NASA TECHNICAL NOTE

NASA TN D-2368

NASA TN D-2368

AERODYNAMIC CHARACTERISTICS OF A FULL-SCALE FAN-IN-WING MODEL INCLUDING RESULTS IN GROUND EFFECT WITH NOSE-FAN PITCH CONTROL

by Jerry V. Kirk, David H. Hickey, and Leo P. Hall

Ames Research Center
Moffett Field, Calif.

NATIONAL AERONAUTICS AND SPACE ADMINISTRATION • WASHINGTON, D. C. • JULY 1964

AERODYNAMIC CHARACTERISTICS OF A FULL-SCALE FAN-IN-WING MODEL INCLUDING RESULTS IN GROUND EFFECT WITH NOSE-FAN PITCH CONTROL

By Jerry V. Kirk, David H. Hickey, and Leo P. Hall

Ames Research Center
Moffett Field, Calif.

NATIONAL AERONAUTICS AND SPACE ADMINISTRATION

For sale by the Office of Technical Services, Department of Commerce,
Washington, D.C. 20230 -- Price $2.75

AERODYNAMIC CHARACTERISTICS OF A FULL-SCALE FAN-IN-WING MODEL INCLUDING RESULTS IN GROUND EFFECT WITH NOSE-FAN PITCH CONTROL

By Jerry V. Kirk, David H. Hickey,
and Leo P. Hall

Ames Research Center
Moffett Field, Calif.

SUMMARY

An investigation was conducted to determine the low-speed aerodynamic characteristics (in and out of ground effect) of a full-scale fan-in-wing VTOL model incorporating a fan in the nose of the fuselage for trim and pitching-moment control. The model had a midmounted wing of aspect ratio 3.1. Results were obtained with the wing at 3.85, 2.2, 1.7, and 1.0 fan diameters above the tunnel floor. The high position was considered out of ground effect.

The effects on longitudinal characteristics of lift-fan performance were obtained at all positions tested while longitudinal characteristics with the pitch fan operating were obtained for only the three positions considered in ground effect. Longitudinal and lateral-directional characteristics were studied in the high position with the lift fans operating and with various settings of the fan exit vanes to control fan thrust and produce yaw and roll. Various trailing-edge flap deflections were tested with the model in the high position, and the optimum setting of 45° was then used throughout the remainder of the program.

Six-component force and moment data were obtained with the model in the high position and three-component data for the three lower positions. Control power of the pitch-fan installation, control power of the horizontal tail, trim characteristics, temperature rise at the fan and gas generator inlets (attributed to exhaust gas reingestion), and downwash at the horizontal tail are included.

INTRODUCTION

Previous theoretical studies and wind-tunnel investigations (refs. 1 through 4) have shown the feasibility of using the lifting fan concept for functional V/STOL aircraft.

Results of a previous large-scale investigation on the fan-in-wing concept are presented in reference 1. The purpose of the present study was to investigate the aerodynamic characteristics in and out of ground effect of a model with a midmounted wing having approximately 50 percent larger fan-to-wing area ratio than the model reported in reference 1, a pitch fan for longitudinal control, and other aerodynamic controls required for a practical aircraft.

The X-353-5B lift fans and the X-376 pitch-control fan were used during the investigation. Fan performance, general aerodynamic characteristics, longitudinal stability and control, and lateral-directional stability and control results are presented without the pitch control fan operating out of ground effect. Lift-fan and pitch-fan performance, general aerodynamic characteristics, and longitudinal stability and control characteristics were obtained in ground effect. The effects on aerodynamic characteristics of throttling the lift-fan exit vanes to control fan thrust, of differential deflection to produce yaw and roll, plus modulating the pitch-fan thrust for pitching-moment control are shown.

Fan and gas generator inlet temperature rise due to exhaust gas ingestion was measured. Means of alleviating the adverse effects of ingestion on performance are discussed.

NOTATION

A fan exit area, sq ft, or wing aspect ratio

b wing span, ft

c wing chord parallel to plane of symmetry, or vane chord, ft

$\bar{c}$ mean aerodynamic chord, $\frac{2}{S}\int_0^{b/2} c^2\,dy$

C_l rolling-moment coefficient, $\frac{l}{qSb}$

C_L lift coefficient, $\frac{L}{qS}$

C_D drag coefficient, $\frac{D}{qS}$

C_m pitching-moment coefficient, $\frac{M}{qS\bar{c}}$

C_n yawing-moment coefficient, $\frac{N}{qSb}$

C_y side-force coefficient, $\frac{Y}{qS}$

D drag, lb, or rotor diameter, ft

h vertical distance from the lower surface of the fan hub to the ground plane, ft

i_t horizontal-tail incidence angle, deg

l	rolling moment, ft-lb
L	total lift on model, lb
M	pitching moment, ft-lb
N	yawing moment, ft-lb
p_s	test section static pressure, lb/sq ft
p_o	standard atmospheric pressure, 2116 lb/sq ft
q	free-stream dynamic pressure, lb/sq ft
R	Reynolds number or fan radius
RPM	corrected fan rotational speed
S	wing area, sq ft
T	complete ducted fan thrust in the lift direction with $\alpha = 0^\circ$ and $\beta = 0^\circ$, $\rho A v_j^2$, lb
ΔT	average temperature rise in the fan and gas generator inlets, $^\circ F$
v	air velocity, ft/sec
V	free-stream air velocity, knots
W	gross weight, lb
x	distance from the leading edge of the wing, ft
y	spanwise distance perpendicular to the plane of symmetry, ft
Y	side force, lb
z	perpendicular distance from the chord line to the airfoil, ft
α	angle of attack of the wing chord plane, deg
β	fan exit-vane deflection angle from the fan axis, deg
$\Delta\beta$	difference in exit-vane angle of alternate vanes, or difference between exit-vane angles of the left and right fans, $\beta_L - \beta_R$, deg
β_s	sideslip angle, deg
δ	relative static pressure, $\frac{p_s}{p_o}$

δ_f	trailing-edge flap deflection measured normal to the hinge line, deg
δ_m	thrust modulator setting measured normal to the hinge line
$\Delta\epsilon$	change in average downwash angle at the horizontal tail, deg
η	fraction of wing semispan, $\frac{2y}{b}$
λ	wing taper ratio
μ	tip-speed ratio, $\frac{V}{\omega R}$
ρ	density, lb-sec^2/ft^4
ω	fan rotational speed, radians/sec

Subscripts

a	average
f	fan
gg	gas generator
j	fan exit
r	in a direction to produce roll
L	left
LF	lift fan
PF	pitch control fan
R	right
s	static conditions
t	in a direction to reduce thrust
u	uncorrected
v	forward speed condition
y	in a direction to produce yaw
α	variable angle of attack
β	variable exit-vane angle

MODEL AND APPARATUS

Model

Photographs of the model mounted on the normal strut system and the variable height strut system in the Ames 40- by 80-Foot Wind Tunnel are shown in figure 1. Figure 2 is a sketch of the model including pertinent dimensions.

Wing geometry.- The midmounted wing had an aspect ratio of 3.11 and a taper ratio of 0.32. Sweepback at the quarter-chord line for the inboard section was 16° and for the wing-tip section 25°. An NACA 65-210 (modified) airfoil section (coordinates are in table I) was basic for the inboard section of the wing from $\eta = 0$ to $\eta = 0.69$. The wing tapered from this point to a standard NACA 65-210 airfoil section at the wing tip. The fan inlet was designed for an untapered wing; the resultant bulge and fairing increased wing thickness to 12 percent at the outboard edge of the fan ($\eta = 0.51$). Normal contour was regained at $\eta = 0.59$.

High-lift devices.- Details of the single-slotted flap are shown in figure 3. The flap extended from 13.4- to 53.5-percent semispan and was tested at deflections of 0°, 30°, 45°, and 50°. With the model in the high position, the flap had a 7-inch-spanwise, 12.3-inch-chordwise hole cut in the leading edge between flap stations 59 and 66. Its purpose was to accommodate the bracket for the lift-fan exit-vane actuator. This hole was covered in the three lower positions.

Figure 3 shows details of the Krüger flaps used during limited testing. The leading-edge flap extended from 69-percent semispan to the wing tip. Split flaps simulating drooped ailerons were also tested. The flaps were deflected 30° and extended from 69-percent semispan to the wing tip. Details are shown in figure 3.

Fuselage.- The fuselage was slab sided with rounded corners. It was approximately 4 feet wide and housed two J-85 gas generators mounted side by side. The J-85 inlets were high on the fuselage. The nose section of the fuselage housed the T-58 gas generator and the pitch-fan installation.

Tail.- Figure 2 shows the location and geometrical details of the tail. The all-movable horizontal tail was pivoted about the quarter-chord line. Tail incidence was varied between 0° and 20°. Both the horizontal and vertical tail were removed during tail-off testing.

Propulsion and Control System

The X-353-5B lifting fan engine has been thoroughly described in references 1, 2, and 3. J85-5 gas generators were used to drive the wing-mounted lift fans. The X-376 pitch-control fan used during the second phase of the test program was similar to the X-353-5B lift fan but with a smaller diameter and was propelled by exhaust gas from a T-58. All three fans rotated counterclockwise as viewed from above the model.

Lift-fan installation.- Location of the wing-mounted fans, hereafter referred to as lift fans, is shown in figure 3. The fan installation is shown in figure 4(a). The fans were completely enclosed within the wing with the exception of the hub, which protruded from the upper wing surface. T-shaped diverter valves mounted aft of the gas generators were used to divert exhaust gases to propel the lift fans or to provide direct thrust.

Figure 4(b) is a sketch of the lift-fan inlet used exclusively throughout the investigation. Details of the inlet vanes are given in table II. Inlet covers were installed during a major portion of the test (fig. 4(a)). The covers had a bulge on the lower surface to cover the fan hub during conventional flight. Unless otherwise stated, data presented will be for the configuration with inlet covers.

The high disk-loading lift fan consists of a single rotor with 36 blades. The fan is 62.5 inches in diameter and has a single row of stators below the rotor. Exit vanes mounted downstream from the stators extended across the tip turbine exhaust and were used for vectoring and throttling the fan exhaust or as a covering for the undersurface of the fan during cruising flight. Alternate vanes were linked together to provide two separate gangs on each fan. Independent actuators allowed differential vane control to provide fan thrust modulation, yaw, and roll control. Symmetrical actuation provided thrust vectoring. The vane airfoil sections had a maximum thickness of 10-percent chord at 20-percent chord and had a maximum of 2.3-percent chord camber of the mean line at 35-percent chord.

During the initial phase of the test the turbine exhaust and fan exit vanes were connected and deflected together. Midway through the test program, in an attempt to reduce the reingestion of hot gases at the fan and gas generator inlets in ground effect at low speeds, the turbine exhaust vanes were offset 30° aft of the fan exit vanes. Figure 4(c) is a photograph and sketch showing the offset. This configuration will be referred to as staggered louvers. The normal configuration will be called straight louvers.

Pitch-fan installation.- Details on the location of the fan in the nose of the fuselage are found in figure 2. This fan will be referred to as the pitch fan. The pitch-fan rotor plane of rotation was 2 inches below the wing chord plane.

The X-376 pitch control fan is 36 inches in diameter and is aerodynamically similar to the X-353-5B lift fan. The pitch fan was designed to be operated in conjunction with the X-353-5B propulsion system and pitch-fan RPM was designed to be 140 percent of lift-fan RPM in this system.

For this investigation the exhaust gas from a modified T-58 gas generator was used to propel the single-stage tip-turbine-driven fan. The T-58 was mounted in the forward section of the fuselage with the inlet facing aft. Air was supplied to the T-58 from the interior of the fuselage and through small ports in the side of the fuselage.

For the majority of the investigation, lift-fan RPM was held at 1700. Corresponding pitch-fan RPM was 2400.

Doors were located below the pitch fan (figs. 1(d) and 2) and operated together to give varying degrees of thrust modulation to provide trim and pitching-moment control. Door positions tested varied from fully open (0°) to 70° closure. Fairings enclosed the pitch-fan installation (figs. 1(b) and (c)) when it was not in use.

TESTING PROCEDURE

Longitudinal force and moment data were obtained for an angle-of-attack range from -4° to $+20^{\circ}$ at the high position. The angle-of-attack range became more limited as the model was placed in the lower ground positions. Lateral-directional force and moment data were obtained at the high ground position. Fan performance was measured utilizing scale force data. Thrust of the pitch fan and left lifting fan was obtained from momentum rakes mounted below the fans. Airspeed varied from 0 to 100 knots corresponding to a maximum Reynolds number of 10.75 million. Fan RPM was varied from 900 to 2400.

Tests at Zero Angle of Attack

At 0° angle of attack, fan speed and wind-tunnel velocity were varied independently. Data were obtained for several exit-vane angles and combinations of differentially deflected vane angles, three flap deflections, and with the tail on and off at the various positions tested.

Limited static tests were performed outside the wind tunnel with the wing at 1 fan diameter from the ground. Only ingestion was measured.

Tests With Variable Angle of Attack

When angle of attack was varied, fan RPM was held essentially constant. Results were obtained for several fan speeds and tunnel airspeeds. Model variables were the same as those listed above except that four flap deflections were tested.

CORRECTIONS

Force data gathered with the fans not operating (power off) at the high position ($h/D = 3.85$) were corrected for the effects of wind-tunnel wall interference in the following manner:

$$\alpha = \alpha_u + 0.64\ C_{L_u}$$

$$C_D = C_{D_u} + 0.0198\ C_{L_u}^2$$

$$C_m = C_{m_u} + 0.0104\ C_{L_u} \text{ (tail-on tests only)}$$

All longitudinal data were corrected for the influence of struts.

Power-off results in ground effect have been corrected for a 1° flow inclination caused by the ground plane and variable-height strut installation. Corrections have been applied, where appropriate, to dynamic pressure due to blockage of the wind-tunnel test section.

No wind-tunnel wall corrections were applied to results obtained with the fans operating since the effect of fan air flow on wind-tunnel corrections is unknown.

RESULTS

Tests were conducted at four ground heights, $h/D = 3.85$, 2.2, 1.7, and 1.0. The study at $h/D = 3.85$ was conducted on the normal strut system while the remaining tests were conducted on the variable-height struts.

Lift-fan tip-speed ratio will be used as the independent parameter in the presentation of results unless otherwise stated. Figure 5 shows the relationship between tip-speed ratio and free stream to fan velocity ratio for the lift fans.

Table III is an index to the figures. The first section of figures is devoted to lift-fan data and aerodynamic characteristics with only the lift fans operating. Aerodynamic characteristics with the pitch fan operating and general aerodynamic characteristics with three fans operating comprise the second section. The third section presents control power results. Horizontal-tail effectiveness, pitch fan and thrust modulator control power, effec~~ts~~ of pitch-fan control power on longitudinal characteristics, exit-vane angle deflection to control fan thrust, and the effect of differential control to produce yaw and roll are included. Short sections follow in order on trim and on measured temperature rise at the fan and gas generator inlets.

Lift-Fan Characteristics

The effects of test and model configuration variables on fan performance as installed in the wing are presented by the following: Figure 6 shows the zero airspeed performance of the fans. Figure 6(a) presents lift with individual fans operating. Figure 6(b) shows the thrust of the left fan as measured by an equal area momentum rake for three ground heights, h/D = 2.2, 1.7, and 1.0. Figure 6(c) presents the total lift from both fans. The effect of forward speed on fan thrust is shown in figure 7. Figures 8(a) and (b) present the effect of forward speed and fan RPM on lift for three flap deflections and different ground heights, respectively.

Aerodynamic Characteristics With Only the Lift Fans Operating

The following results present the effect of wing fan operating conditions and model configuration on longitudinal and lateral-directional characteristics.

Angle of attack of zero.- Figures 9 through 12 show the effects of airspeed and fan RPM (tip-speed ratio) on longitudinal characteristics. Figure 9 presents results for h/D = 3.85, several exit-vane deflection angles, straight louvers, and three flap deflections. Results at h/D = 2.2, 1.7, and 1.0 are shown in figures 10, 11, and 12. Data are for a flap deflection of 45°, tail off and on, and straight and staggered louvers.

The incremental variation of average downwash at the horizontal tail for the different ground positions at 0° exit-vane deflection is shown in figure 13. Results were computed from data in figures 9 through 12 and from measured tail effectiveness.

Variable angle of attack.- Figures 14 through 28 present variation of longitudinal characteristics with angle of attack. Power-off data are shown in figures 14 through 17. Figure 14 shows the effect of flap deflection with the tail on and off at h/D = 3.85. Effectiveness of the leading-edge Krüger flaps is also shown. Reynolds number effect is presented at h/D = 3.85, tail on, and at h/D = 2.2, tail off, in figure 15 while the effect of ground height on power-off longitudinal characteristics is shown in figure 16. Various inlet closures and exit-vane deflection angles were tested at h/D = 3.85 and the results are given in figure 17.

Data obtained at low tunnel speed with the lift fans operating (low tip-speed ratios) are plotted as forces in figures 18 and 19. Figures 20 through 28 show the variation of longitudinal characteristics, in coefficient form, with the fans operating at higher tip-speed ratios. Tail-off longitudinal characteristics for different exit-vane deflection angles are given for three ground heights in figures 20 through 22. Corresponding tail-on results are shown at four ground heights in figures 23 through 26. The longitudinal characteristics with Krüger flaps on, 0° exit-vane deflection and h/D = 3.85 are presented in figure 27. Figure 28 shows results with the split-flaps deflected 30° at h/D = 2.2 and 0° fan exit-vane deflection.

Aerodynamic characteristics with sideslip.- The variation of longitudinal and lateral-directional characteristics for variable angle of attack at sideslip angles of -12°, 0°, and +12 at $h/D = 3.85$ is shown in figures 29 through 31. Figure 29 presents power-off longitudinal and lateral-directional characteristics. Low tunnel speed (low tip speed) results plotted as forces are in figure 30. Higher speed results for -12° sideslip, in coefficient form, are shown in figure 31.

Constant angle-of-attack results at $h/D = 3.85$ are presented in figures 32 through 34. Power-off longitudinal and lateral-directional characteristics at 0° and 8° angle of attack are shown in figure 32. Results at 0° angle of attack with the fans operating are presented in figure 33. Similar results for 8° angle of attack are in figure 34.

Characteristics With the Pitch Fan Operating

Performance of the pitch fan and thrust modulator with zero airspeed is shown in figure 35. The variation of pitch-fan thrust with forward speed and the relationship between pitch-fan tip-speed ratio and velocity ratio are presented in figure 36. Pitch-fan tip-speed ratio was approximately 140 percent of lift-fan tip-speed ratio.

Angle of attack zero.- Figures 37 and 38 present the variation of longitudinal characteristics with velocity and lift fan RPM (tip-speed ratio) for several exit-vane angles at two ground heights. Two flap positions and pitch-fan thrust modulator settings are shown at $h/D = 2.2$ in figure 37. Similar results at $h/D = 1.0$ are given in figure 38. Figure 38(d) shows characteristics with the split flaps installed.

Variable angle of attack.- Variation of longitudinal characteristics with angle of attack is shown in figures 39 through 43. Tail-off results obtained with only the pitch fan operating, the lift-fan apertures closed, $h/D = 2.2$, and with the thrust modulator at 60° are presented in figure 39. Data shown in figures 40 through 43 are for the pitch-control fan operating in conjunction with the lift fans. Low tip-speed ratio results for two ground positions and two exit-vane angles, plotted as forces, are shown in figure 40. Figure 41 through 43 present characteristics at higher tip speeds in coefficient form. Results at $h/D = 2.2$ for 0° exit-vane deflection and 60° thrust modulator setting are shown in figure 42. Longitudinal characteristics at $h/D = 1.0$ are shown in figure 43.

Control Power

Horizontal-tail effectiveness is presented in figure 44. Control power of the pitch-fan and thrust modulator installation is shown in figure 45. The variation of longitudinal characteristics with velocity and fan RPM (tip-speed ratio) for the pitch-fan and modulator installation at two ground heights is shown in figure 46.

Figure 47 presents the effect of thrust control on longitudinal characteristics for various tip-speed ratios at $h/D = 3.85$. The effect of roll control and yaw control on longitudinal and lateral-directional characteristics at $h/D = 3.85$ is shown in figures 48 through 53. Results in figures 48 through 51 are at 0° sideslip while figures 52 and 53 present data at -12° sideslip. Low-speed characteristics plotted as forces are shown in figures 48 and 50. Results in figures 49 and 51 are in coefficient form. Longitudinal and lateral-directional results at -12° sideslip for low tunnel speed (low tip-speed ratios), plotted as forces, are shown in figure 52. Similar results for higher tip-speed ratios, in coefficient form, are presented in figure 53.

Trim

The variation of longitudinal characteristics with angle of attack near trimmed conditions is shown in figure 54. Data are presented for three ground heights with and without the pitch fan operating.

Ingestion

Temperature rise above ambient at the fan and gas generator inlets as a measure of exhaust gas reingestion is shown in figures 55 through 57. Figure 55 presents the temperature rise at the fan and gas generator inlets for $h/D = 1.0$, low forward speed (0 to 5 knots), and straight and staggered louvers. The rise in temperature at the lift-fan inlets for higher forward speeds at $h/D = 2.2$, 1.7, and 1.0, exit-vane angles of 0°, 15°, and 30° with staggered louvers is shown in figure 56. Similar results with straight and staggered louvers are presented for the gas generator inlets in figure 57.

DISCUSSION

Lift-Fan Performance

Lift-fan performance was measured under static conditions and with forward speed, in and out of ground effect. Temperature probes were placed at the fan and gas generator inlets to measure the temperature rise attributable to exhaust gas reingestion in ground effect during hovering and STOL conditions.

Zero speed.- At zero forward speed, measured fan thrust for the model of this investigation was comparable to that of the previous fan-in-wing study (ref. 1). The effect of ground proximity on fan thrust with the lift fans operating (fig. 6(b)) indicated a fan thrust loss of approximately 15 percent near the ground. The fan-in-fuselage model (ref. 3) had an adverse ground effect amounting to 23 percent of the total lift out of ground effect of which 14 percent was attributed to fan thrust loss and 9 percent to adverse effects on the model. In spite of the thrust loss, the model of this investigation showed no effect of ground proximity on total lift (fig. 6(c)); thus a favorable ground effect on lift was sufficient to compensate for the adverse effect on fan thrust. The effect of exhaust gas reingestion in hover was minor. During these conditions the fan flow spread radially along the ground surface, except near the line of symmetry where it was confined to fore and aft flow. During windy conditions, the hot gas was picked up and blown back in the vicinity of the model so that both the fan inlets and gas generator inlets could ingest the hot air. In light winds, temperature rise in all inlets was under 10°.

Forward speed.- The variation of fan thrust with forward speed was nearly identical with that reported in reference 1 (see fig. 58). Fan thrust for both fan-in-wing investigations decreased with increasing air speed at tip-speed ratios above 0.12. With forward speed, ingestion was a significant problem because the blowback of hot gases became more severe. The path between fan exit and inlet was short, so that a temperature rise in excess of 50° occurred in the fan inlets. Temperature rise at the gas generator inlets exceeded 30°. Vectoring the fan turbine exhaust 30° aft of the fan exit vanes (staggered louvers, see fig. 4(c)) was beneficial in reducing ingestion. With 0° exit-vane deflection, increasing distance above the ground from $h/D = 1.0$ to 2.2 reduced the maximum speed at which ingestion occurred from approximately 70 to 40 knots with a maximum temperature recorded of 50° at $h/D = 1.0$ and 40° at $h/D = 2.2$. With 15° exit-vane deflection, a maximum temperature rise of 30° was measured at $h/D = 1.0$ with the maximum speed for ingestion of approximately 50 knots but increasing h/D to 2.2 eliminated ingestion. With 30° exit-vane deflection, ingestion was negligible at all ground heights tested. The largest temperature rise measured at the fan inlets with staggered louvers would require a 4.5-percent increase in fan speed to compensate for the thrust loss.

Aerodynamic Characteristics With the Lift Fans Operating

Out of ground effect.- With only the lift fans operating out of ground effect, total lift increased with increasing airspeed. Comparison of the two large-scale fan-in-wing studies (fig. 58) shows a smaller increase in lift with airspeed for the configuration of this investigation than for the configuration of the previous program (ref. 1). Lift with the fans operating is comprised of aerodynamic lift and fan thrust. Fan thrust and airfoil camber were essentially the same for the two tests. Comparisons were made at 0° angle of attack with the flaps up; therefore, the smaller increase in total lift with airspeed in this investigation is due to less induced lift. Figure 59 is a comparison of the variation of induced lift with airspeed for the two investigations. At a tip-speed ratio of 0.30, induced lift was 50 percent less for the subject model. The increased fan area to wing area ratio of the model for this investigation and differences in wing geometry and fan spacing are probably responsible for this smaller value.

Lift induced by fan operation is a significant part of the total lift in wing fan installations. A method of estimating induced lift is presented in reference 5.

In ground effect.- Figure 60 presents the variation of lift-to-static-thrust ratio with velocity ratio (at constant fan speed) for three ground heights. In the low position (h/D = 1.0), with straight louvers, a reduction in lift below the static value was caused by ingestion in the lift fans. This lift loss was eliminated by staggering the turbine exhaust louvers 30° aft which reduced the temperature rise of the air ingesting into the lift fans. As these results were compared at a constant fan RPM, the above comparison may not be valid. If results are compared at a constant throttle setting, and the gas generators are free of ingestion, an increase in fan speed occurs when the fans ingest exhaust gases, thus compensating for the lift loss. This type of operation and constant RPM operation are compared in figure 61 for an h/D of 1.0. Constant power operation had a much larger increase in lift with airspeed because of the compensation for hot gas ingestion in the fan. Figure 62 presents the variation of lift with airspeed for constant power at the four ground heights tested; low-speed results are similar while at higher speeds a favorable ground effect is evident.

Aerodynamic Characteristics With the Pitch Fan Operating

The aerodynamic effects of operating a pitch-control fan forward of the wing, necessary in this model for hovering and low-speed pitching-moment control, are shown in figures 63 and 64 for ground heights of 2.2 and 1.0 fan diameters.

Effect on lift.- As shown by the results in figure 63, at an h/D = 2.2 with the thrust modulator positioned at 0° and 60°, the pitch-fan contribution to total lift decreased with increasing airspeed. Measured pitch-fan thrust was essentially constant over the speed range tested, and a variation in pitching moment did not accompany the lift loss, indicating that induced effects at the nose of the aircraft were negligible. These facts indicate the lift loss with a 0° modulator setting is attributable to an unloading of the wing behind the pitch fan due to downwash. This conclusion is verified by the data at an h/D of 1.0, where downwash on the wing is of a lower order of magnitude due to constraint of flow by the ground plane; the results show an increase in lift with airspeed. The lift loss for an h/D = 2.2 and the thrust modulator doors at 60° is caused by the pitch-fan exhaust blowing across the doors and exiting in a horizontal plane at right angles to the free-stream air flow. This flow probably blocks the free-stream air flow resulting in less dynamic pressure over the wing and therefore less lift. A similar flow interaction has been reported when a target type thrust reverser was used on a single engine jet aircraft (see ref. 6). Results shown in figure 64(a) also support this explanation. At an h/D = 2.2, with tail off, and with the thrust modulator doors at 60° and only the pitch fan operating, the lift-curve slope is significantly reduced at low forward speeds. The power-off value of the lift-curve slope is not approached until a pitch-fan tip-speed ratio of 0.30 is reached. Whereas the reduction in lift contributed by operation of the pitch fan was significant, total model lift with all three fans operating was not reduced below the static value throughout the transition speed range.

Effect on pitching moment.- The change in static margin due to pitch-fan operation is shown in figure 64(b) for an $h/D = 2.2$ and thrust modulator positions of 0° and 60°. With only the pitch fan operating for the tail-off configuration, modulator doors at 60°, a significant destabilizing effect is present below a pitch-fan tip-speed ratio of 0.25. Similar results are shown with the pitch fan operating in conjunction with the lift fans for the tail-on configuration, straight louvers, with the thrust modulator doors at 60°. (The shaded area in the figure represents the band of uncertainty in the results.) These results indicate that the thrust modulator doors at 60° act as a small canard. Pitch-fan exhaust blowing over the doors increases the canard effectiveness in the low-speed range, resulting in the unstable trend in static margin. With all three fans operating for the tail-off configuration, staggered louvers, and with the modulator doors at 0°, a pitch down or stabilizing contribution from the pitch fan for the tip-speed range is indicated.

Effect of pitch-fan operation on transition performance.- Power and control requirements for balanced flight as computed from the test results for an aircraft weight of 9500 pounds are presented in figure 65 to illustrate the effects of pitch-fan operation on transition performance. Two possible flight plans are outlined. The first consists of maintaining a constant angle of attack of 0° throughout transition, varying fan speed, and operating the pitch fan continuously, providing as much trim as necessary for balanced flight. The second plan involves maintaining a constant throttle setting, turning the pitch fan off at approximately 50 knots, and varying angle of attack to maintain balanced conditions.

Continuous operation of the pitch fan as outlined in the first profile results in a maximum possible conversion speed of approximately 105 knots (corresponding to 120 percent of stall speed on a standard day). Altering the flight plan by either exit louver deflection or angle of attack will not significantly alter the maximum conversion speed since 100-percent fan speed would be exceeded with fan exit-vane deflection angles of 40°, and further deflection of the exit vanes at 0° or lower angles of attack would result in a significant lift loss. Increasing angle of attack and fan exit-vane deflection would not provide sufficient lift and thrust to extend the conversion speed. The maximum conversion speed can be extended by turning the pitch fan off at approximately 50 knots when it is no longer needed for trim or pitching-moment control. In so doing, drag is reduced, power requirements are decreased, and, by varying angle of attack, required lift-fan exit-vane deflection angles are reduced. A speed of 120 knots is reached before fan exit-vane deflection angles of 40° are necessary; however, in this case, angle of attack, fan speed, and exit-vane deflection can be varied to extend the conversion speed somewhat. Results of the foregoing discussion indicate that continuous operation of the pitch fan throughout transition when it is not needed for trim or control lowers the maximum possible conversion speed by approximately 20 knots.

Horizontal-tail incidence and tail angle of attack required to maintain balanced flight are essentially the same for the two methods outlined.

SUMMARY OF RESULTS

A full-scale wind-tunnel investigation of a V/STOL fan-in-wing model has shown positive lift induced by fan operation was present at all ground positions tested, although the amount of induced lift was less in this investigation than in the previous large-scale fan-in-wing study.

The adverse effect on lift-fan performance by the ingestion of exhaust gases during STOL operation can be minimized by (1) vectoring the exhaust gases away from the fan inlets and placing the gas generator inlets to reduce ingestion, and (2) designing the fans to permit constant power operation.

Pitch-fan operation and thrust modulator door position produced detrimental effects on the aerodynamic characteristics of the model. The pitch-fan contribution to total lift decreased significantly with increasing airspeed as distance from the ground increased. The contribution of the pitch fan to static margin was destabilizing at low tip-speed ratios when the thrust modulator doors were positioned at 60°; however, with the doors fully open a stabilizing contribution was present.

Continuous operation of the pitch fan throughout transition when it is not needed for trim or pitching-moment control lowers the maximum possible conversion speed by approximately 20 knots.

Ames Research Center
National Aeronautics and Space Administration
Moffett Field, Calif., Jan. 30, 1964

REFERENCES

1. Hickey, David H., and Hall, Leo P.: Aerodynamic Characteristics of a Large-Scale Model With Two High Disk-Loading Fans Mounted in the Wing. NASA TN D-1650, 1963.

2. Aoyagi, Kiyoshi, Hickey, David H., and deSavigny, Richard A.: Aerodynamic Characteristics of a Large-Scale Model With a High Disk-Loading Lifting Fan Mounted in the Fuselage. NASA TN D-775, 1961.

3. deSavigny, Richard A., and Hickey, David H.: Aerodynamic Characteristics in Ground Effect of a Large-Scale Model With a High Disk-Loading Lifting Fan Mounted in the Fuselage. NASA TN D-1557, 1963.

4. Maki, Ralph L., and Hickey, David H.: Aerodynamics of a Fan-in-Fuselage Model. NASA TN D-789, 1961.

5. Goldsmith, Robert H., and Hickey, David H.: Characteristics of Aircraft With Lifting-Fan Propulsion Systems for V/STOL. IAS 63-27, 1963.

6. Tolhurst, William H., Jr., Kelly, Mark W., and Greif, Richard K.: Full-Scale Wind-Tunnel Investigation of the Effects of a Target-Type Thrust Reverser on the Low-Speed Aerodynamic Characteristics of a Single-Engine Jet Airplane. NASA TN D-72, 1959.

TABLE I.- COORDINATES OF WING AIRFOIL SECTION (NACA 65-210 MODIFIED) PARALLEL TO MODEL PLANE OF SYMMETRY

Upper surface		Lower surface	
x/c	z/c	x/c	z/c
0	0	0	0
.00435	.00819	.00569	-.00776
.00678	.00999	.00827	-.00925
.01169	.01273	.01337	-.01141
.02408	.01757	.02598	-.01498
.04898	.02491	.05110	-.02014
.07394	.03069	.07614	-.02431
.09894	.03555	.10417	-.02812
.14899	.04338	.13889	-.03194
.19909	.04938	.17361	-.03486
.24921	.05397	.20833	-.03708
.29936	.05732	.27778	-.03868
.34951	.05954	.34722	-.03910
.39968	.06067	.41667	-.03924
.44984	.06058	.48611	-.03861
.50000	.05915	.55556	-.03618
.55014	.05625	.62500	-.03146
.60027	.05217	.65972	-.02806
.65036	.04712	.69954	-.02404
.70043	.04128	.74952	-.01867
.75045	.03479	.79953	-.01325
.80044	.02783	.84959	-.00803
.85038	.02057	.89970	-.00344
.90028	.01327	.94985	-.00009
.95014	.00622	1.00000	0
1.00000	0		
Leading-edge radius: 0.00687 Slope of radius through leading-edge: 0.084			

TABLE II.- INLET VANE DETAILS

	Circular vane	Fixed vane 1	Fixed vane 2	Fixed vane 3	Fixed vane 4	Fixed vane 5
Maximum thickness, percent	12.0	9.0	9.7	9.0	9.9	9.1
Location of maximum thickness, percent	25.5	20.0	20.0	20.0	20.0	20.0
Camber of mean line, percent	9.7	3.0	3.0	3.0	1.5	0
Location of camber of mean line, percent	46.8	40.0	50.0	45.0	40.0	0
Chord	5.12	6.0	6.0	6.0	6.0	5.85

TABLE III.- LIST OF FIGURES

Figure	h/D	α, deg	β, deg	V, knots	i_t, deg	δ_f, deg	Turbine louvers	Remarks
Lift-fan characteristics								
5	---	---	0	---	---	---	---	Relationship of velocity ratio to tip-speed ratio
6	---	0		0	---	---	---	Lift fan performance
7	---			Variable	---	---	---	Effect of forward speed on fan thrust
8(a)	3.85			Variable	Off	Variable	Straight	Effect of forward speed and fan RPM on lift
8(b)	Variable			Variable	0	45°	Both	Effect of forward speed and fan RPM on lift
Longitudinal data at zero angle of attack (lift fans operating)								
9(a)	3.85	0	Variable	Variable	Off	0	Straight	
9(b)						0		Inlet covers off
9(c)						30		
9(d)						45		
9(e)					0			
10(a)	2.2				Off		Staggered	Inlet covers off
10(b)					Off		Staggered	
10(c)					0		Straight	
10(d)							Straight	
10(e)							Staggered	Split flaps
11(a)	1.7				Off		Staggered	
11(b)					0		Straight	
11(c)					0		Staggered	
12(a)	1.0				Off		Staggered	Inlet covers off
12(b)					0		Straight	
12(c)					0		Staggered	
13	3.85,2.2 1.7,1.0		0		0		---	Average downwash at horizontal tail

TABLE III.- LIST OF FIGURES - Continued

Figure	h/D	α, deg	β, deg	V, knots	i_t, deg	δ_f, deg	Turbine louvers	Remarks
Longitudinal data at variable angle of attack (lift fans operating)								
14(a)	3.85	Variable	90	80	0	0,30,45,50	Sealed	Power off
14(b)					Off	0,45,50		
14(c)					0	45		Effect of Krüger flaps
15(a)				20,40,60,80	0,20	0,45	Sealed	Power off Reynolds number effect
15(b)	2.2			20,40,60,80	Off	0,45		
16	Variable			80	Off	45		Effect of ground height
17	3.85		Variable	80	0	45	Straight	Effects of fan inlet and exit closure
18(a)	3.85		0	20,30	Off	30,45	Straight	
18(b)	2.2		0,20	30		45	Staggered	
18(c)	1.7		20	30			Staggered	
19(a)	3.85		0,8,12	20,30	0,16,20		Straight	
19(b)	2.2		0,20	30	0		Both	
19(c)	1.7		0,20	30			Straight	
19(d)	1.0		0,20	30			Both	
20(a)	3.85		0	40,60,80	Off	30	Straight	
20(b)	3.85		0	40,60,80		45		
20(c)			20	40,60				
20(d)			35	60,80				
21(a)	2.2		0	40,60			Staggered	
21(b)	2.2		20	30,40,60,80				
22(a)	1.7		0	40,60				
22(b)	1.7		20	40,60,80				
23(a)	3.85		0	40,60,80	0		Straight	
23(b)	3.85		40	80,100			Straight	
24(a)	2.2		0	40,60,80			Both	
24(b)			20	40,60			Straight	
24(c)			35	40,60,80			Straight	
25(a)	1.7		0	40,60,80			Both	
25(b)			20	40,60			Straight	
25(c)			35	40,60,80			Straight	

TABLE III.- LIST OF FIGURES - Continued

Figure	h/D	α, deg	β, deg	V, knots	i_t, deg	δ_f, deg	Turbine louvers	Remarks
26(a)	1.0	Variable	0	40,60,80	0	45	Straight	
26(b)			20	40,60			Both	
26(c)			35	40,60,80			Straight	
27	3.85		0	40,60,80			Straight	Krüger flaps installed
28	2.2		0	40,60,80			Straight	Split-flaps
Aerodynamic characteristics with sideslip; variable angle of attack (lift fans operating)								
29(a)	3.85	Variable	90	60	0	45	Sealed	Power-off longitudinal characteristics
29(b)			90	60	0		Sealed	Power-off lateral-directional characteristics
30(a)			8,12	20,30	20		Straight	Longitudinal characteristics
30(b)			8,12	20,30				Lateral-directional characteristics
31(a)			16,25	40,60				Longitudinal characteristics
31(b)			16,25	40,60				Lateral-directional characteristics
Aerodynamic characteristics with sideslip; constant angle of attack								
32(a)	3.85	0,8	90	80	0	45	Sealed	Power-off longitudinal characteristics
32(b)		0,8	90	80	0		Sealed	Power-off lateral-directional characteristics
33(a)		0	8,12,16,25	20,30,40,60	20		Straight	Longitudinal characteristics
33(b)		0	8,12,16,25 90	20,30,40,60 80				Lateral-directional characteristics
34(a)		8	16,25	40,60				Longitudinal characteristics
34(b)		8	16,25,90	40,60,80				Lateral-directional characteristics

TABLE III.- LIST OF FIGURES - Continued

Figure	h/D	α, deg	β, deg	V, knots	i_t, deg	δ_f, deg	Turbine louvers	Remarks
Pitch fan and thrust modulator characteristics								
35(a)	---	0	---	0	---	---	---	Variation of lift with RPM
35(b)	---	↓	---	0	---	---	---	Thrust reverser characteristics
36(a)	---	↓	---	Variable	---	---	---	Variation of thrust with forward speed
36(b)	---	↓	---	Variable	---	---	---	Relationship of velocity ratio to tip-speed ratio
Longitudinal data at zero angle of attack (three fans operating)								
37(a)	2.2	0	Variable	Variable	Off	45	Staggered	δ_m = 0
37(b)	2.2	↓	↓	↓	↓	0	↓	δ_m = 60
38(a)	1.0	↓	↓	↓	↓	0	↓	δ_m = 60
38(b)	↓	↓	↓	↓	↓	45	↓	δ_m = 0
38(c)	↓	↓	↓	↓	↓	↓	↓	δ_m = 60
38(d)	↓	↓	↓	↓	↓	↓	↓	δ_m = 60, split flaps
Longitudinal data at variable angle of attack (pitch fan only operating)								
39	2.2	Variable	90	20,30,40,60,80	Off	45	Sealed	δ_m = 60
Longitudinal data at variable angle of attack (three fans operating)								
40	2.2,1.0	Variable	0,20	30	0	45	Straight	δ_m = 45,60
41(a)	2.2	↓	0	40,60,80	Off	↓	Staggered	δ_m = 0
41(b)		↓	20	40	Off	↓	Staggered	δ_m = 0,30,45,60
42		↓	0	30,40,60	0	↓	Straight	δ_m = 60
43	1.0	↓	20	40,60	0	↓	Straight	δ_m = 60

TABLE III.- LIST OF FIGURES - Continued

Figure	h/D	α, deg	β, deg	V, knots	i_t, deg	δ_f, deg	Turbine louvers	Results
Control power								
44	---	---	---	40,60	Variable	---	---	Horizontal-tail effectiveness
45	---	---	---	0	---	---	---	Pitch-fan and thrust modulator control power
46(a)	2.2	0	0		0	45	Straight	δ_m = 0,30,45,60,70
46(b)	1.0		20		0			δ_m = 0,30,45,60,70
47	3.85		8,12,18,25	20,30,40,60	0			Thrust control
48(a)			8	20	+1			Roll control
48(b)			8	20				
49(a)			12,18,25	30,40,60				
49(b)			12,18,25	30,40,60				
50(a)			8	20				Yaw control
50(b)			8	20				
51(a)			12,18,25	30,40,60				
51(b)			12,18,25	30,40,60				
52(a)			8	20	20			Yaw and roll control, β_s = -12
52(b)			8	20				
53(a)	3.85	Variable	12,18,25	30,40,60				
53(b)	3.85	Variable	12,18,25	30,40,60				
Trim characteristics								
54(a)	3.85	Variable	18,25,36,38	40,50,70,80	16,20	45	Straight	δ_m = 0,60
54(b)	2.2		22,35,45	40,60,72	16,17			δ_m = 60
54(c)	1.7		32,45	40,50	12,16			

TABLE III.- LIST OF FIGURES - Concluded

Figure	h/D	α, deg	β, deg	V, knots	i_t, deg	δ_f, deg	Turbine louvers	Remarks
Exhaust gas reingestion								
55(a)	1.0	0	0	0-5	---	45	Straight	Fan and gas generator inlets
55(b)	1.0	↓	0	0-5	↓	↓	Staggered	Fan and gas generator inlets
56(a)	1.0,1.7, 2.2	↓	0	Variable	↓	↓	↓	Wing-mounted lift-fan inlets
56(b)	↓	↓	15	↓	↓	↓	↓	↓
56(c)	↓	↓	30	↓	↓	↓	↓	↓
57(a)	↓	↓	0,15,30	↓	↓	↓	Straight	J-85 gas generator inlets
57(b)	↓	↓	0,15,30	↓	↓	↓	Staggered	J-85 gas generator inlets
Discussion								
58.- Comparison of large-scale fan-in-wing variation of lift with airspeed.								
59.- Comparison of the variation of fan induced lift with airspeed.								
60.- Constant fan RPM.								
61.- Effect of constant power.								
62.- Equivalent power setting.								
63.- Effect of airspeed on the variation of lift and moment due to pitch-fan operation.								
64.- Effect of pitch-fan operation on lift-curve slope and longitudinal stability.								
65.- Power and longitudinal control requirements for unaccelerated flight.								

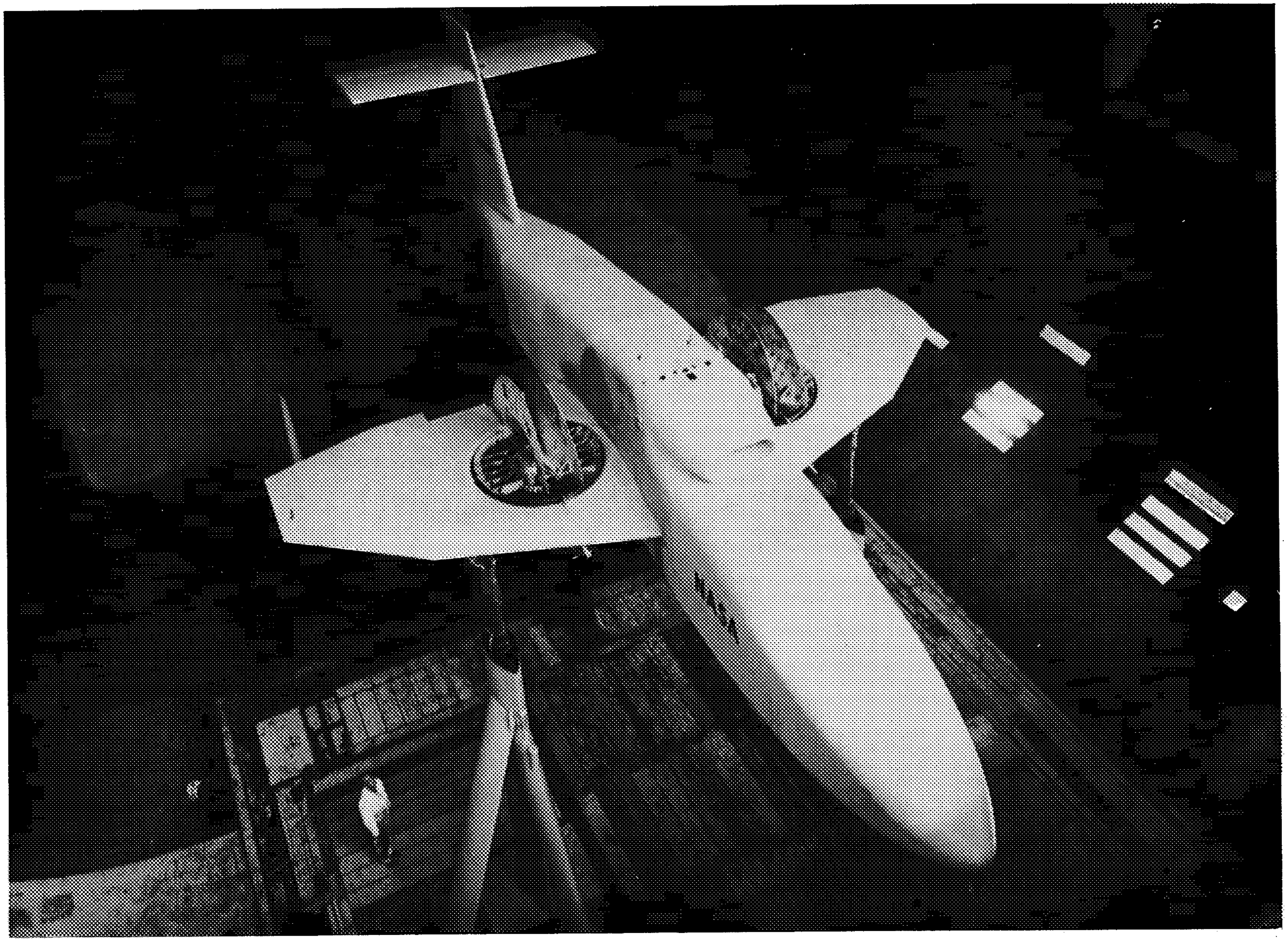

A-29509

(a) Ground height $h/D = 3.85$.

Figure 1.- Photographs of the model mounted in the Ames 40- by 80-foot wind tunnel.

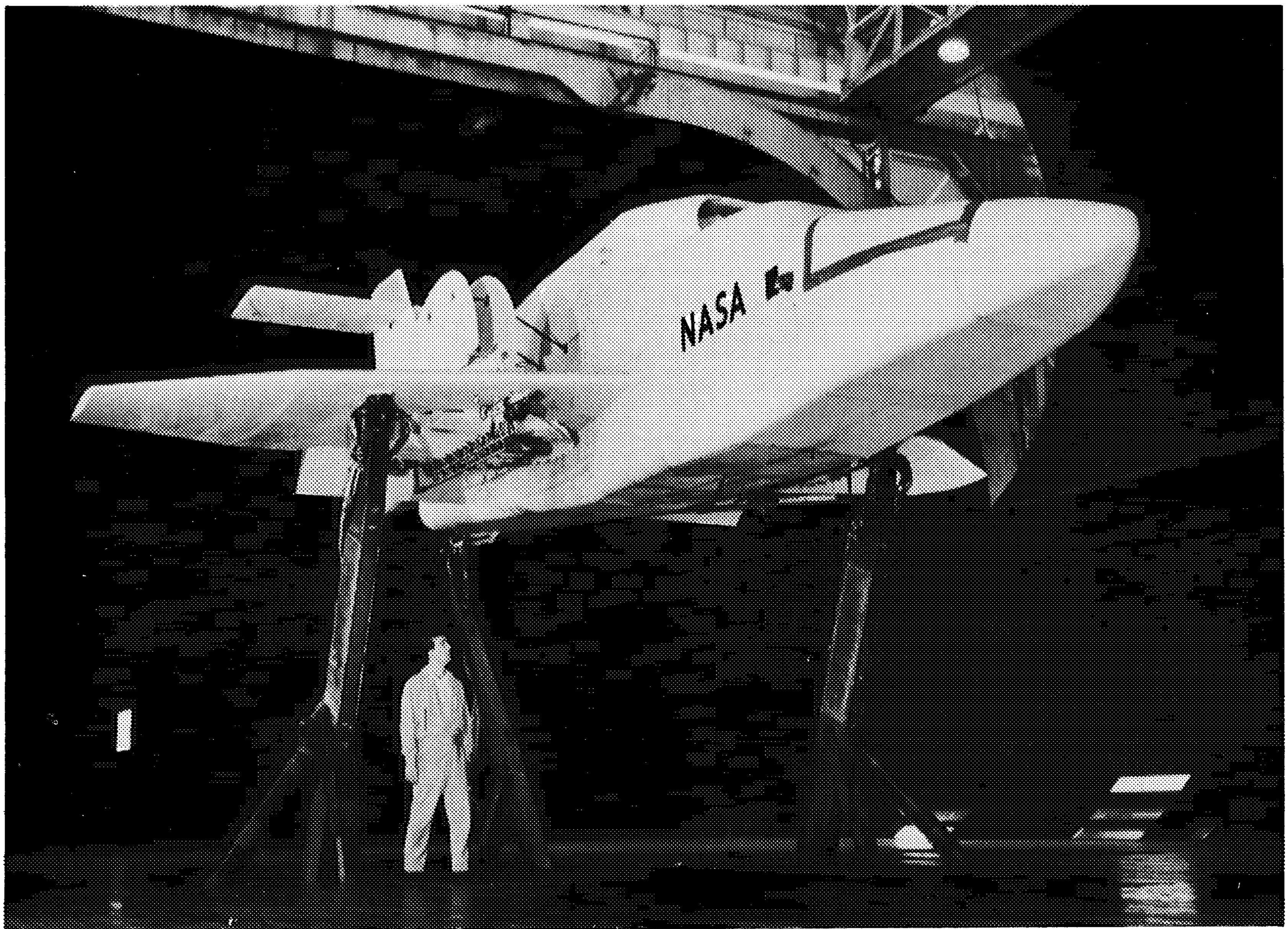

A-30197

(b) Ground height h/D = 2.2.

Figure 1.- Continued.

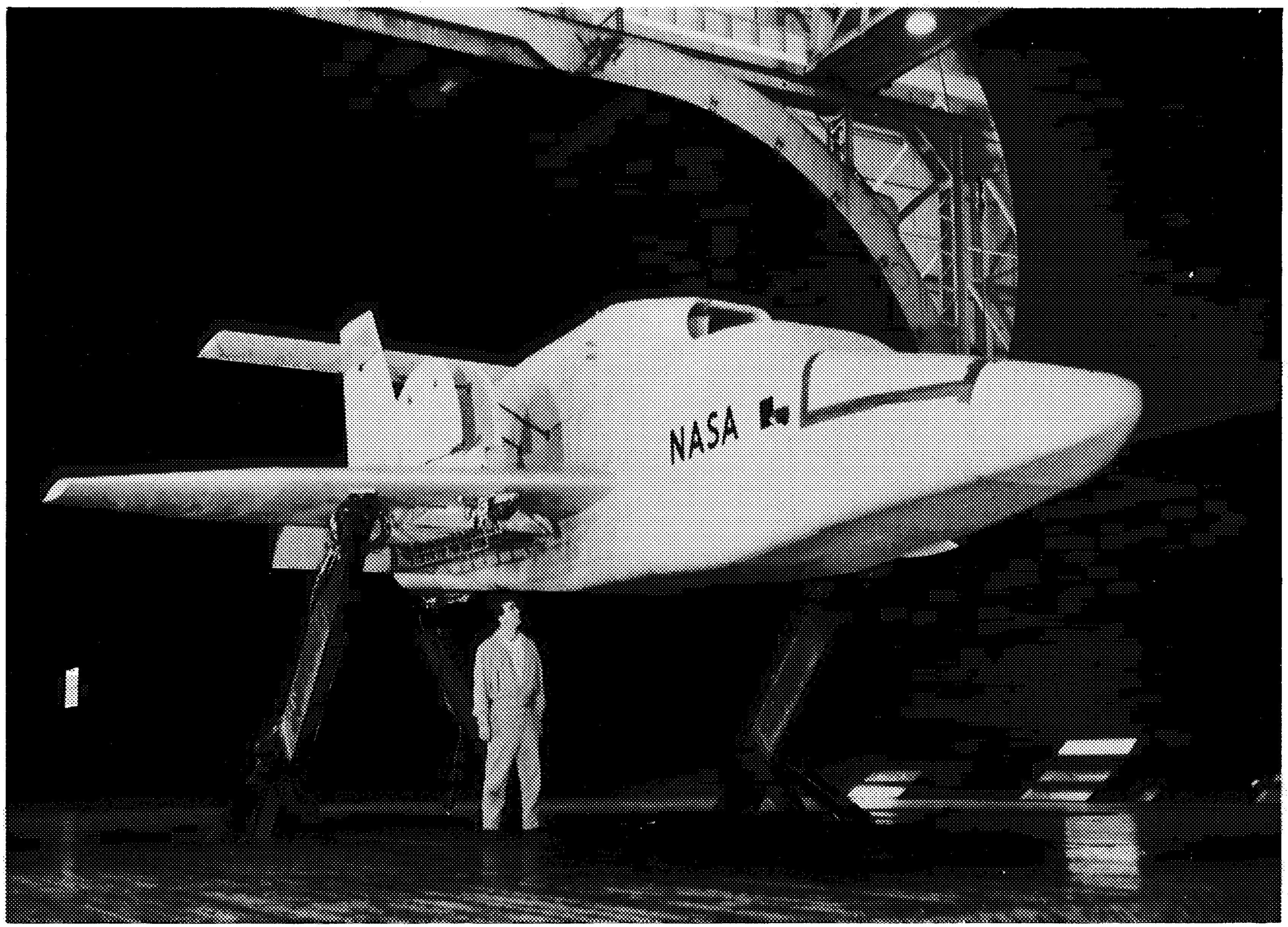

A-30195

(c) Ground height h/D = 1.7.

Figure 1.- Continued.

A-30211

(d) Ground height $h/D = 1.0$.

Figure 1.- Concluded.

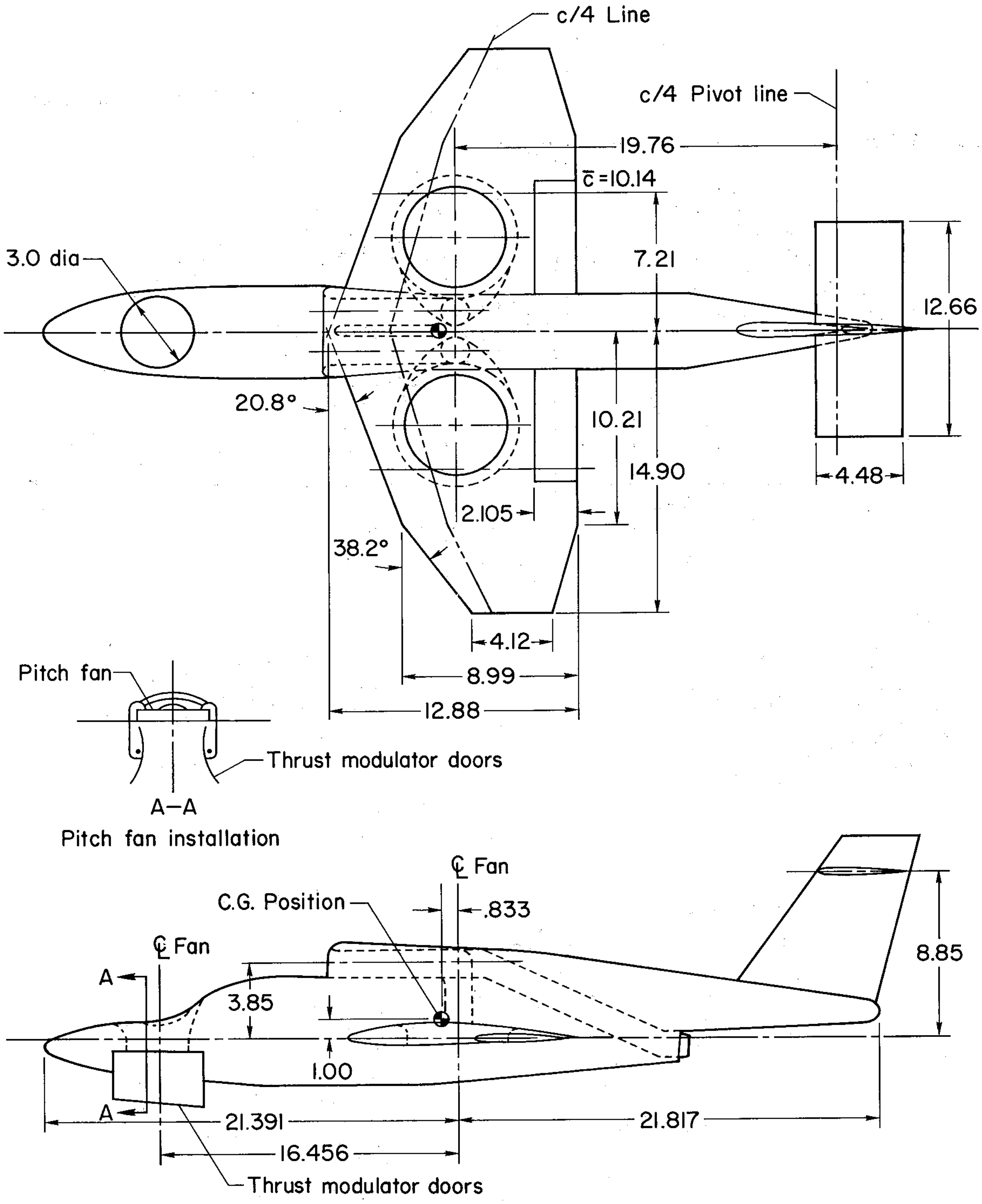

	Wing	Horizontal tail
Area	285.6	56.7
Aspect ratio	3.11	2.82
Taper ratio	.32	1.00
Airfoil section	65-210 (Mod.)	63-009

All dimensions in feet unless otherwise noted

Figure 2.- Geometric characteristics of the model.

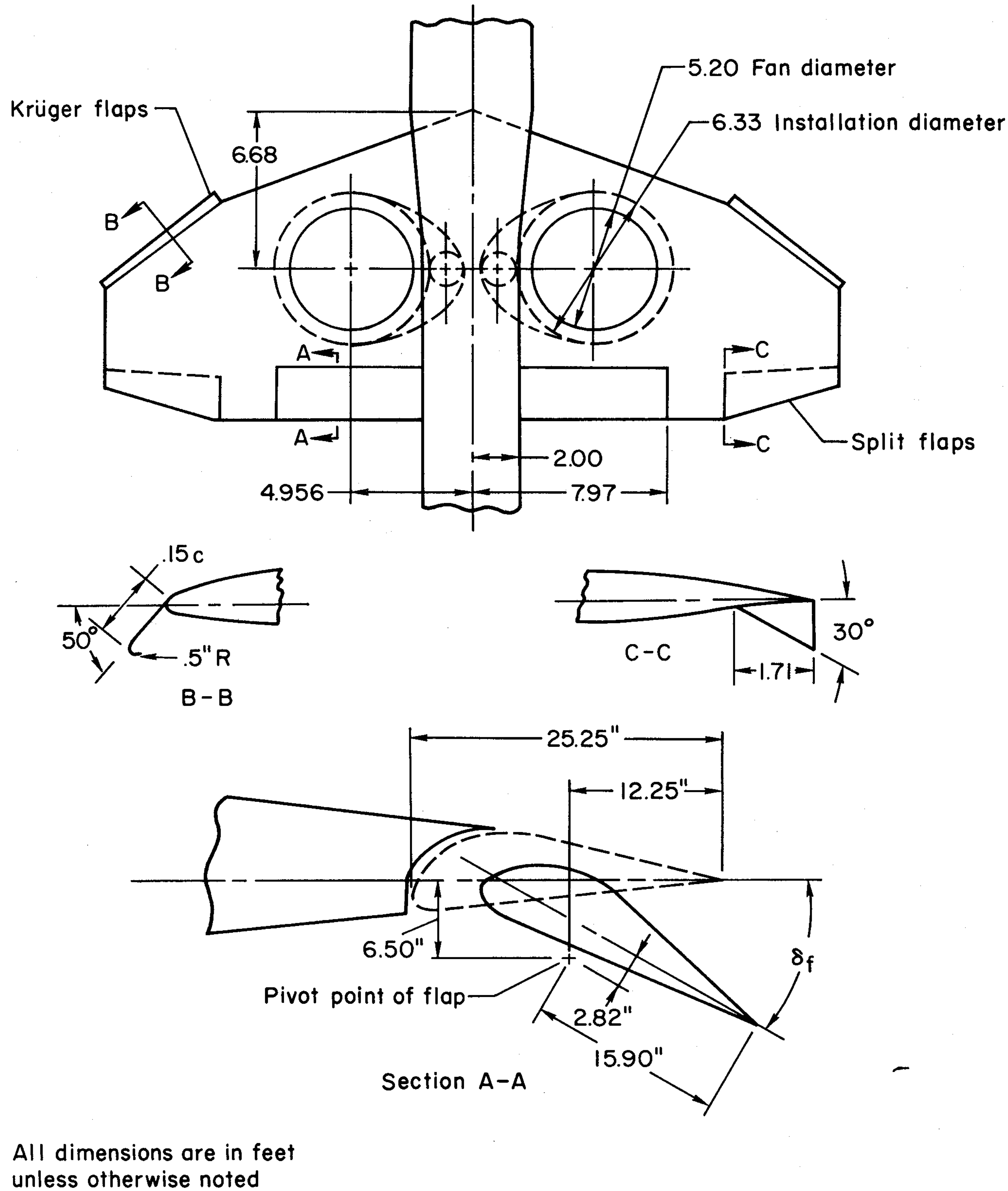

Figure 3.- Details of the high lift devices and location of the lift fans.

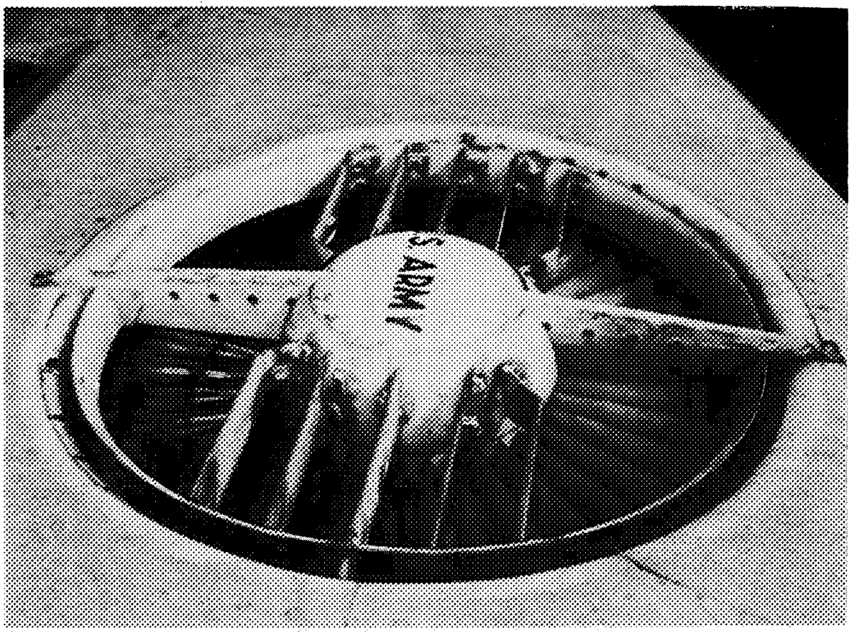

A-30114-1

Inlet covers removed.

Inlet covers installed.

(a) Photographs of the lift-fan inlet.

Figure 4.- Details of the lift-fan installation.

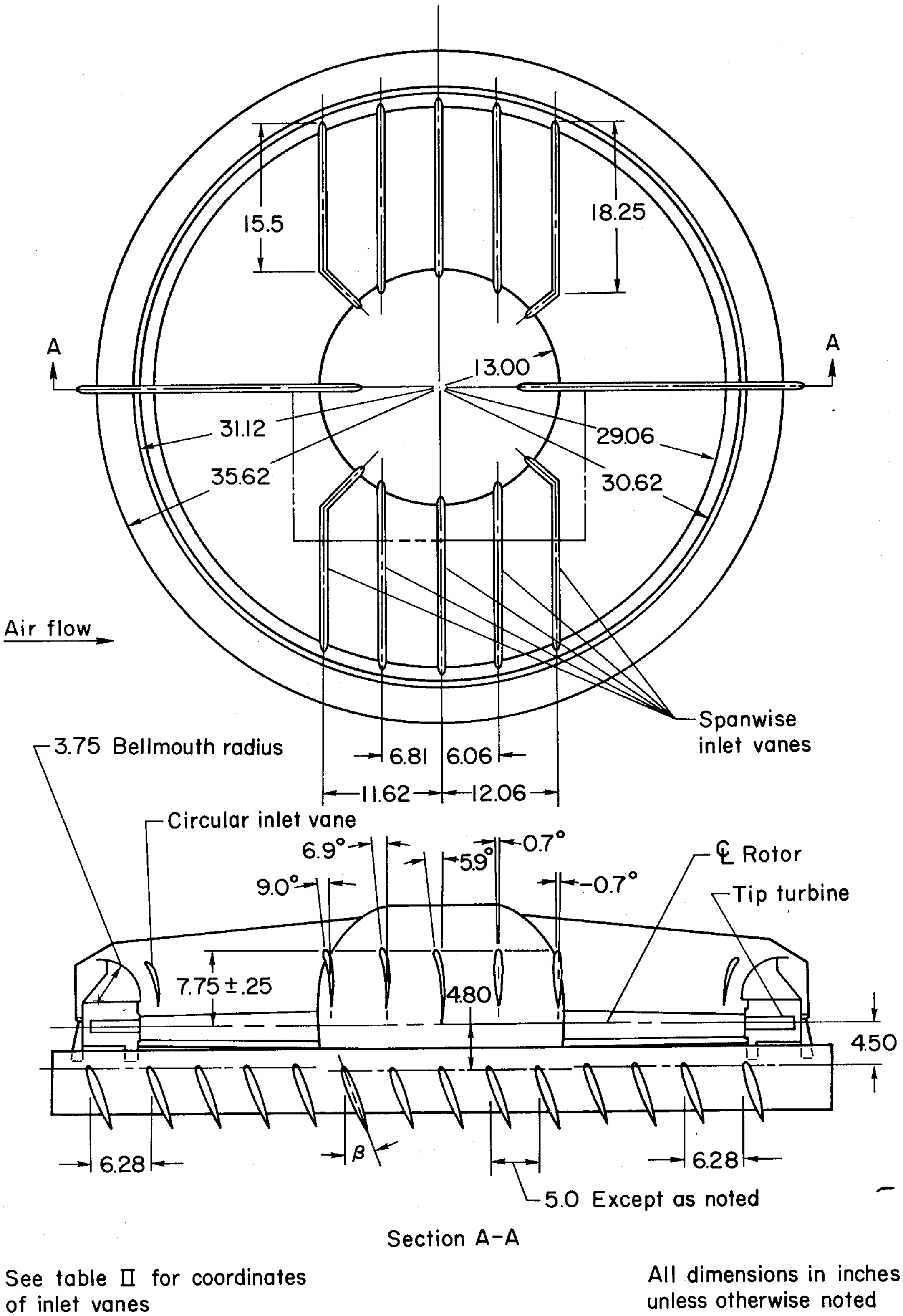

(b) Details of the fan inlet.

Figure 4.- Continued.

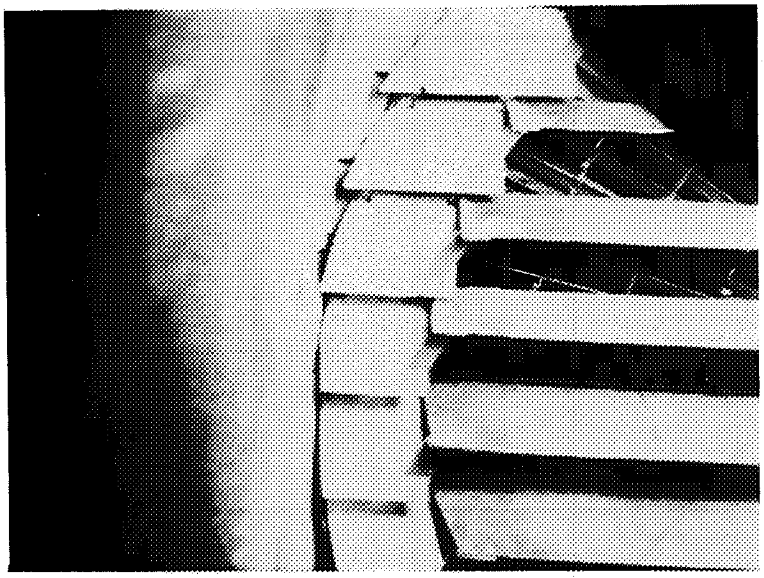

Underside of fan.

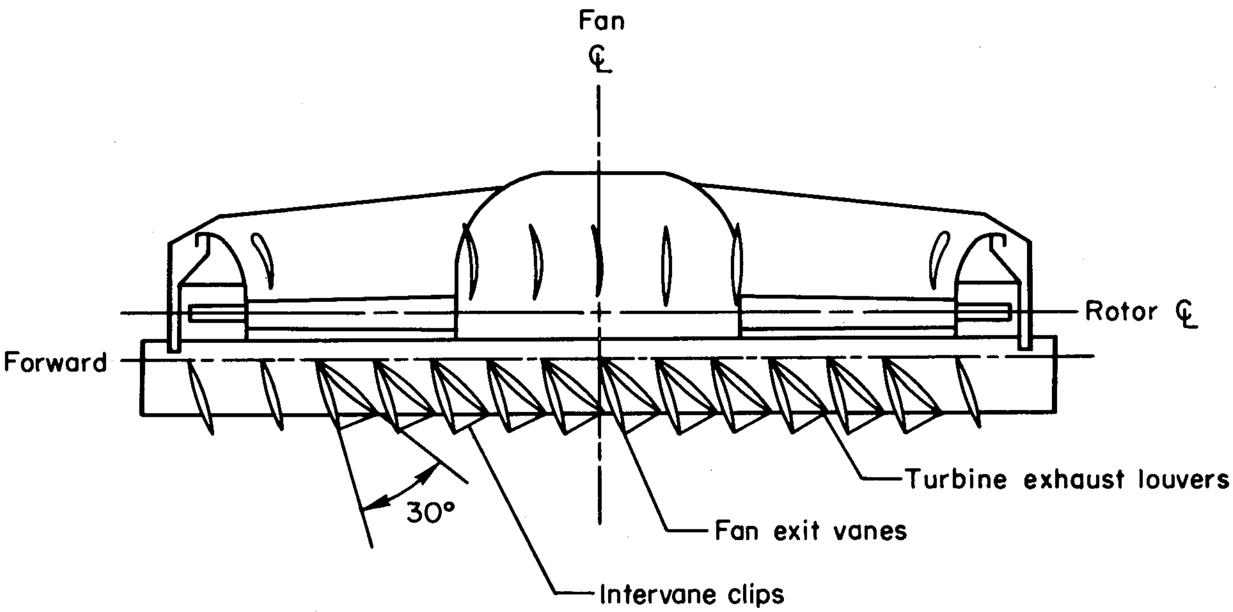

(c) Staggered louvers.

Figure 4.- Concluded.

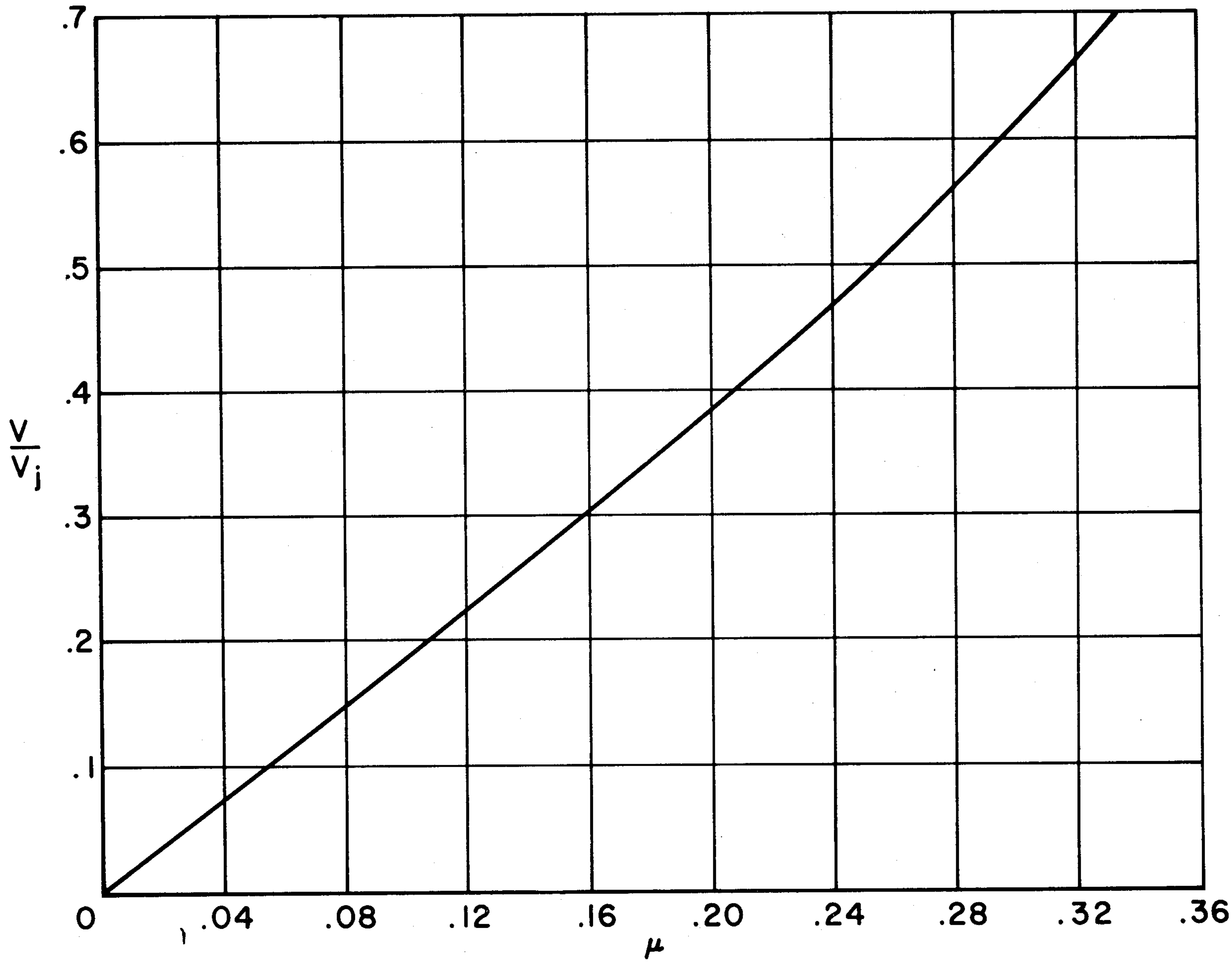

Figure 5.- The variation of average velocity ratio with tip-speed ratio; $\beta = 0^{\circ}$.

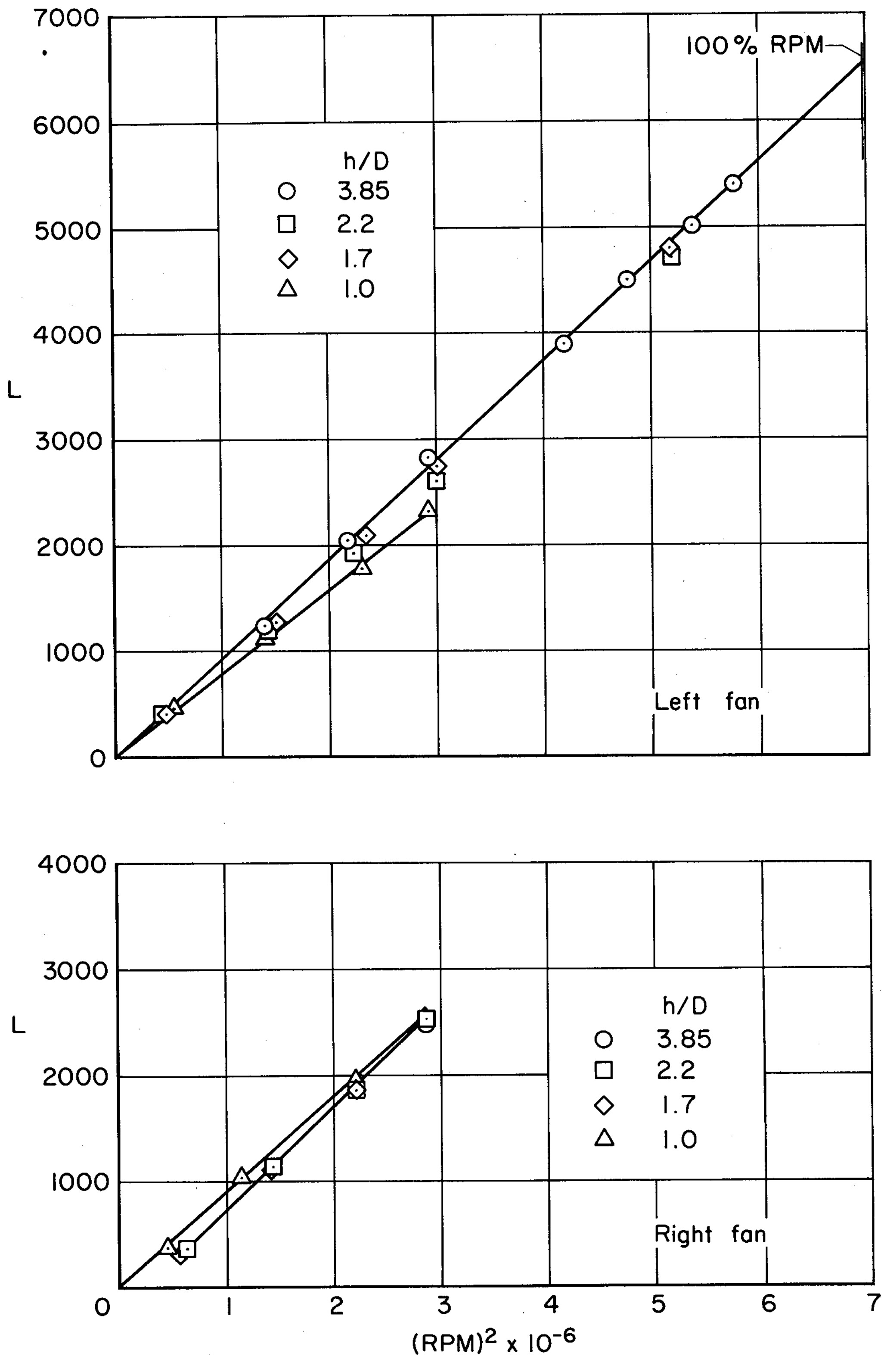

(a) Lift with individual fans operating.

Figure 6.- Zero airspeed performance of the model; $\alpha = 0^{\circ}$, $\beta = 0^{\circ}$.

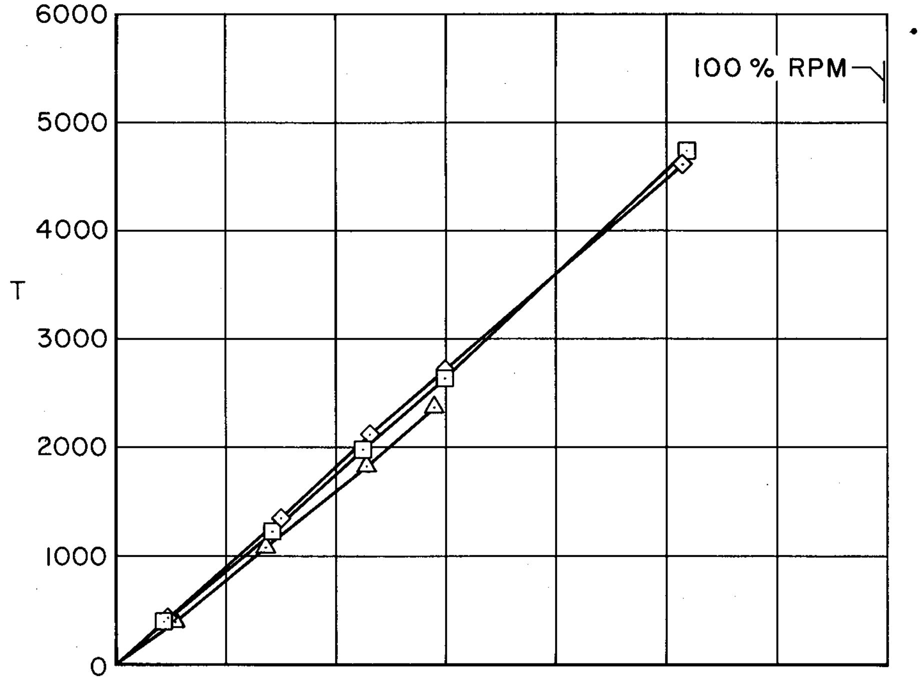

(b) Thrust of the left fan.

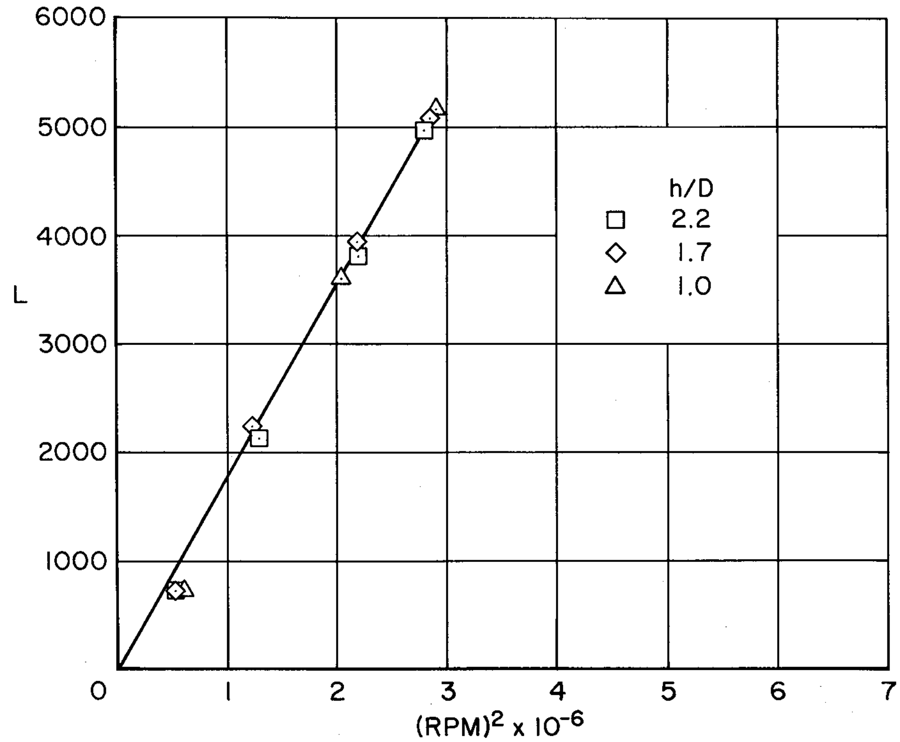

(c) Total lift with both fans operating.

Figure 6.- Concluded.

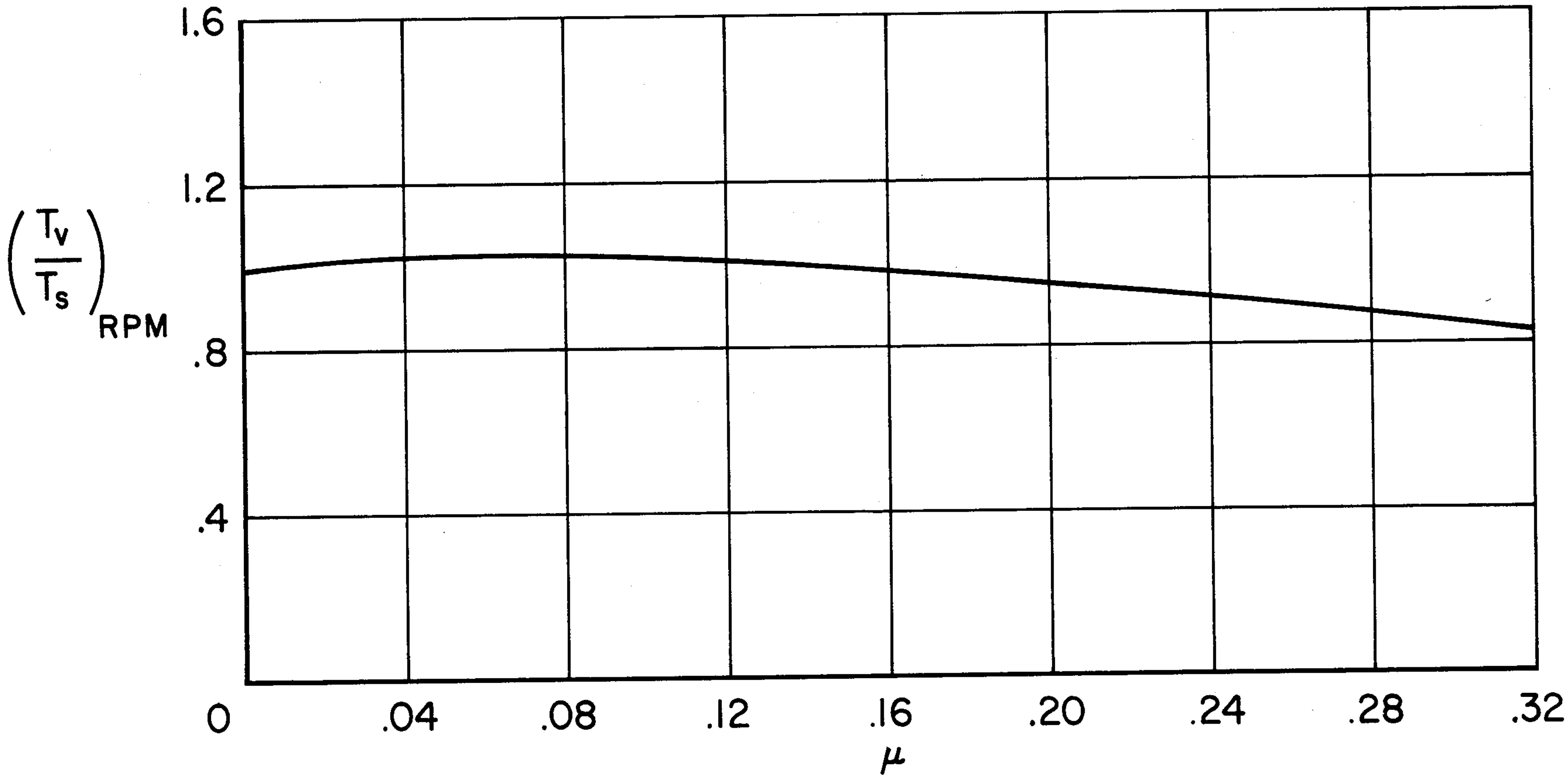

Figure 7.- The effect of forward speed (tip-speed ratio) on average fan thrust; $\alpha = 0^{\circ}$, $\beta = 0^{\circ}$, 1700 RPM.

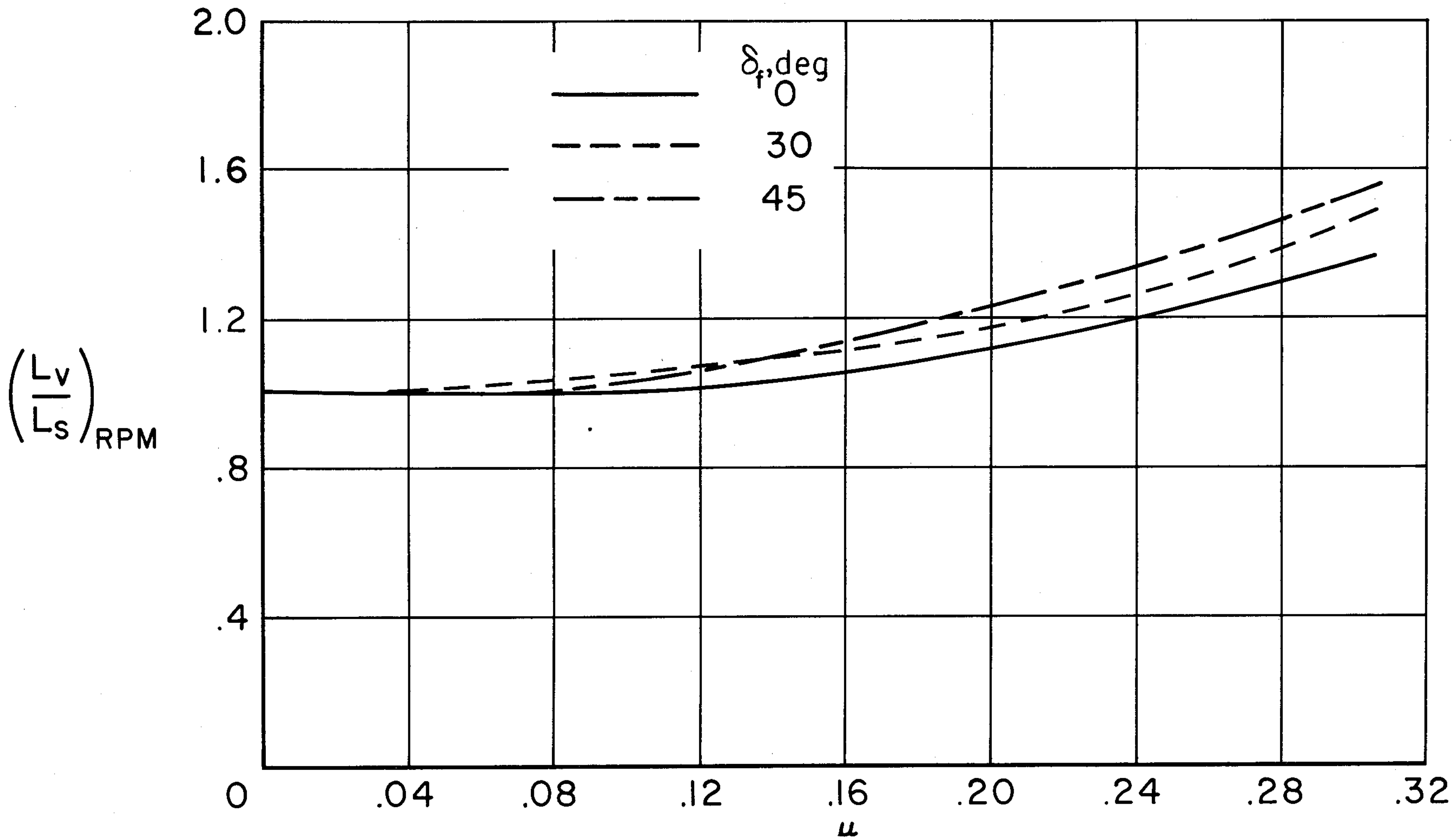

(a) Effect of trailing-edge flap deflection; h/D = 3.85, tail off.

Figure 8.- The effect of forward speed and fan RPM (tip-speed ratio) on lift at constant fan RPM; $\alpha = 0^{\circ}$, $\beta = 0^{\circ}$, 1700 RPM.

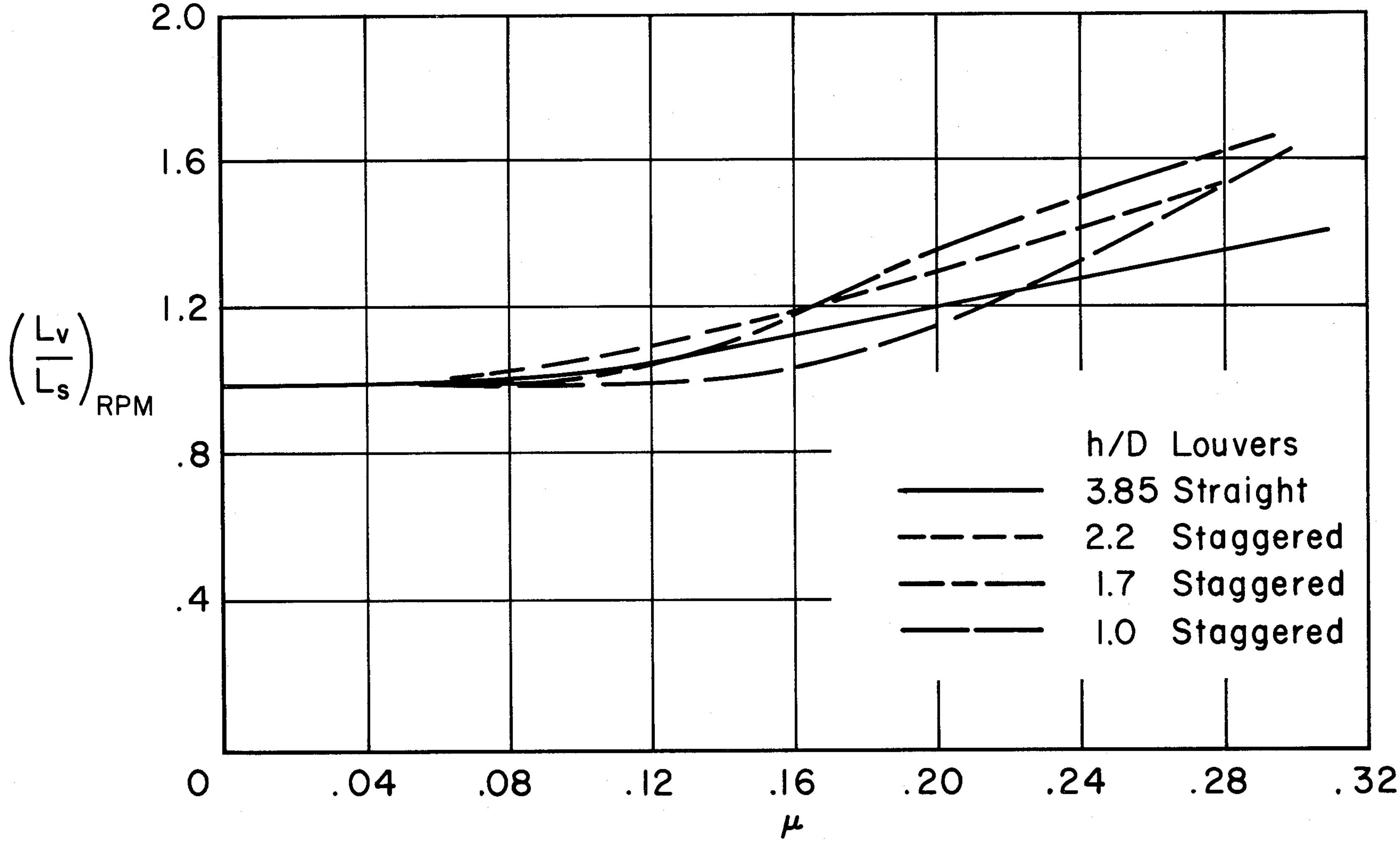

(b) Effect of ground height; tail on, $\delta_f = 45^\circ$.

Figure 8.- Concluded.

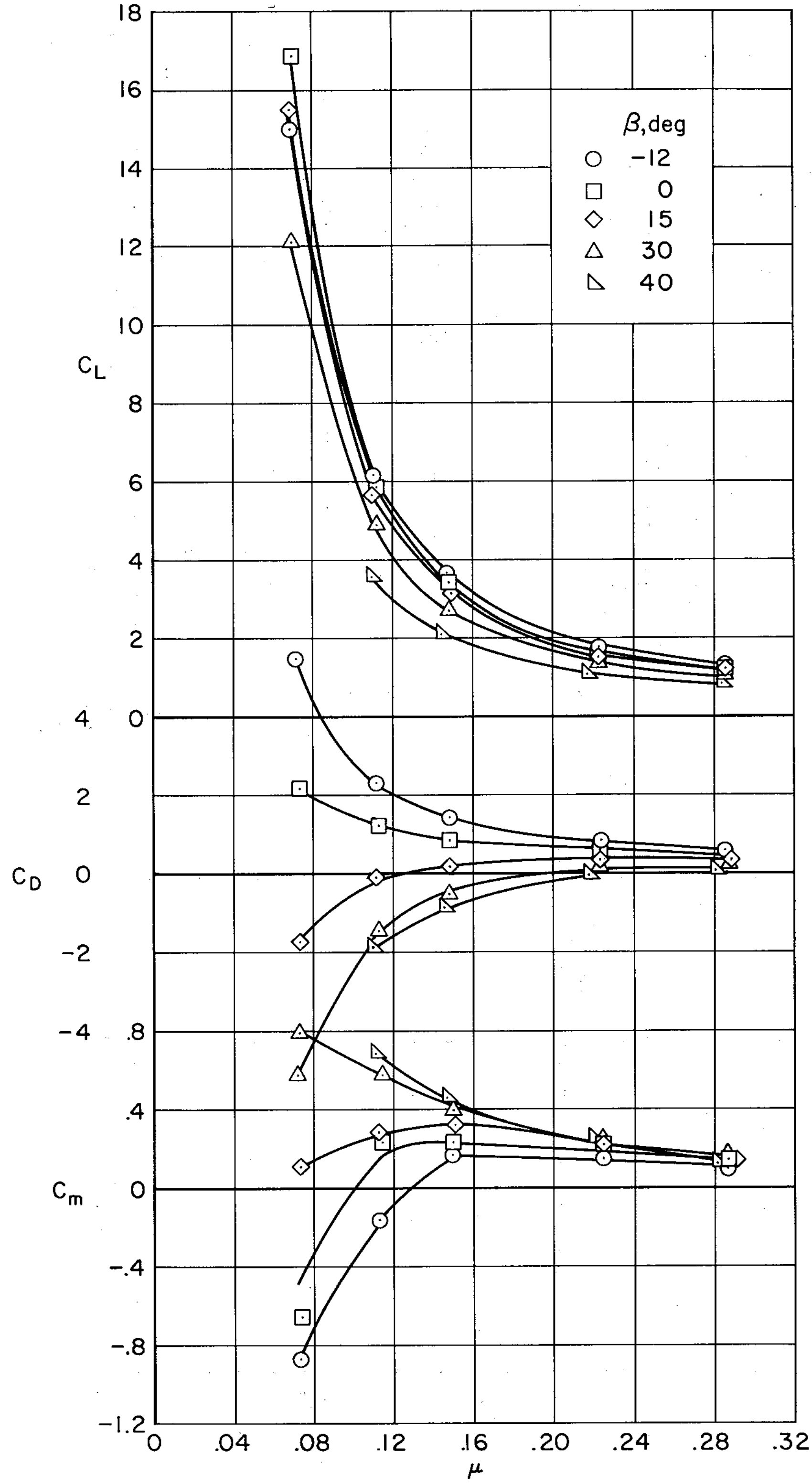

(a) Tail off, $\delta_f = 0^{\circ}$.

Figure 9.- Variation of longitudinal characteristics with tip-speed ratio; $h/D = 3.85$, $\alpha = 0^{\circ}$, straight louvers, 1700 RPM.

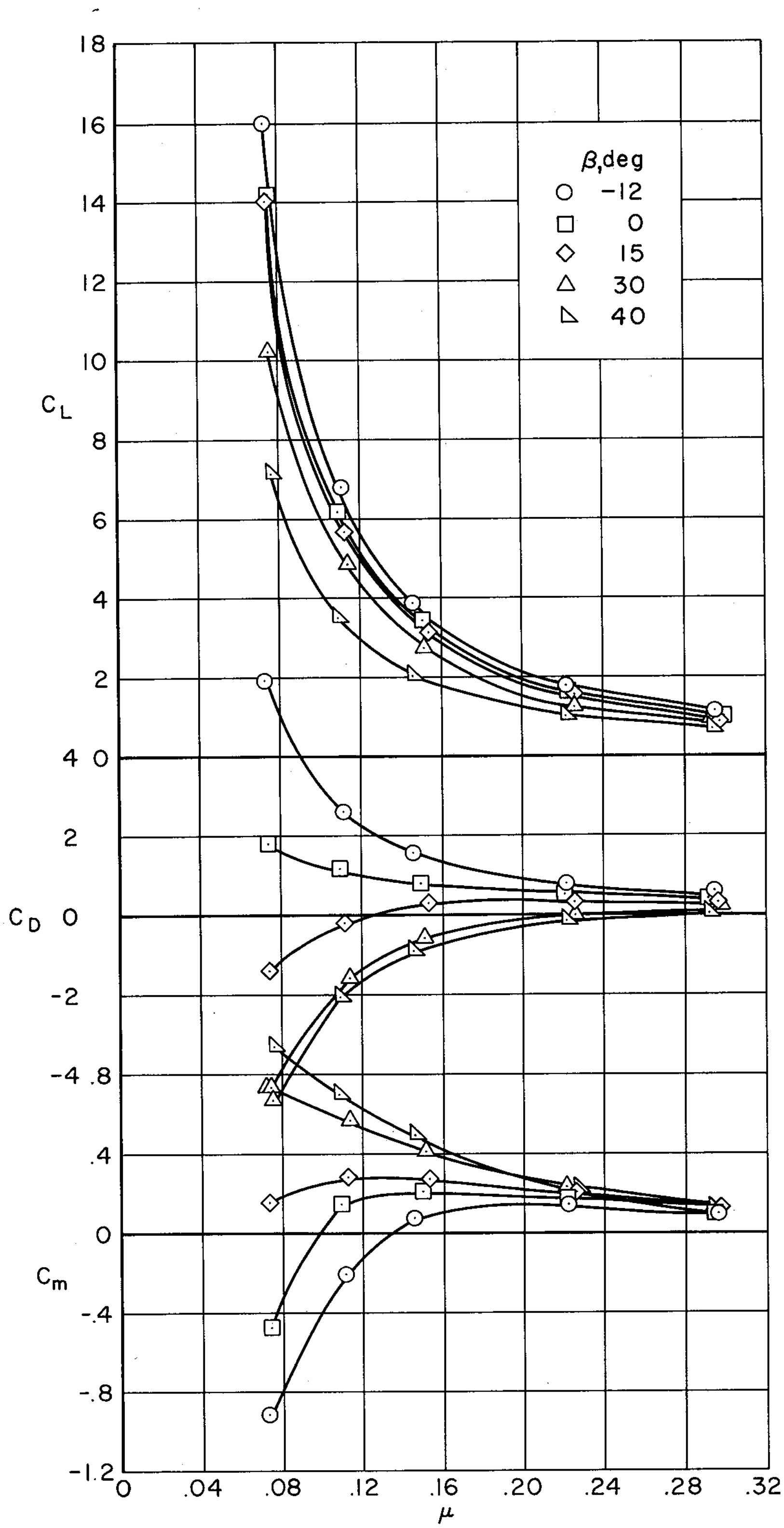

(b) Tail off, $\delta_f = 0^{\circ}$, inlet covers off.

Figure 9.- Continued.

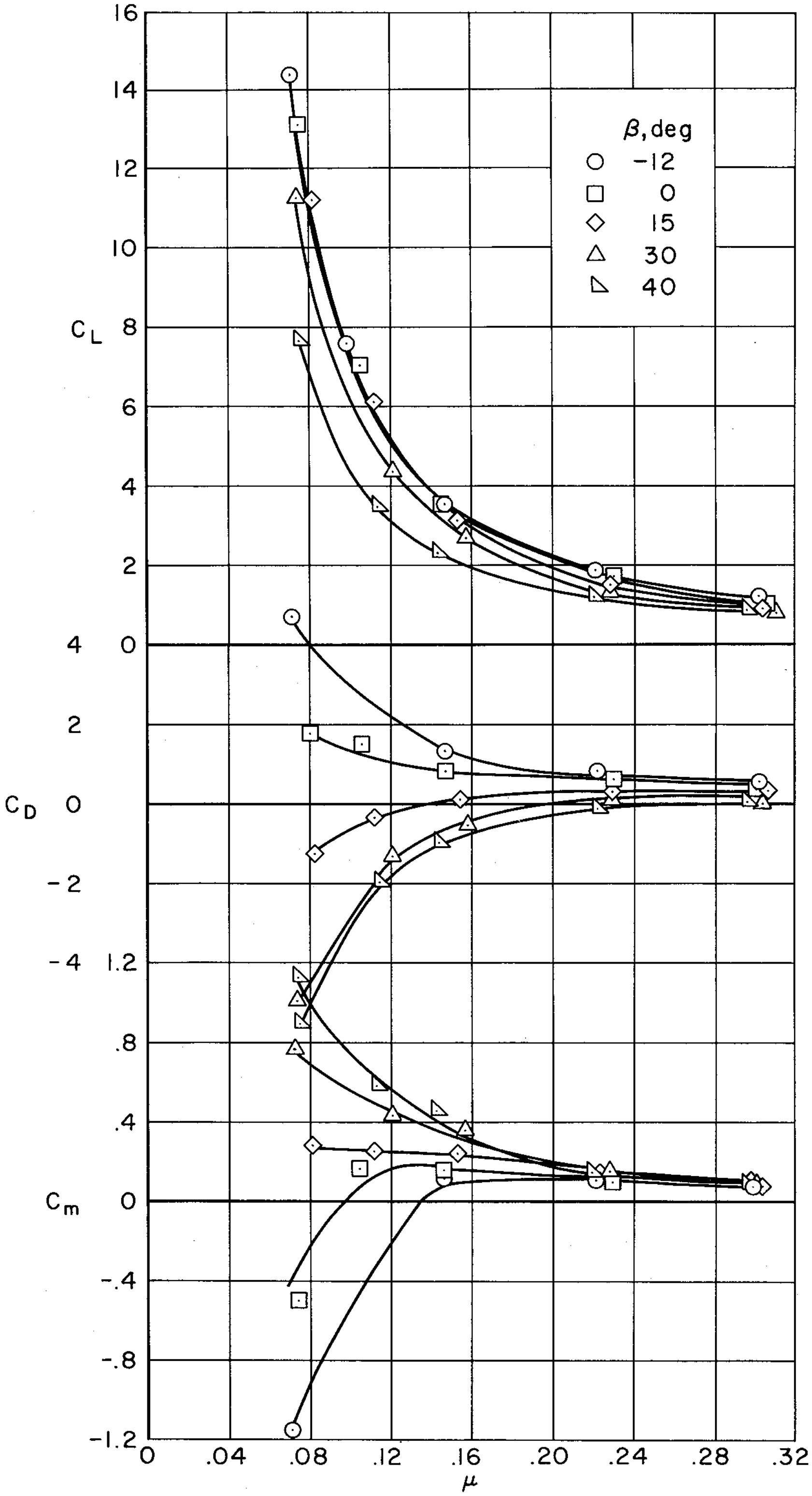

(c) Tail off, $\delta_f = 30^o$.

Figure 9.- Continued.

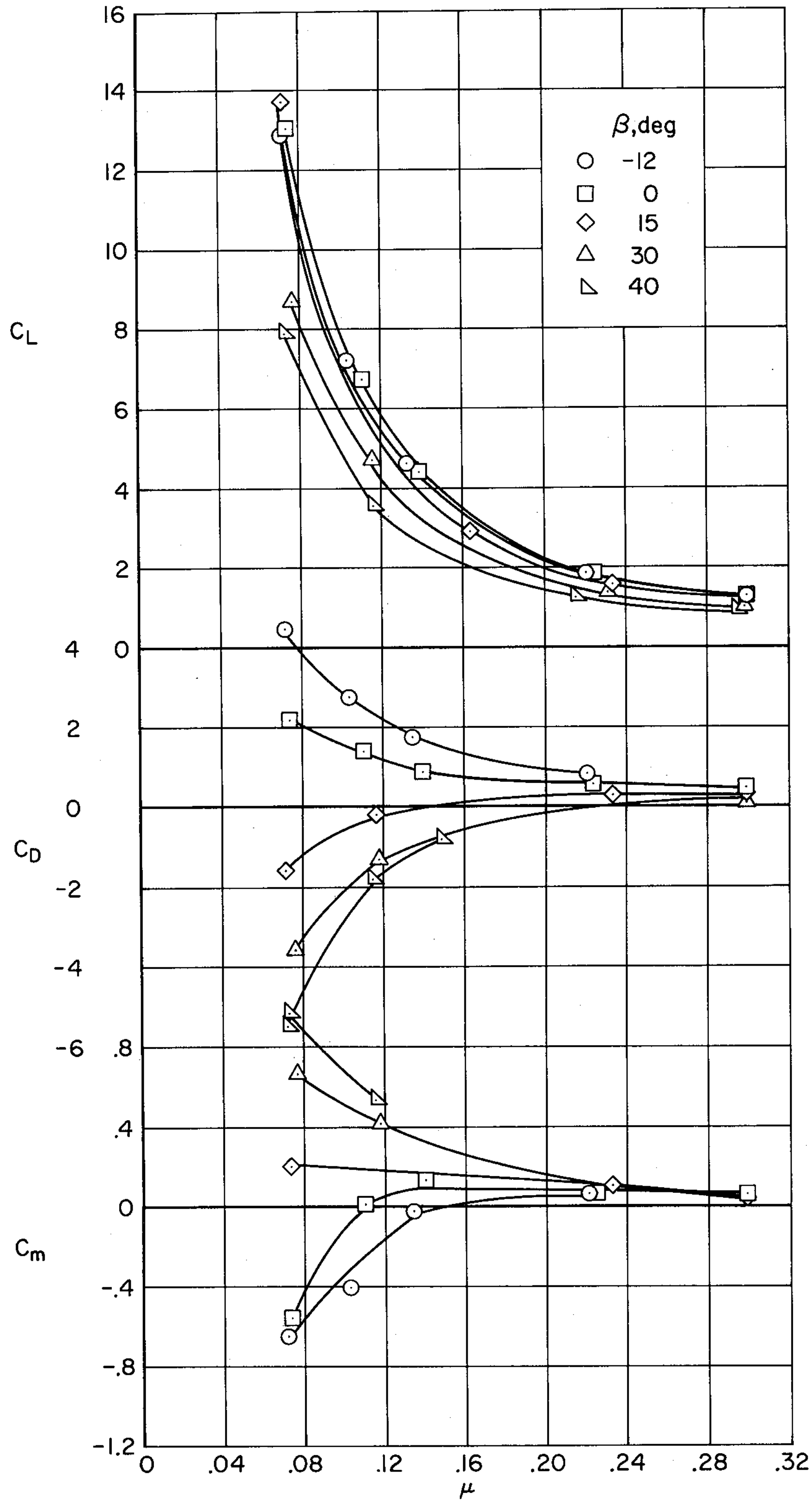

(d) Tail off, $\delta_f = 45^\circ$.

Figure 9.- Continued.

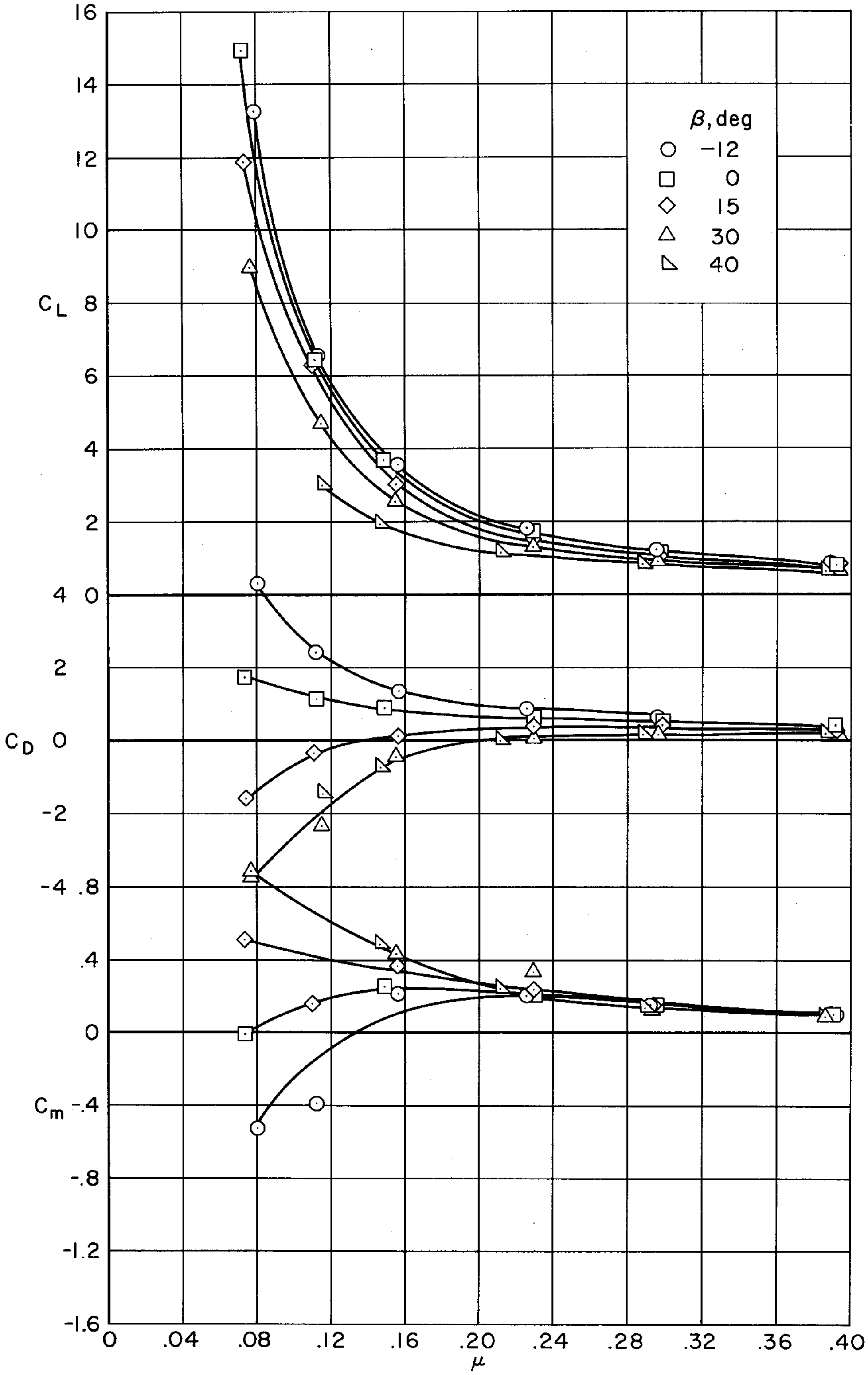

(e) Tail on, $\delta_f = 45^\circ$.

Figure 9.- Concluded.

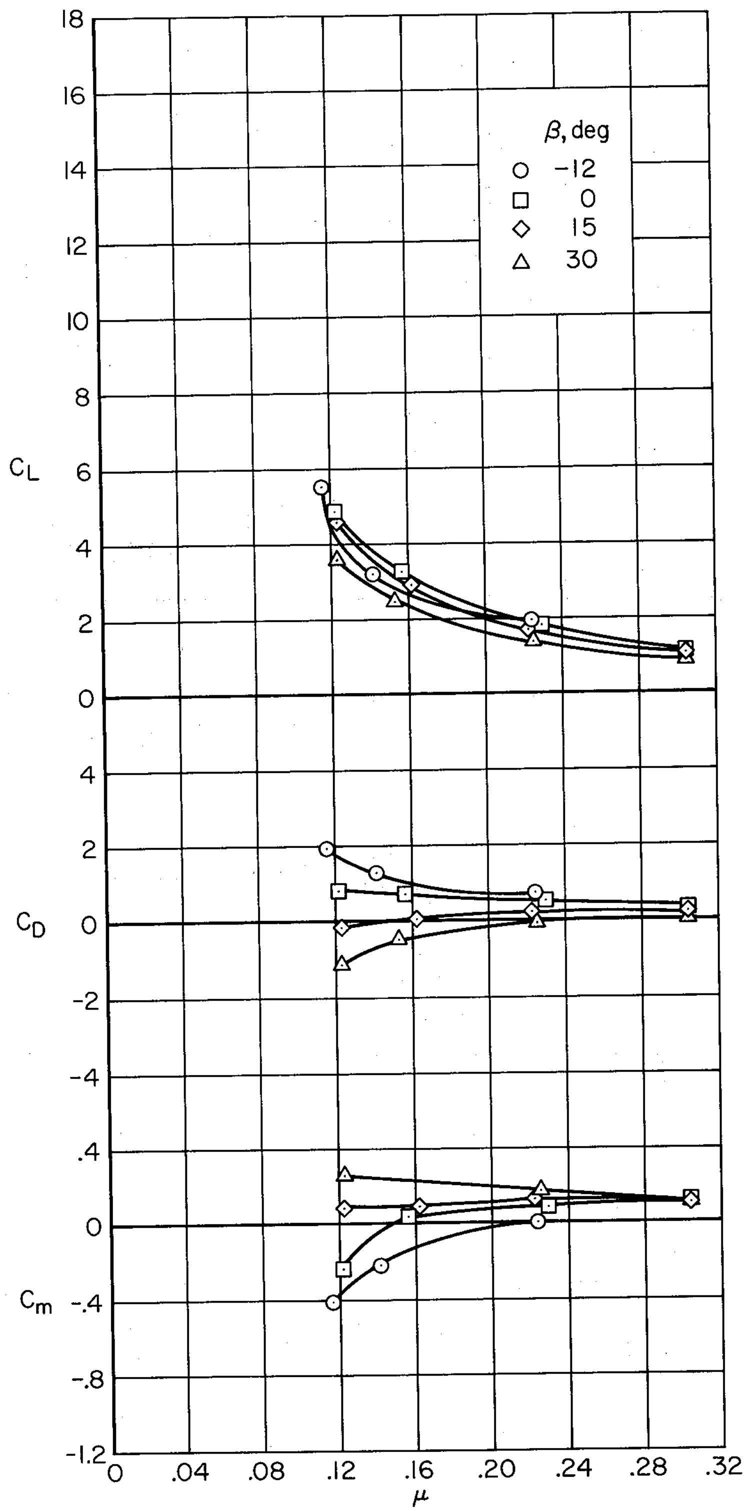

(a) Tail off, staggered louvers, inlet covers off.

Figure 10.- Variation of longitudinal characteristics with tip-speed ratio; $h/D = 2.2$, $\alpha = 0^\circ$, $\delta_f = 45^\circ$, 1700 RPM.

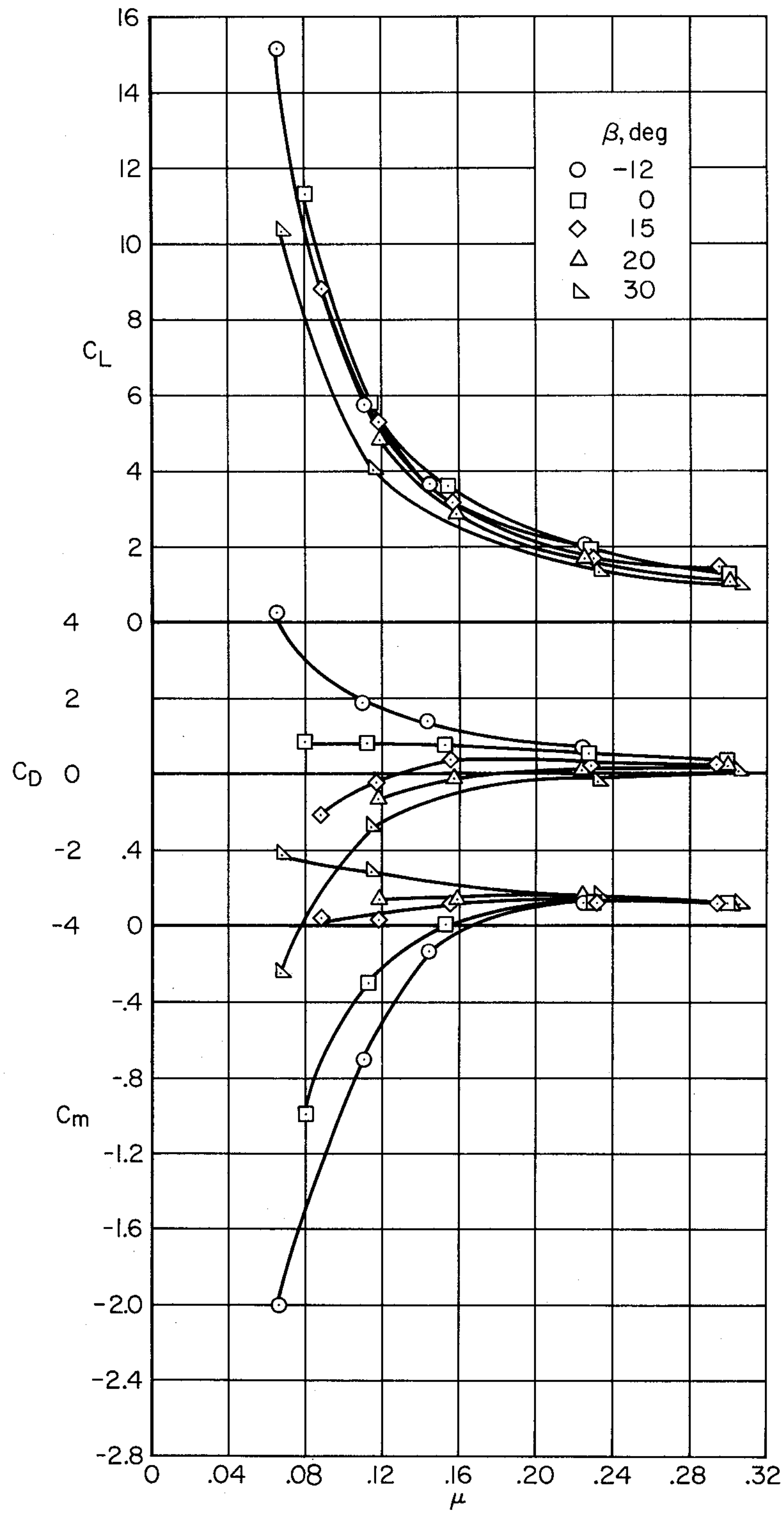

(b) Tail off, staggered louvers, inlet covers on.

Figure 10.- Continued.

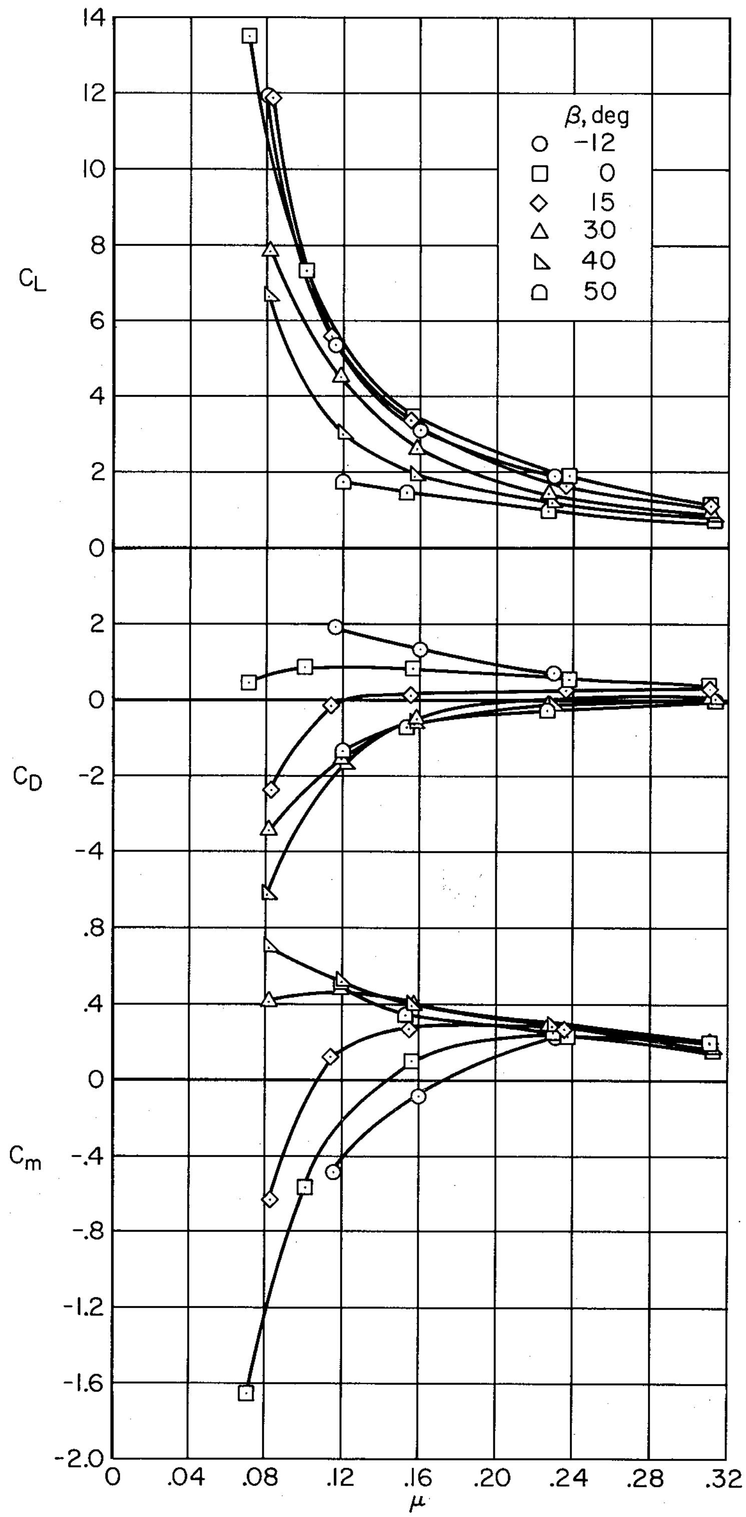

(c) Tail on, straight louvers.

Figure 10.- Continued.

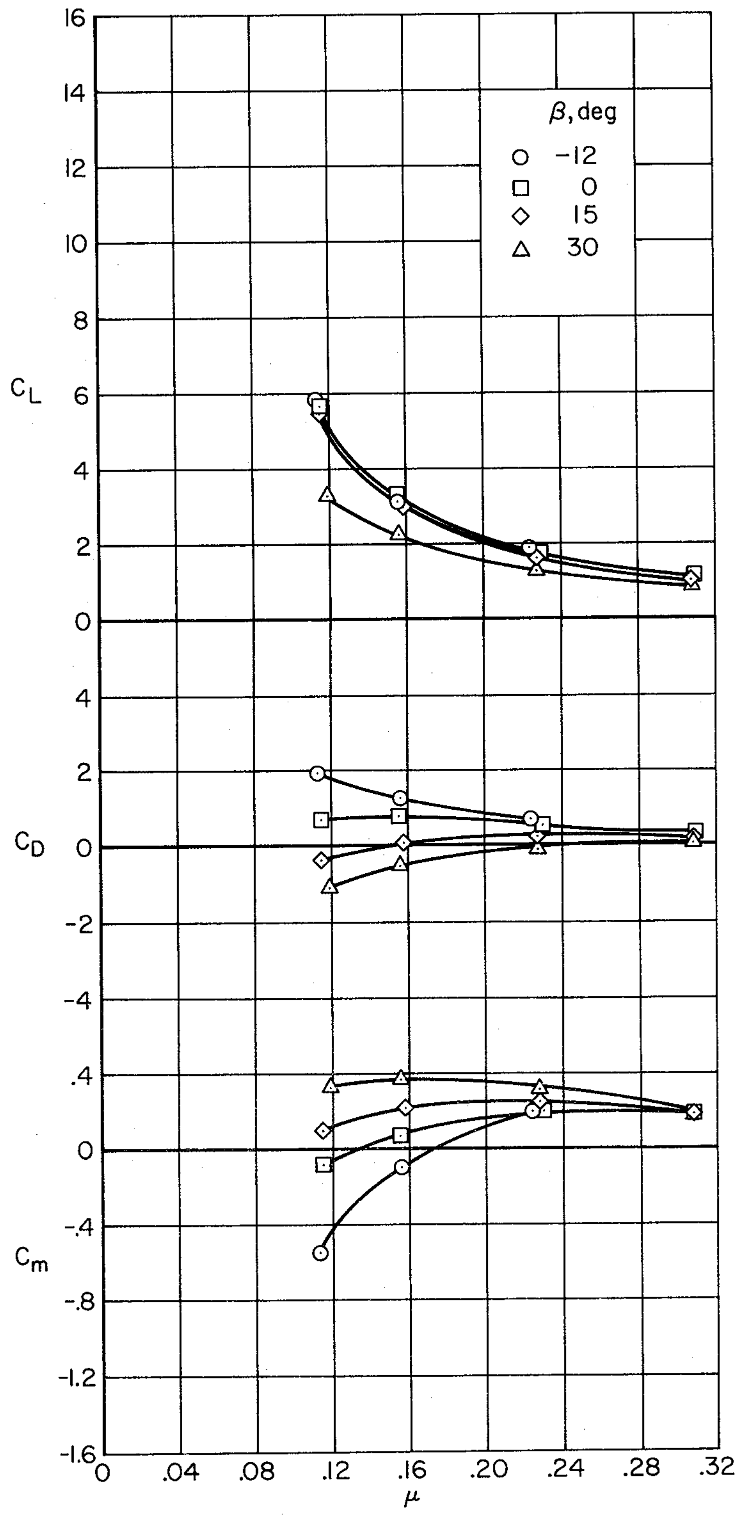

(d) Tail on, staggered louvers.

Figure 10.- Continued.

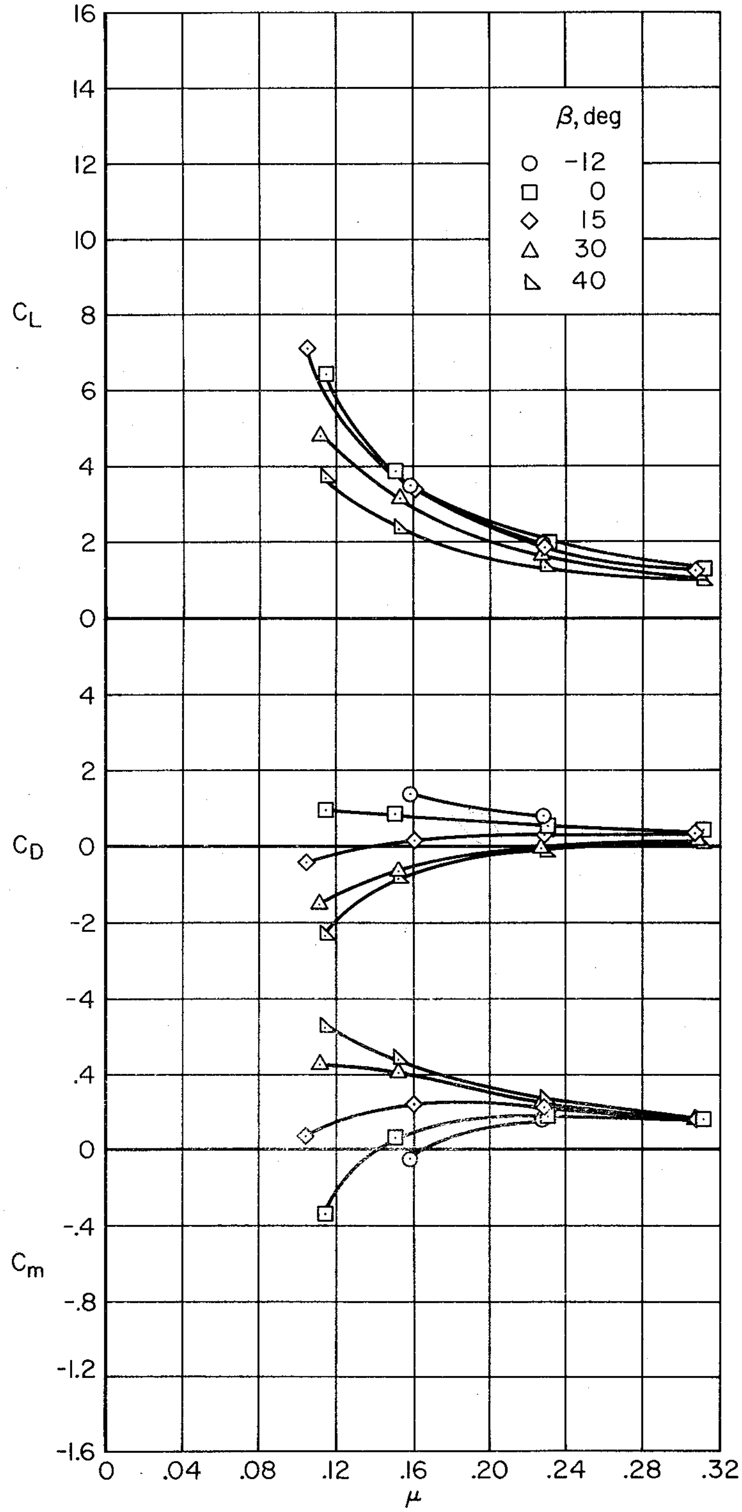

(e) Tail on, straight louvers, split flaps.

Figure 10.- Concluded.

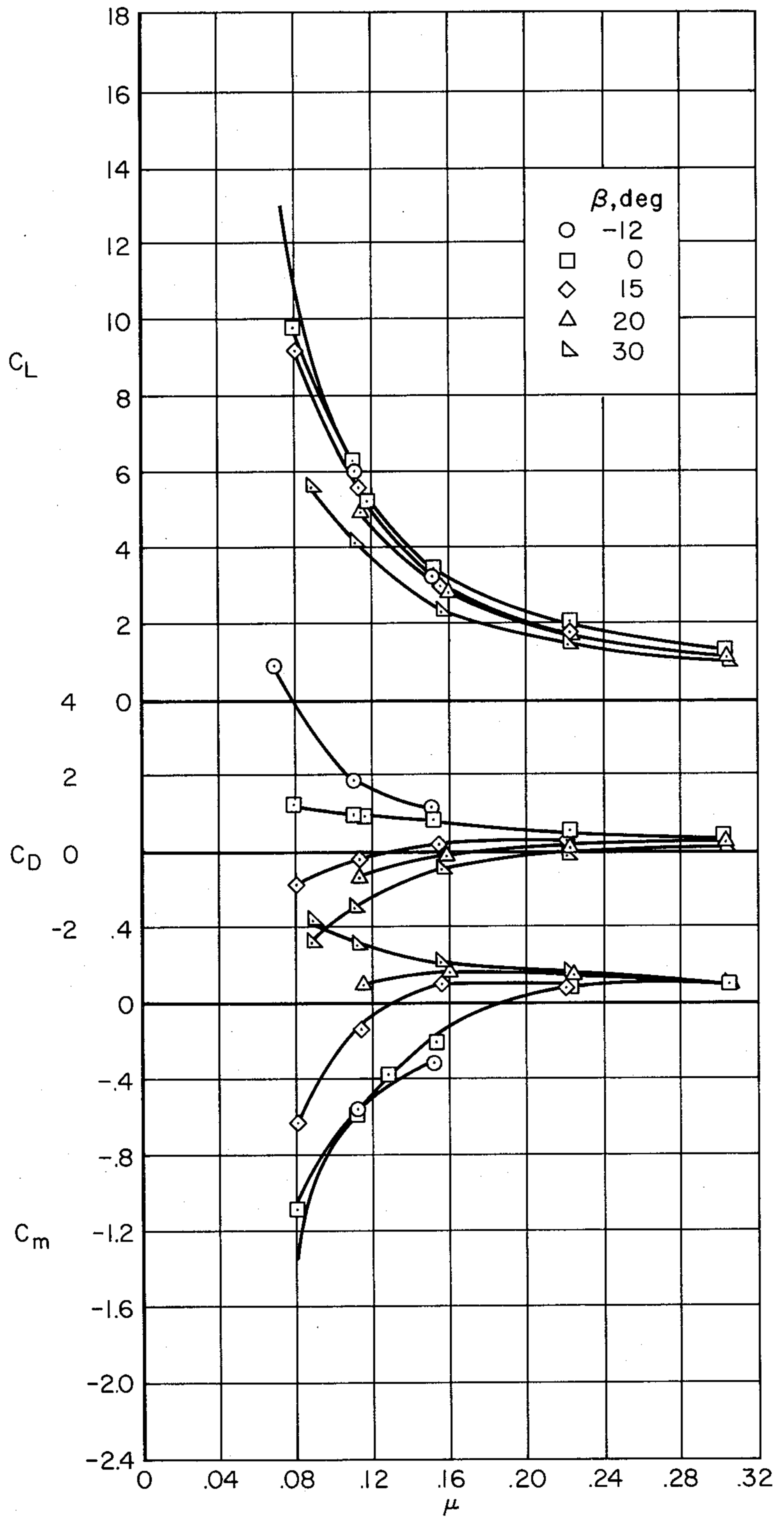

(a) Tail off, staggered louvers.

Figure 11.- Variation of longitudinal characteristics with tip-speed ratio; $h/D = 1.7$, $\alpha = 0^{\circ}$, $\delta_f = 45^{\circ}$, 1700 RPM.

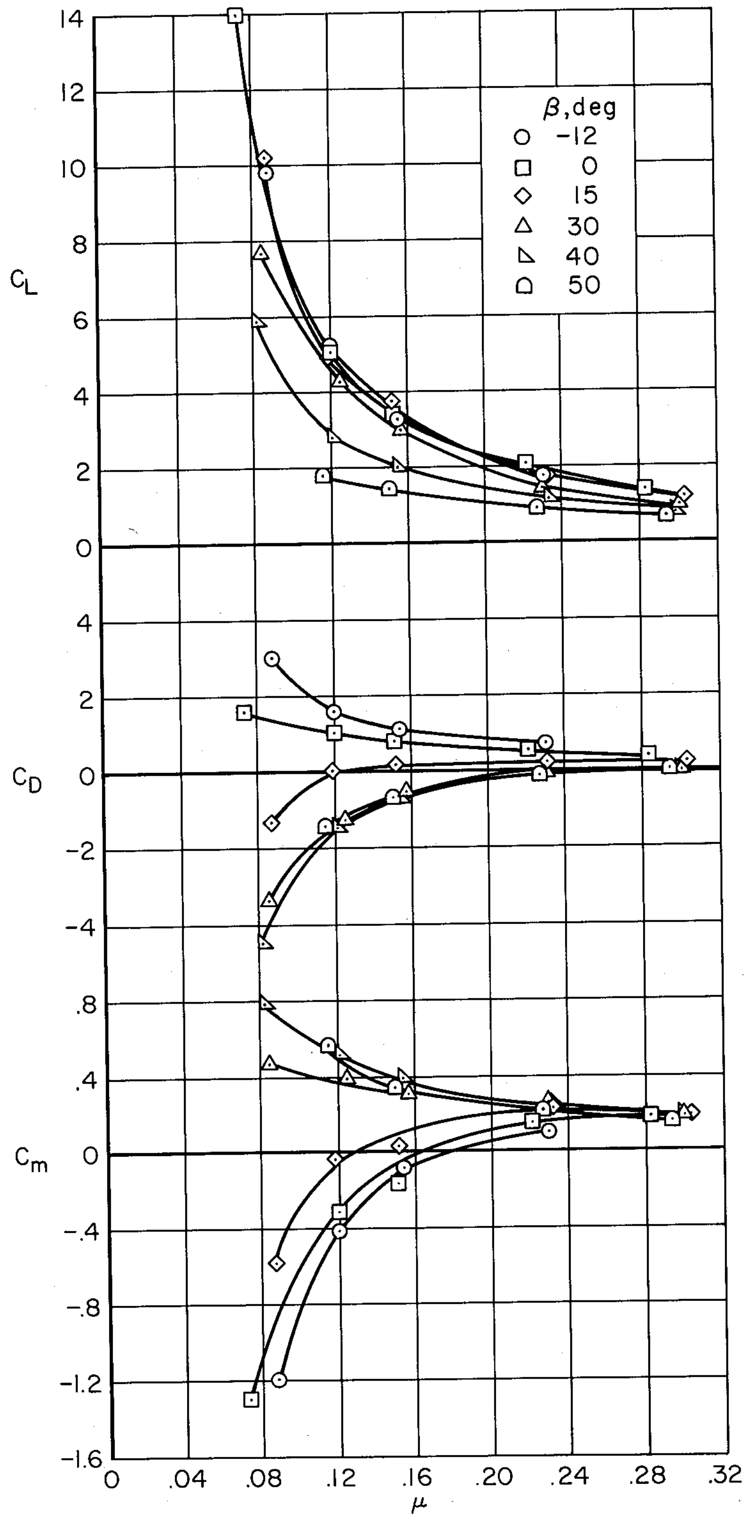

(b) Tail on, straight louvers.

Figure 11.- Continued.

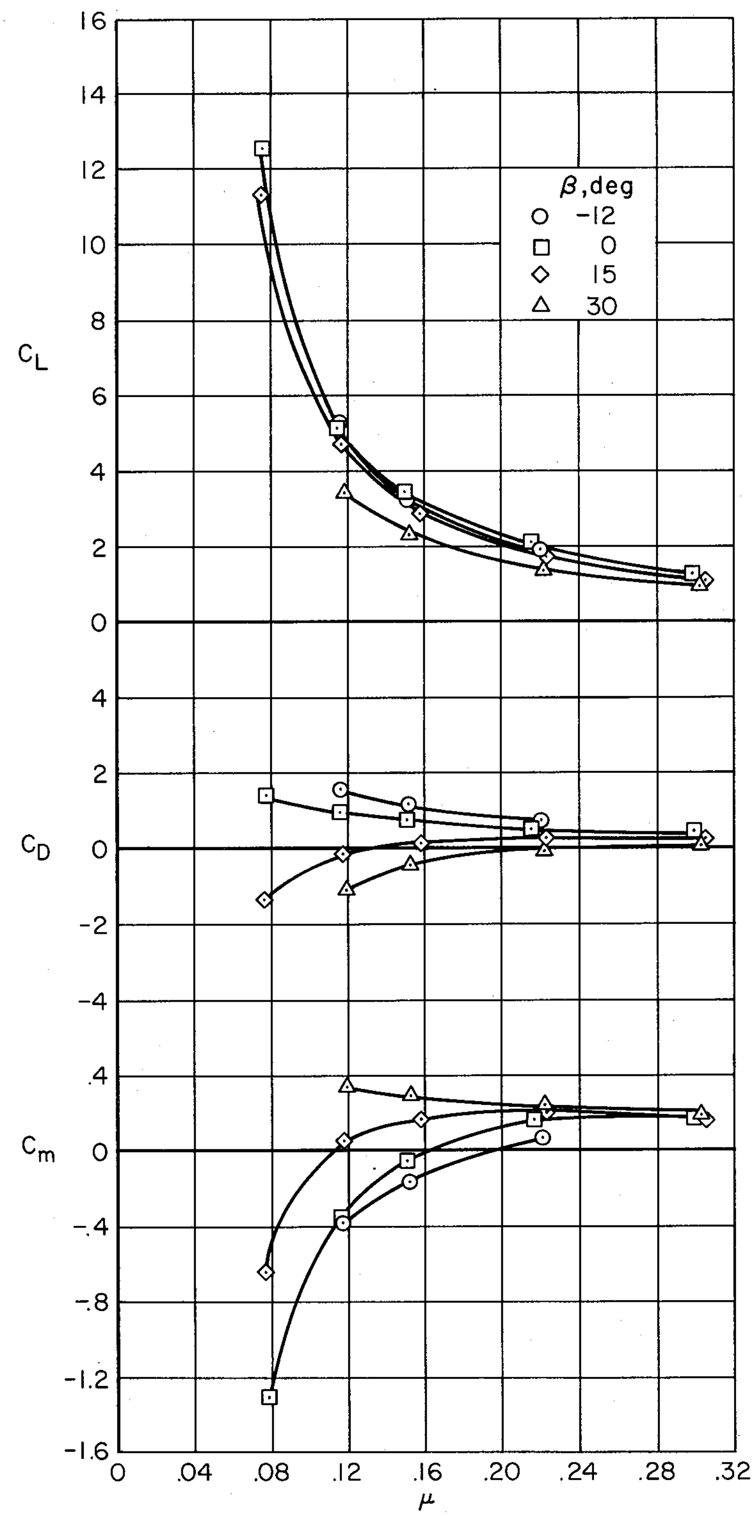

(c) Tail on, staggered louvers.

Figure 11.- Concluded.

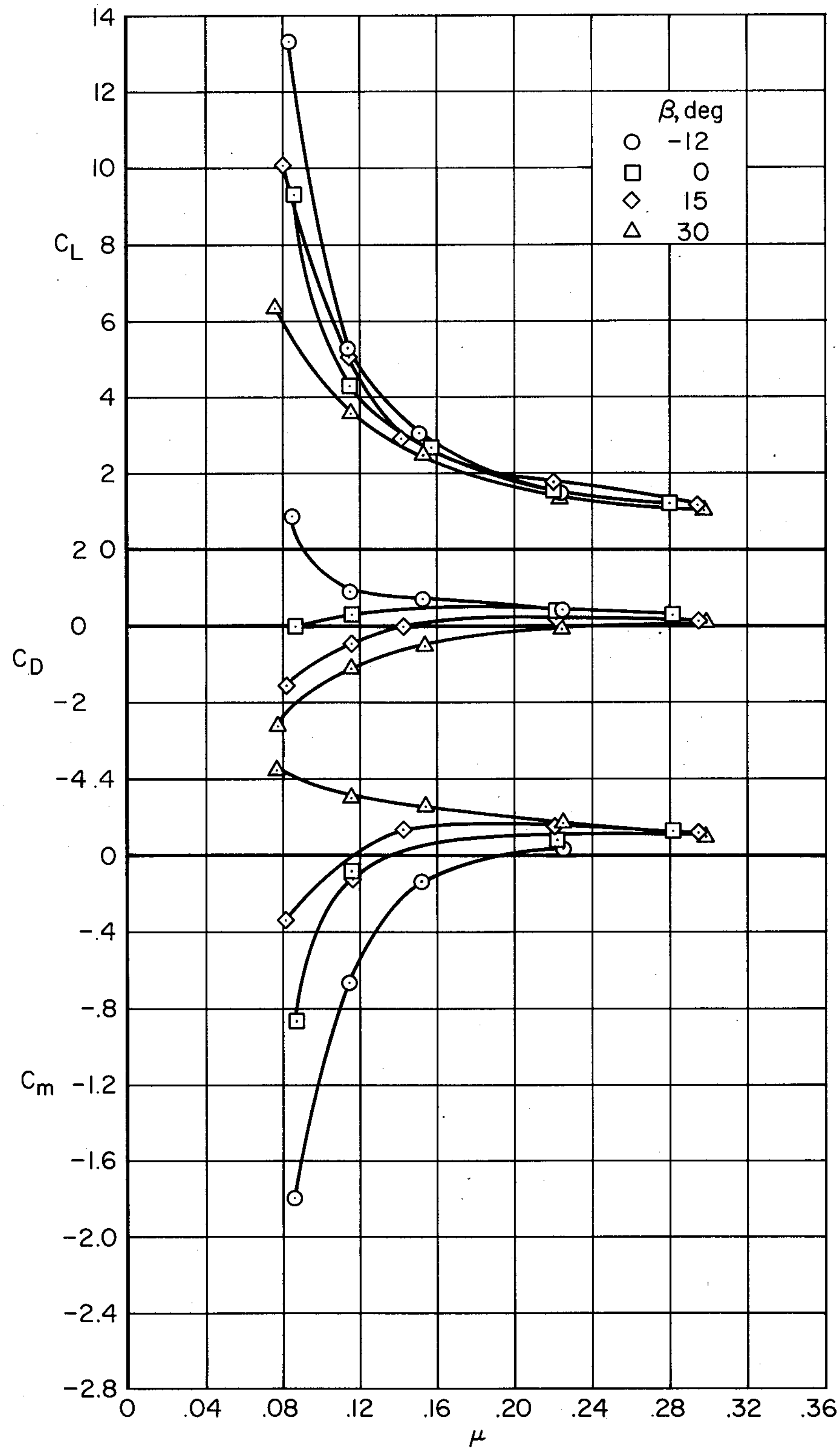

(a) Tail off, staggered louvers, inlet covers off.

Figure 12.- Variation of longitudinal characteristics with tip-speed ratio; $h/D = 1.0$, $\alpha = 0^{\circ}$, $\delta_f = 45^{\circ}$, 1700 RPM.

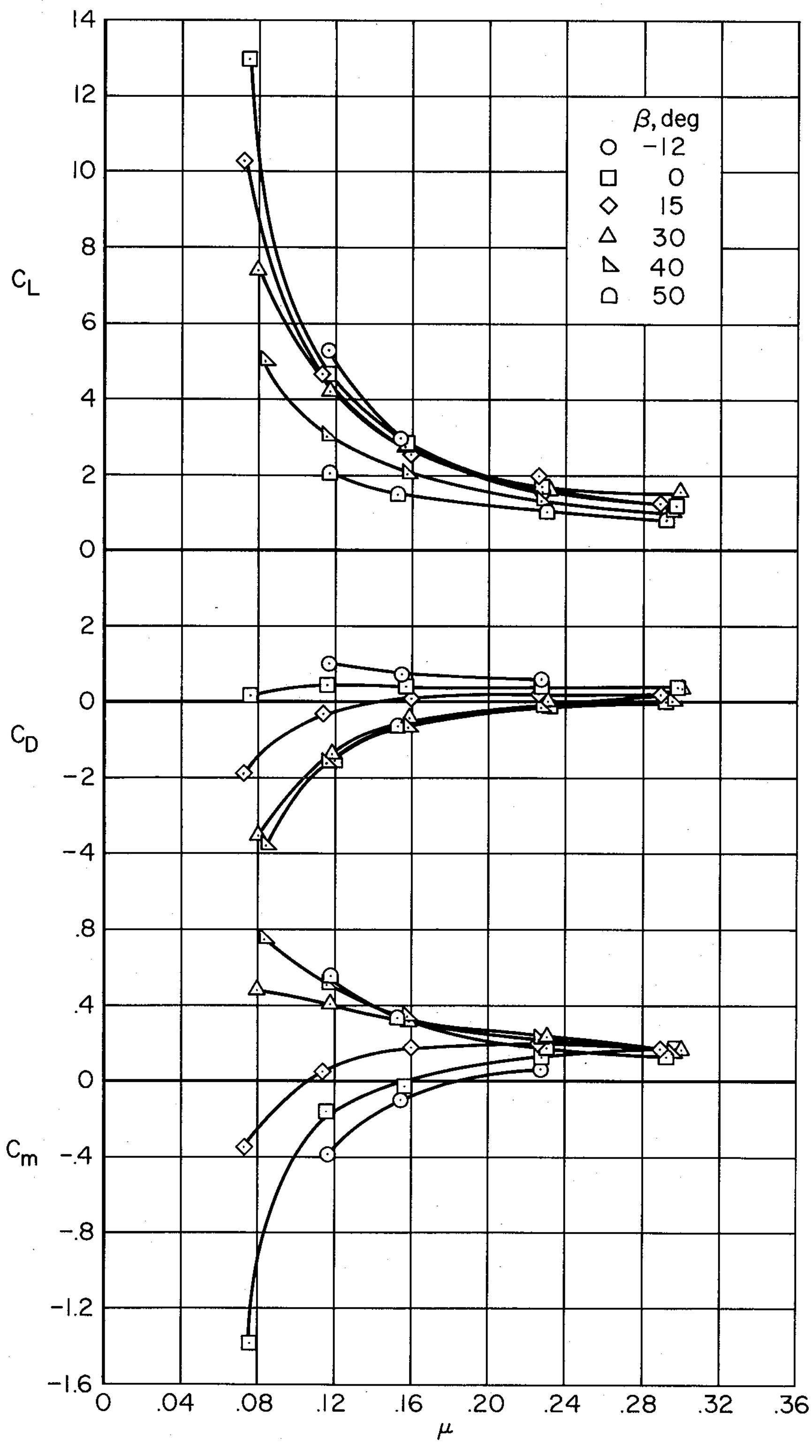

(b) Tail on, straight louvers.

Figure 12.- Continued.

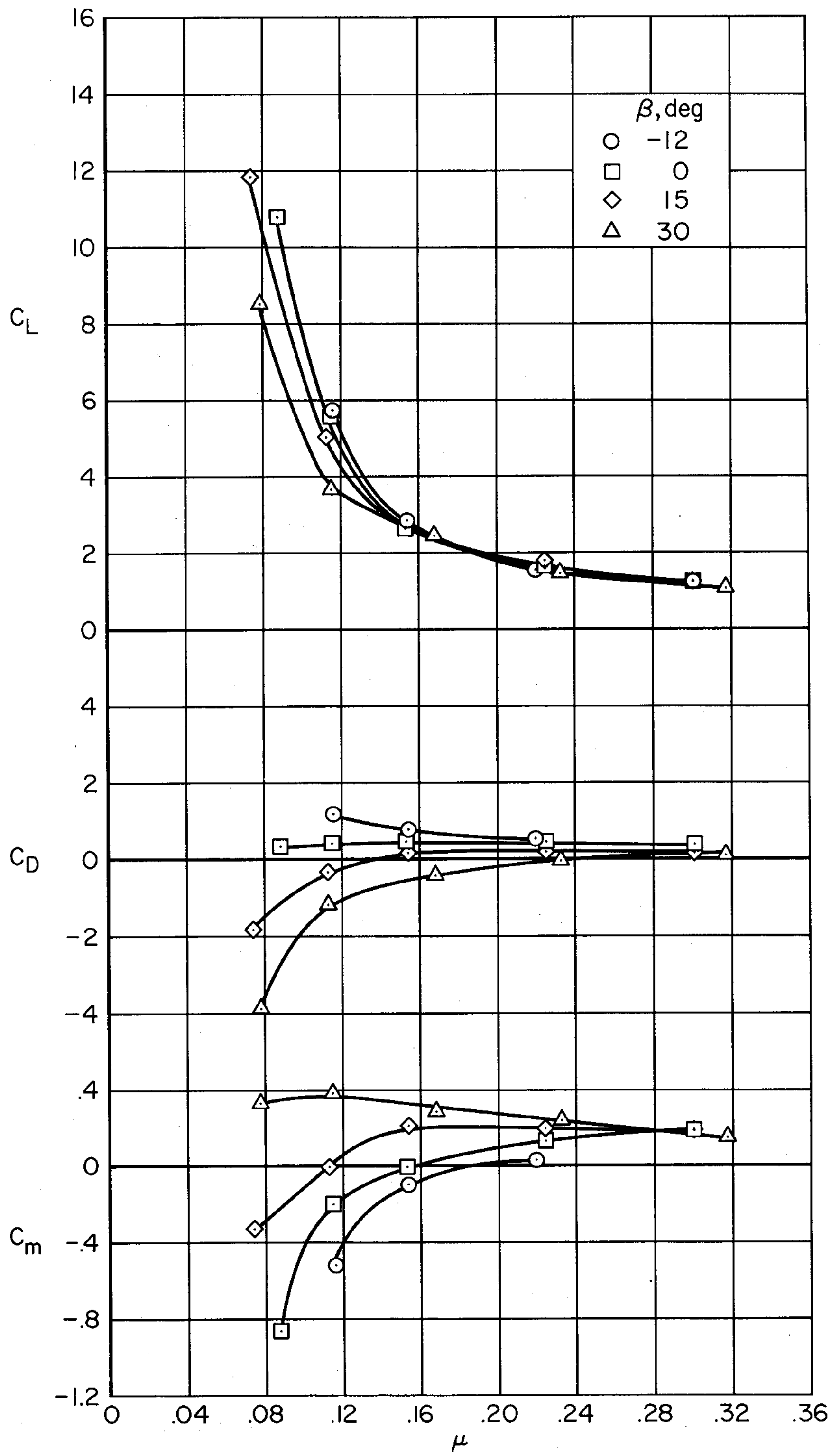

(c) Tail on, staggered louvers.

Figure 12.- Concluded.

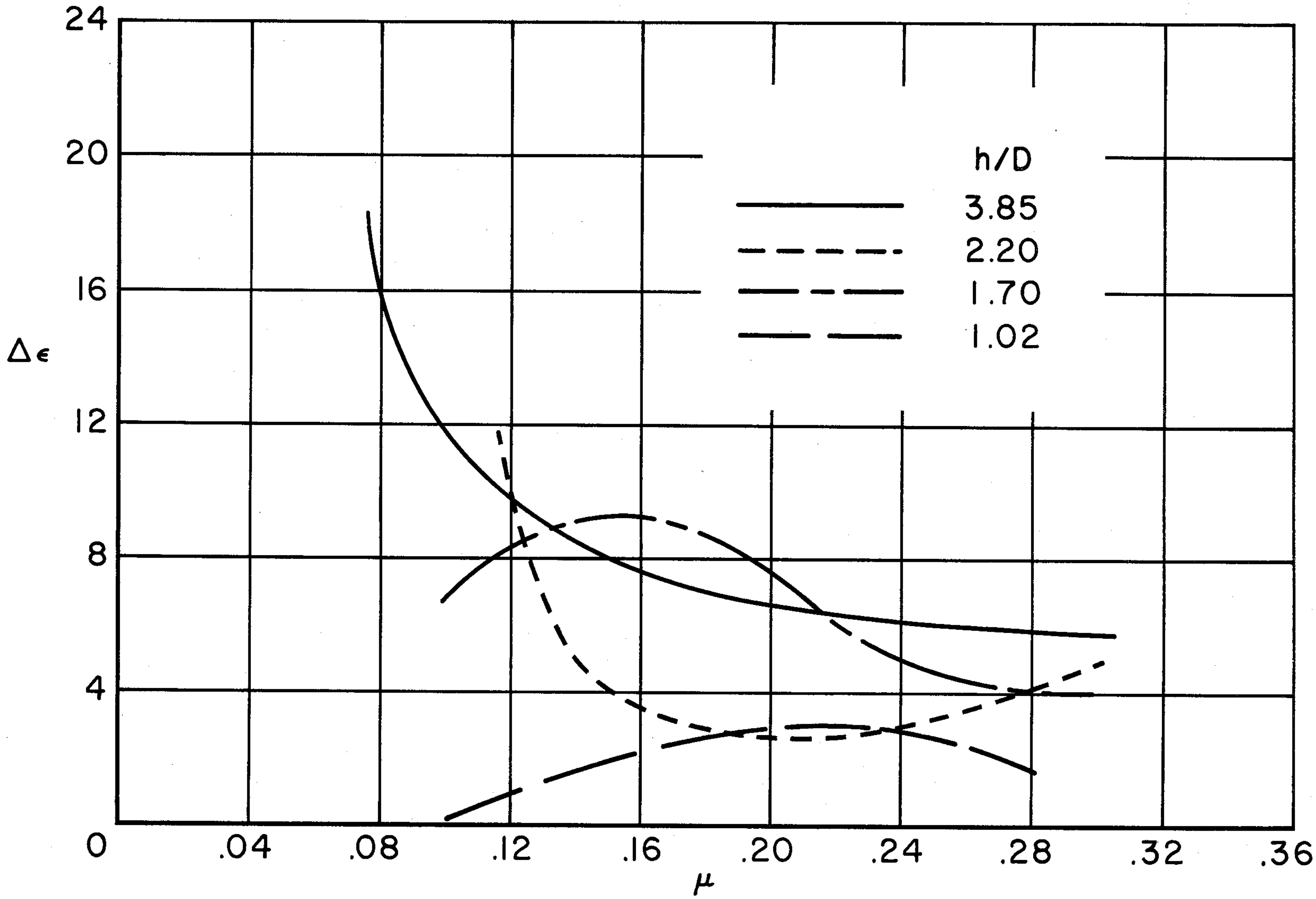

Figure 13.- Average incremental downwash at the tail due to fan operation; $\alpha = 0^{\circ}$, $\beta = 0^{\circ}$, $\delta_f = 45^{\circ}$.

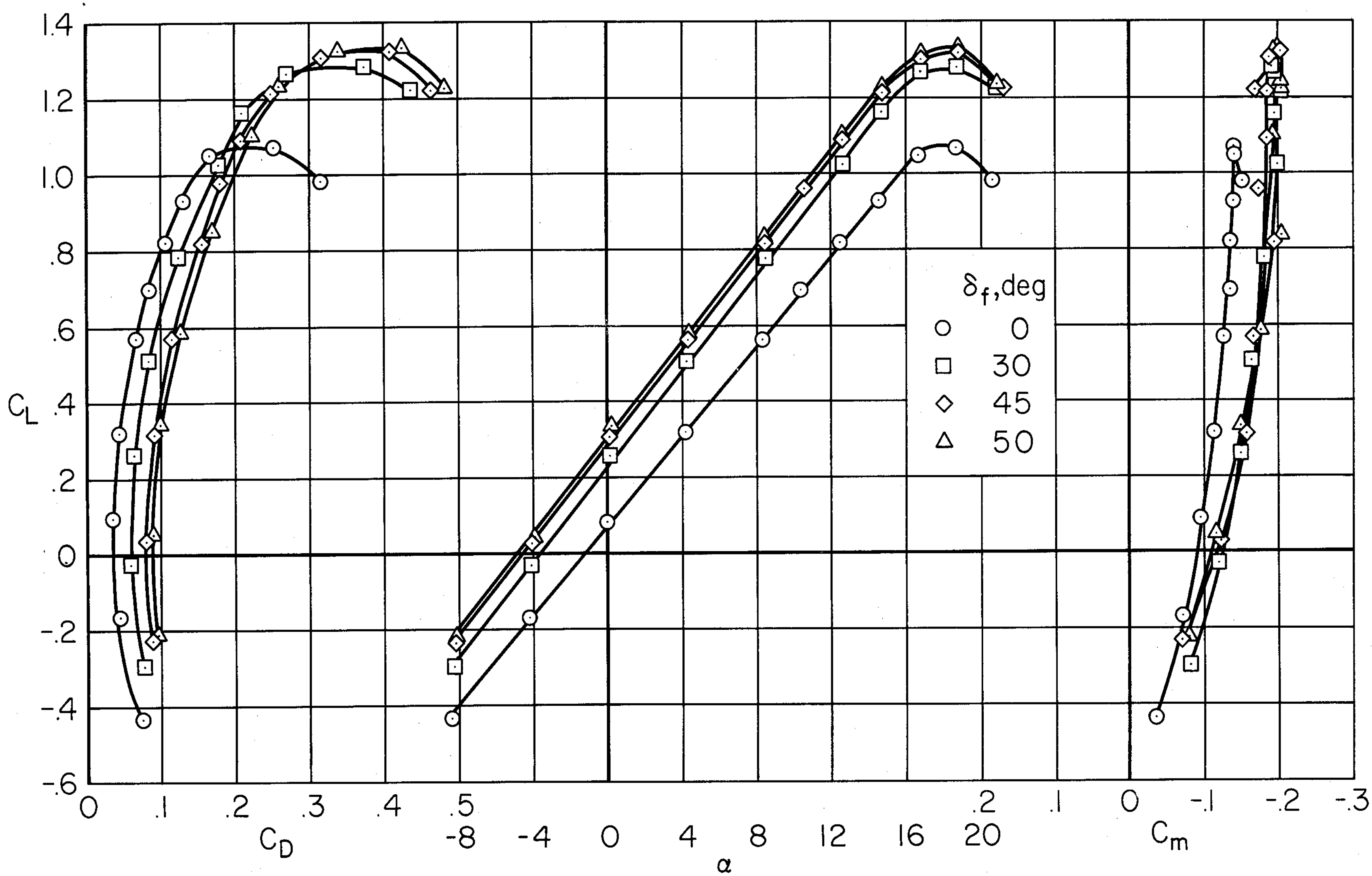

(a) Tail on, $i_t = 0^{\circ}$.

Figure 14.- Longitudinal characteristics with power off; $h/D = 3.85$, $\beta = 90^{\circ}$, inlets sealed, $V = 80$ knots.

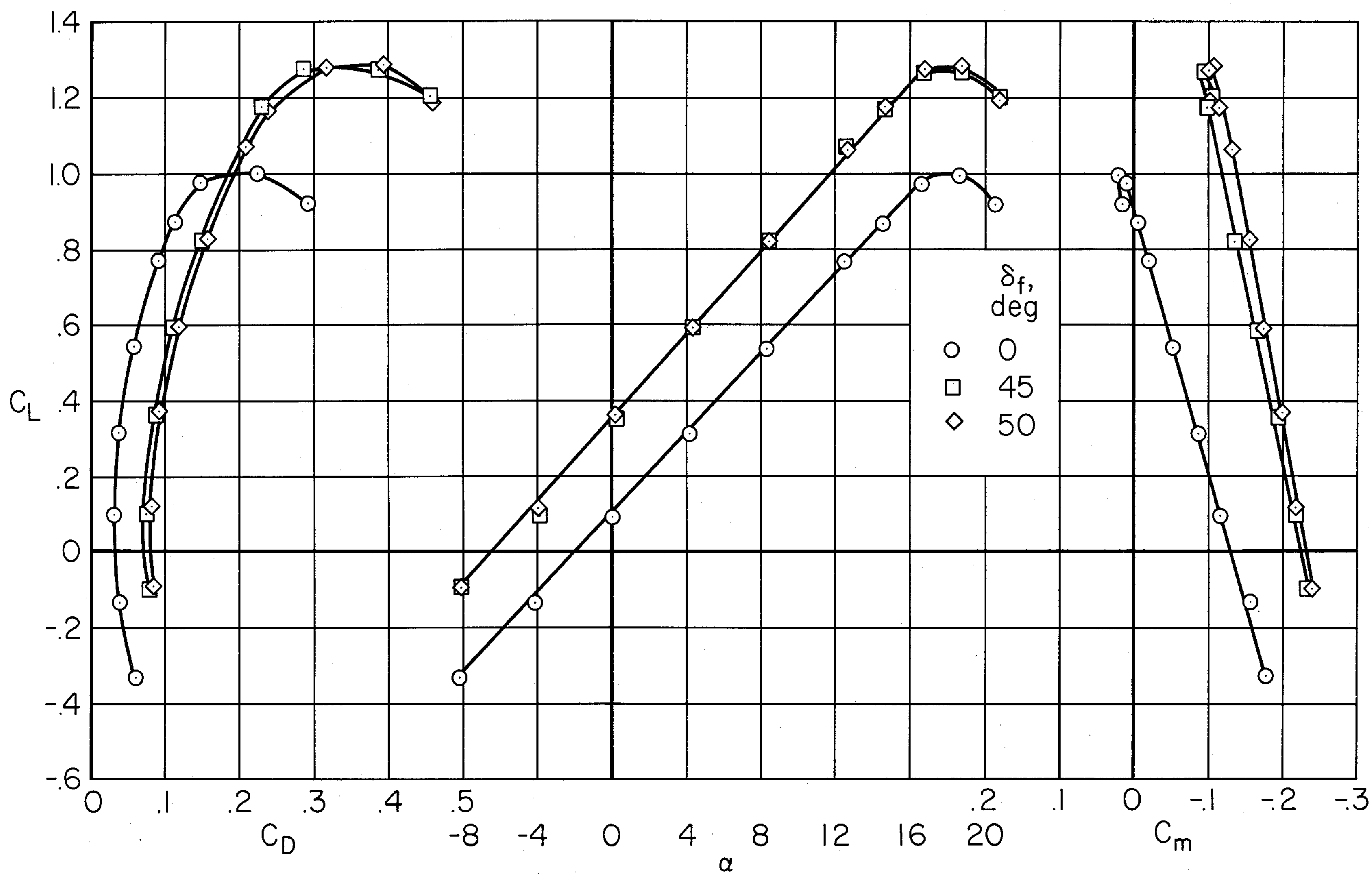

(b) Tail off.

Figure 14.- Continued.

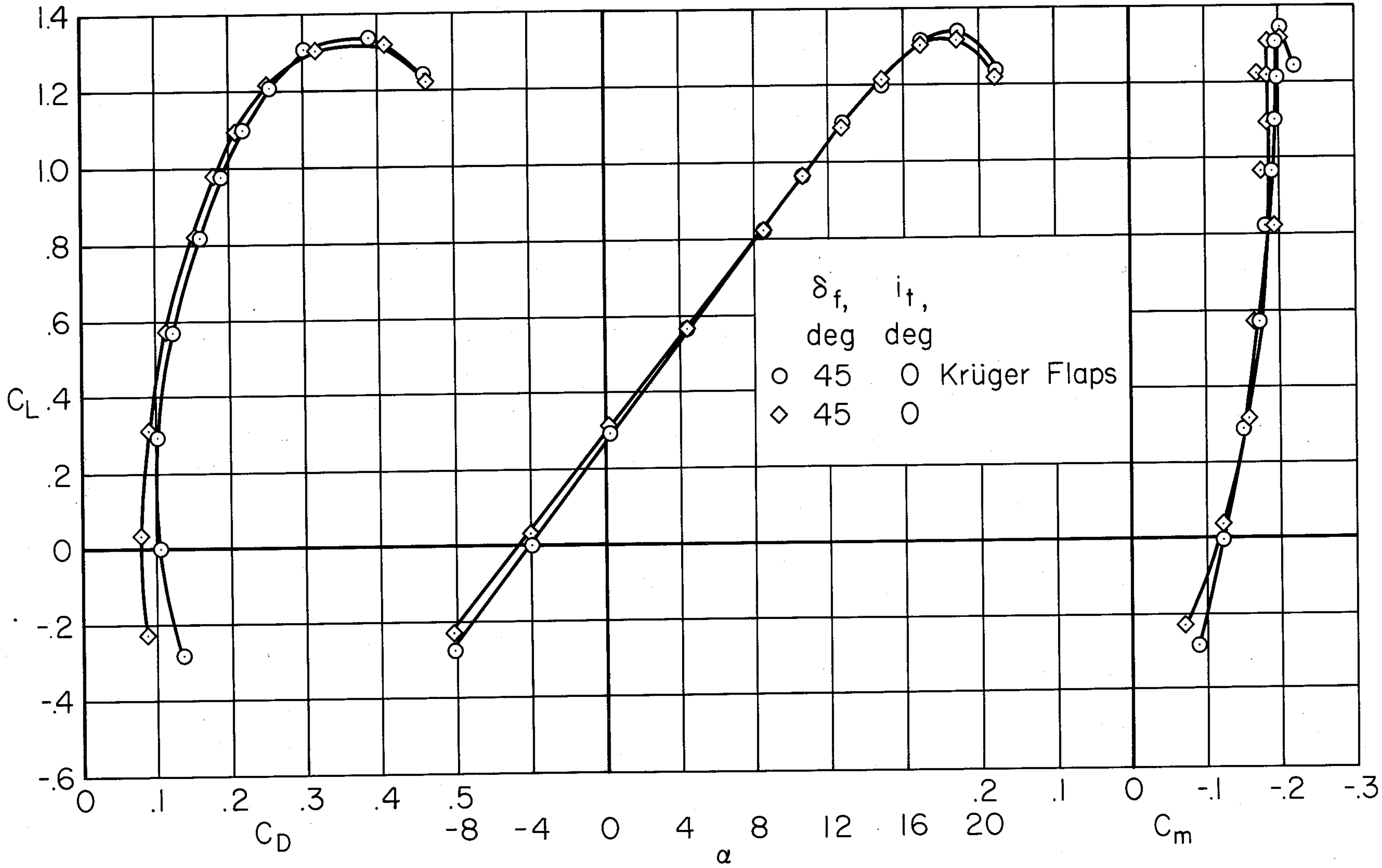

(c) Effect of Krüger flaps; tail on.

Figure 14.- Concluded.

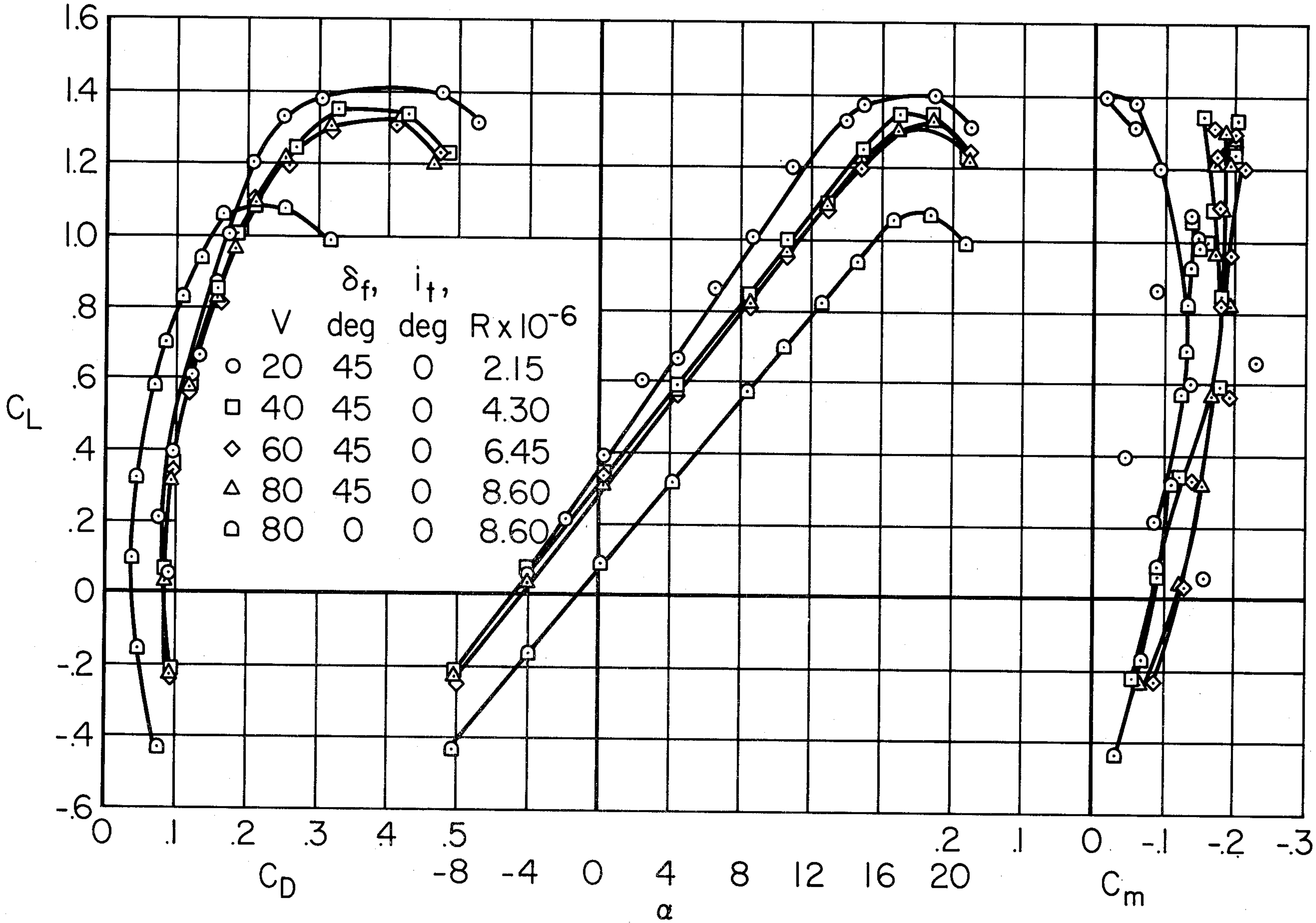

(a) h/D = 3.85, tail on.

Figure 15.- Effect of Reynolds number on power off longitudinal characteristics; $\beta = 90^{\circ}$, inlets sealed.

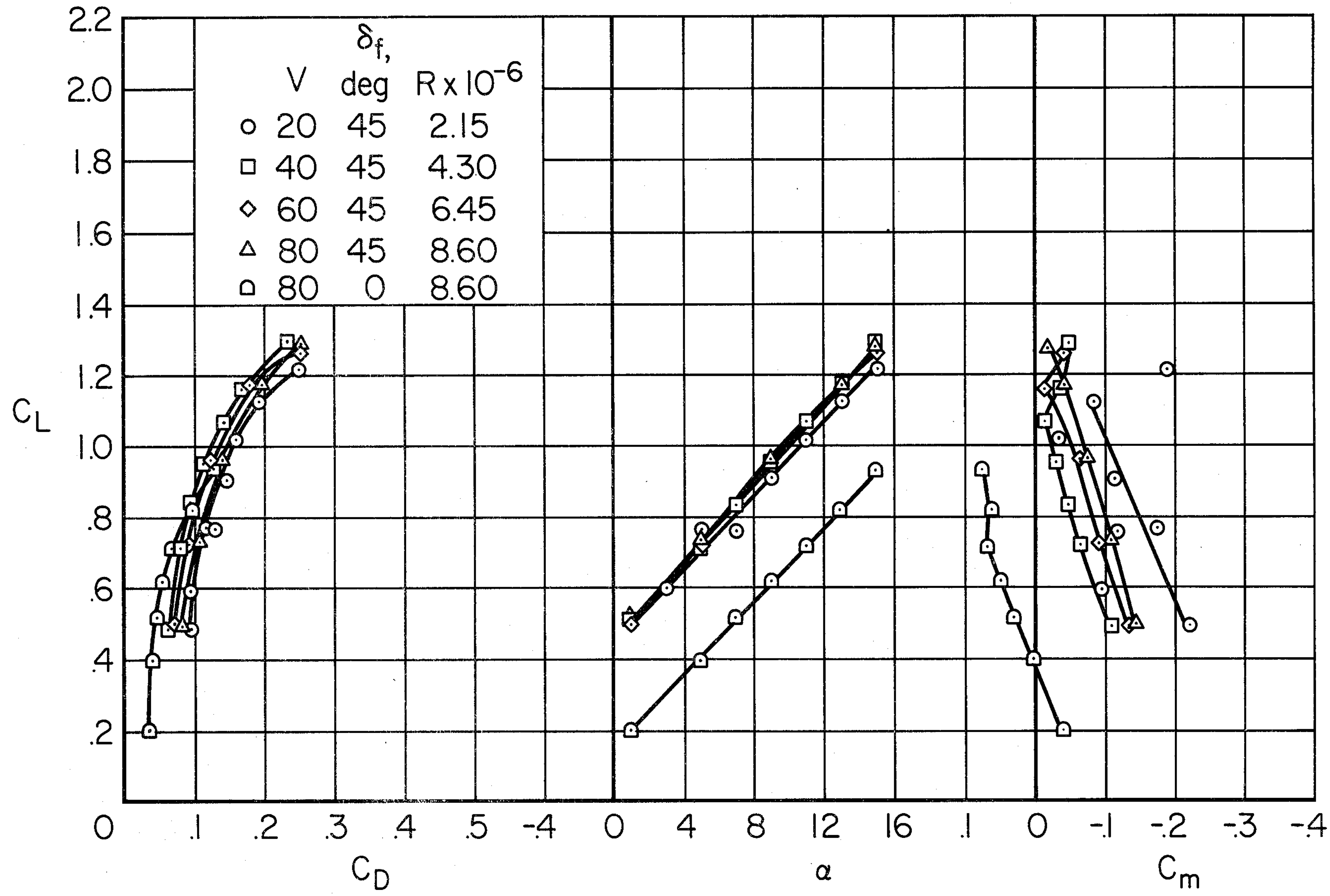

(b) h/D = 2.2, tail off.

Figure 15.- Concluded.

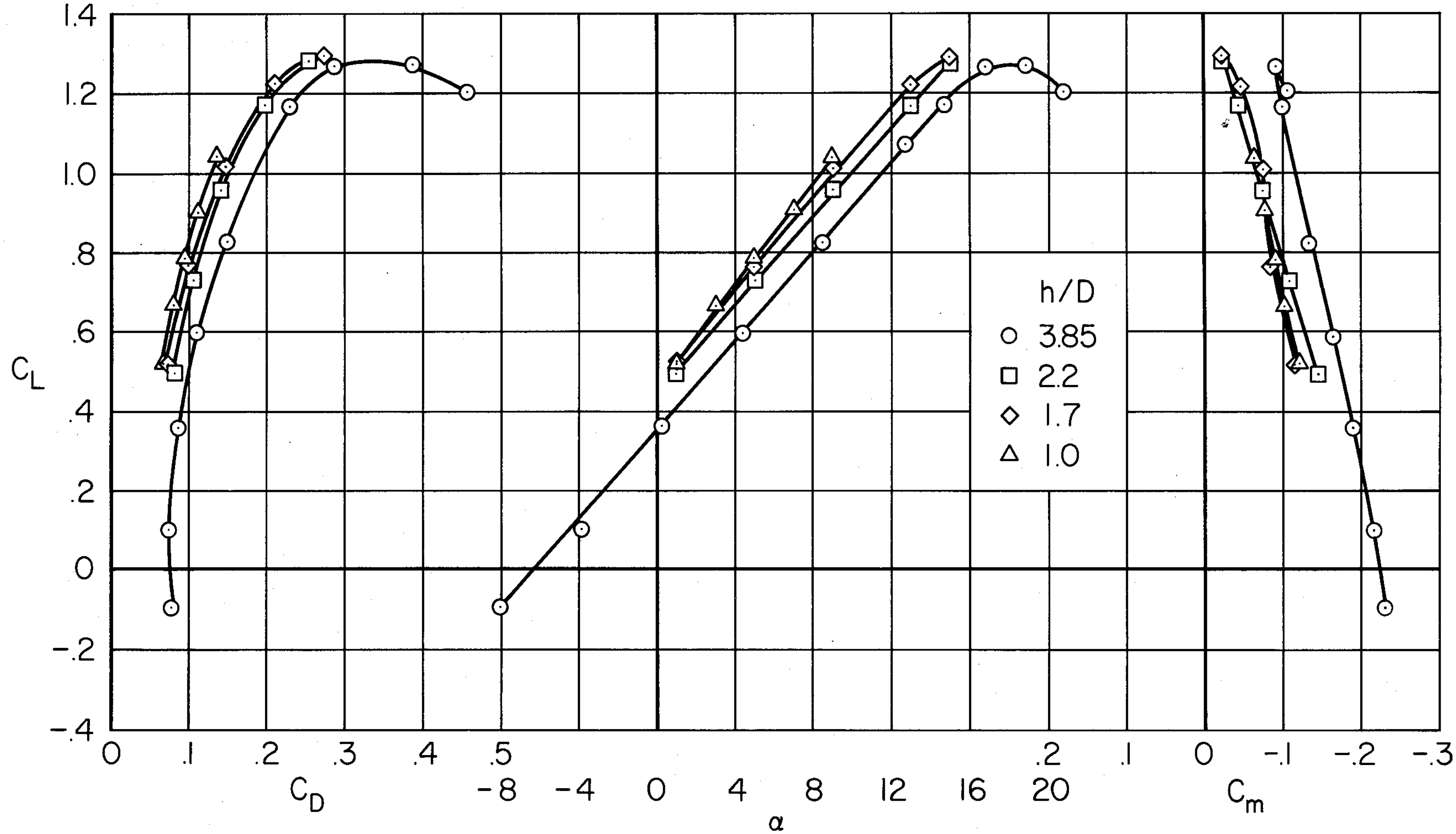

Figure 16.- Effect of ground height on power off longitudinal characteristics; $\beta = 90^{\circ}$, inlets sealed, tail off, $\delta_f = 45^{\circ}$, $V = 80$ knots.

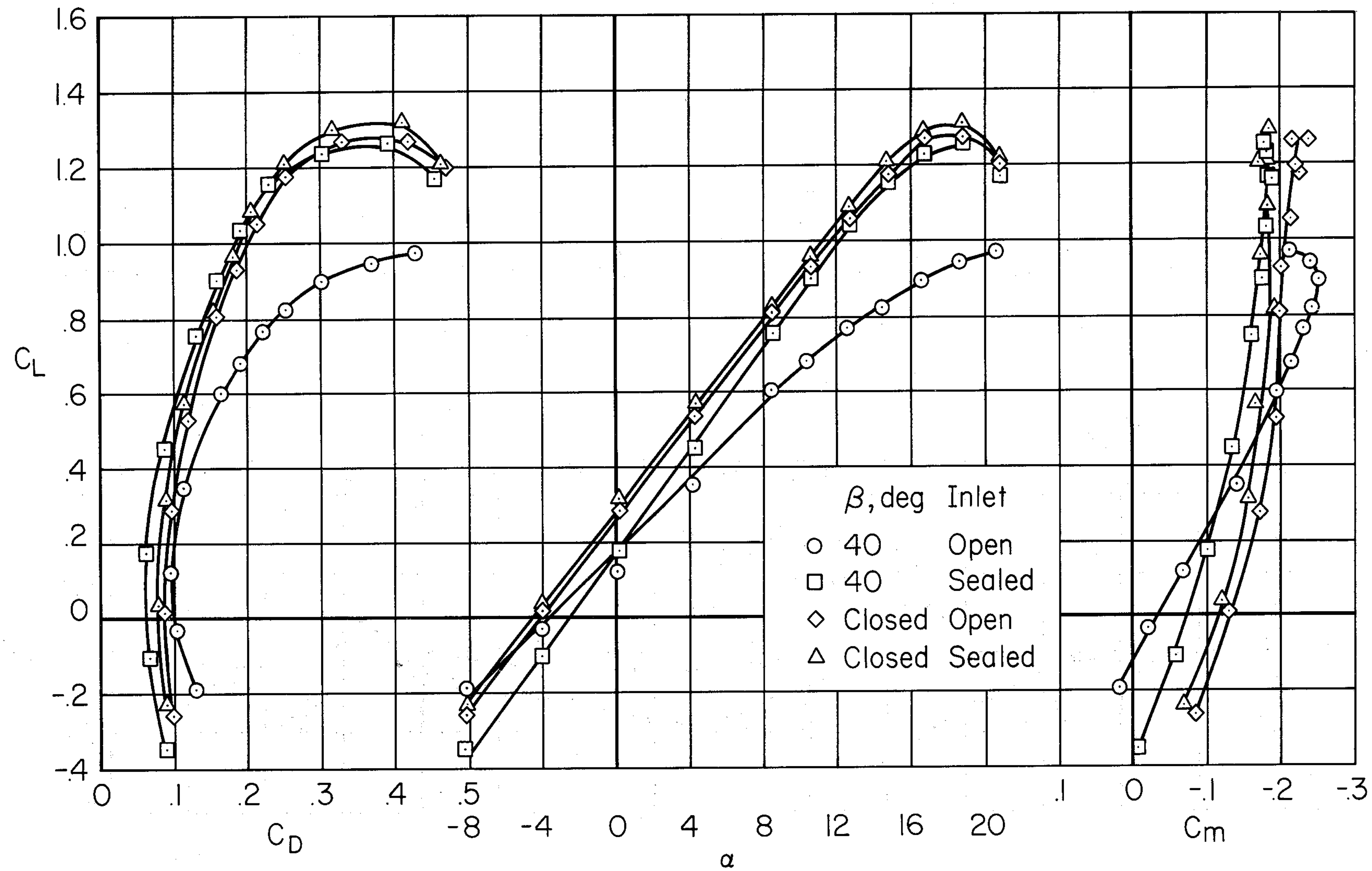

Figure 17.- Effect of various open or partly open fan inlets and exits on longitudinal characteristics with power off; $h/D = 3.85$, tail on, $i_t = 0^o$, $\delta_f = 45^o$, $V = 80$ knots.

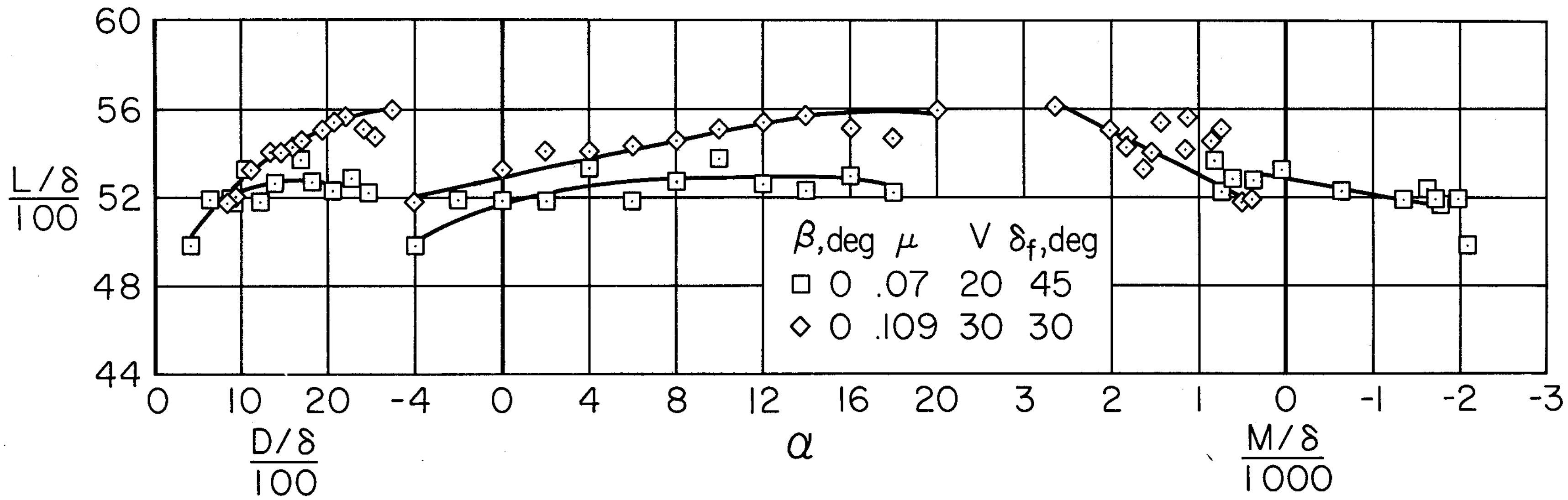

(a) h/D = 3.85, straight louvers.

Figure 18.- Longitudinal characteristics with fans operating at low tip-speed ratios; tail off, 1700 RPM.

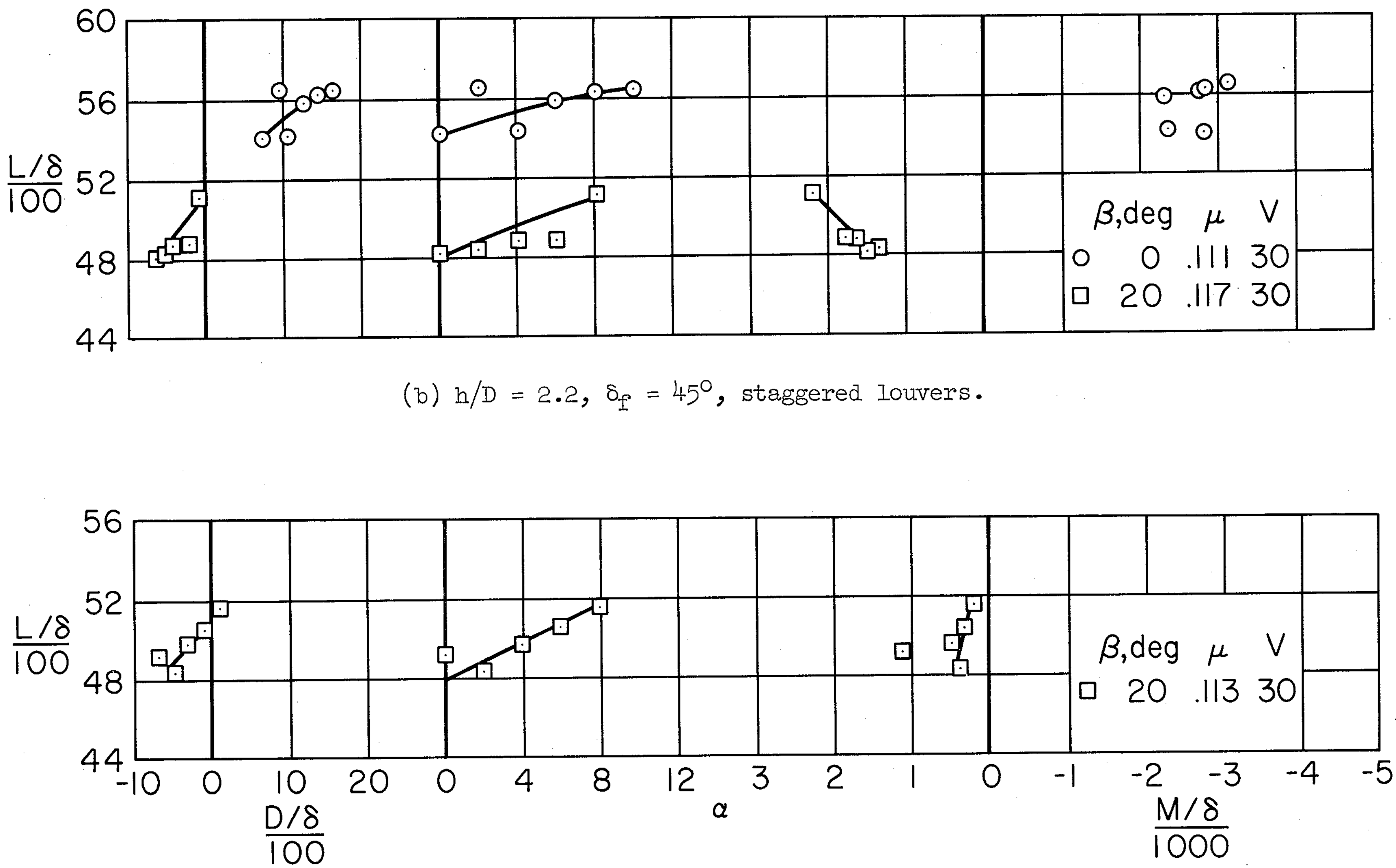

(b) h/D = 2.2, δ_f = 45°, staggered louvers.

(c) h/D = 1.7, δ_f = 45°, staggered louvers.

Figure 18.- Concluded.

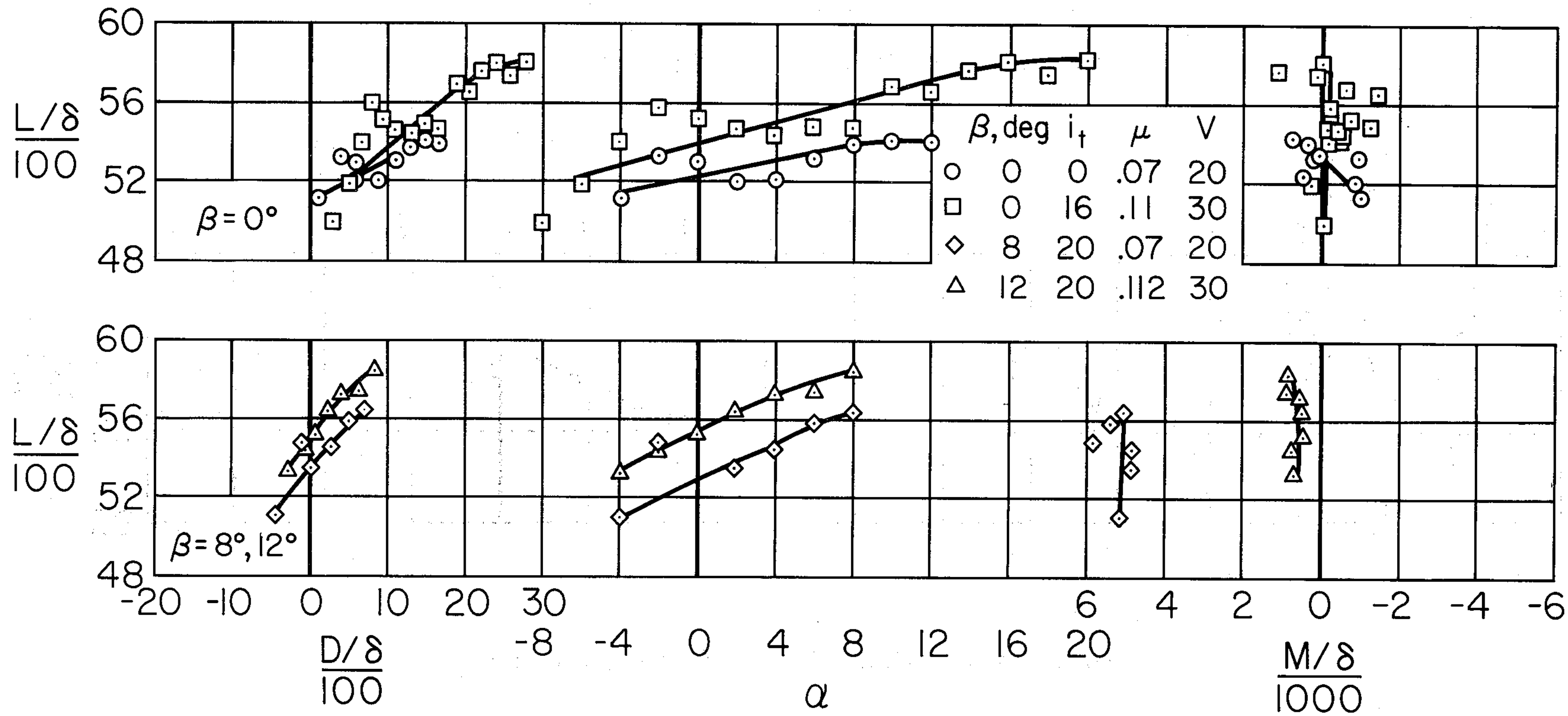

(a) h/D = 3.85

Figure 19.- Longitudinal characteristics with fans operating at low tip-speed ratios; tail on, $\delta_f = 45^o$, straight louvers, 1700 RPM.

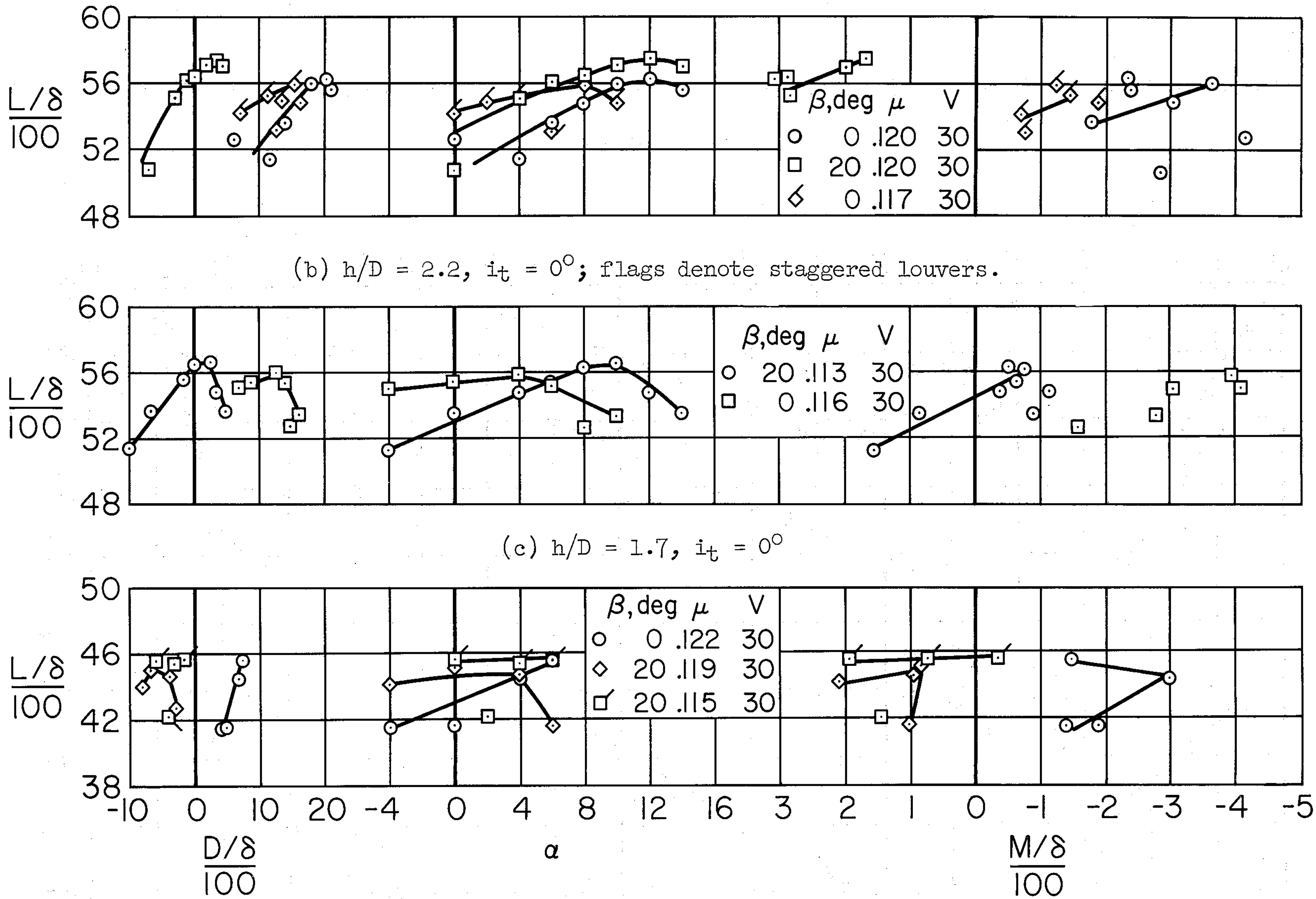

(b) h/D = 2.2, i_t = 0°; flags denote staggered louvers.

(c) h/D = 1.7, i_t = 0°

(d) h/D = 1.0, i_t = 0°; flags denote staggered louvers.

Figure 19.- Concluded.

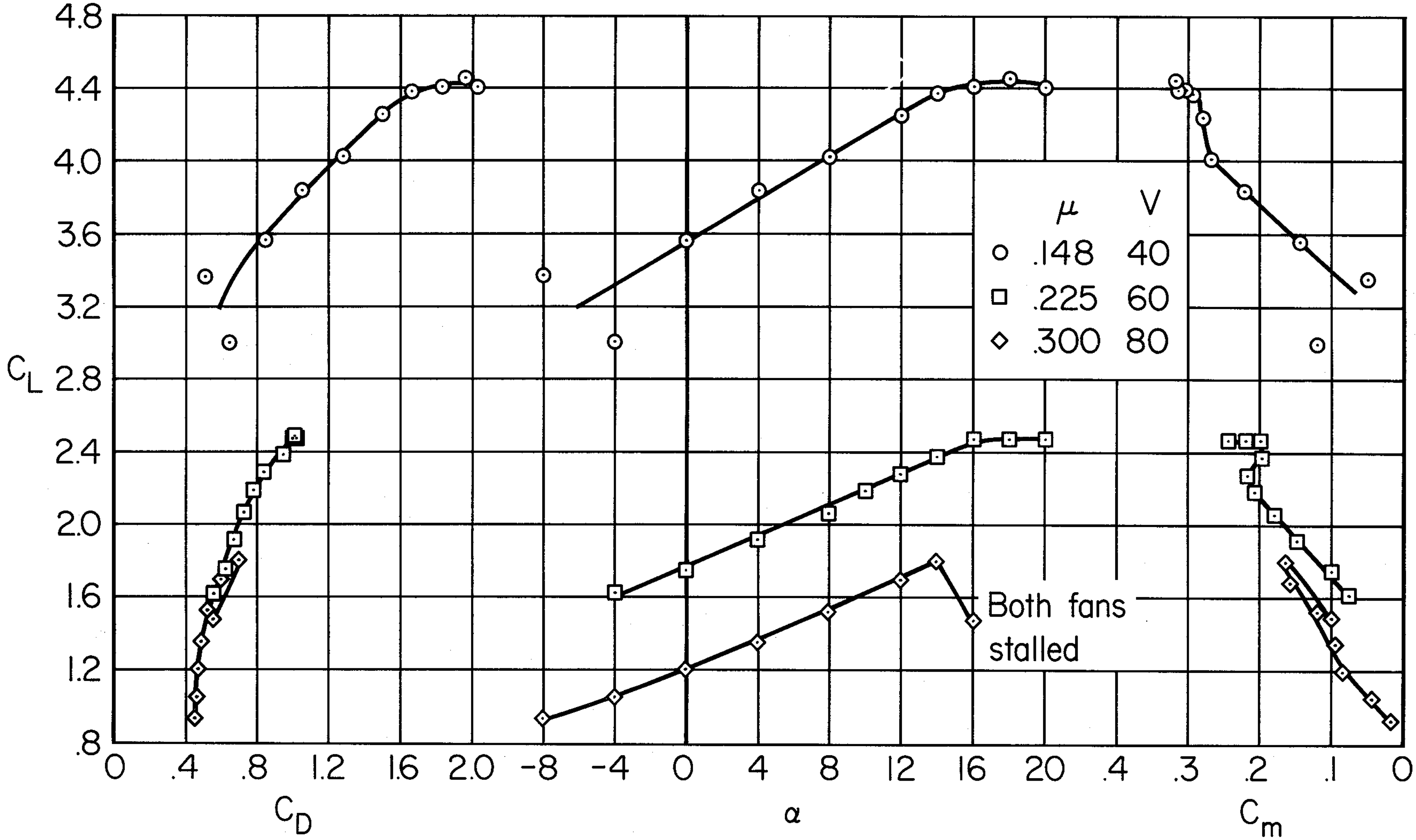

(a) $\beta = 0^{\circ}$, $\delta_f = 30^{\circ}$

Figure 20.- Longitudinal characteristics with fans operating; h/D = 3.85, tail off, straight louvers, 1700 RPM.

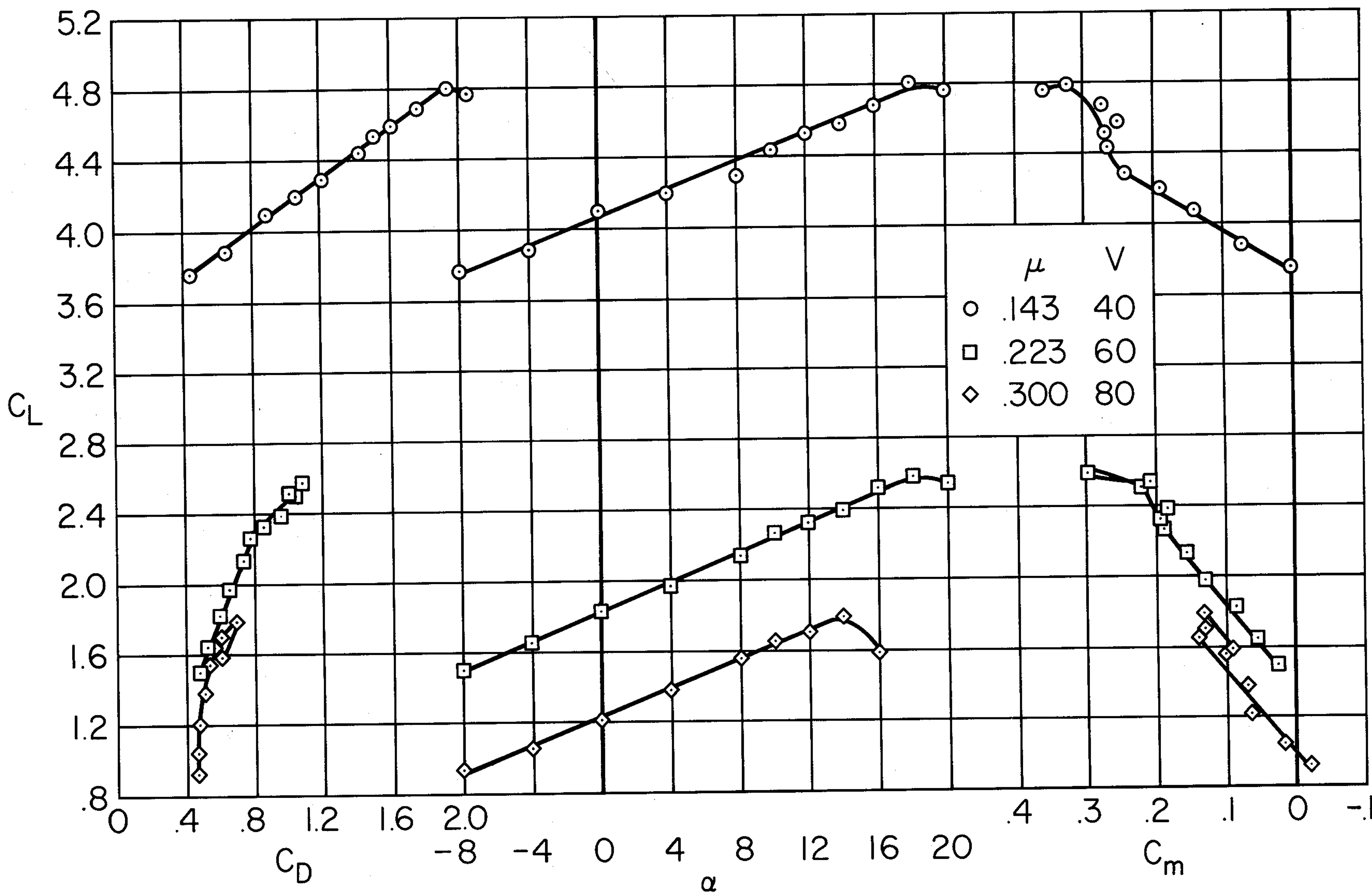

(b) $\beta = 0^{\circ}$, $\delta_f = 45^{\circ}$

Figure 20.- Continued.

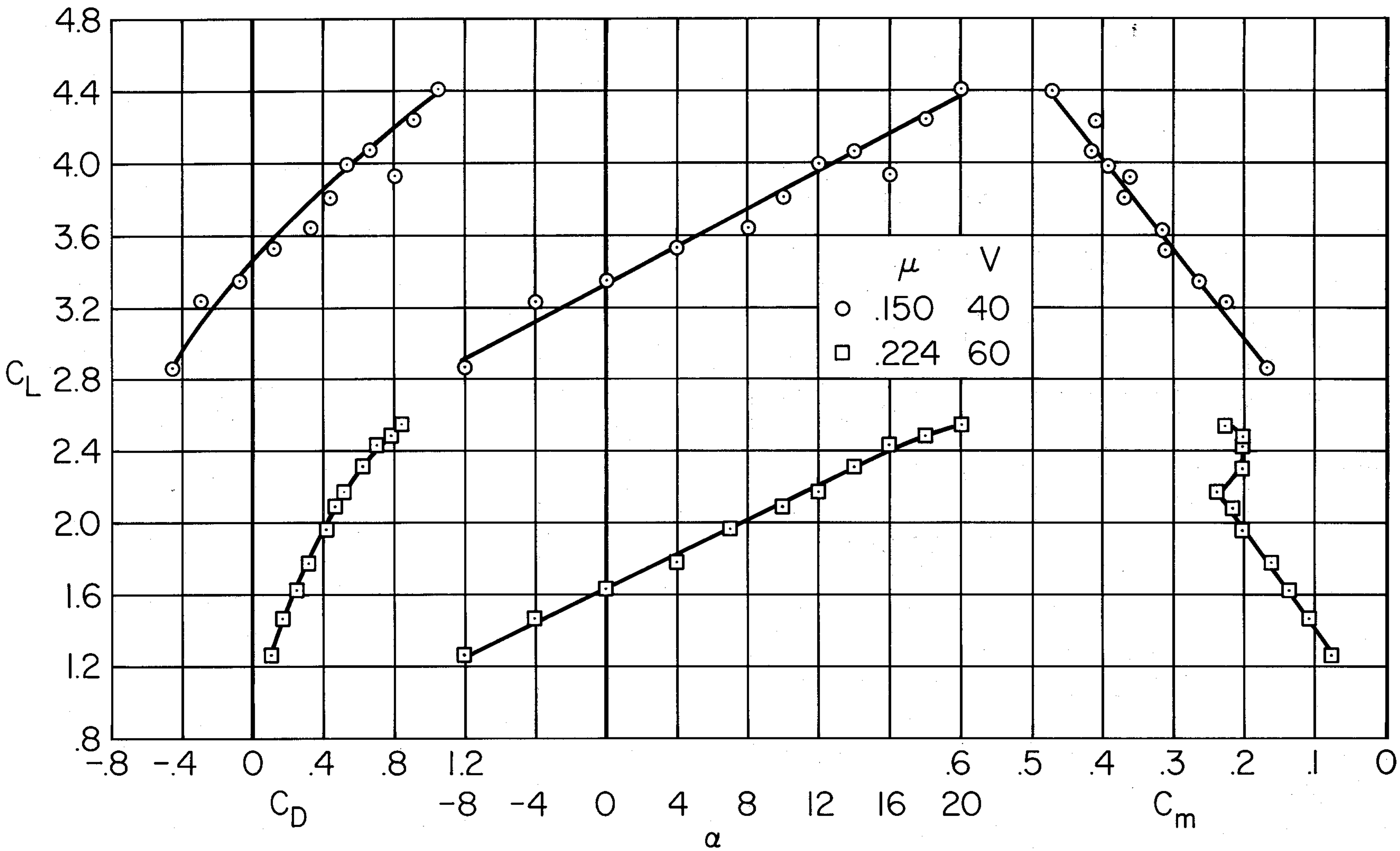

(c) $\beta = 20^{\circ}$, $\delta_f = 45^{\circ}$

Figure 20.- Continued.

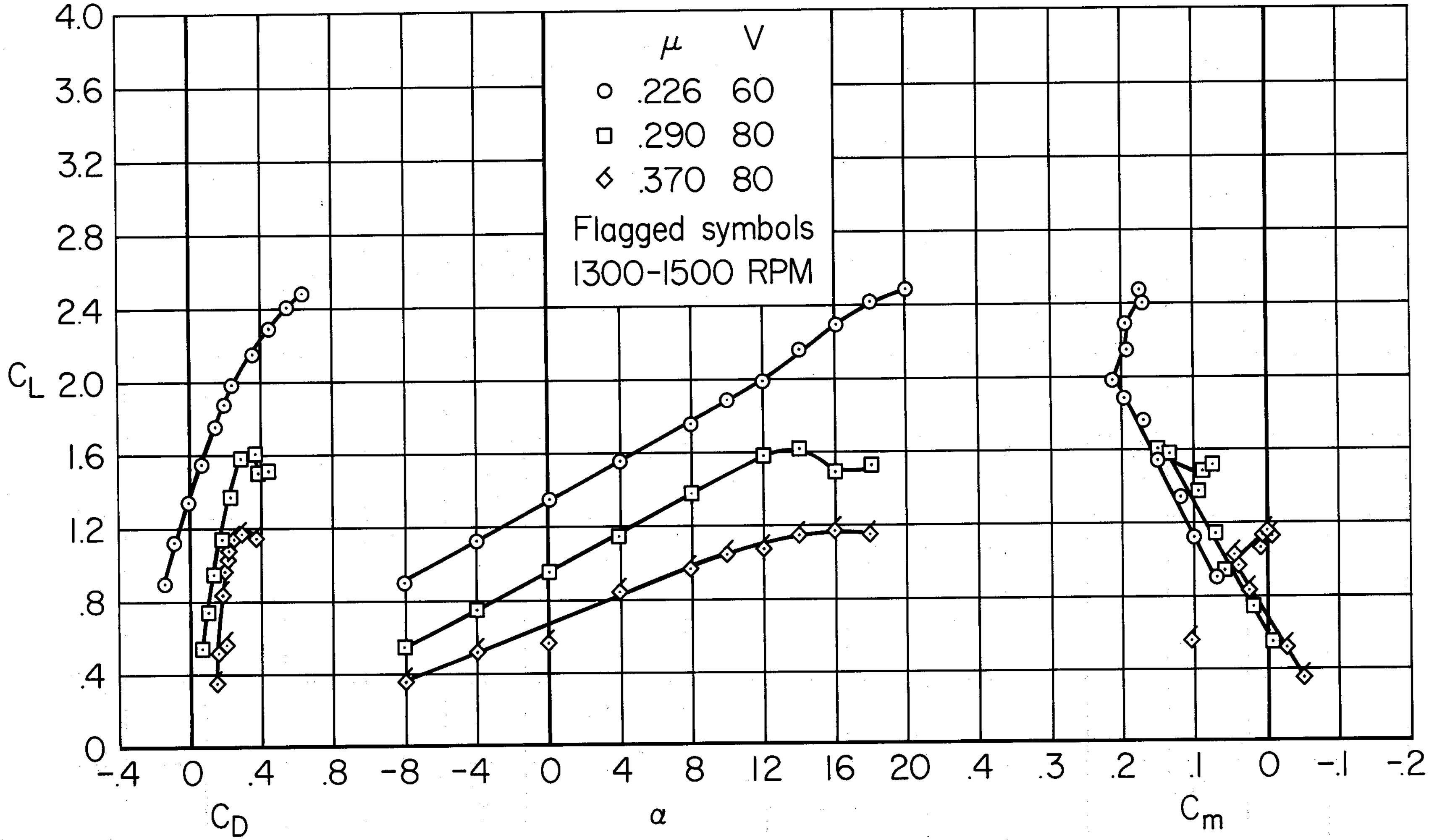

(d) $\beta = 35^{\circ}$, $\delta_f = 45^{\circ}$

Figure 20.- Concluded.

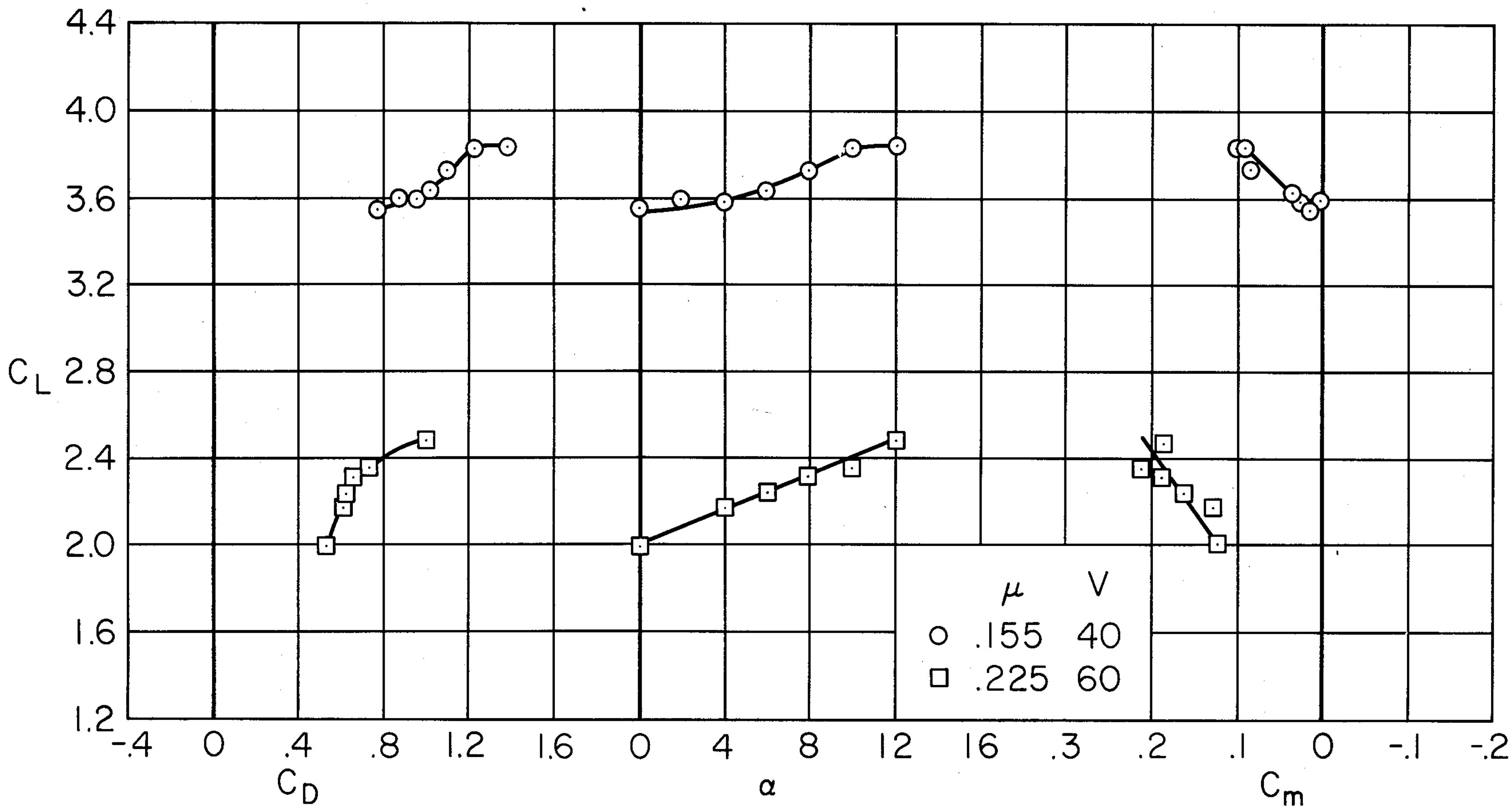

(a) $\beta = 0^{\circ}$

Figure 21.- Longitudinal characteristics with fans operating; $h/D = 2.2$, tail off, $\delta_f = 45^{\circ}$, staggered louvers, 1700 RPM.

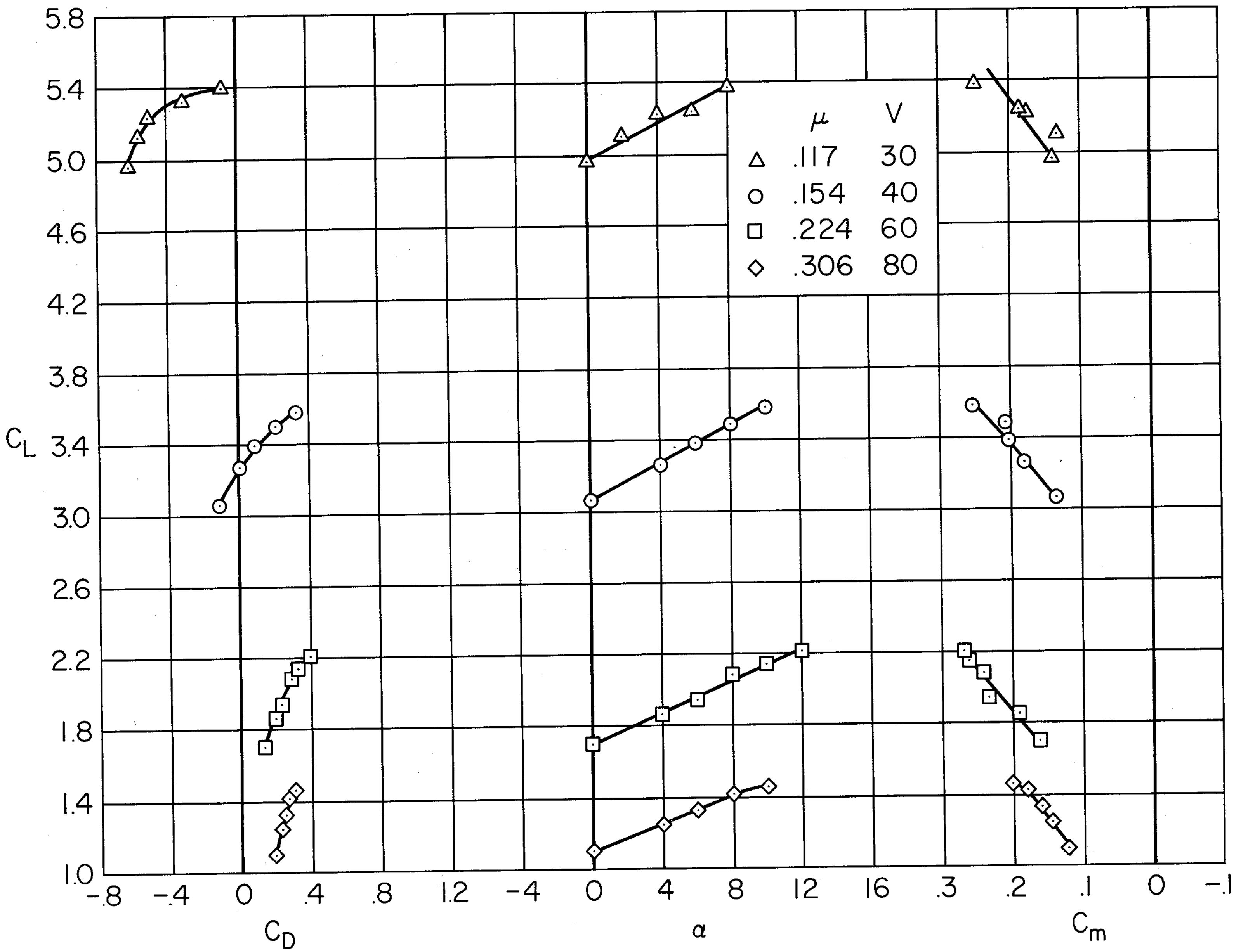

(b) $\beta = 20^{\circ}$

Figure 21.- Concluded.

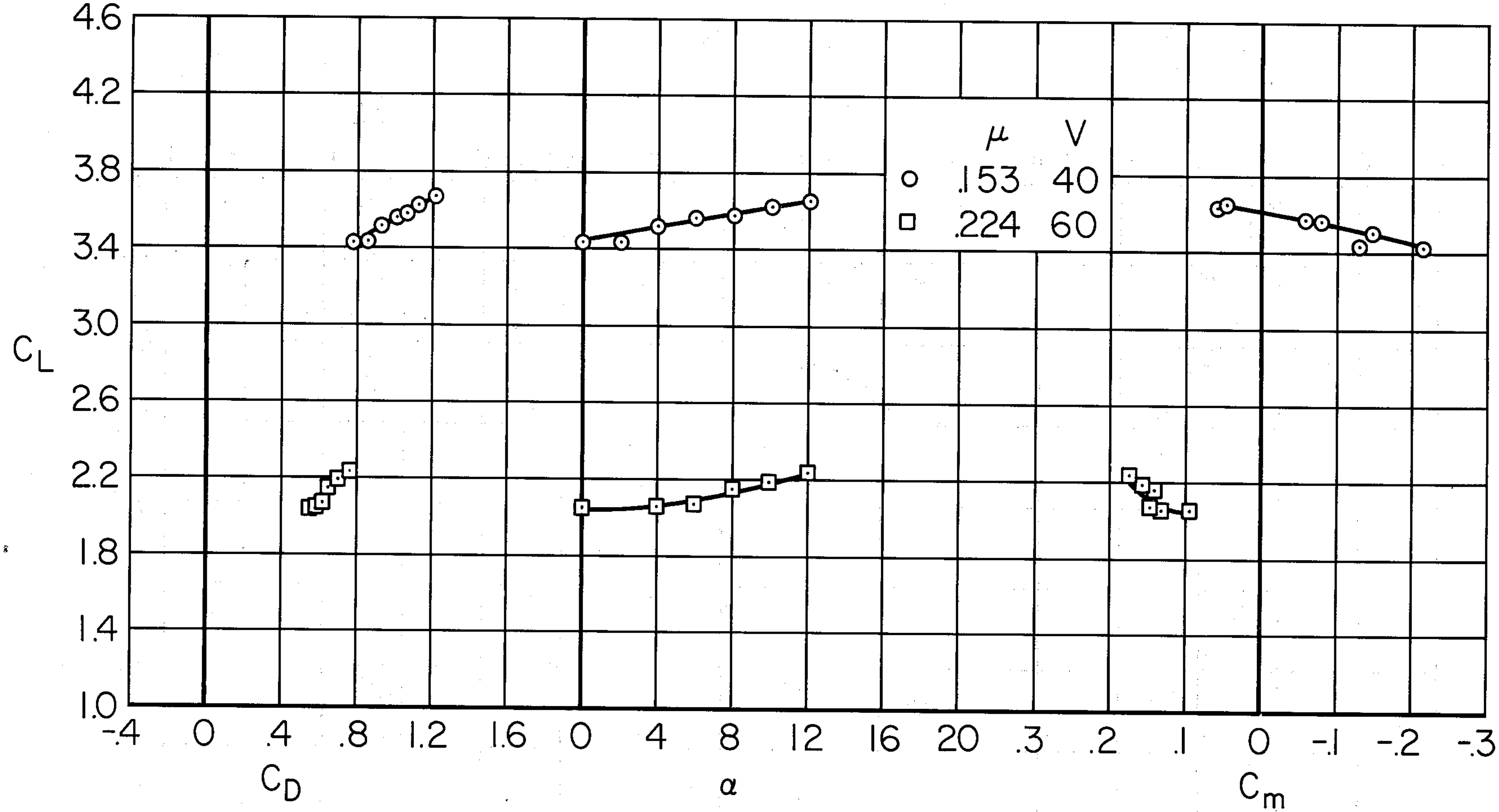

(a) $\beta = 0^{\circ}$

Figure 22.- Longitudinal characteristics with fans operating; $h/D = 1.7$, tail off, $\delta_f = 45^{\circ}$, staggered louvers, 1700 RPM.

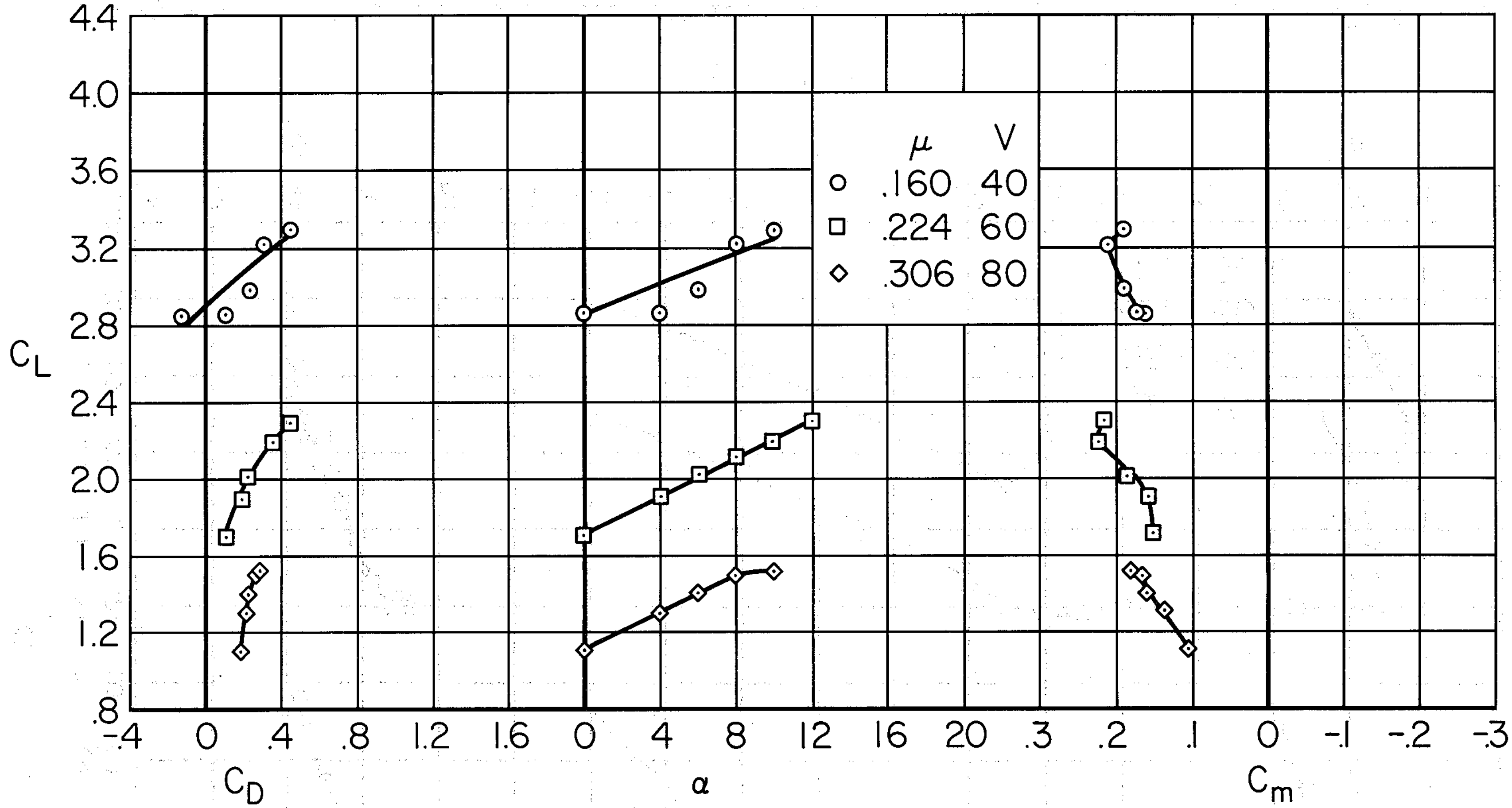

(b) $\beta = 20^{\circ}$

Figure 22.- Concluded.

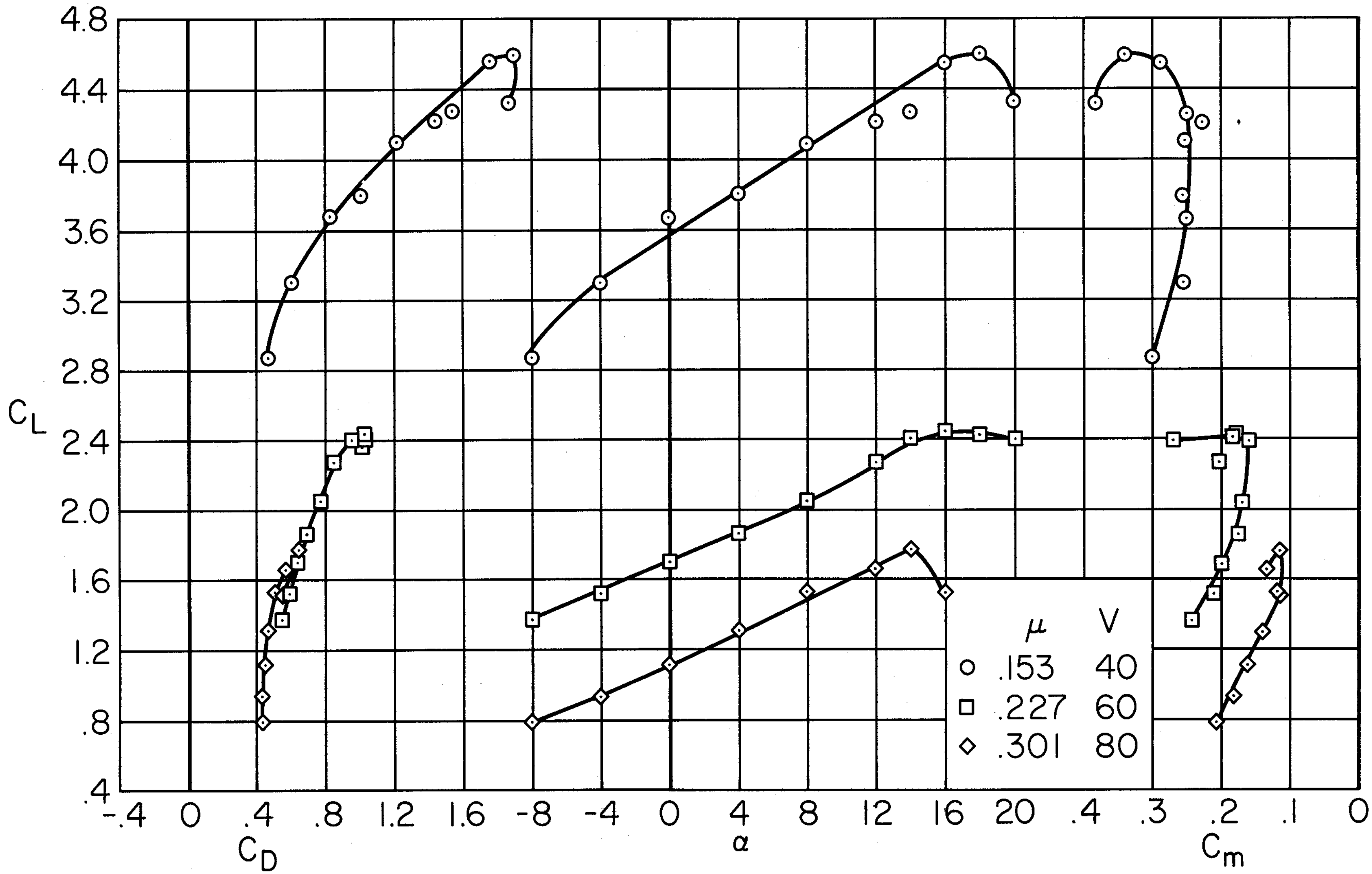

(a) $\beta = 0^{\circ}$

Figure 23.- Longitudinal characteristics with fans operating; $h/D = 3.85$, tail on, $i_t = 0^{\circ}$, $\delta_f = 45^{\circ}$, straight louvers, 1700 RPM.

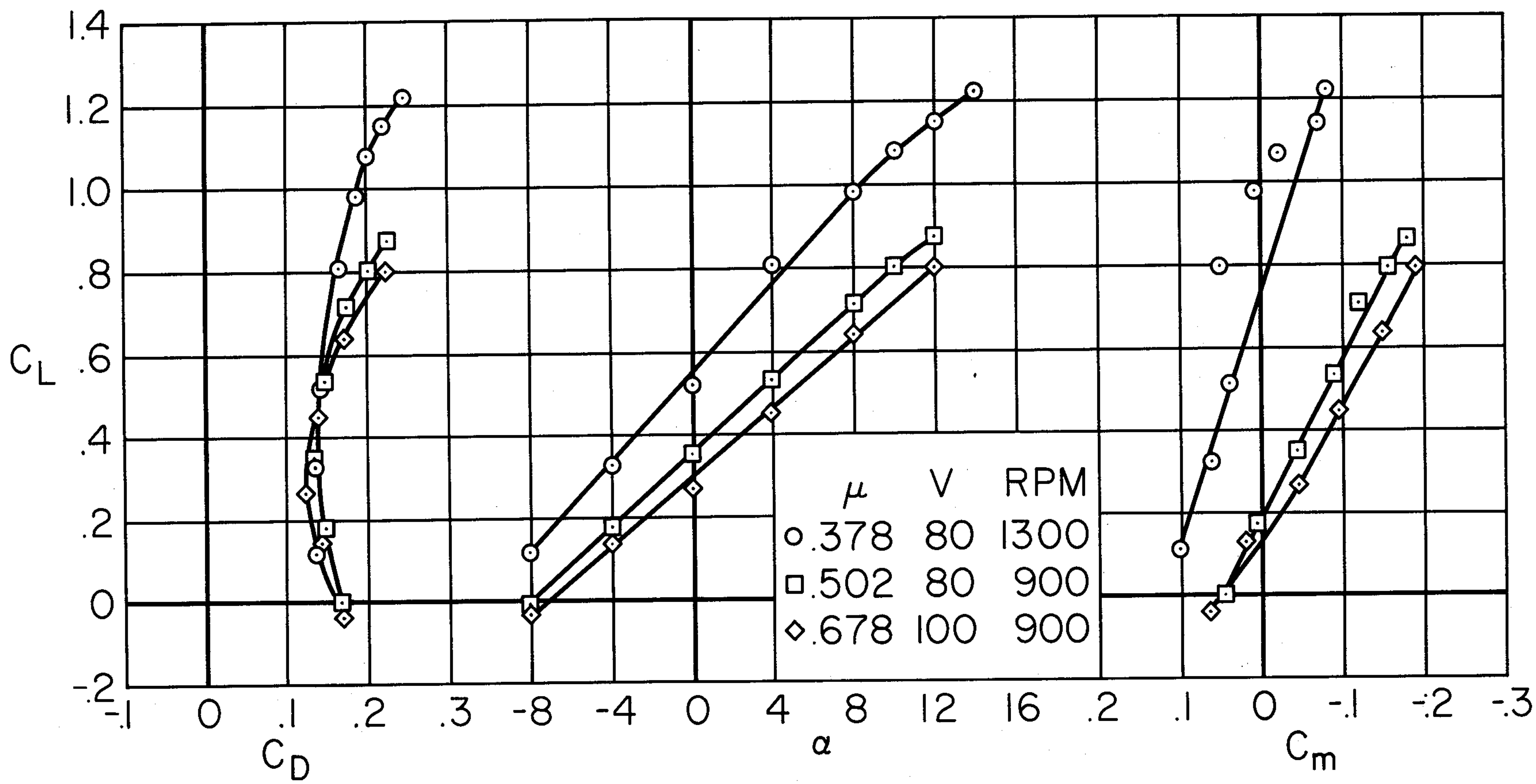

(b) $\beta = 40^{\circ}$

Figure 23.- Concluded.

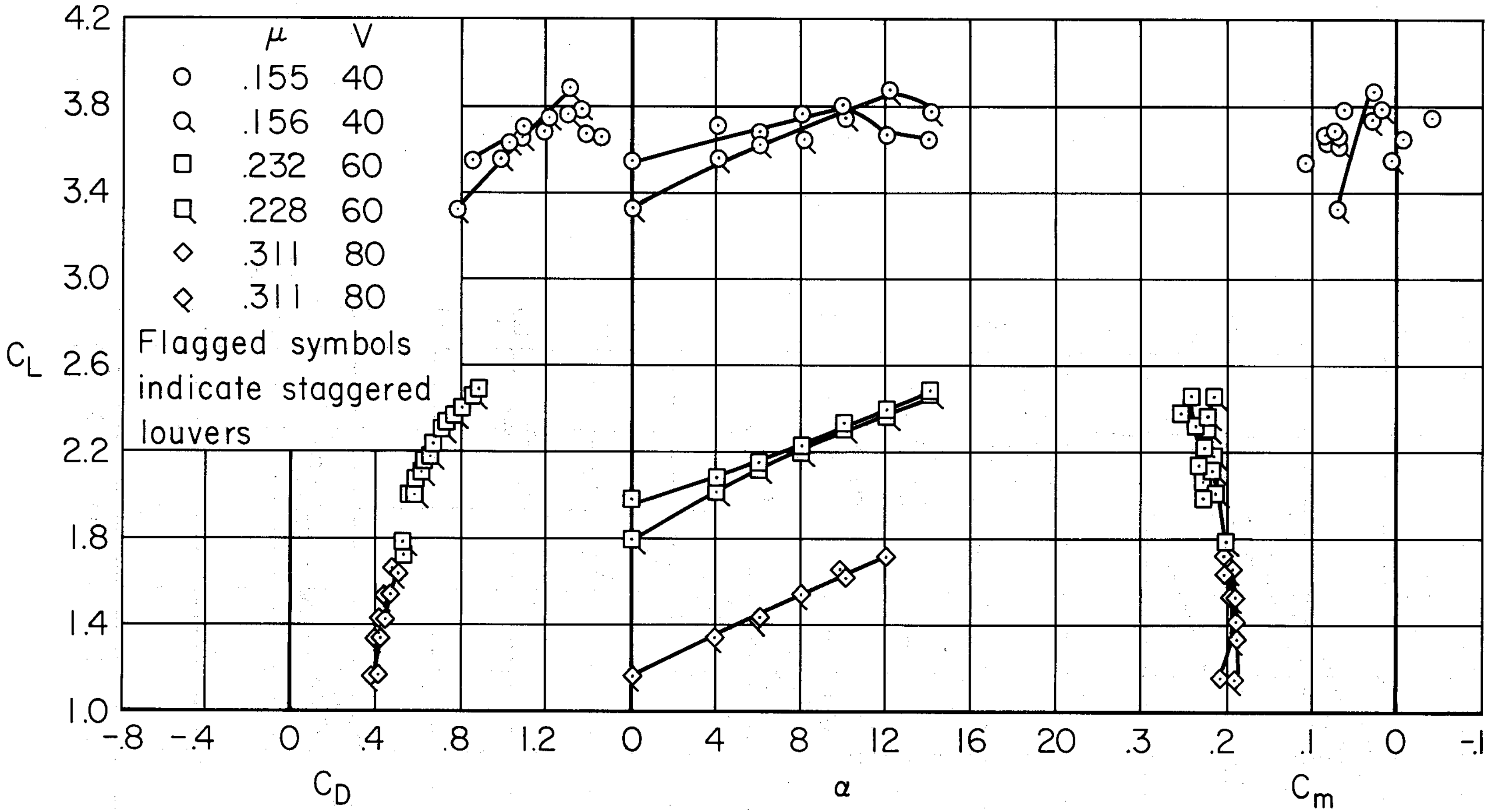

(a) $\beta = 0^{\circ}$

Figure 24.- Longitudinal characteristics with fans operating; $h/D = 2.2$, tail on, $i_t = 0^{\circ}$, $\delta_f = 45^{\circ}$, 1700 RPM.

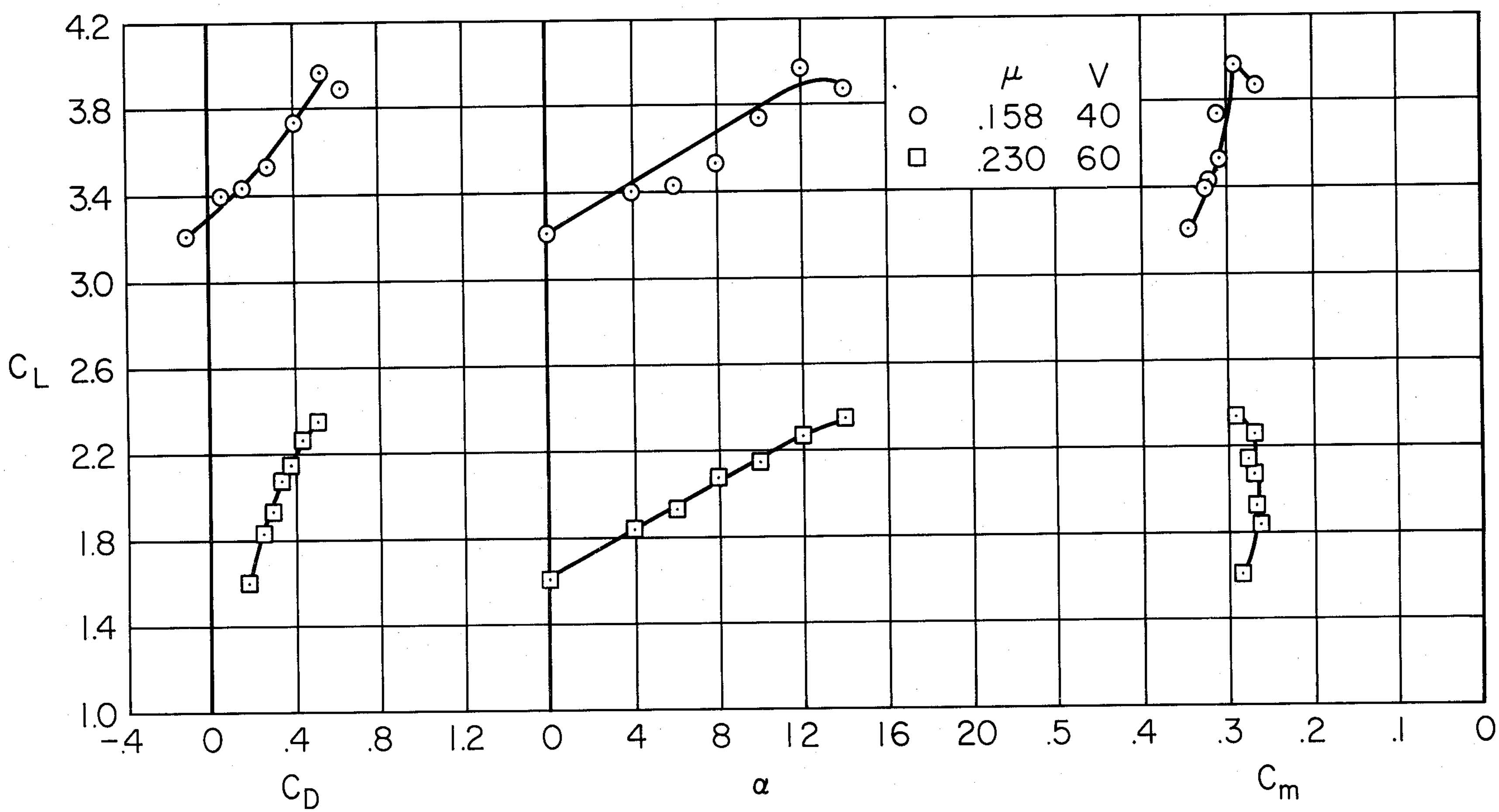

(b) β = 20°

Figure 24.- Continued.

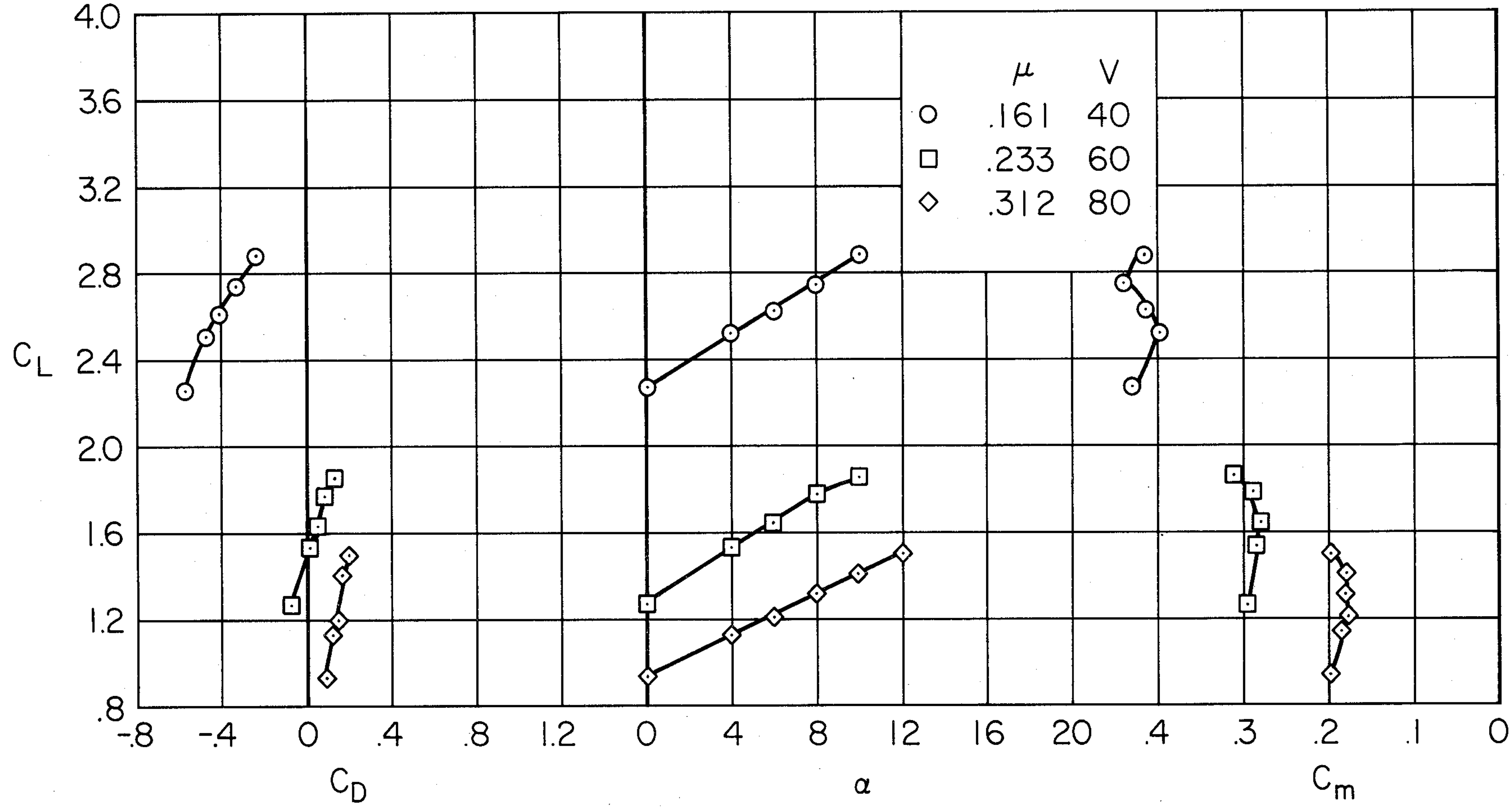

(c) $\beta = 35^{\circ}$

Figure 24.- Concluded.

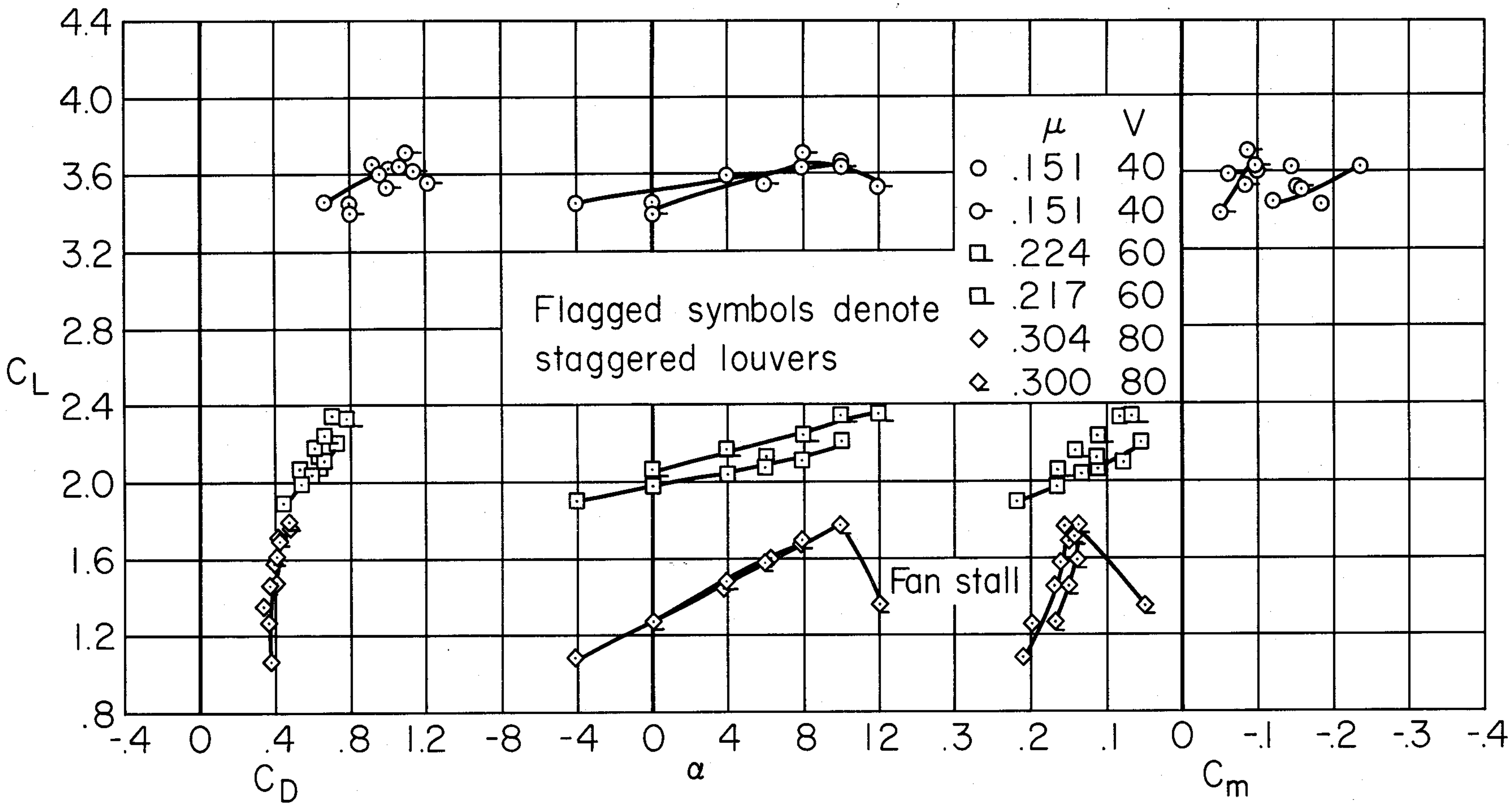

(a) $\beta = 0^{\circ}$

Figure 25.- Longitudinal characteristics with fans operating; $h/D = 1.7$, tail on, $i_t = 0^{\circ}$, $\delta_f = 45^{\circ}$, 1700 RPM.

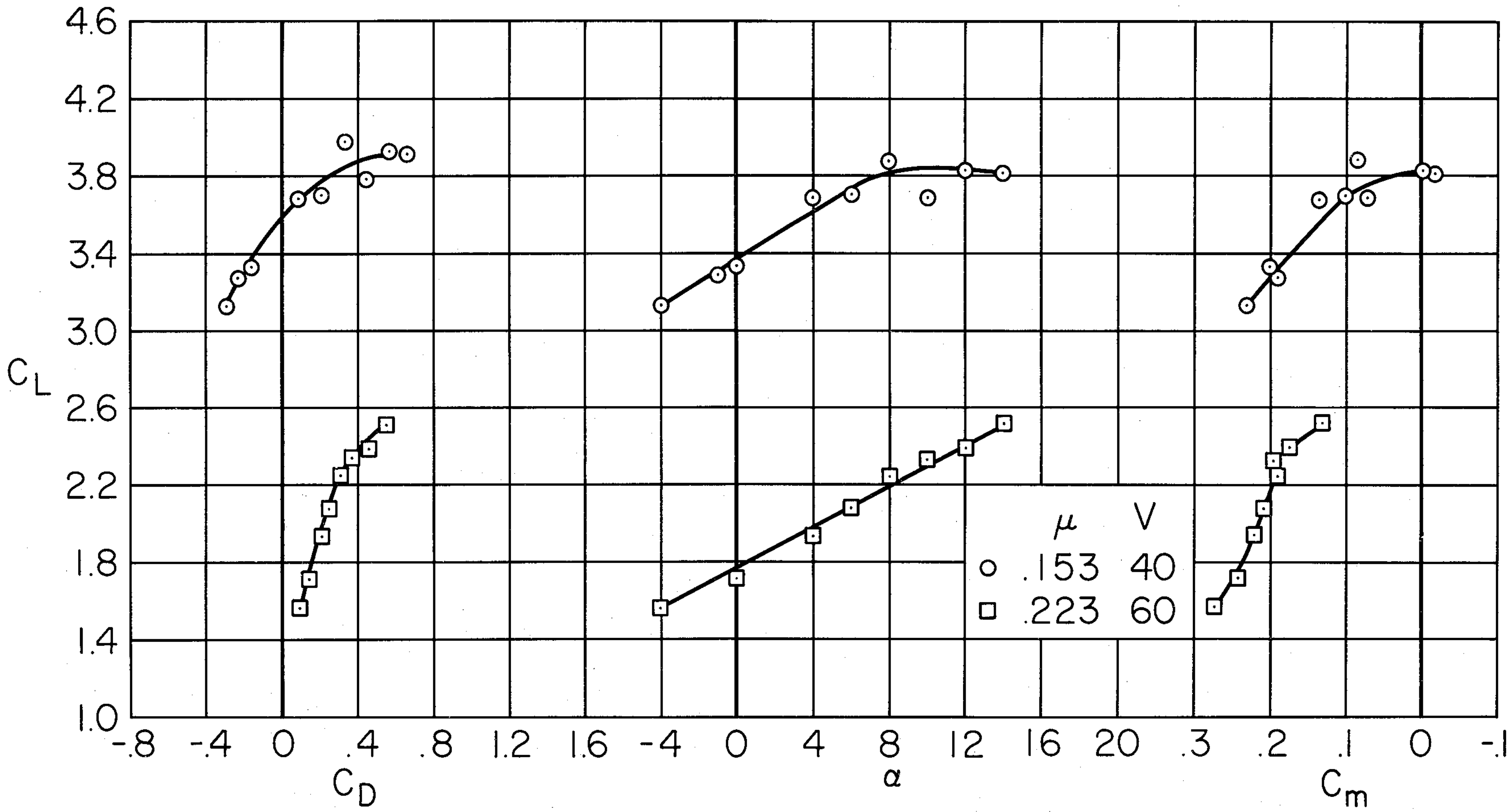

(b) $\beta = 20^{\circ}$

Figure 25.- Continued.

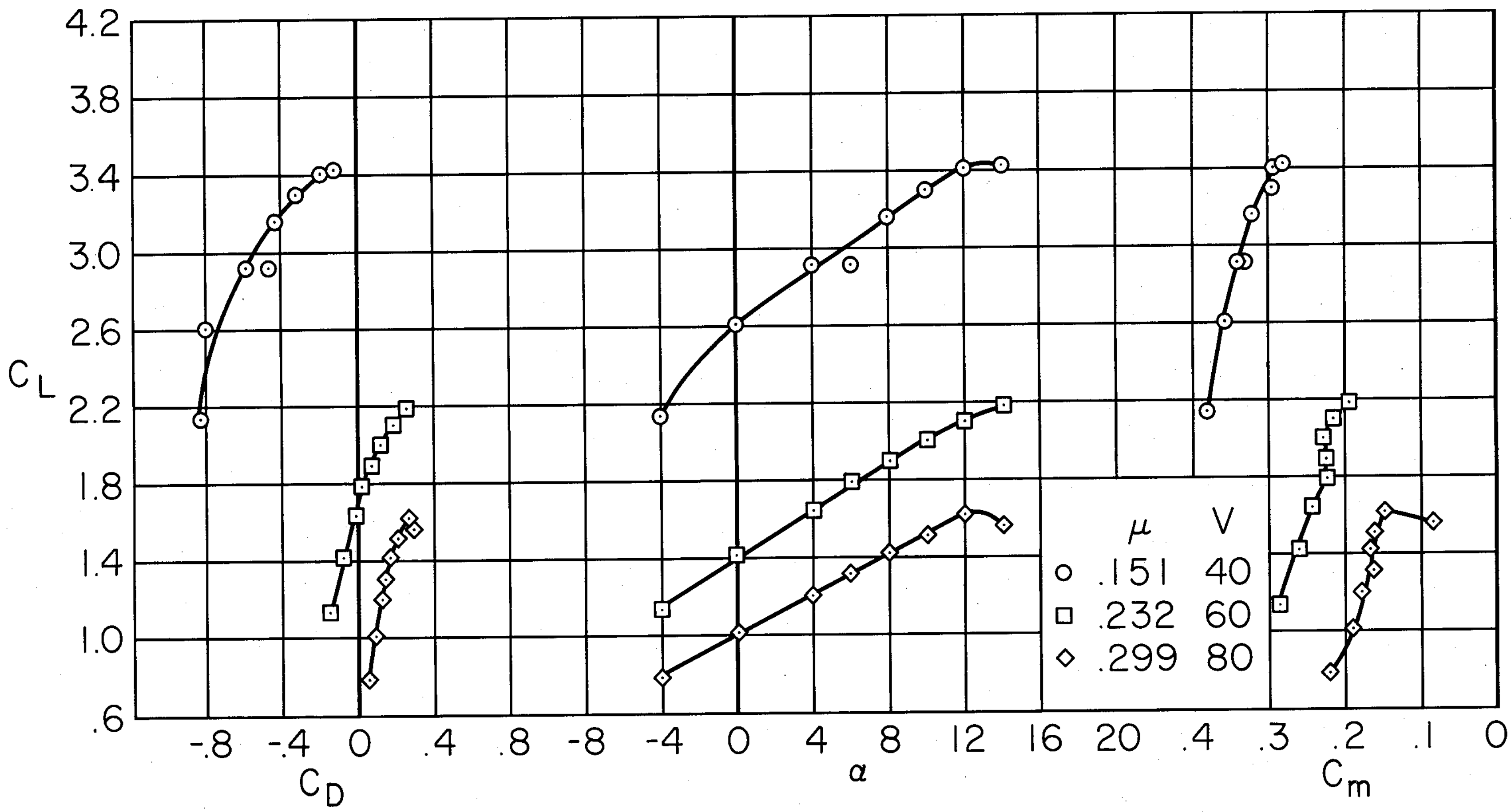

(c) $\beta = 35^{\circ}$

Figure 25.- Concluded.

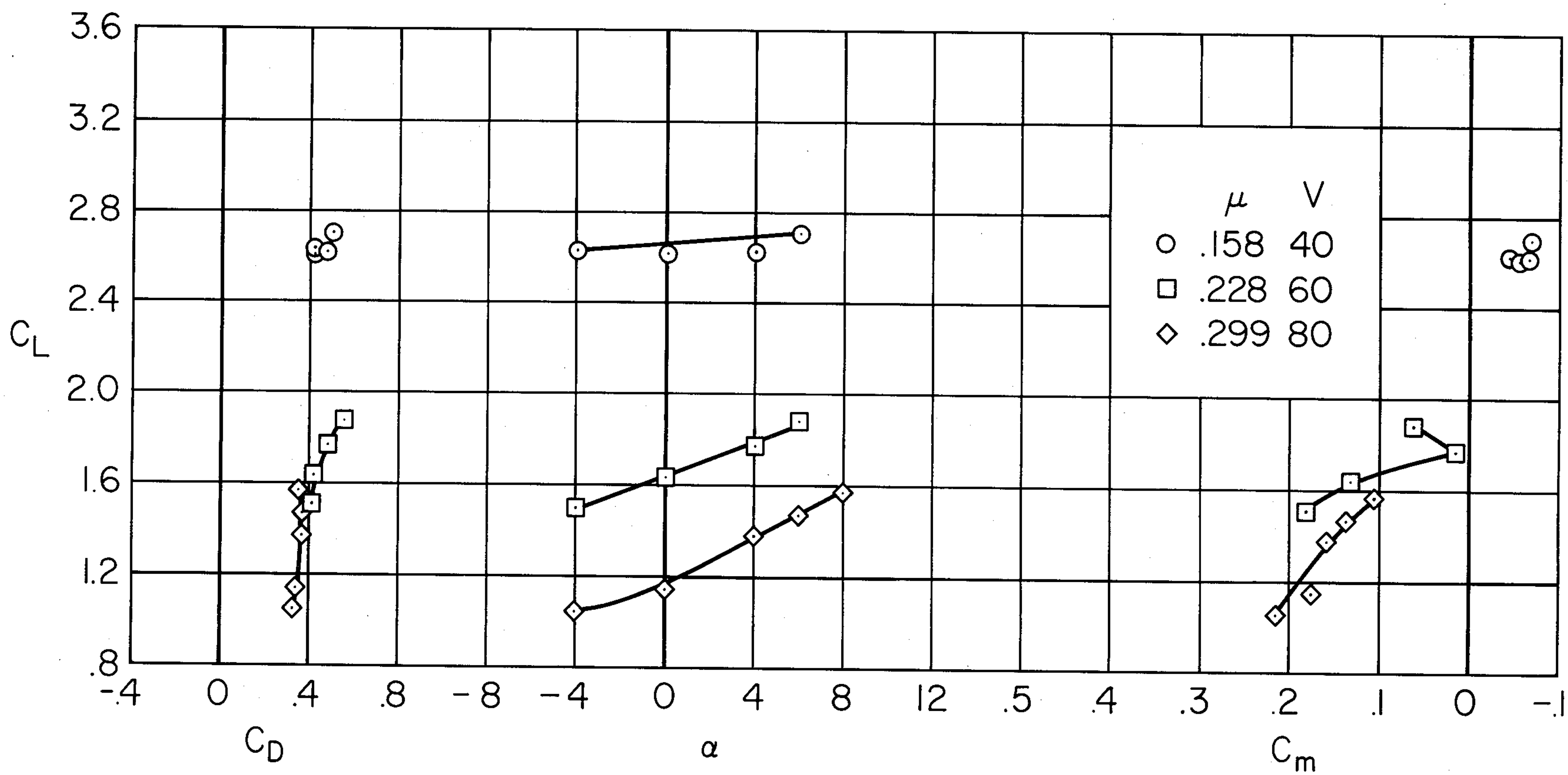

(a) $\beta = 0^{\circ}$

Figure 26.- Longitudinal characteristics with fans operating; $h/D = 1.0$, tail on, $i_t = 0^{\circ}$, $\delta_f = 45^{\circ}$, straight louvers, 1700 RPM.

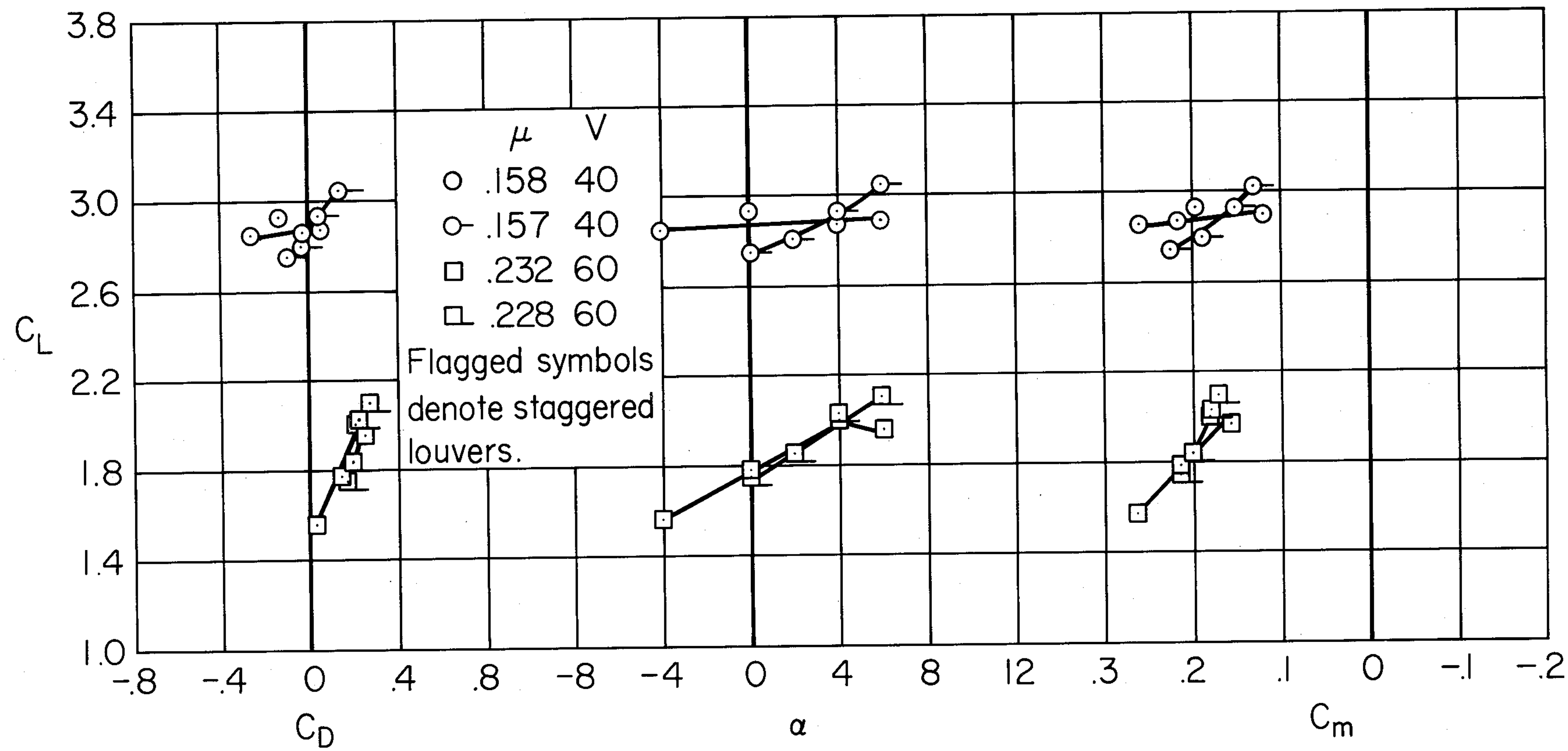

(b) $\beta = 20^{\circ}$

Figure 26.- Continued.

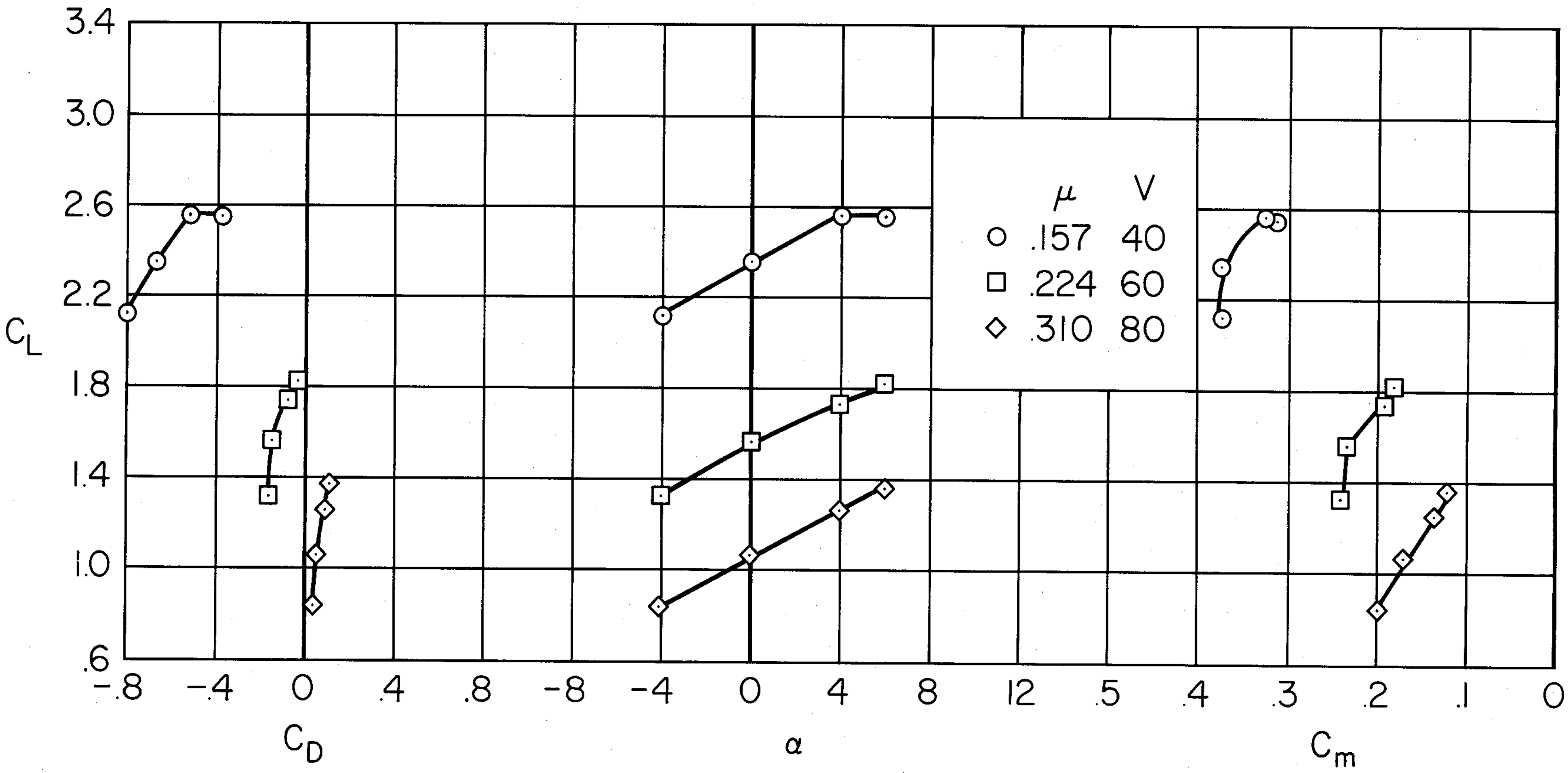

(c) $\beta = 35^{\circ}$

Figure 26.- Concluded.

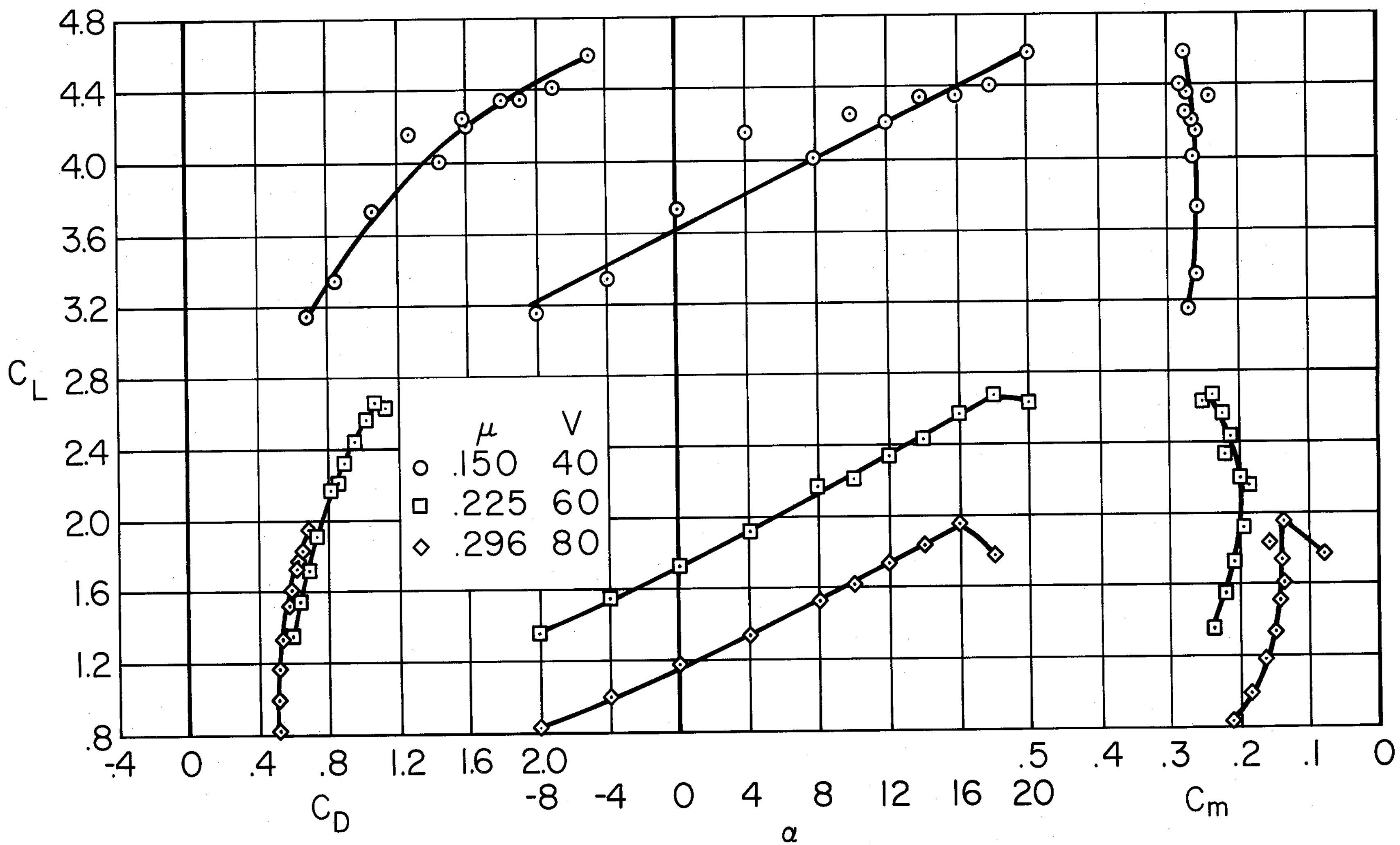

Figure 27.- Longitudinal characteristics with Krüger flaps; $h/D = 3.85$, $\beta = 0^{\circ}$, tail on, $i_t = 0^{\circ}$, $\delta_f = 45^{\circ}$, straight louvers, 1700 RPM.

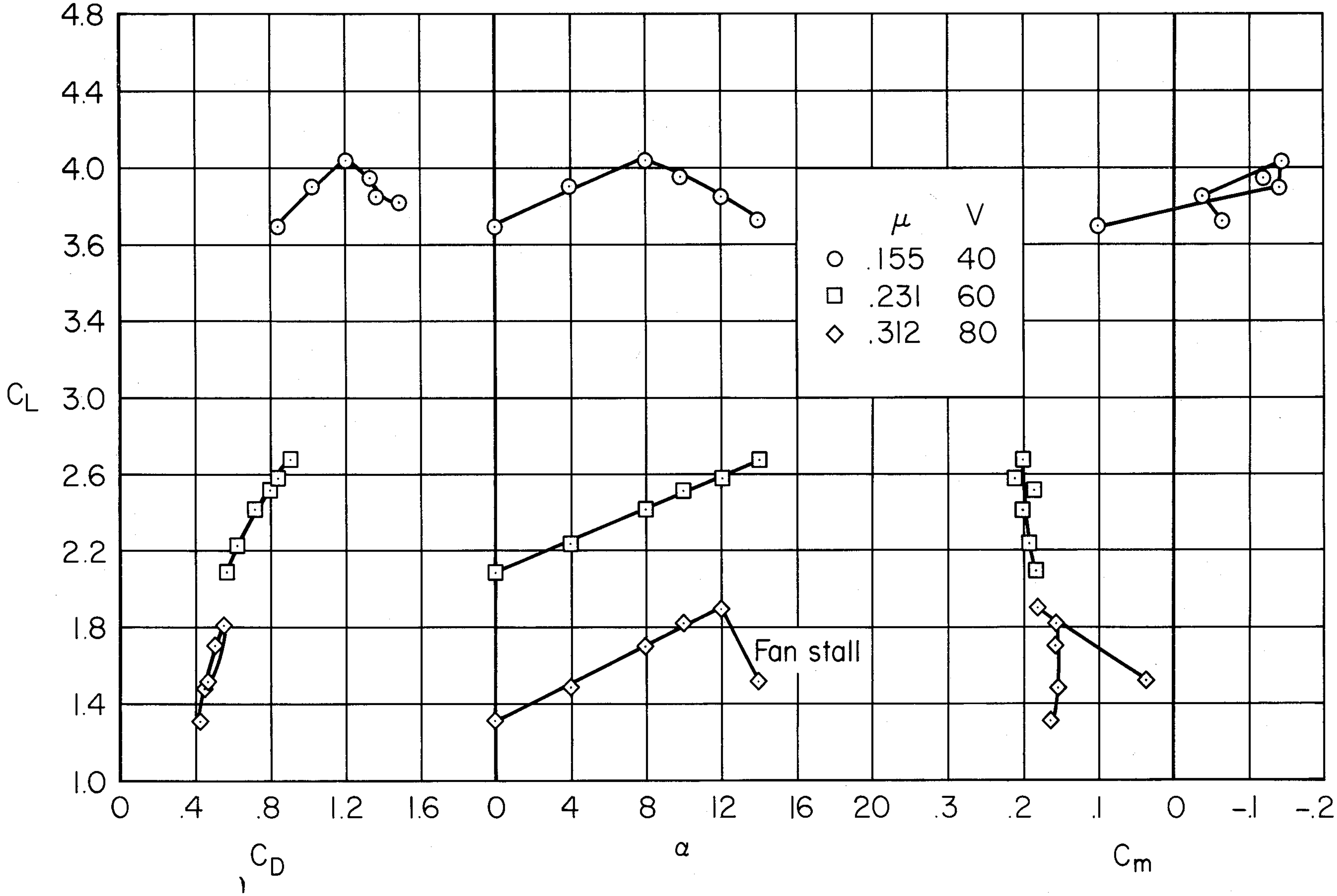

Figure 28.- Longitudinal characteristics with split flaps simulating drooped ailerons; h/D = 2.2, $\beta = 0^{\circ}$, tail on, $i_t = 0^{\circ}$, $\delta_f = 45^{\circ}$, straight louvers, 1700 RPM.

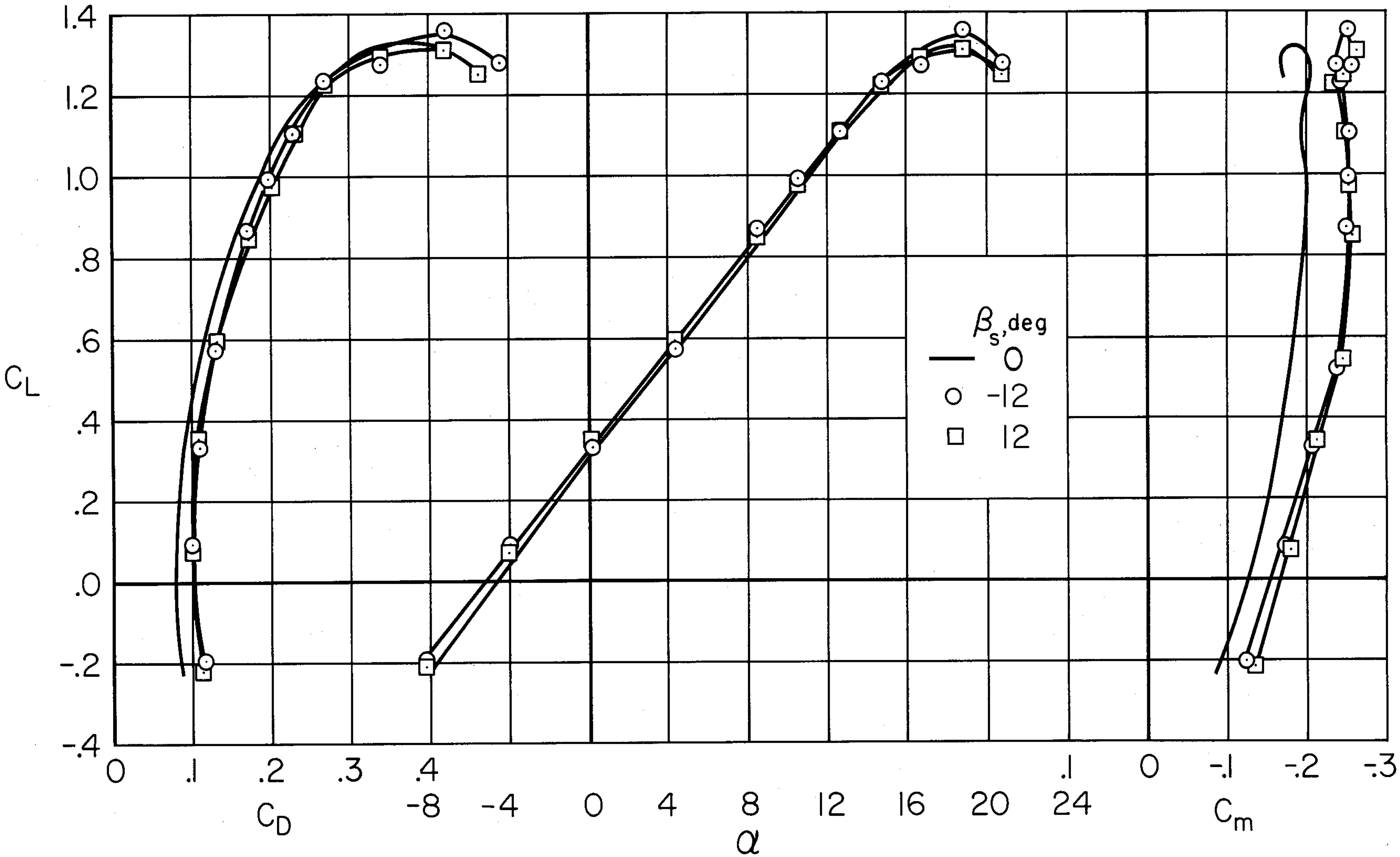

(a) Longitudinal characteristics.

Figure 29.- Effect of sideslip on aerodynamic characteristics; $h/D = 3.85$, $\beta = 90^{\circ}$, inlets sealed, tail on, $i_t = 0^{\circ}$, $\delta_f = 45^{\circ}$, straight louvers, $V = 60$ knots.

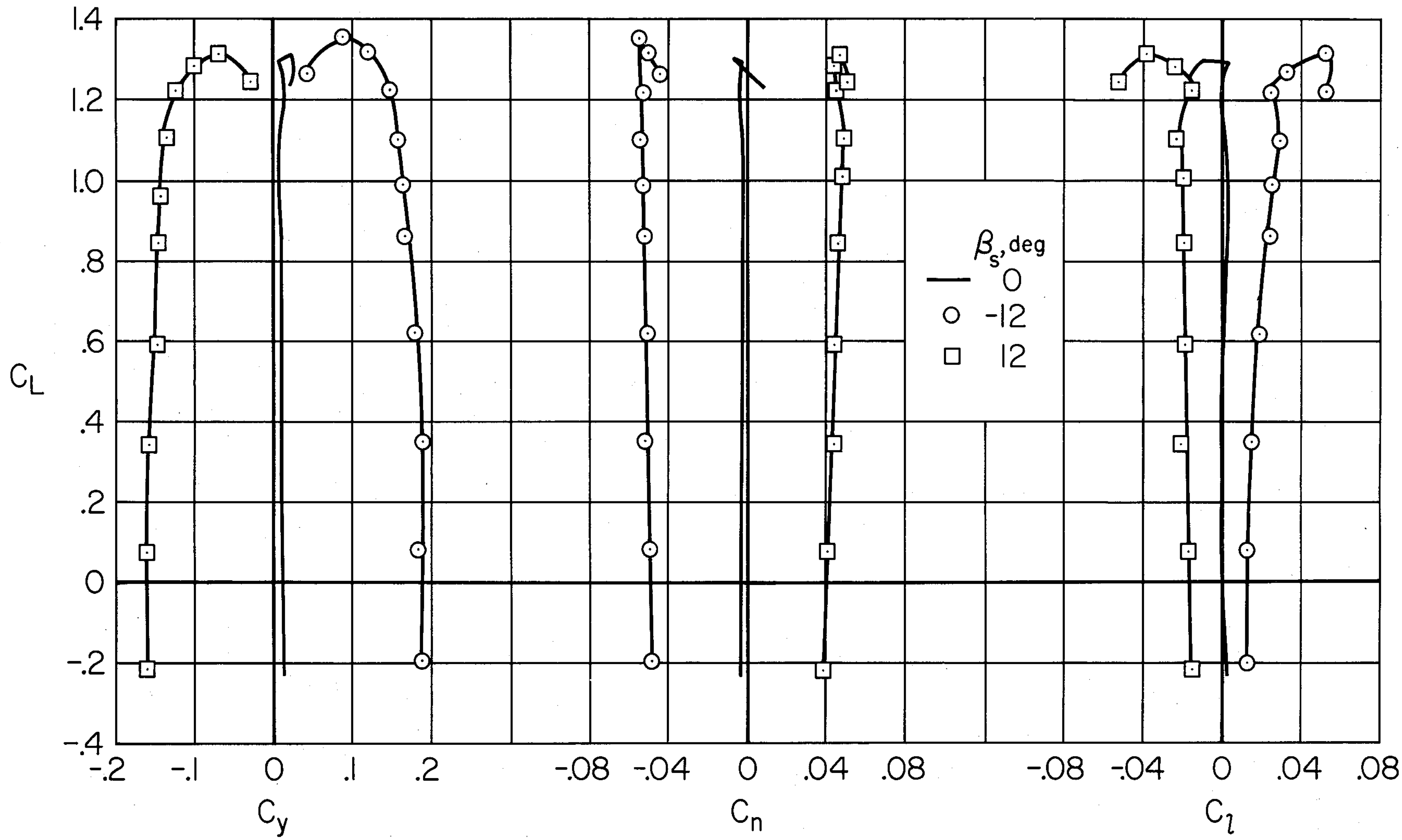

(b) Lateral-directional characteristics.

Figure 29.- Concluded.

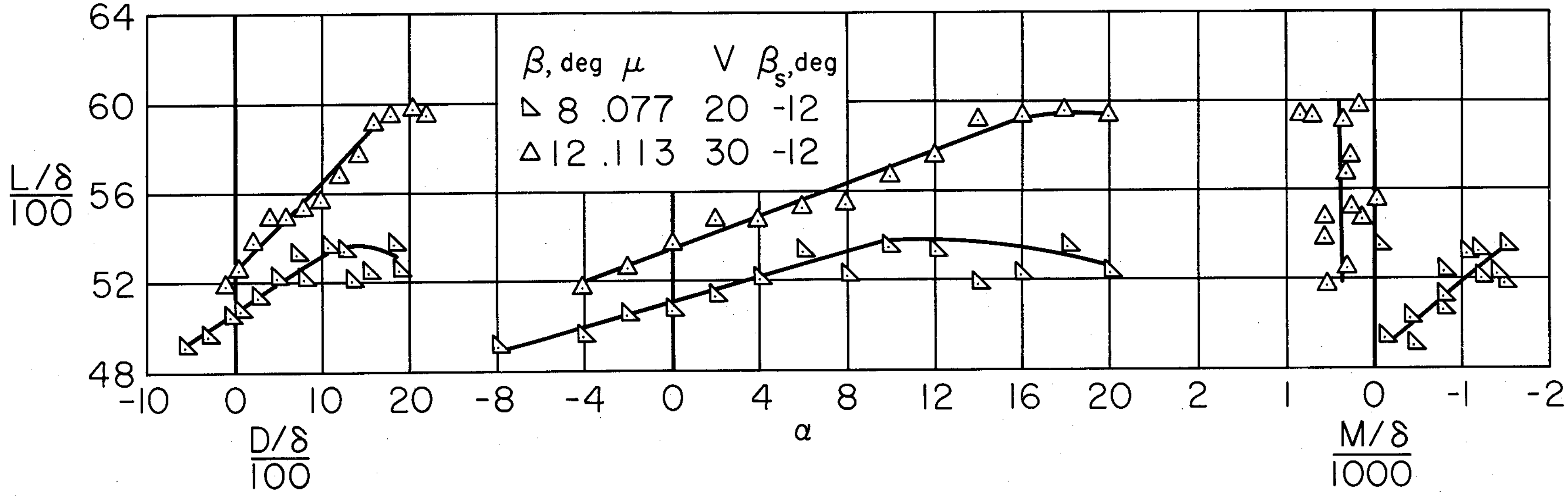

(a) Longitudinal characteristics.

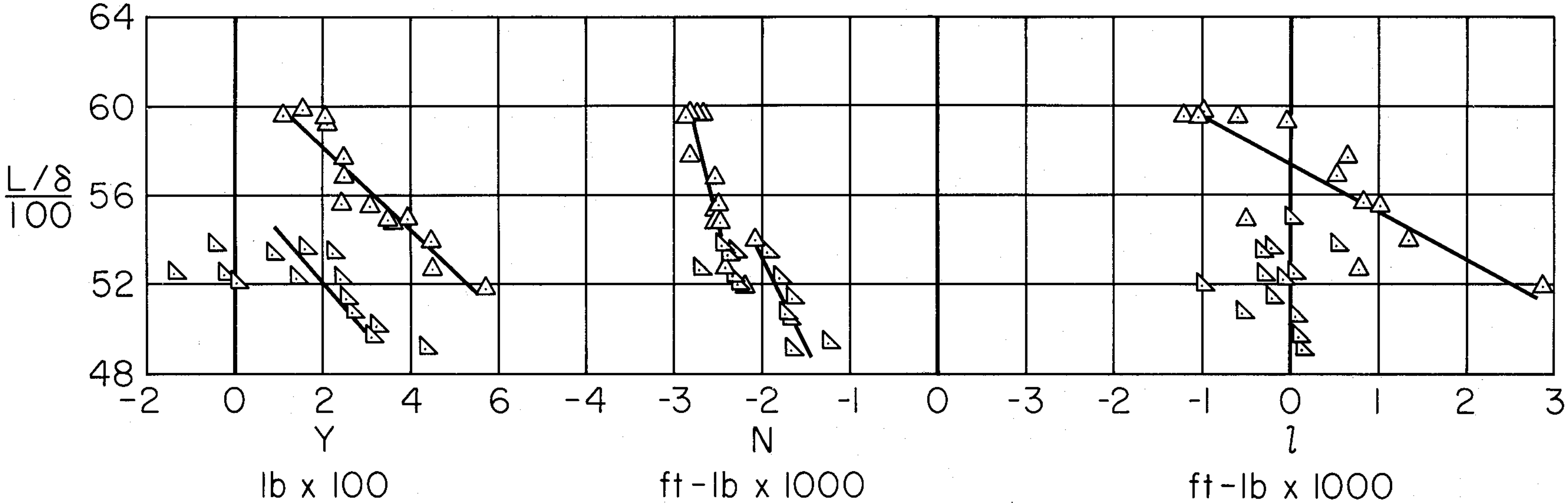

(b) Lateral-directional characteristics.

Figure 30.- Low-speed aerodynamic characteristics at sideslip; $h/D = 3.85$, tail on, $i_t = 20^\circ$, $\delta_f = 45^\circ$, straight louvers, 1700 RPM.

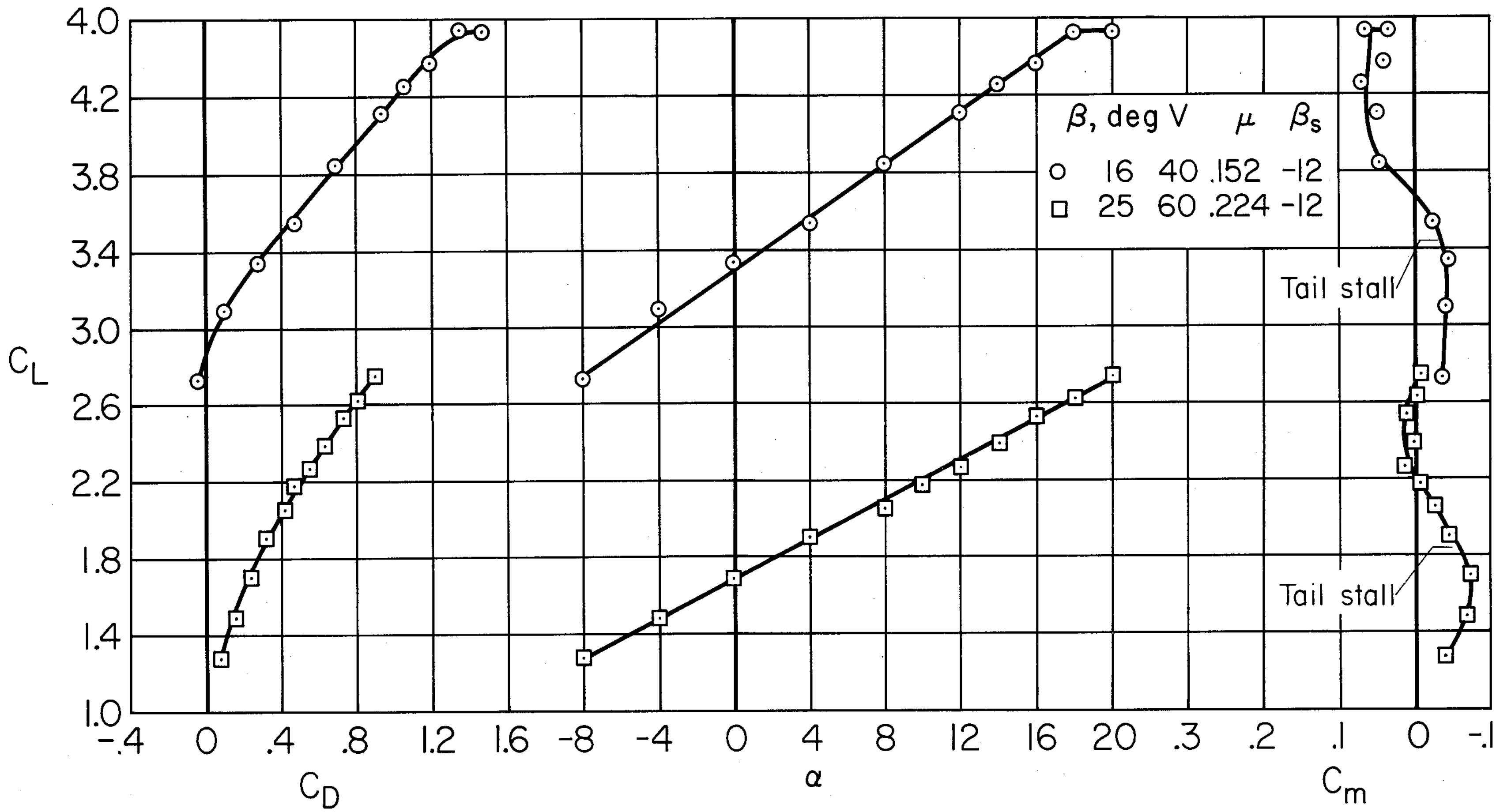

(a) Longitudinal characteristics.

Figure 31.- Aerodynamic characteristics at sideslip; $h/D = 3.85$, tail on, $i_t = 20^{\circ}$, $\delta_f = 45^{\circ}$, straight louvers, 1700 RPM.

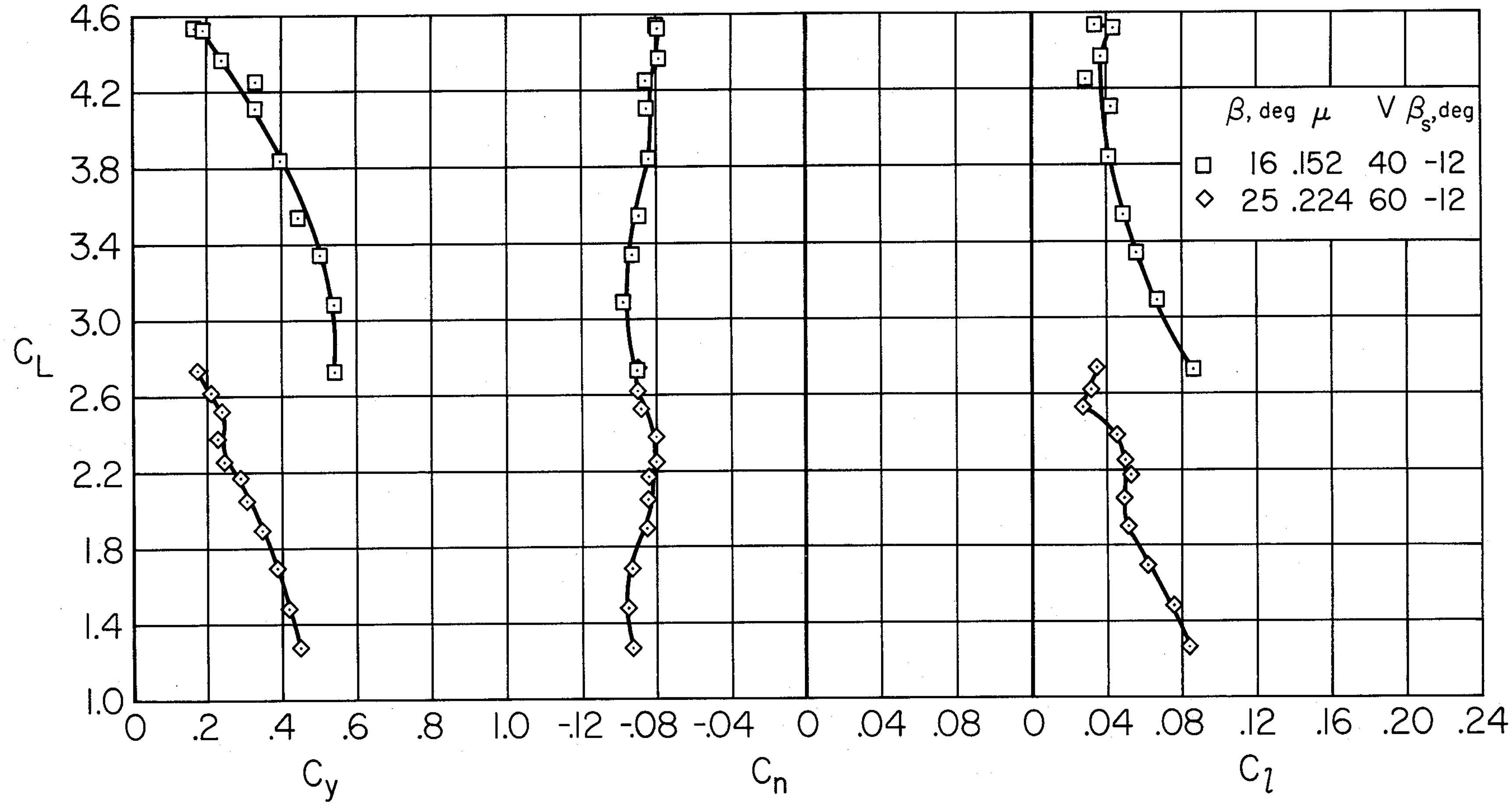

(b) Lateral-directional characteristics.

Figure 31.- Concluded.

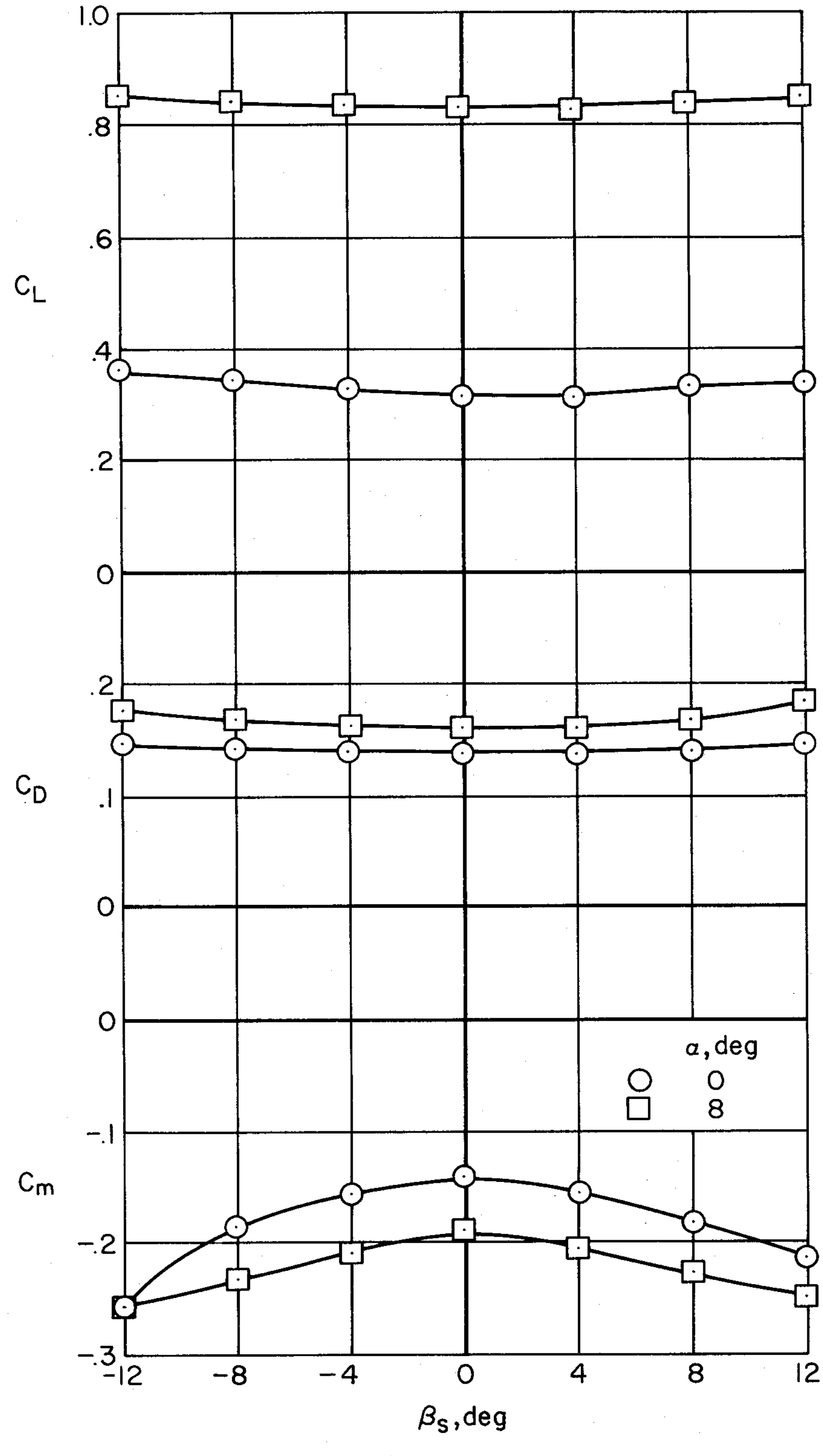

(a) Longitudinal characteristics.

Figure 32.- Effect of sideslip on power off aerodynamic characteristics; $h/D = 3.85$, $\beta = 90^\circ$, inlets sealed, tail on, $i_t = 0^\circ$, $\delta_f = 45^\circ$, $V = 80$ knots.

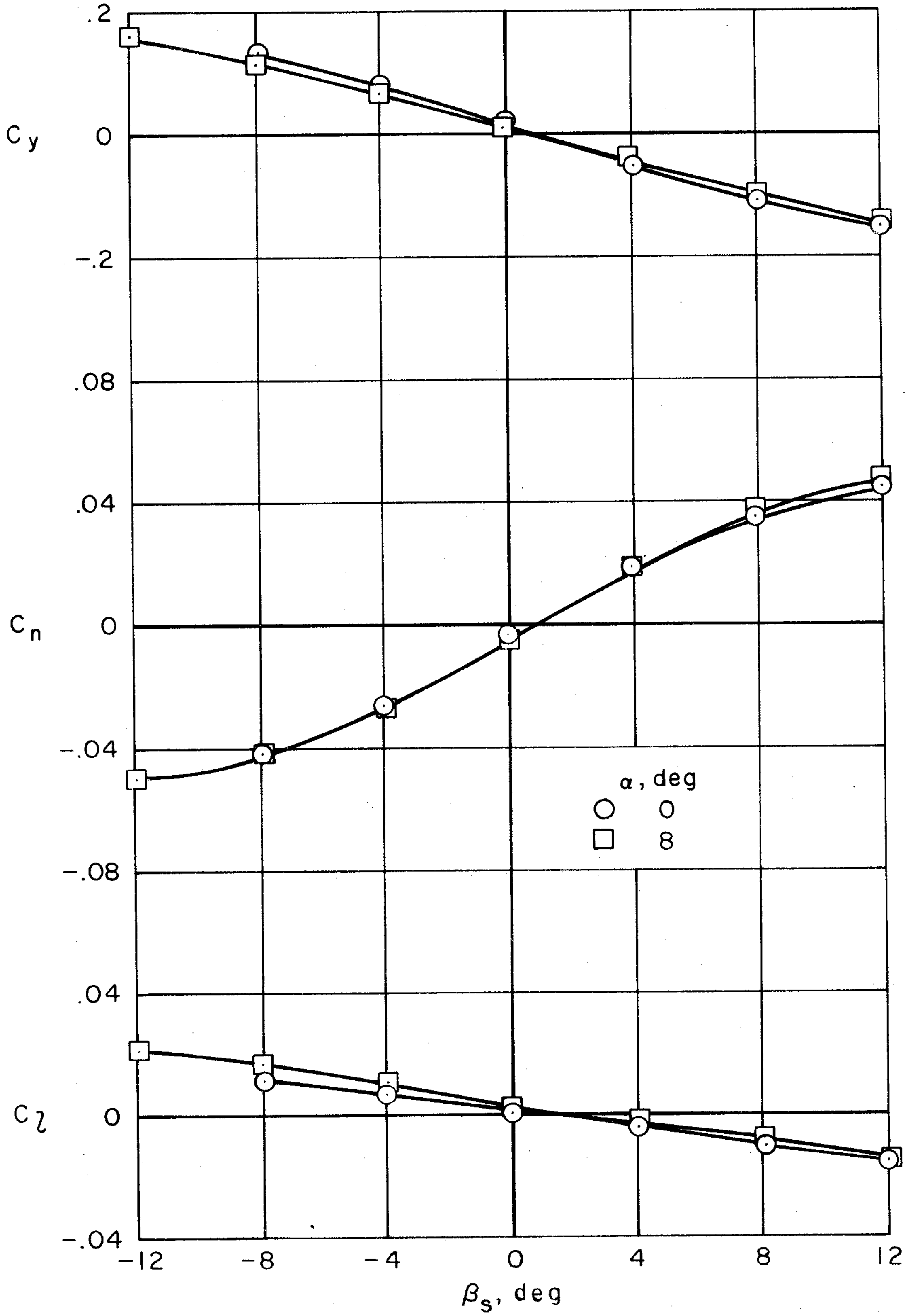

(b) Lateral-directional characteristics.

Figure 32.- Concluded.

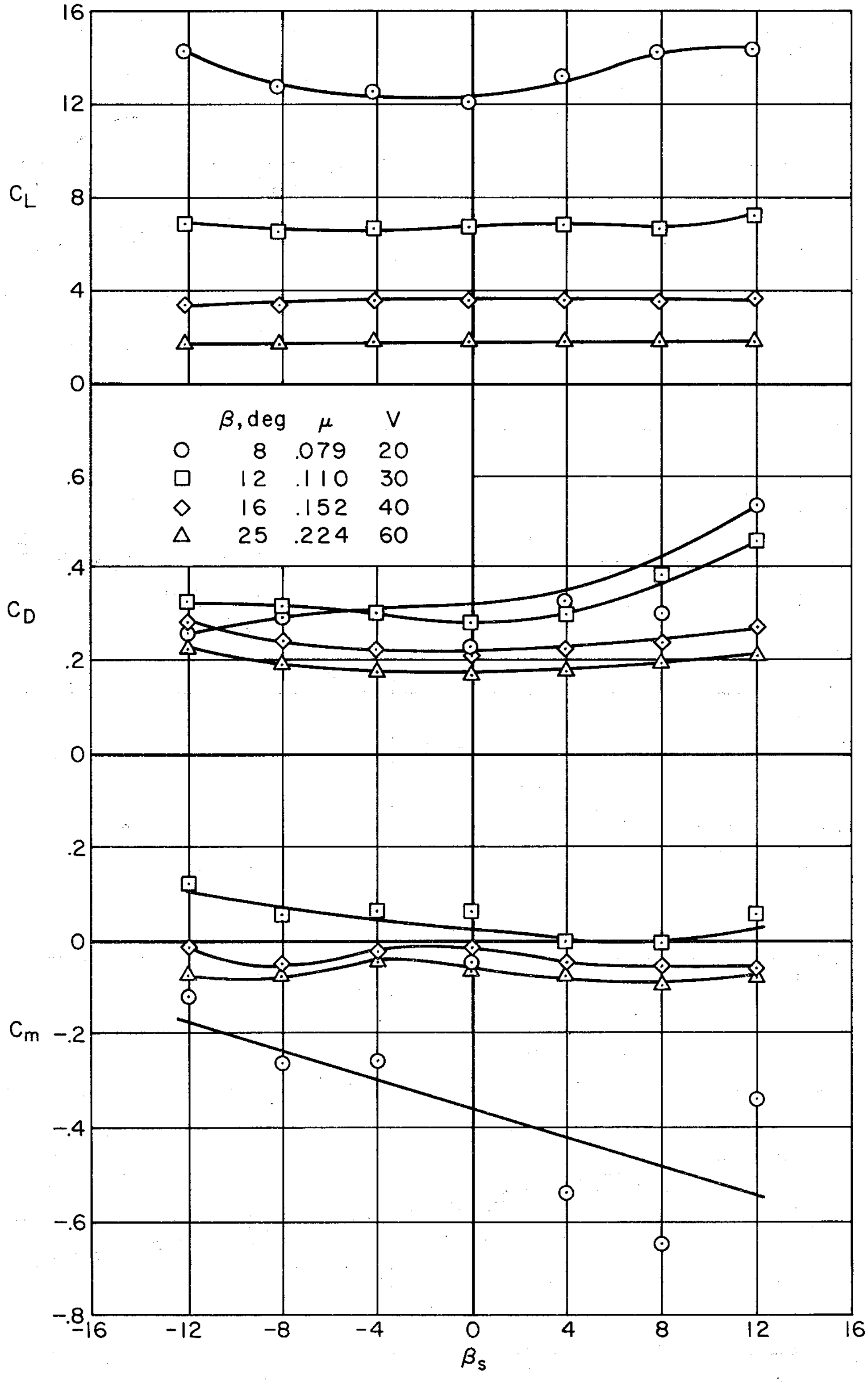

(a) Longitudinal characteristics.

Figure 33.- Effect of sideslip on aerodynamic characteristics; $h/D = 3.85$, $\alpha = 0^{\circ}$, tail on, $i_t = 20^{\circ}$, $\delta_f = 45^{\circ}$, straight louvers, 1700 RPM.

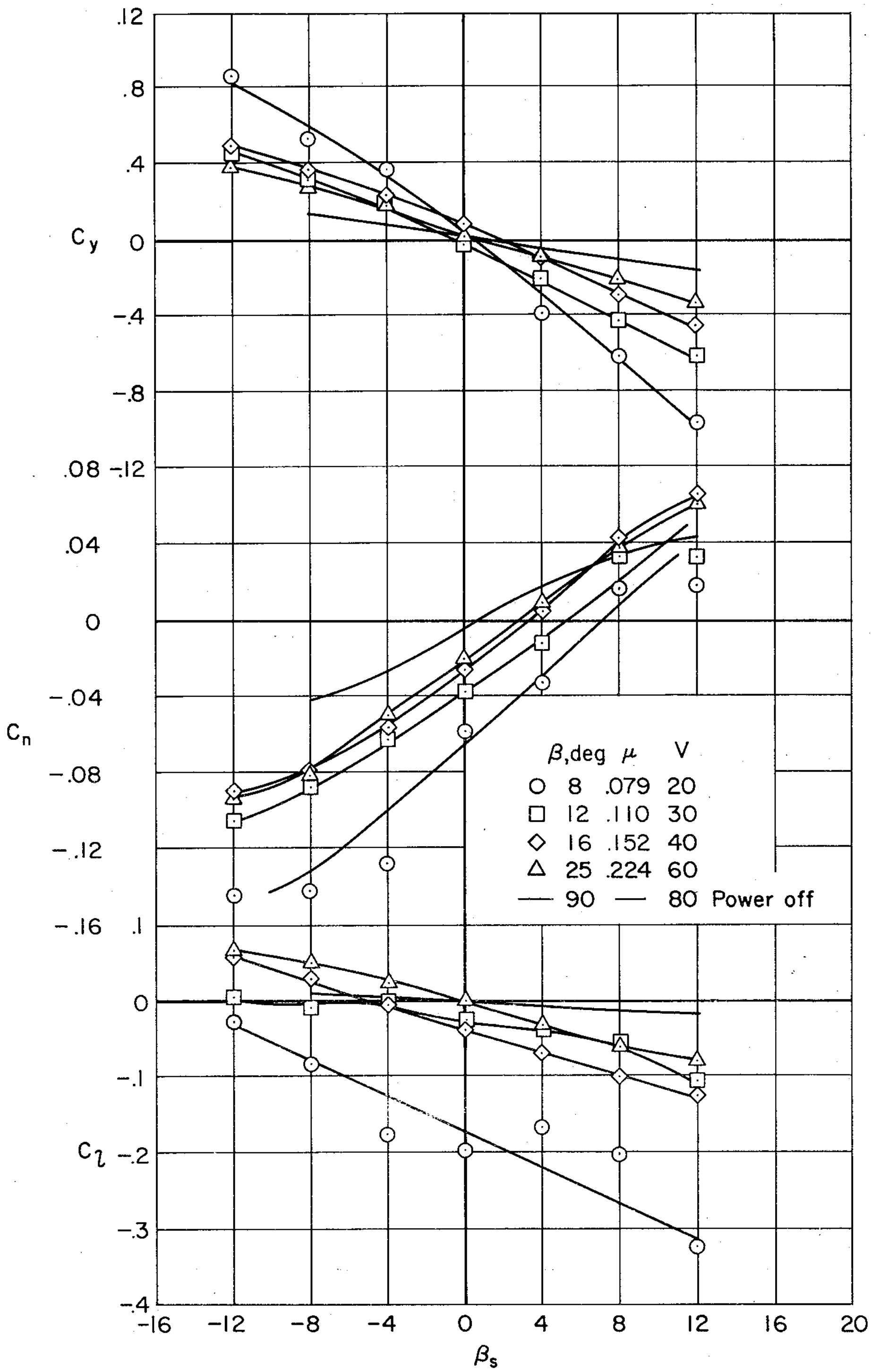

(b) Lateral-directional characteristics.

Figure 33.- Concluded.

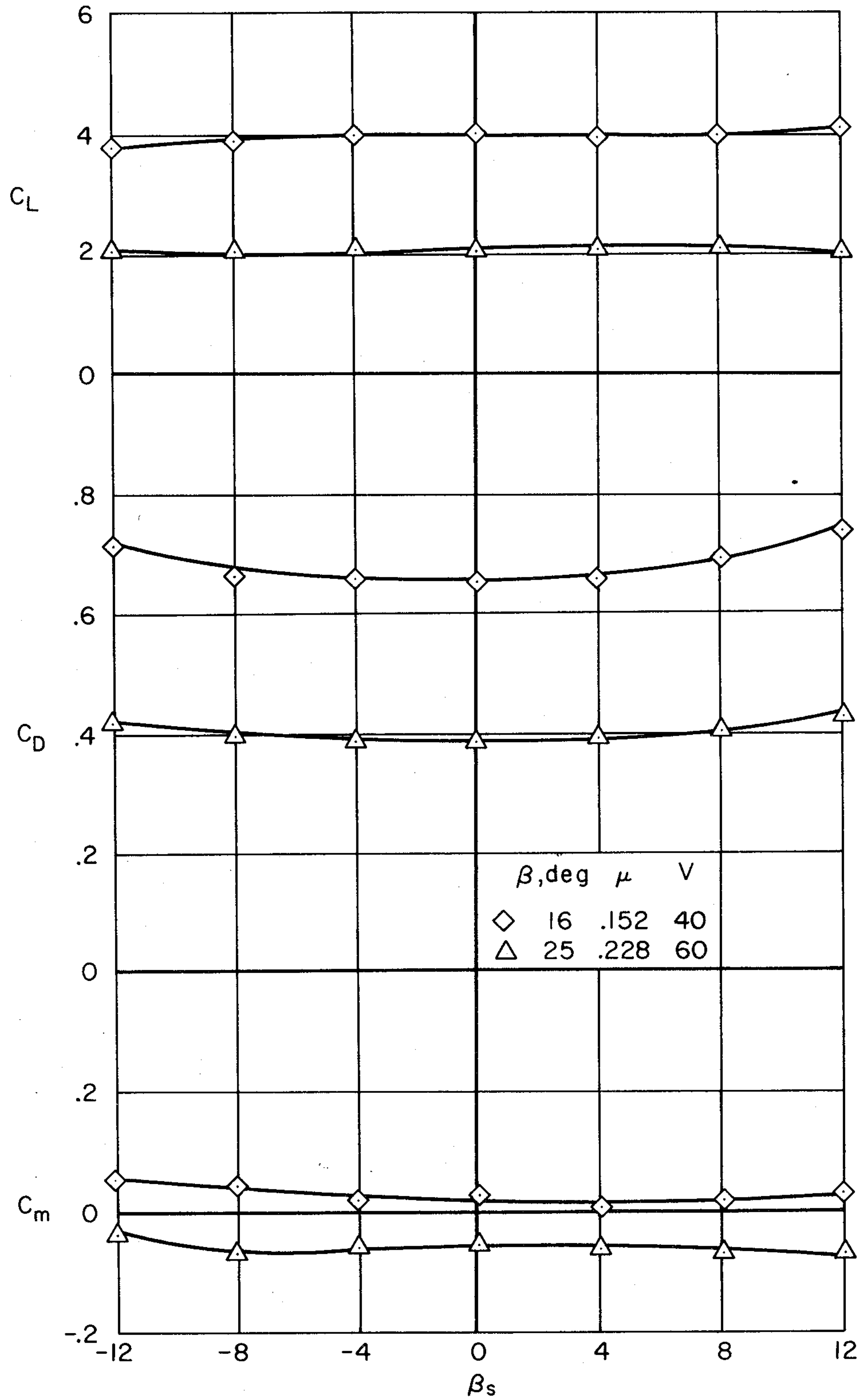

(a) Longitudinal characteristics.

Figure 34.- Effect of sideslip on aerodynamic characteristics; $h/D = 3.85$, $\alpha = 8^\circ$, tail on, $i_t = 20^\circ$, $\delta_f = 45^\circ$, straight louvers, 1700 RPM.

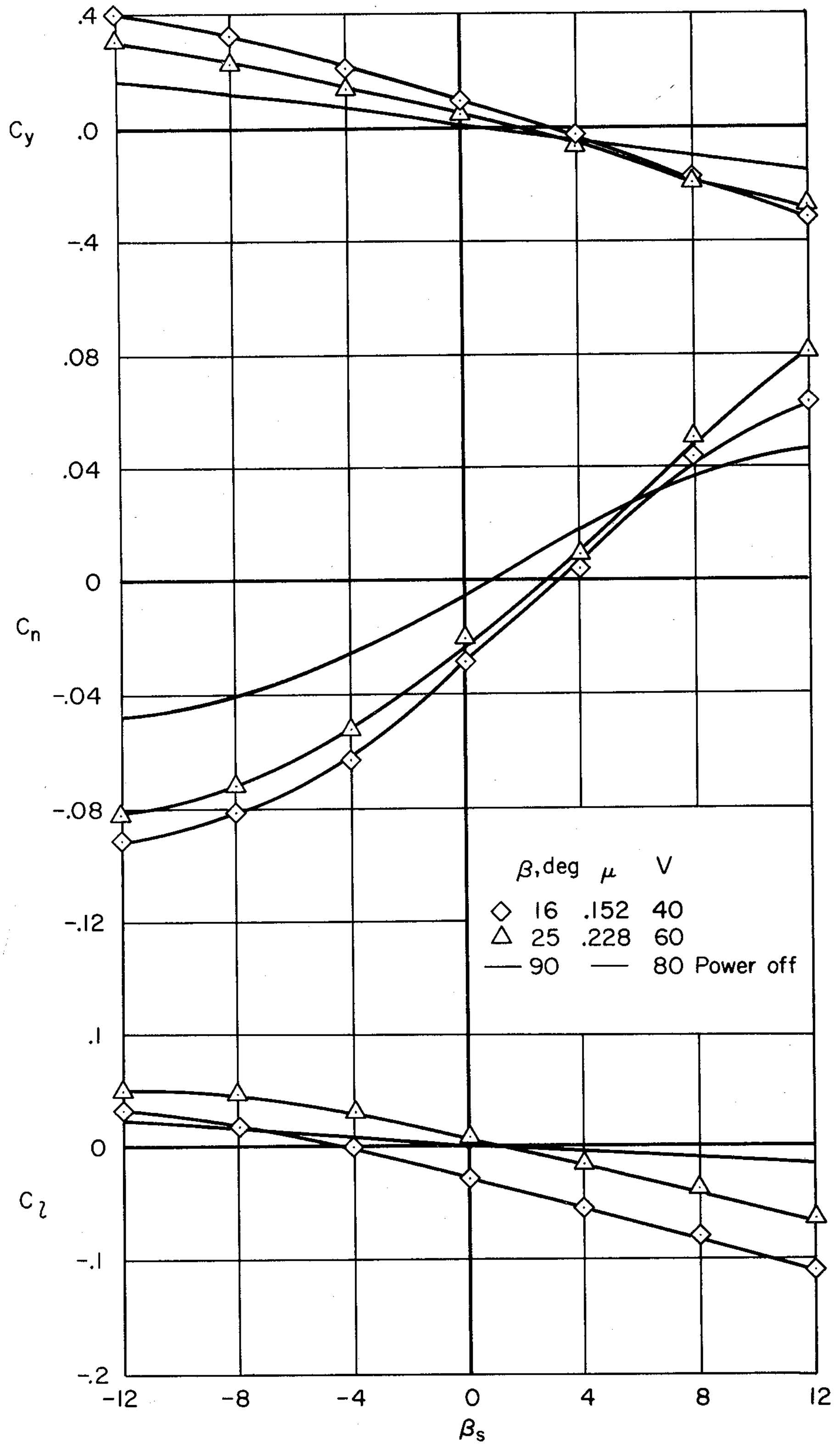

(b) Lateral-directional characteristics.

Figure 34.- Concluded.

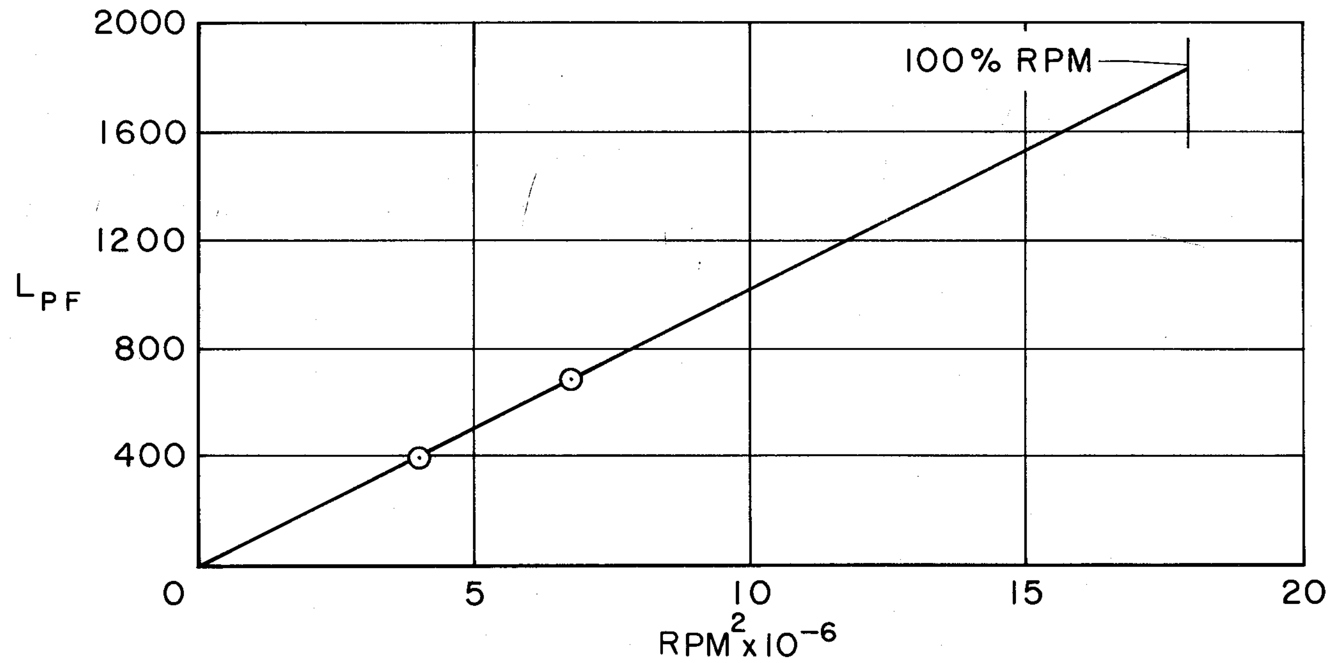

(a) Variation of lift with RPM; $\delta_m = 0^\circ$.

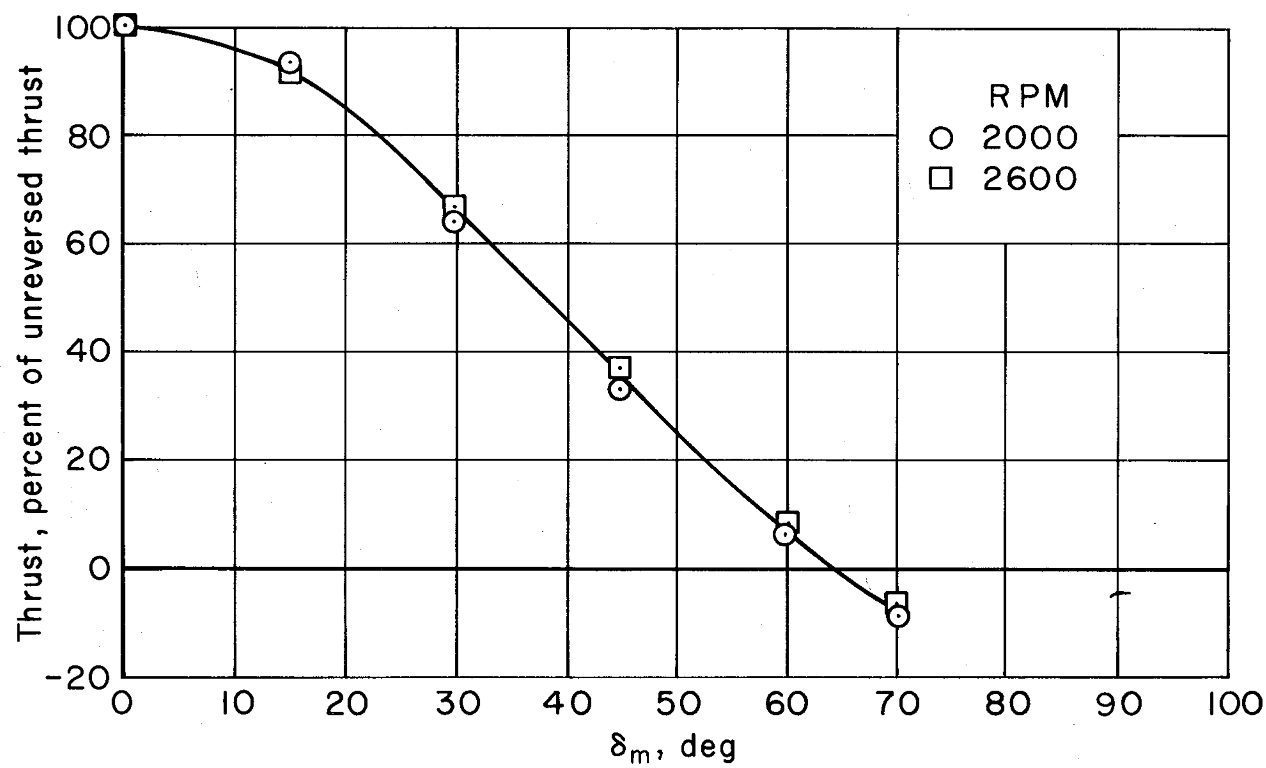

(b) Characteristics of the thrust modulator.

Figure 35.- Zero airspeed performance of the pitch fan; $\alpha = 0^\circ$.

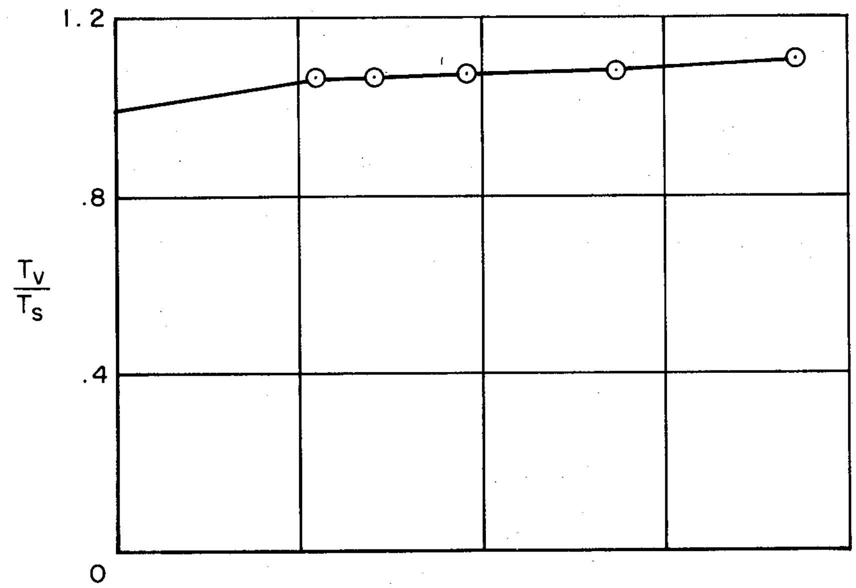

(a) Variation of fan thrust with forward speed.

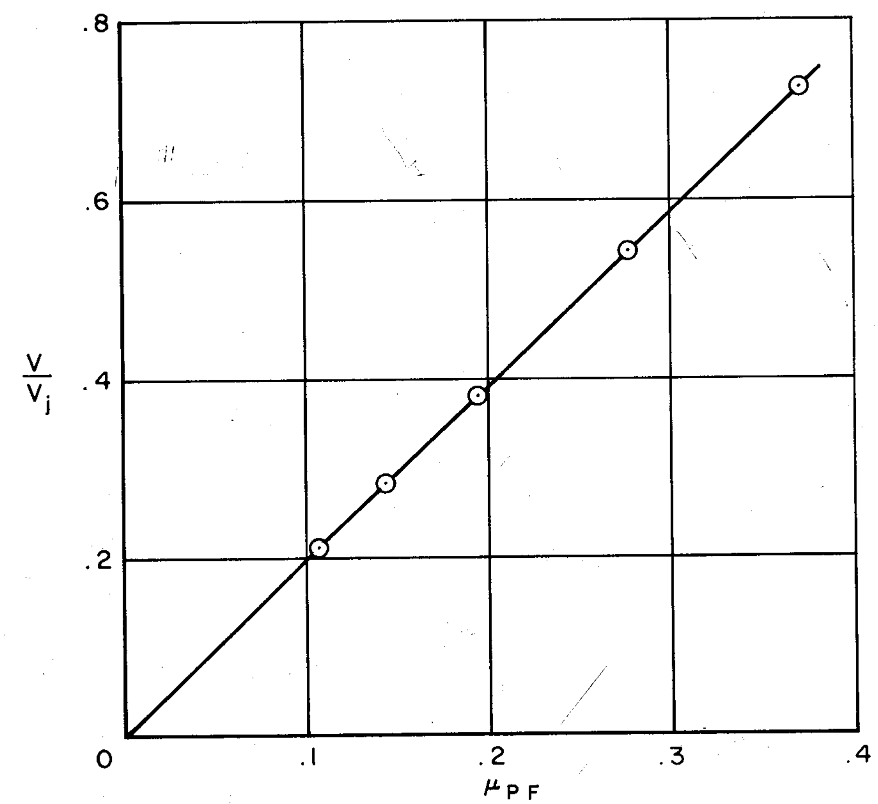

(b) Relationship between tip-speed ratio and velocity ratio.

Figure 36.- Installed characteristics of the pitch fan with forward speed; $\alpha = 0^\circ$, $\delta_m = 0^\circ$.

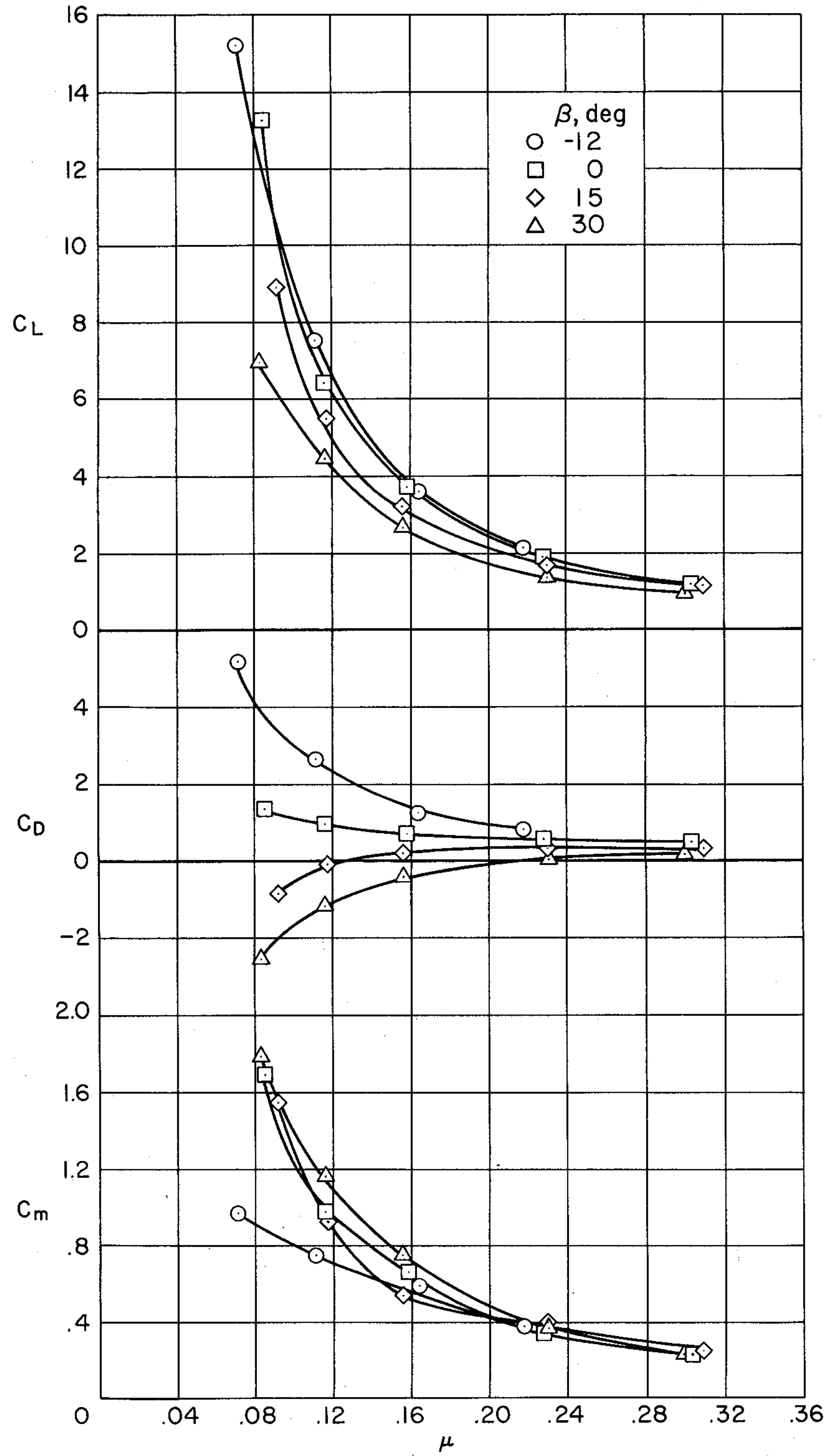

(a) $\delta_f = 45^\circ$, $\delta_m = 0^\circ$

Figure 37.- Variation of longitudinal characteristics with tip-speed ratio; $h/D = 2.2$, $\alpha = 0^\circ$, tail off, staggered louvers, lift fan RPM = 1700, pitch fan RPM = 2400.

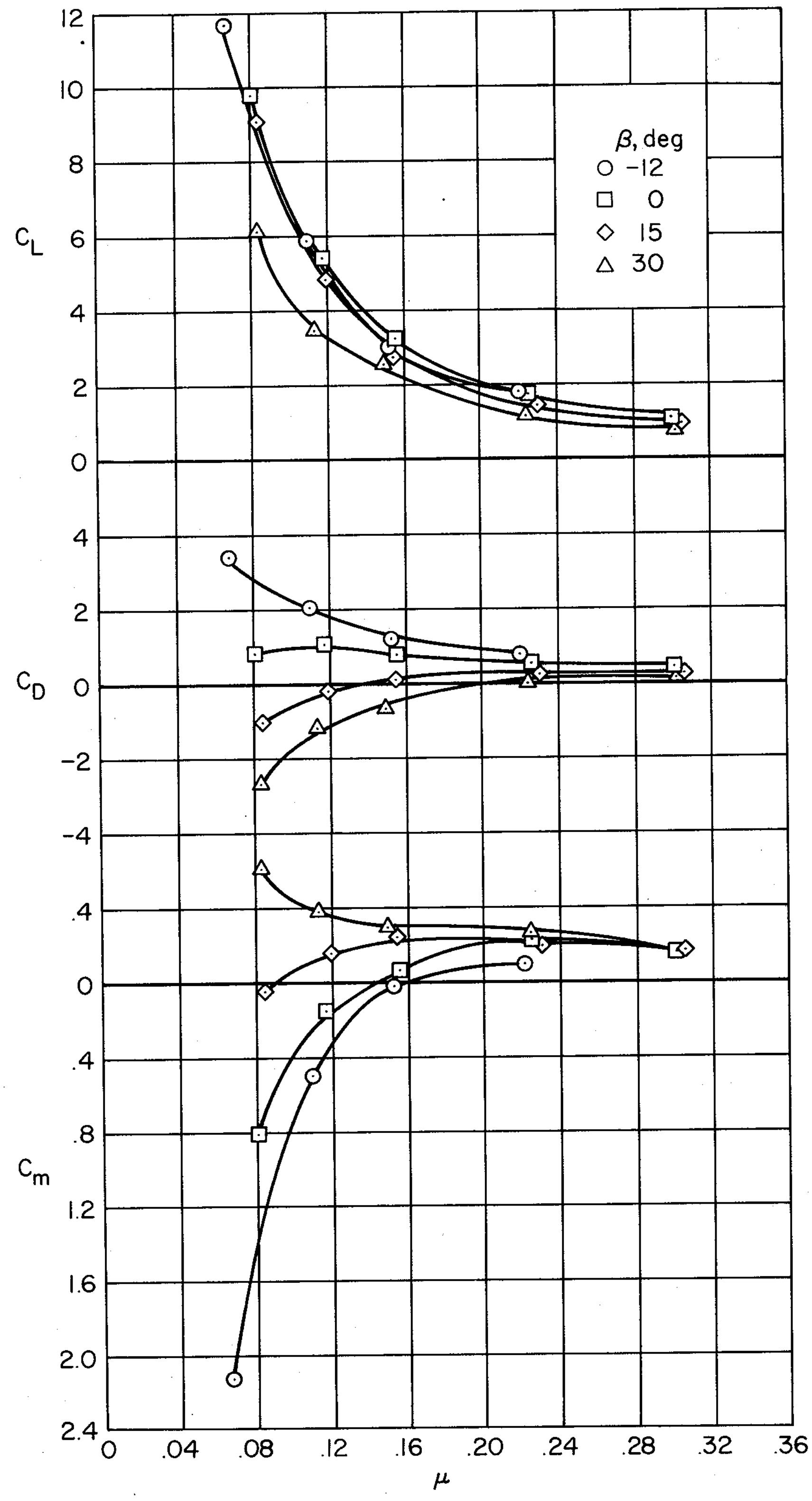

(b) $\delta_f = 0^\circ$, $\delta_m = 60^\circ$

Figure 37.- Concluded.

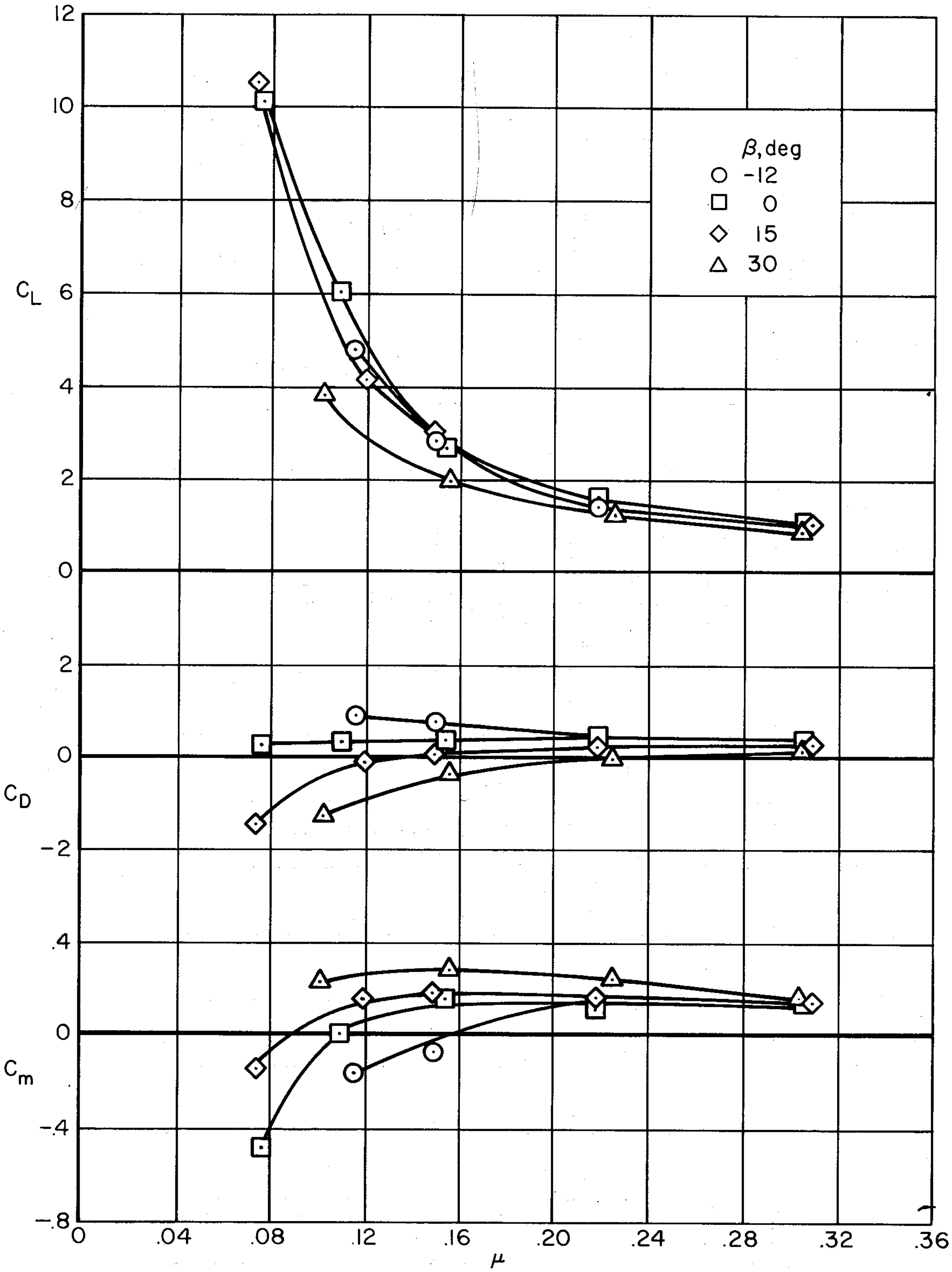

(a) $\delta_f = 0^\circ$, $\delta_m = 60^\circ$

Figure 38.- Variation of longitudinal characteristics with tip-speed ratio; h/D = 1.0, tail off, staggered louvers, lift fan RPM = 1700, pitch fan RPM = 2400.

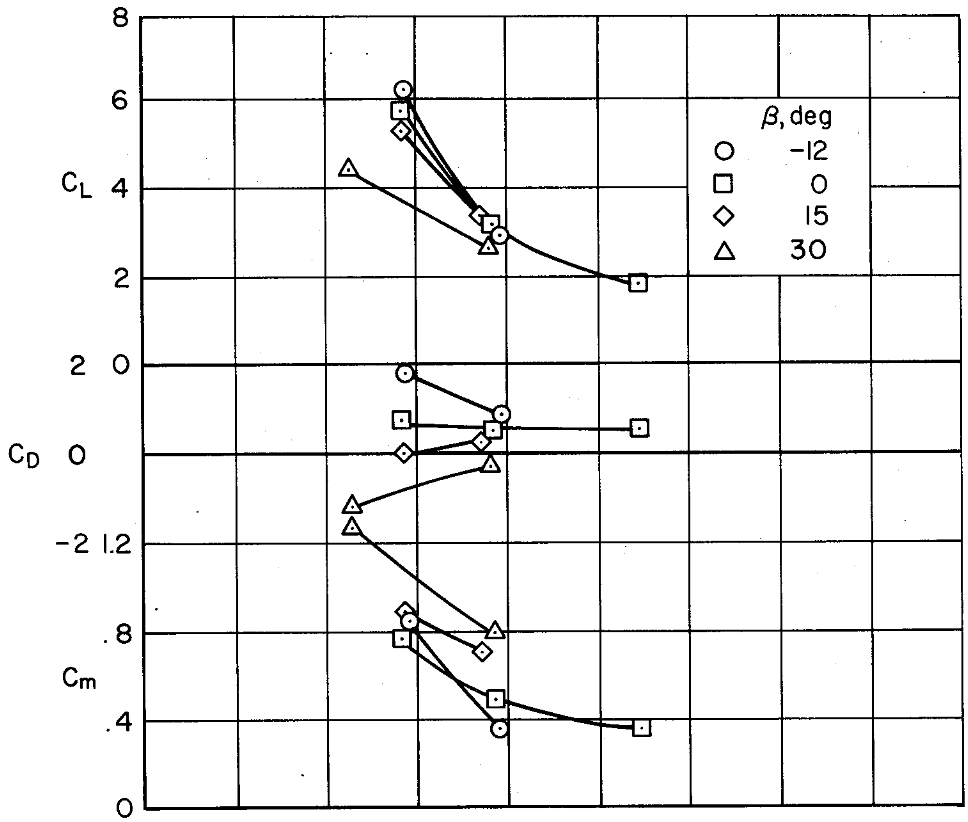

(b) $\delta_f = 45^{\circ}$, $\delta_m = 0^{\circ}$

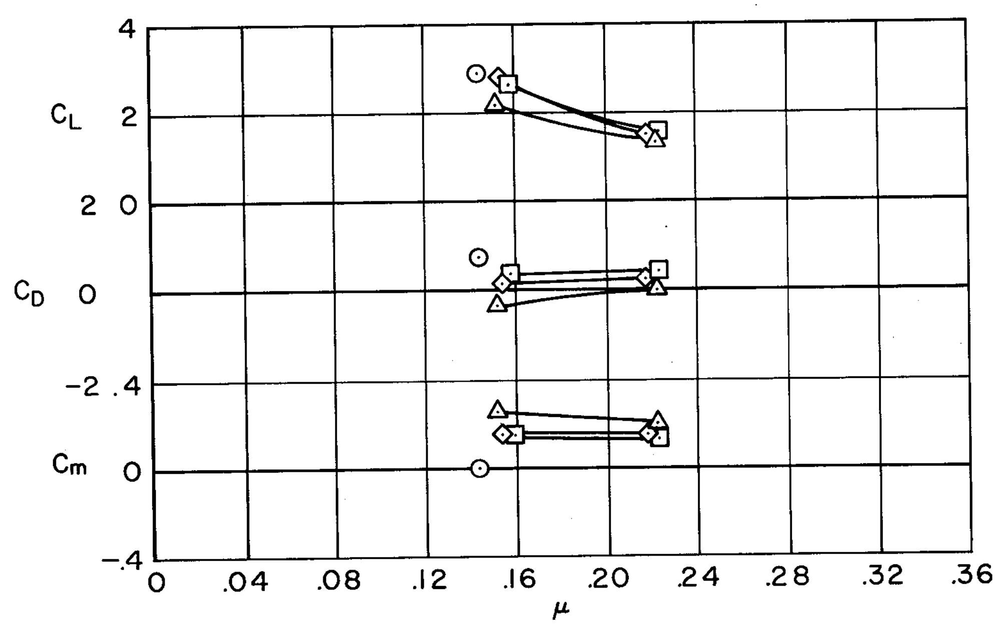

(c) $\delta_f = 45^{\circ}$, $\delta_m = 60^{\circ}$

Figure 38.- Continued.

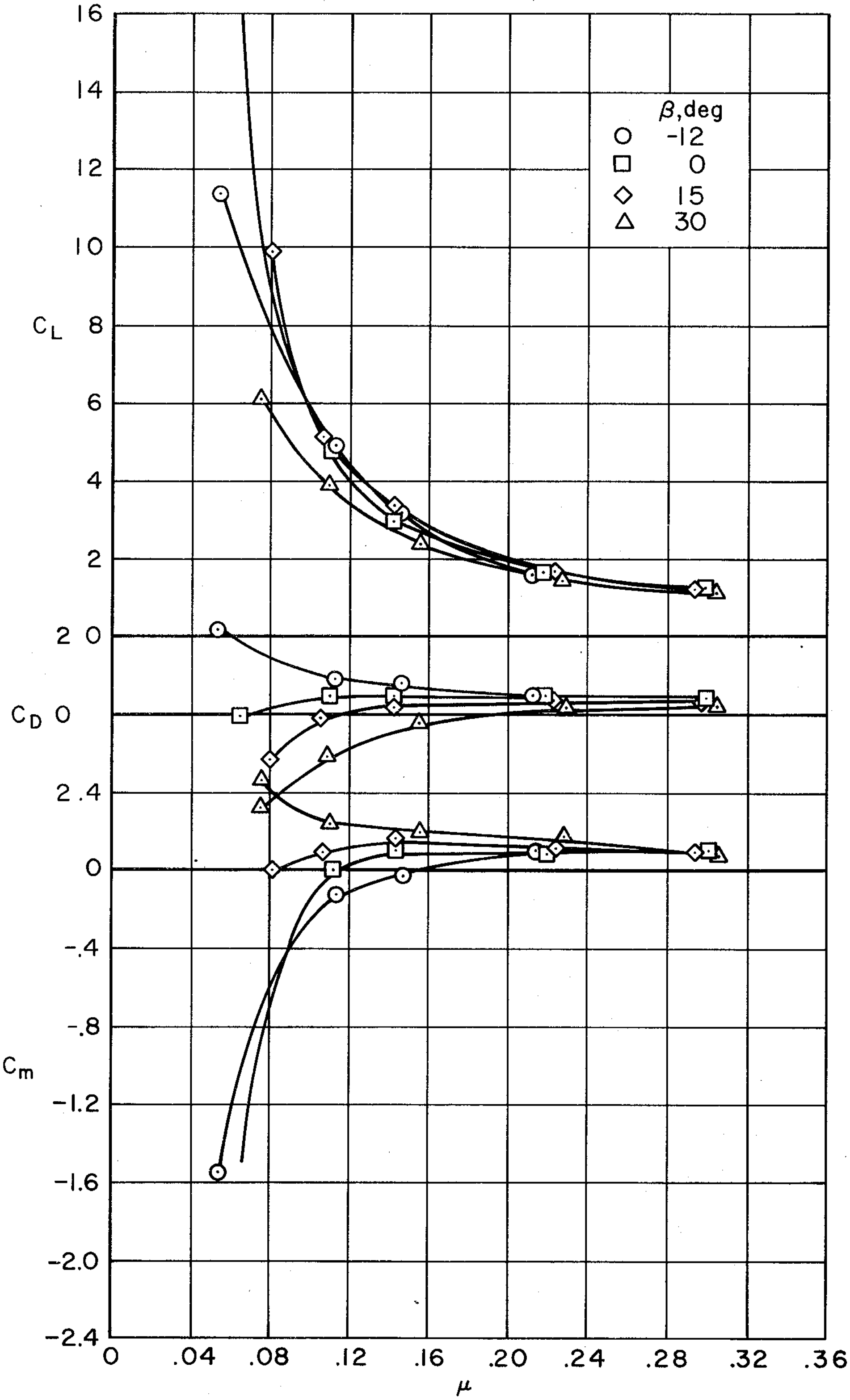

(d) $\delta_f = 45^o$, $\delta_m = 60^o$, split flaps.

Figure 38.- Concluded.

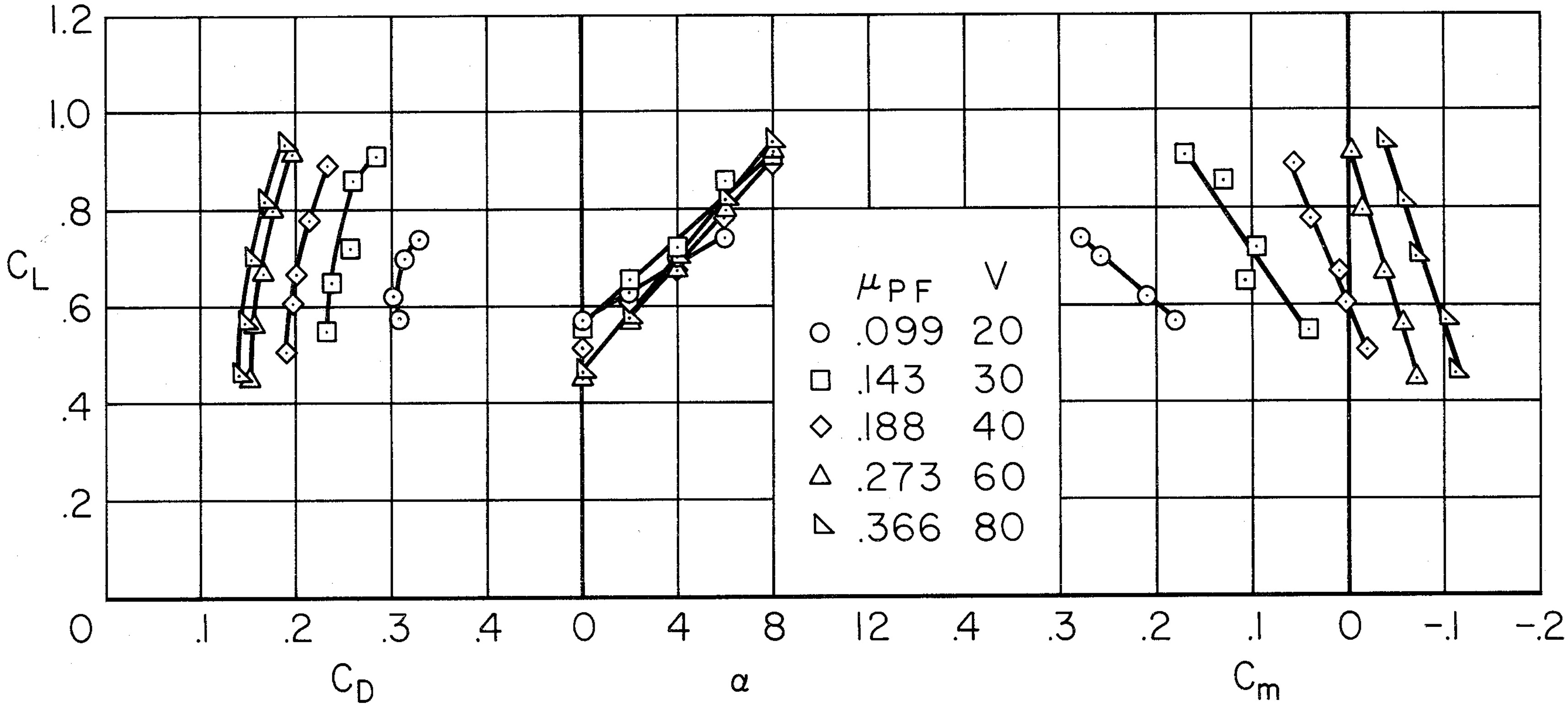

Figure 39.- Longitudinal characteristics with only the pitch fan operating; h/D = 2.2, $\beta = 90^\circ$, inlets sealed, $\delta_m = 60^\circ$, tail off, $\delta_f = 45^\circ$, 2400 RPM.

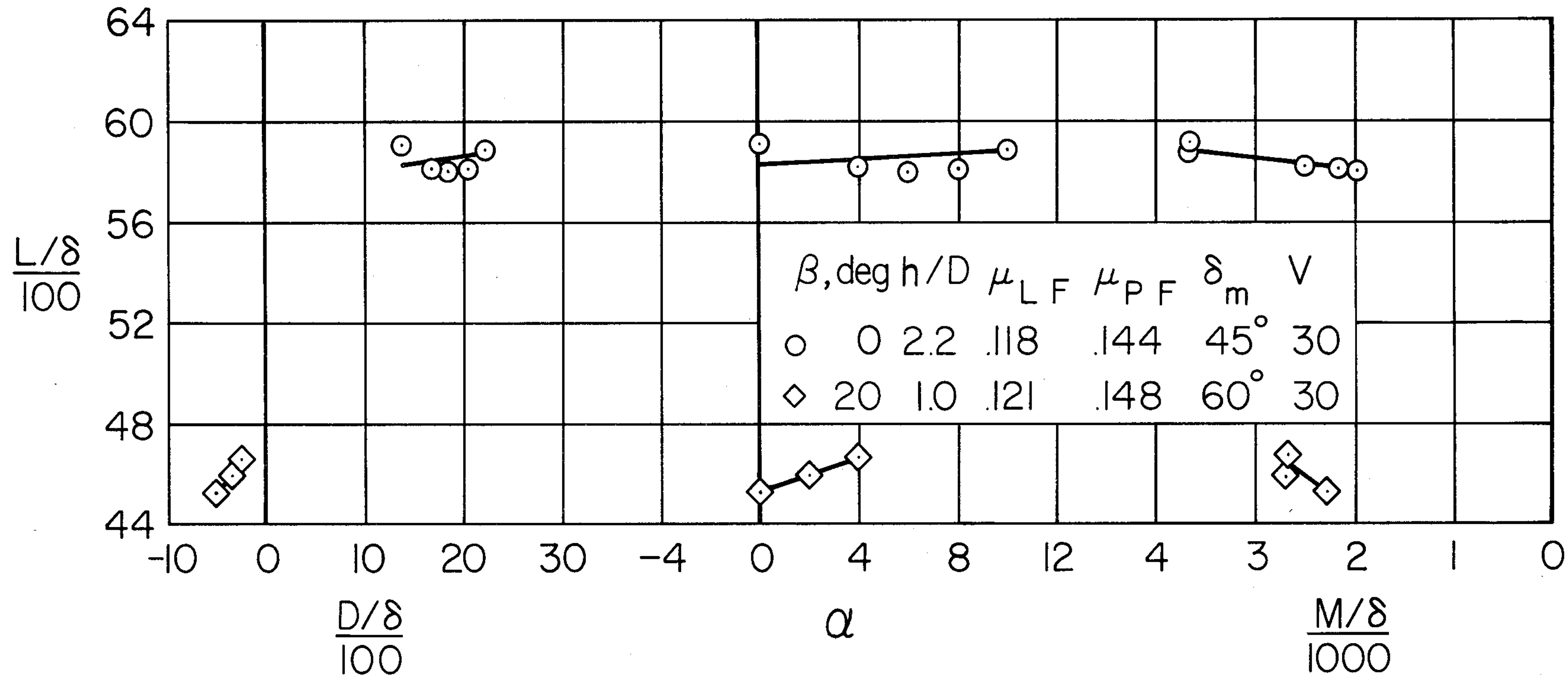

Figure 40.- The effect of three-fan operation on low-speed longitudinal characteristics; tail on, $i_t = 0^\circ$, $\delta_f = 45^\circ$, straight louvers, lift fan RPM = 1700, pitch fan RPM = 2400.

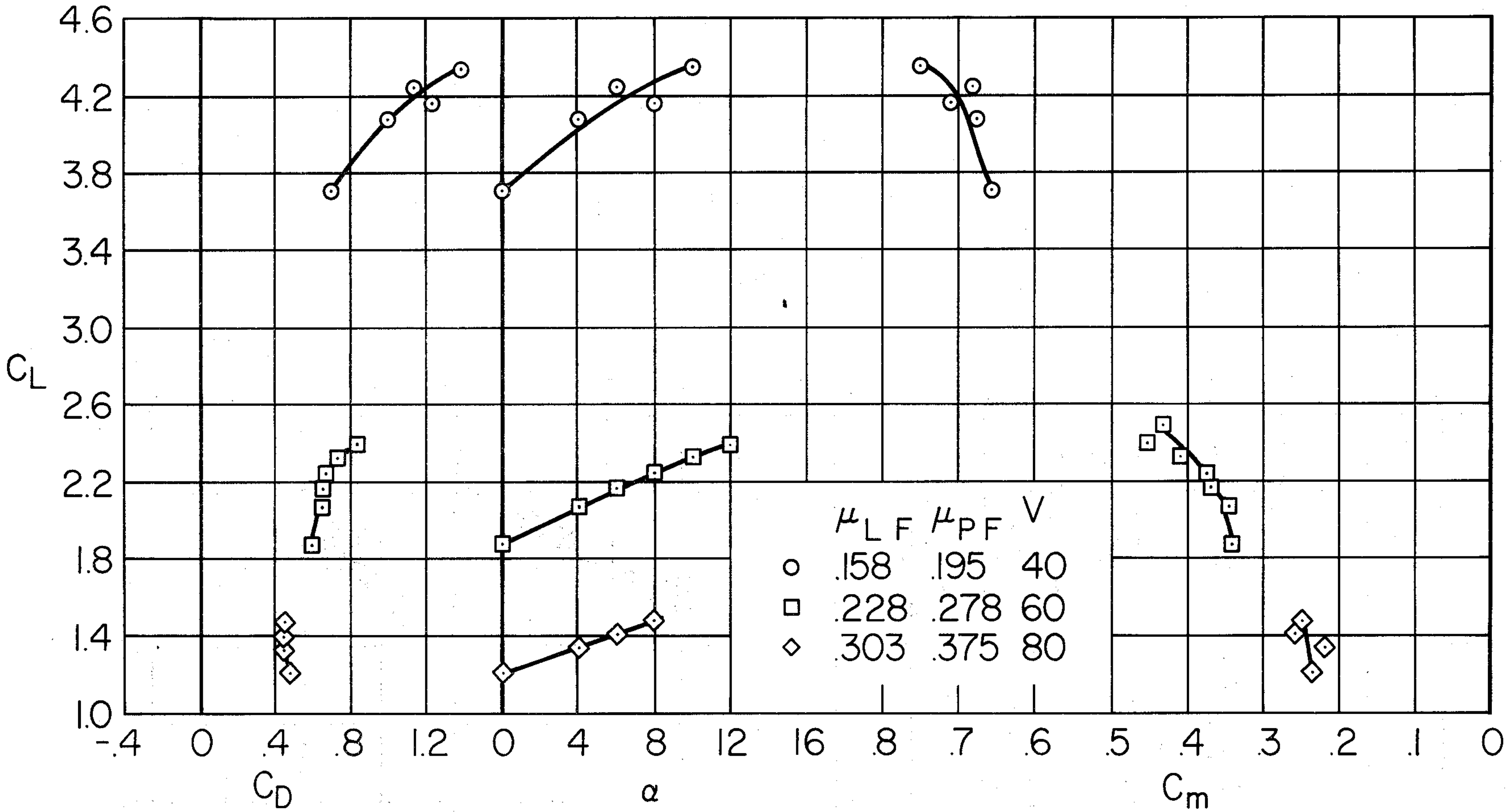

(a) $\beta = 0^{\circ}$, $\delta_m = 0^{\circ}$

Figure 41.- Longitudinal characteristics with three fans operating; $h/D = 2.2$, $\delta_f = 45^{\circ}$, staggered louvers, lift fan RPM = 1700, pitch fan RPM = 2400.

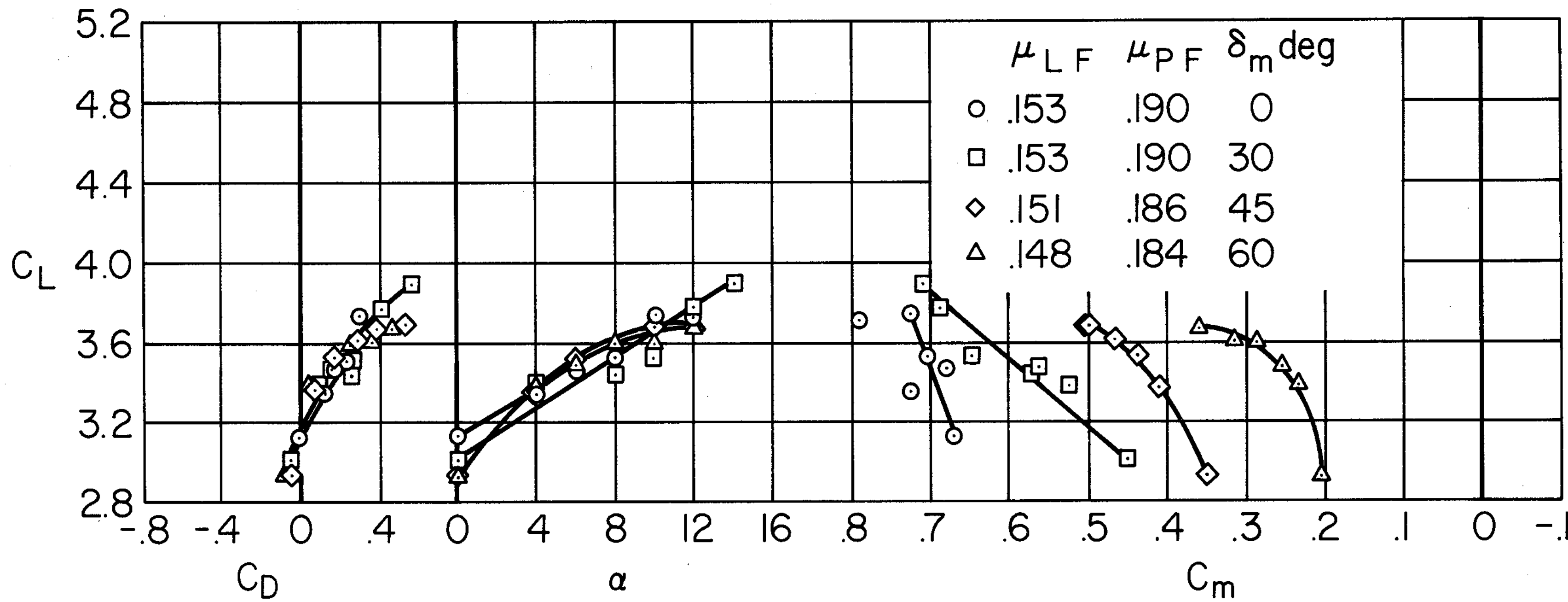

(b) $\beta = 20^{\circ}$, V = 40 knots.

Figure 41.- Concluded.

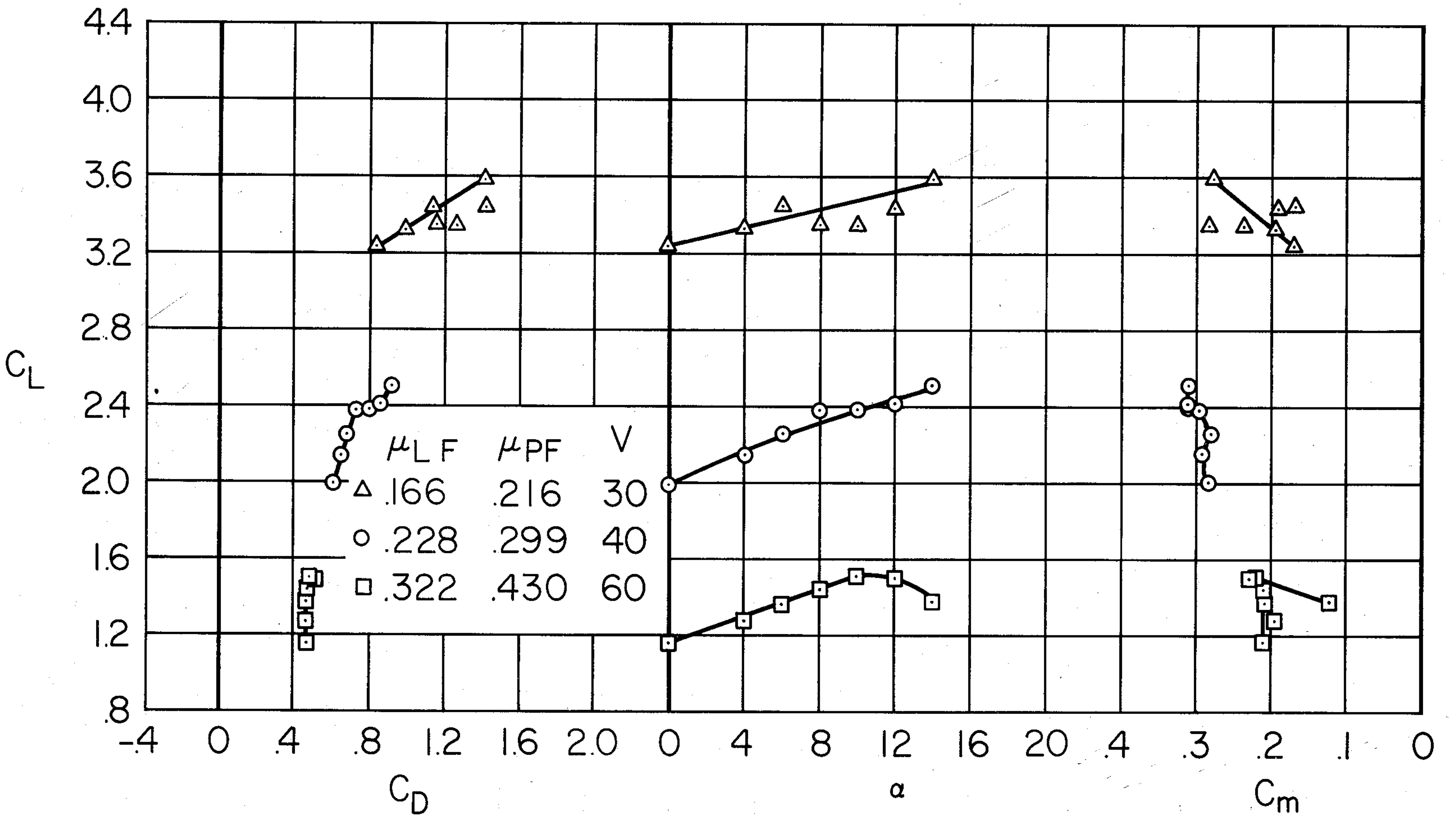

Figure 42.- Longitudinal characteristics with three fans operating; $h/D = 2.2$, $\beta = 0^\circ$, $\delta_m = 60^\circ$, tail on, $i_t = 0^\circ$, $\delta_f = 45^\circ$, straight louvers, lift fan RPM = 1200, pitch fan RPM = 1600.

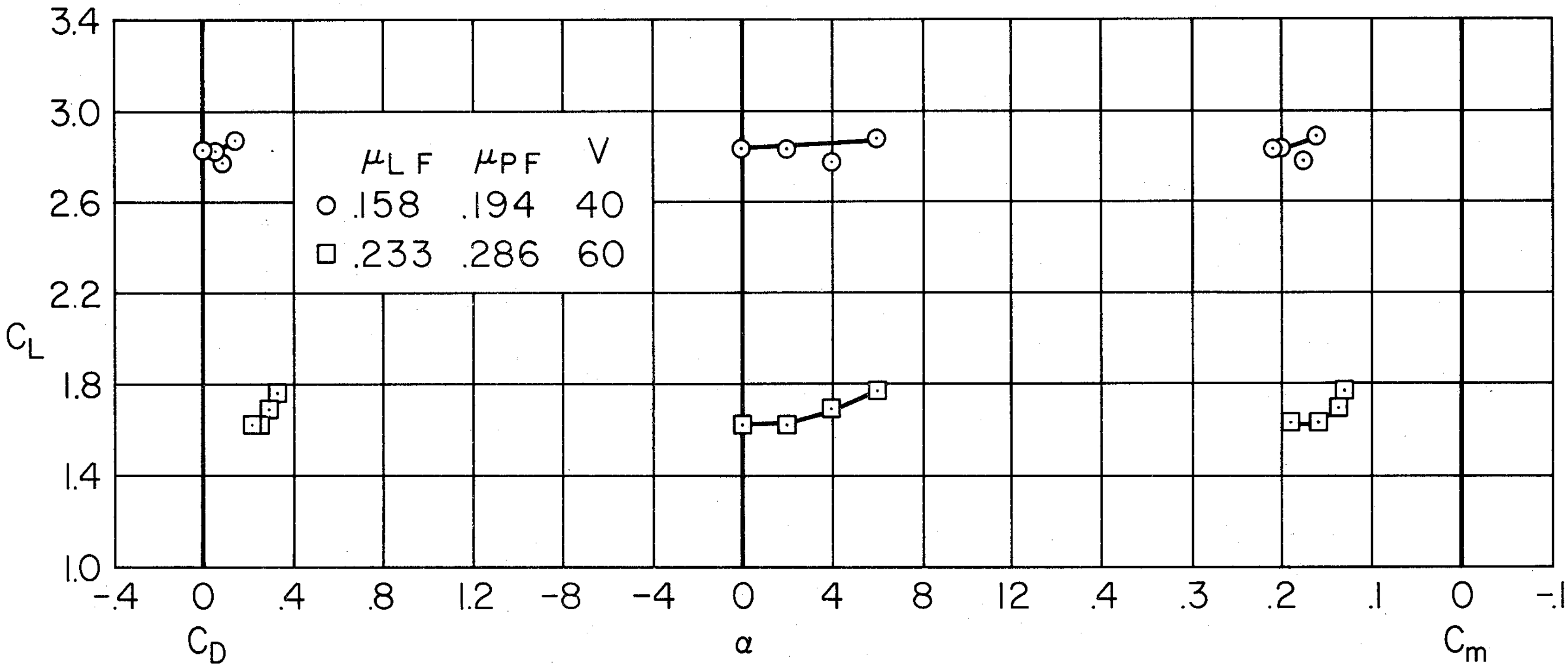

Figure 43.- Longitudinal characteristics with three fans operating; $h/D = 1.0$, $\beta = 20^{\circ}$, $\delta_m = 60^{\circ}$, tail on, $i_t = 0^{\circ}$, $\delta_f = 45^{\circ}$, straight louvers, lift fan RPM = 1200, pitch fan RPM = 1600.

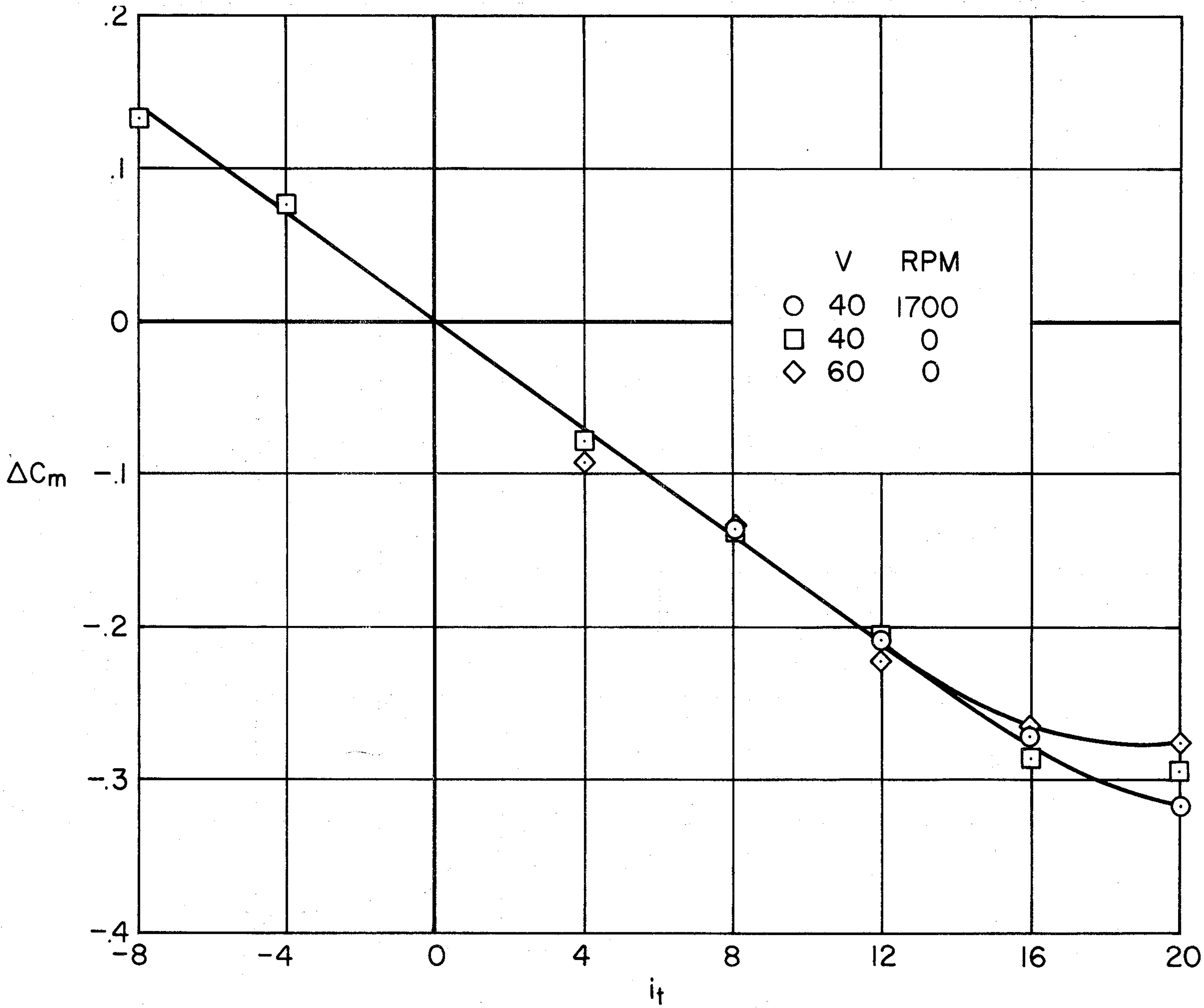

Figure 44.- Control power of the horizontal tail.

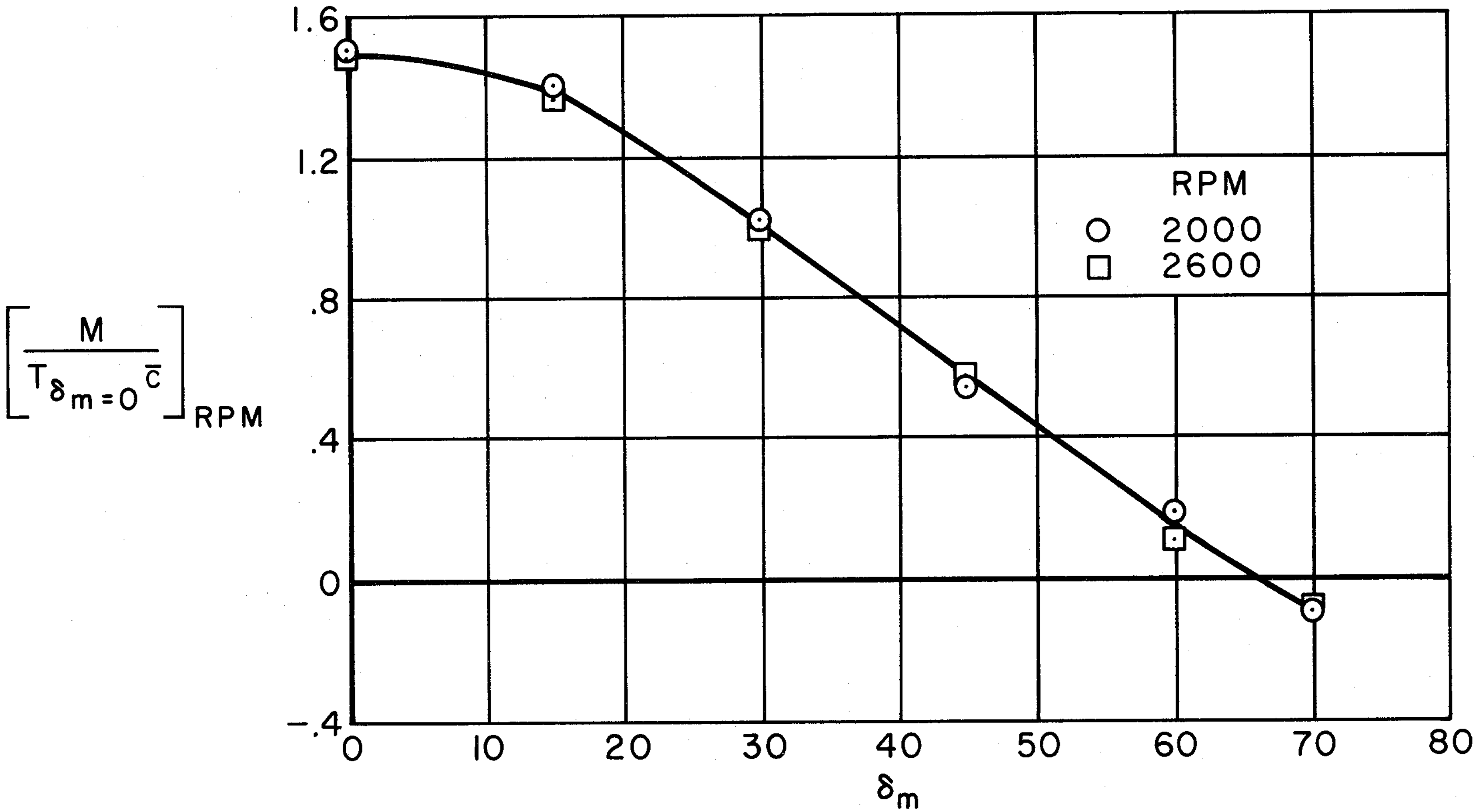

Figure 45.- Control power of the pitch fan and modulator installation; V = 0.

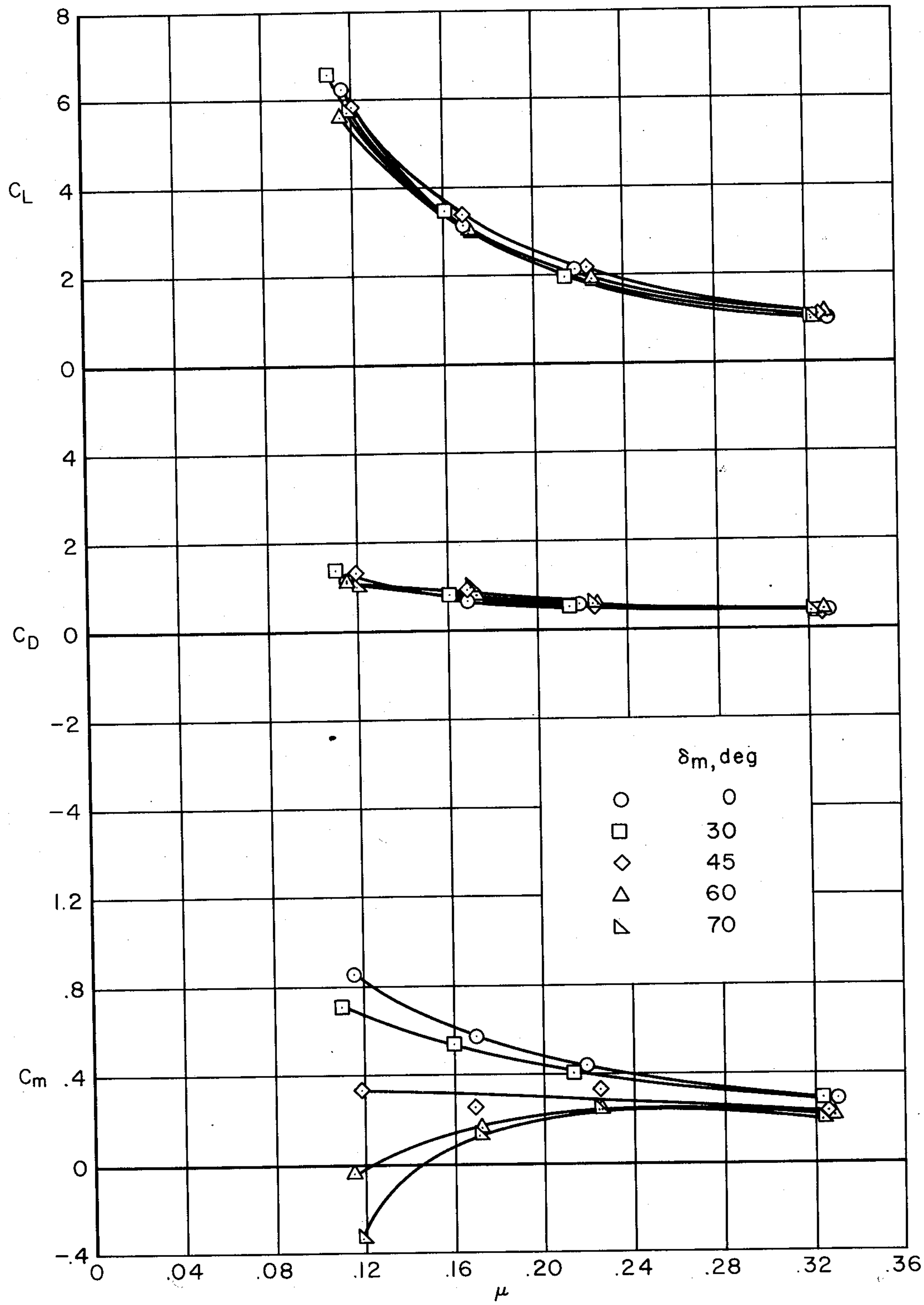

(a) $h/D = 2.2$, $\beta = 0^{\circ}$

Figure 46.- Control power of the pitch fan and its effect on longitudinal characteristics; tail on, $i_t = 0^{\circ}$, $\delta_f = 45^{\circ}$, straight louvers, lift fan RPM = 1700, pitch fan RPM = 2400.

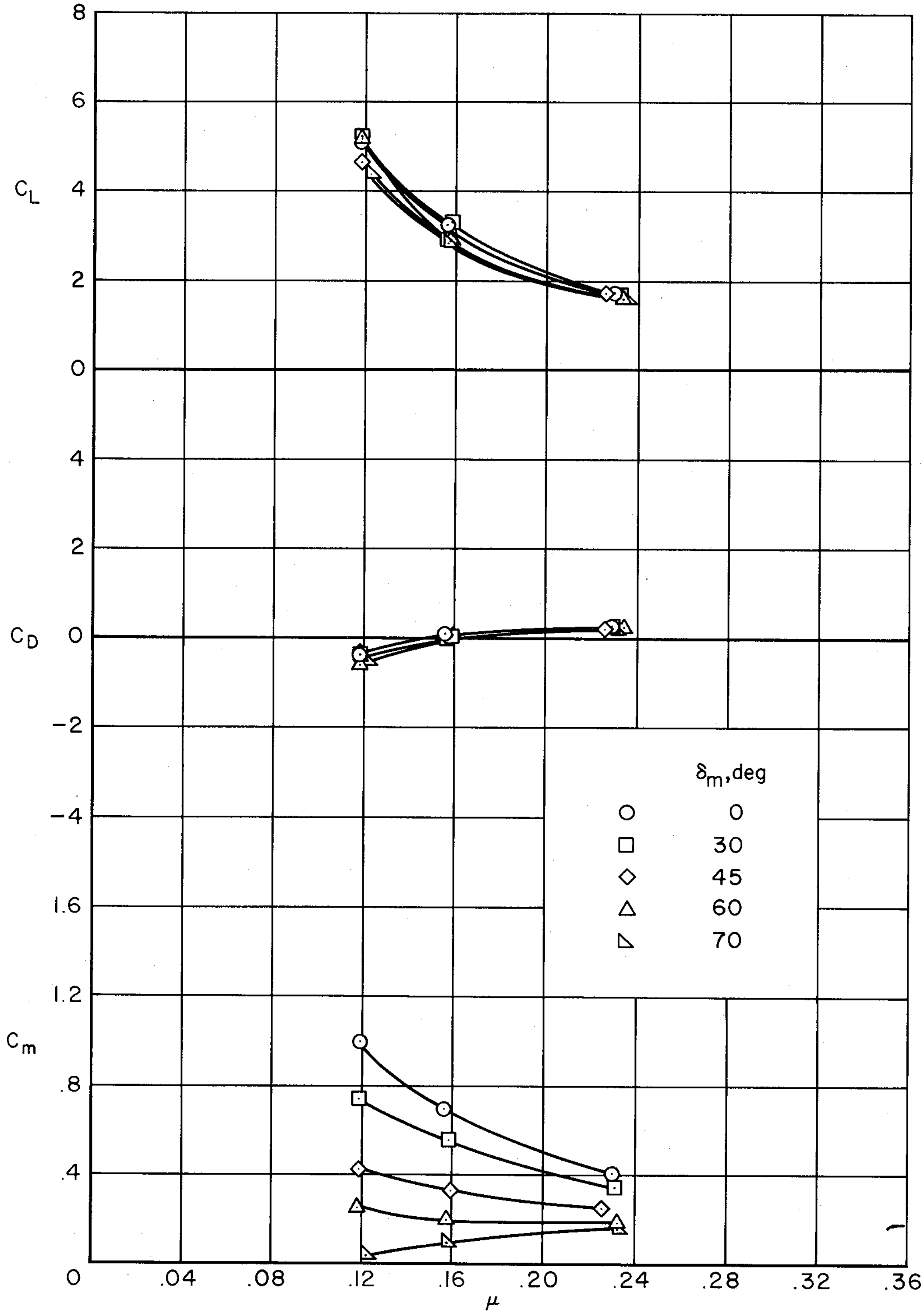

(b) $h/D = 1.0$, $\beta = 20^{\circ}$

Figure 46.- Concluded.

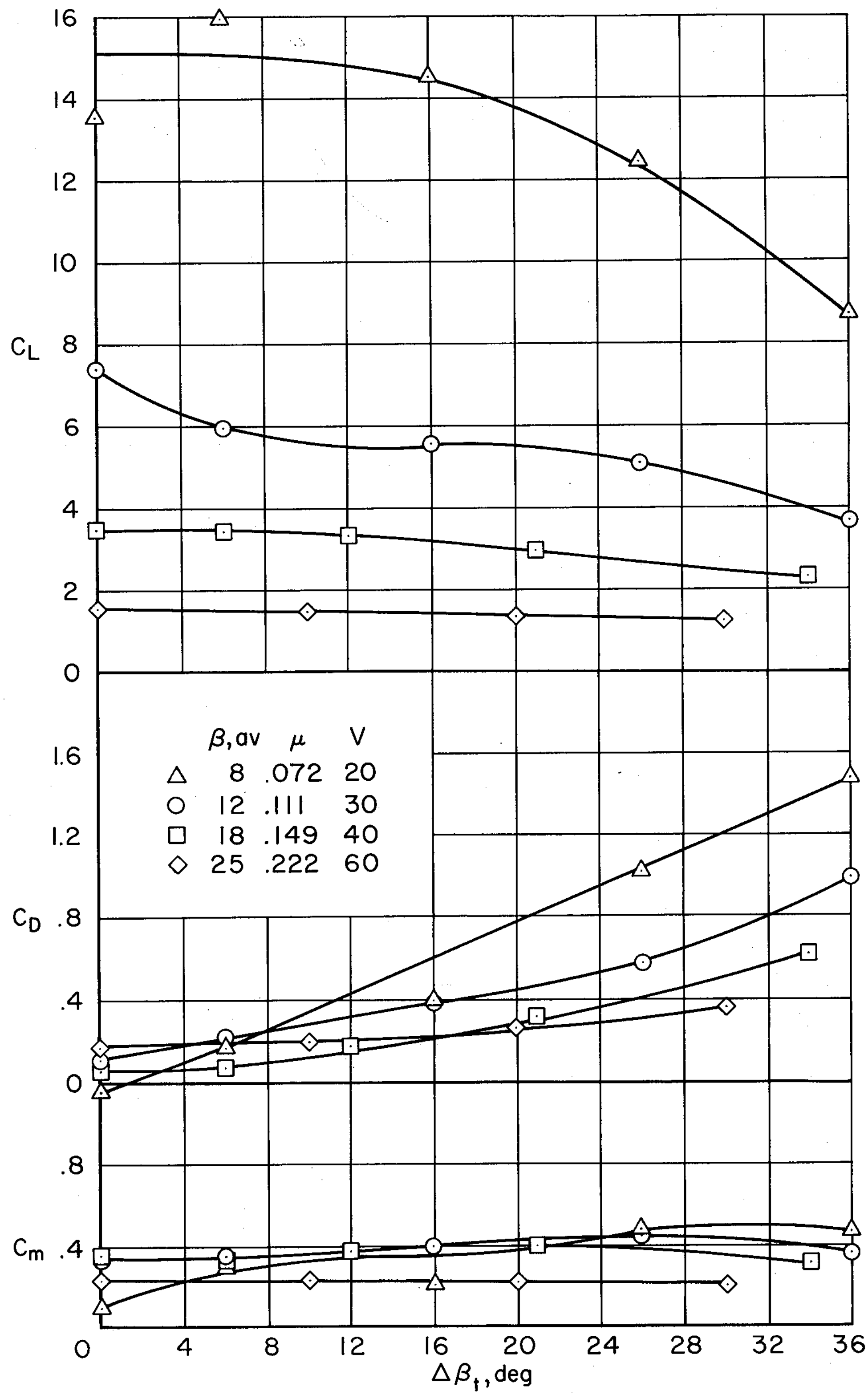

Figure 47.- Effect of thrust control on longitudinal characteristics; $h/D = 3.85$, $\alpha = 0^{\circ}$, $\beta_s = 0^{\circ}$, tail on, $i_t = 0^{\circ}$, $\delta_f = 45^{\circ}$, straight louvers, 1700 RPM.

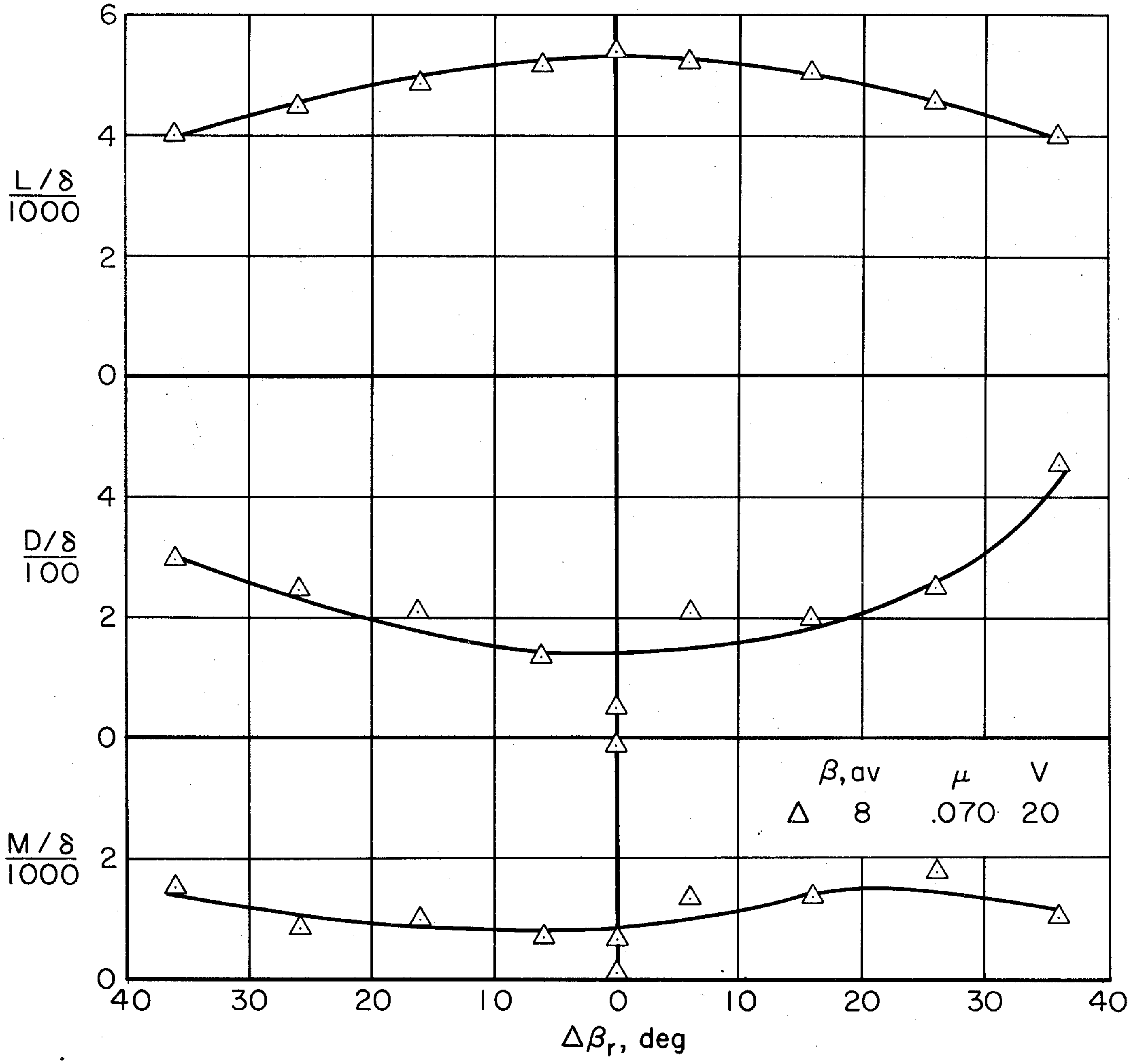

(a) Longitudinal characteristics.

Figure 48.- Effect of roll control on aerodynamic characteristics at low tip-speed ratios; $h/D = 3.85$, $\alpha = 0^{\circ}$, $\beta_s = 0^{\circ}$, tail on, $i_t = 1^{\circ}$, $\delta_f = 45^{\circ}$, straight louvers, 1700 RPM.

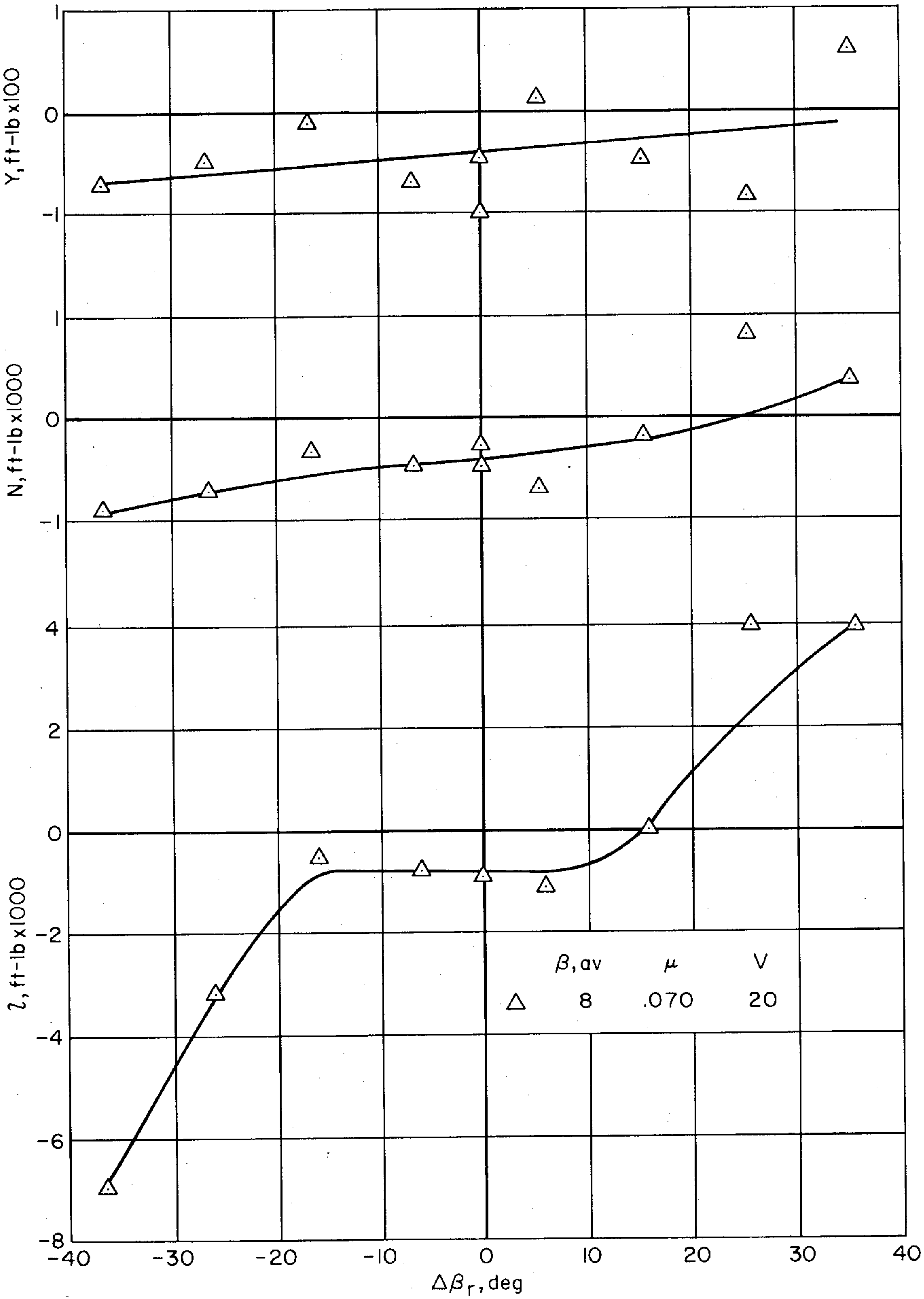

(b) Lateral-directional characteristics.

Figure 48.- Concluded.

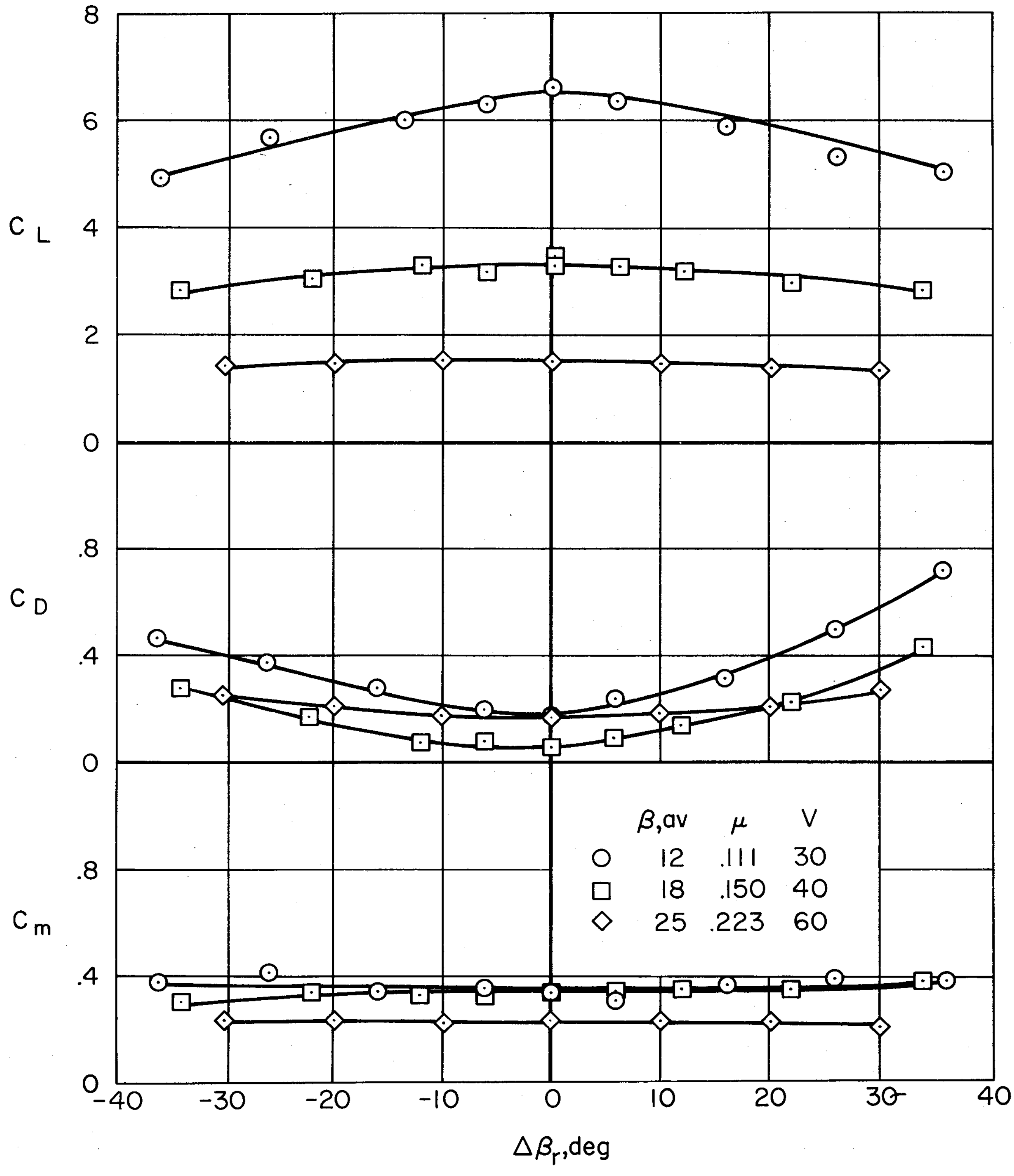

(a) Longitudinal characteristics.

Figure 49.- Effect of roll control on aerodynamic characteristics; $h/D = 3.85$, $\alpha = 0^{\circ}$, $\beta_s = 0^{\circ}$, tail on, $i_t = 1^{\circ}$, $\delta_f = 45^{\circ}$, straight louvers, 1700 RPM.

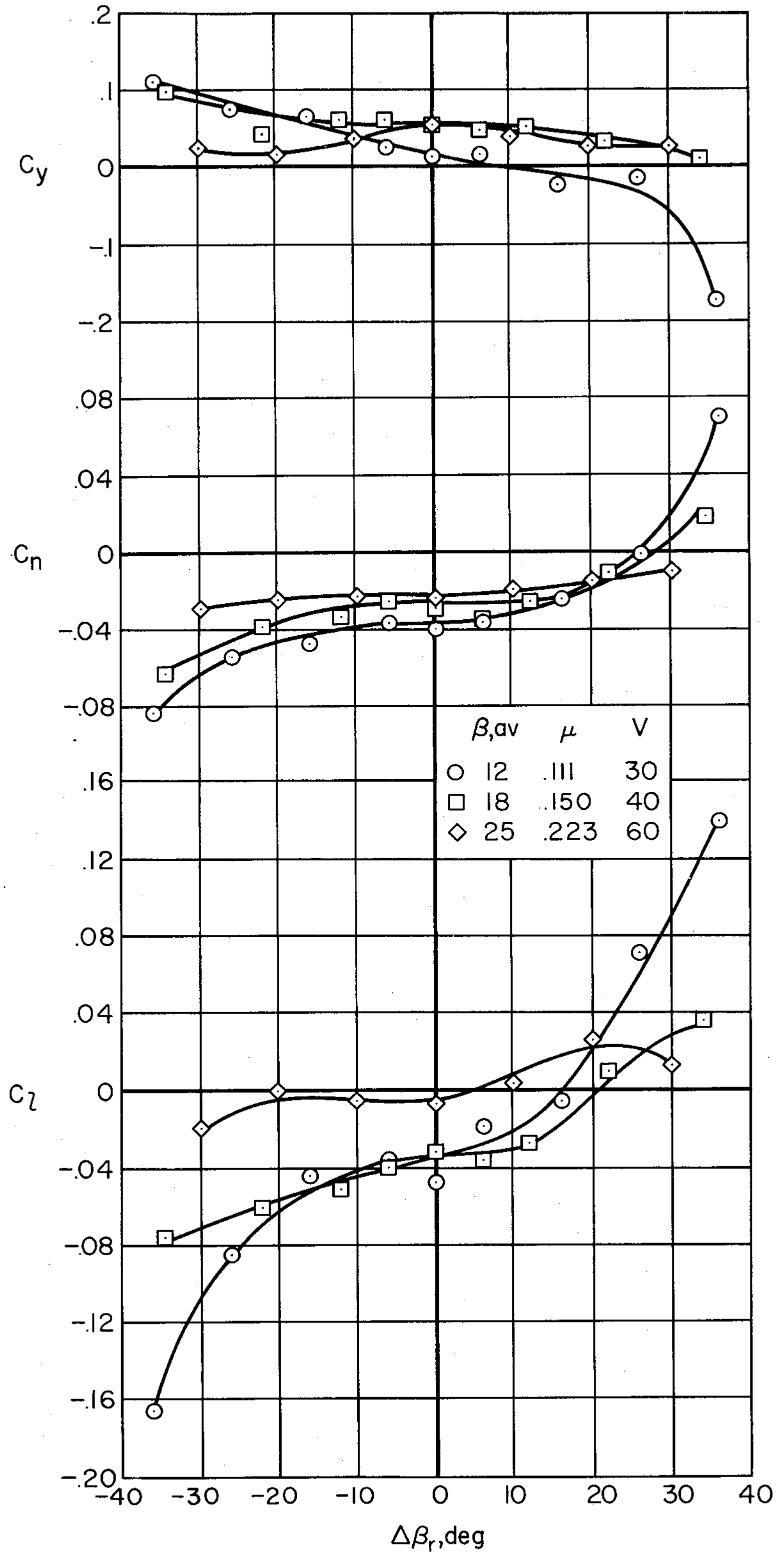

(b) Lateral-directional characteristics.

Figure 49.- Concluded.

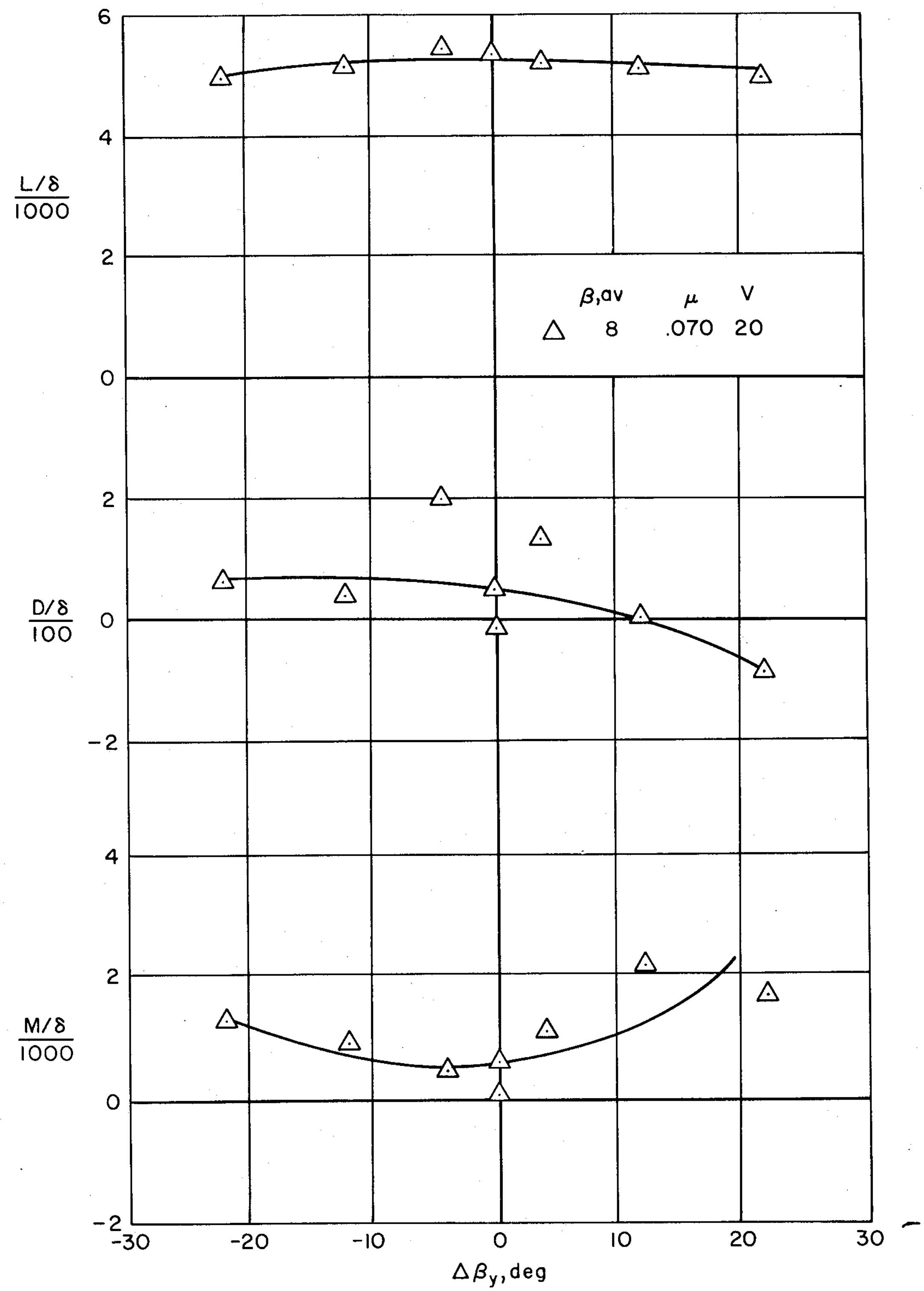

(a) Longitudinal characteristics.

Figure 50.- Effect of yaw control on aerodynamic characteristics at low tip-speed ratios; $h/D = 3.85$, $\alpha = 0^{\circ}$, $\beta_s = 0^{\circ}$, tail on, $i_t = 1^{\circ}$, $\delta_f = 45^{\circ}$, straight louvers, 1700 RPM.

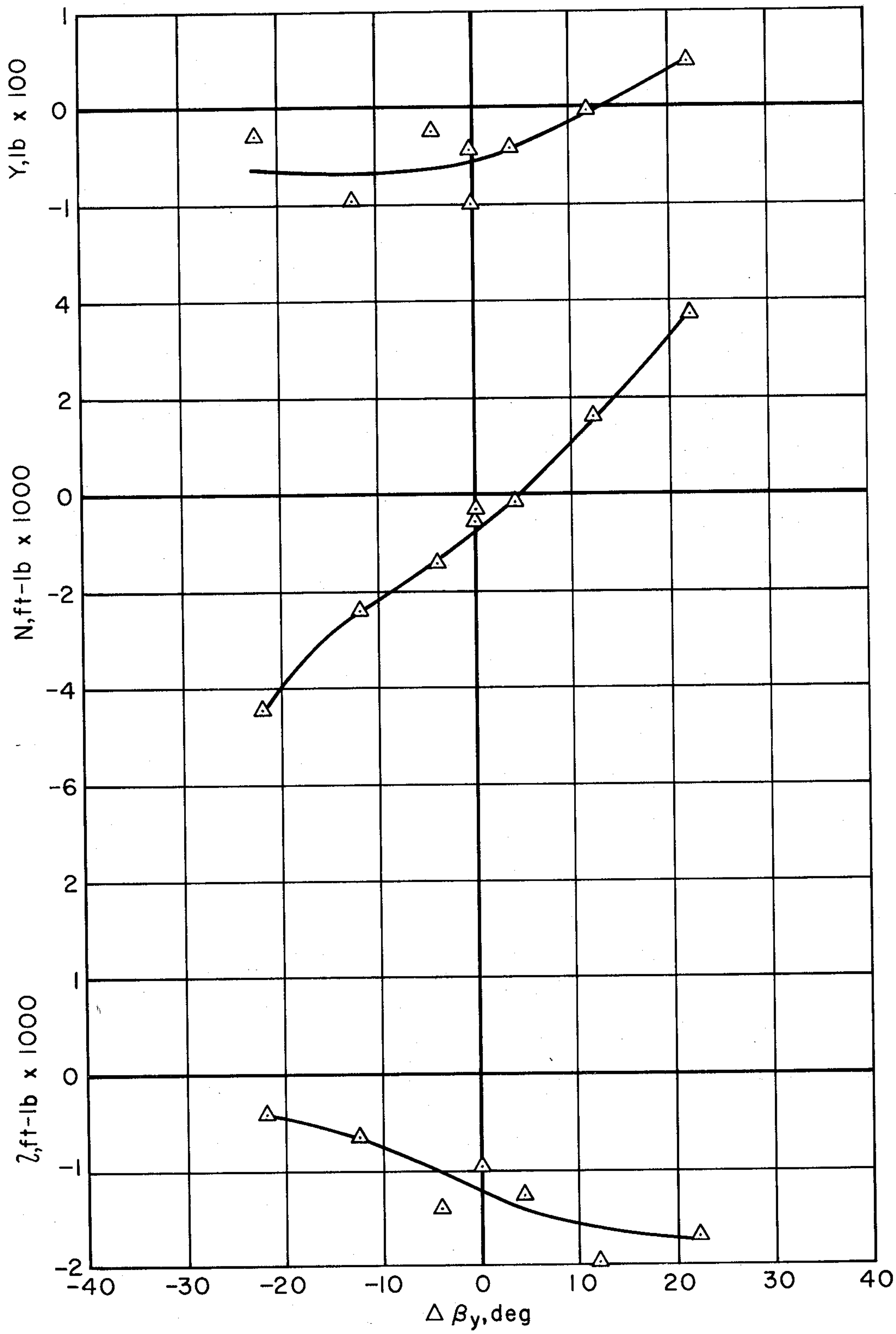

(b) Lateral-directional characteristics.

Figure 50.- Concluded.

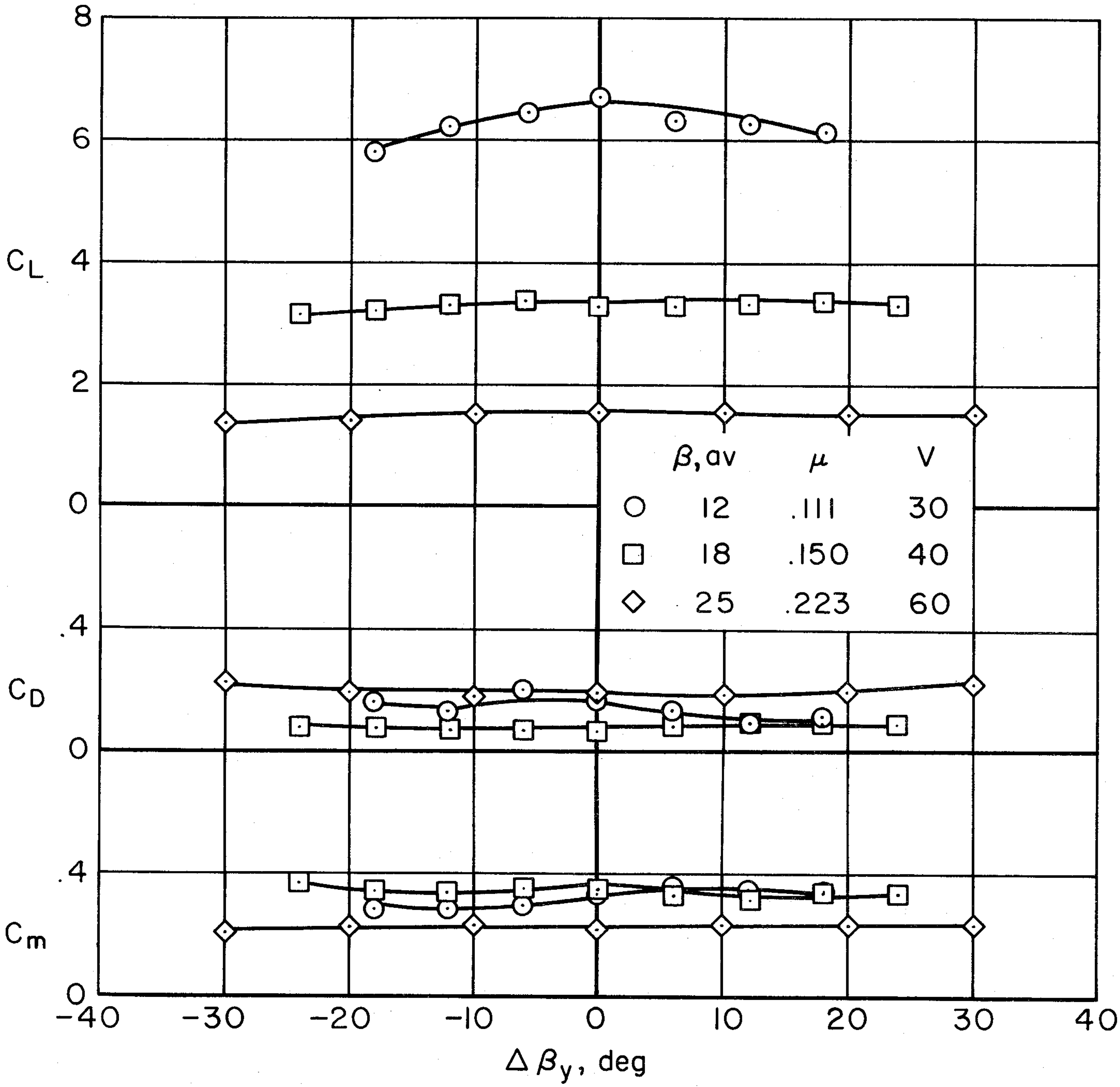

(a) Longitudinal characteristics.

Figure 51.- Effect of yaw control on aerodynamic characteristics; $h/D = 3.85$, $\alpha = 0^{\circ}$, $\beta_s = 0^{\circ}$, tail on, $i_t = 1^{\circ}$, $\delta_f = 45^{\circ}$, straight louvers, 1700 RPM.

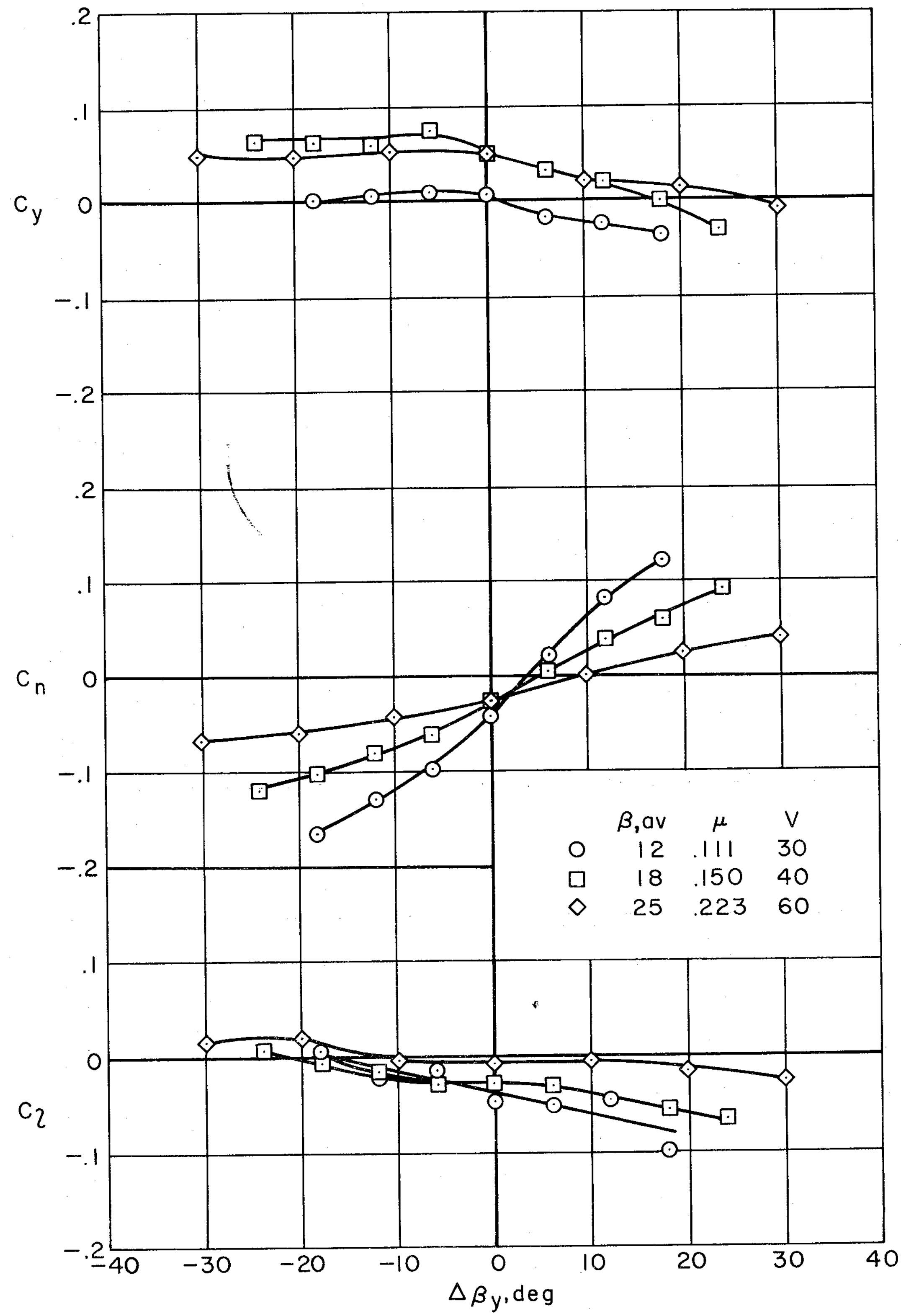

(b) Lateral-directional characteristics.

Figure 51.- Concluded.

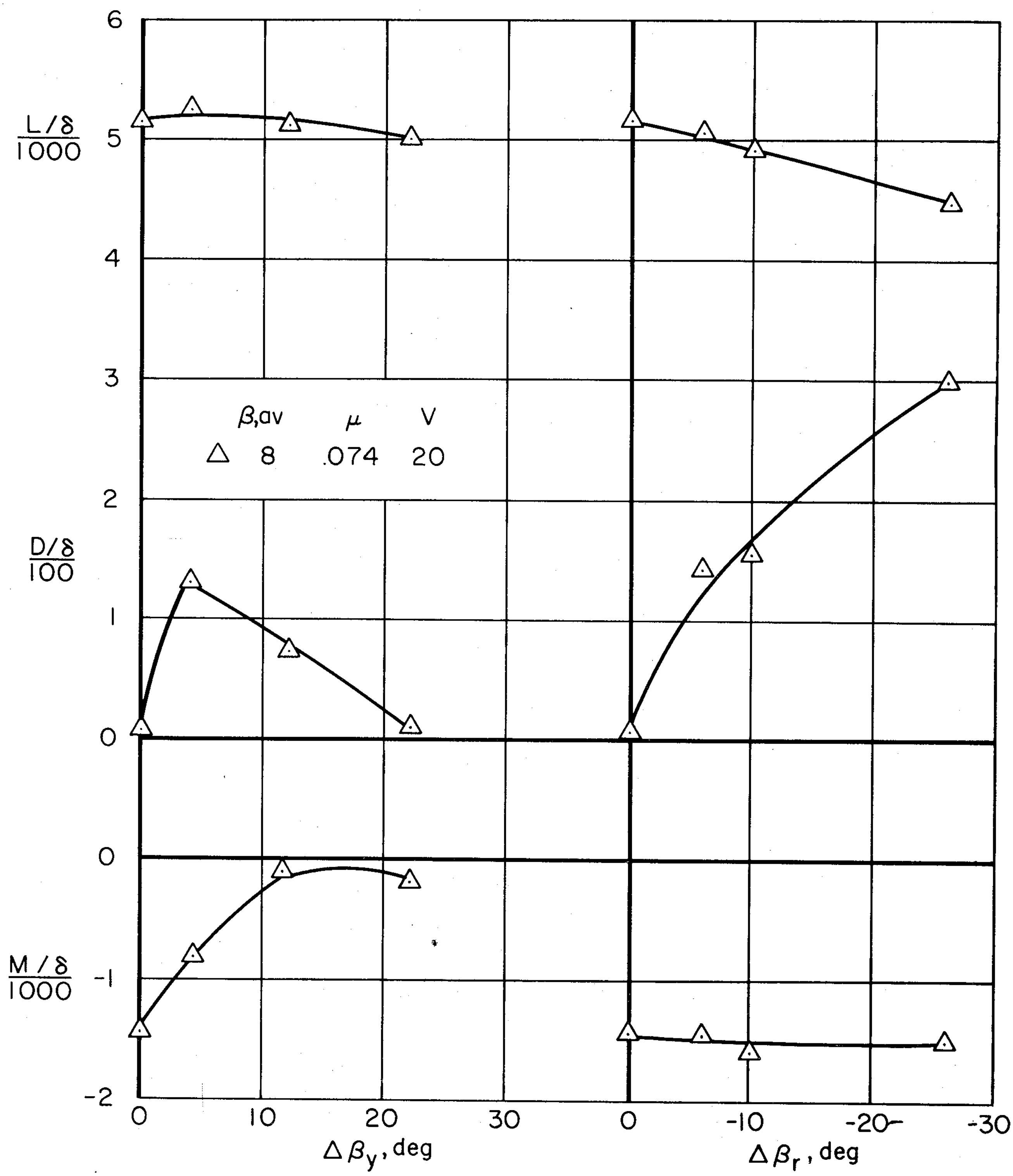

(a) Longitudinal characteristics.

Figure 52.- Effect of yaw and roll control on aerodynamic characteristics at low tip-speed ratios; $h/D = 3.85$, $\alpha = 0^{\circ}$, $\beta_s = -12^{\circ}$, tail on, $i_t = 20^{\circ}$, $\delta_f = 45^{\circ}$, straight louvers, 1700 RPM.

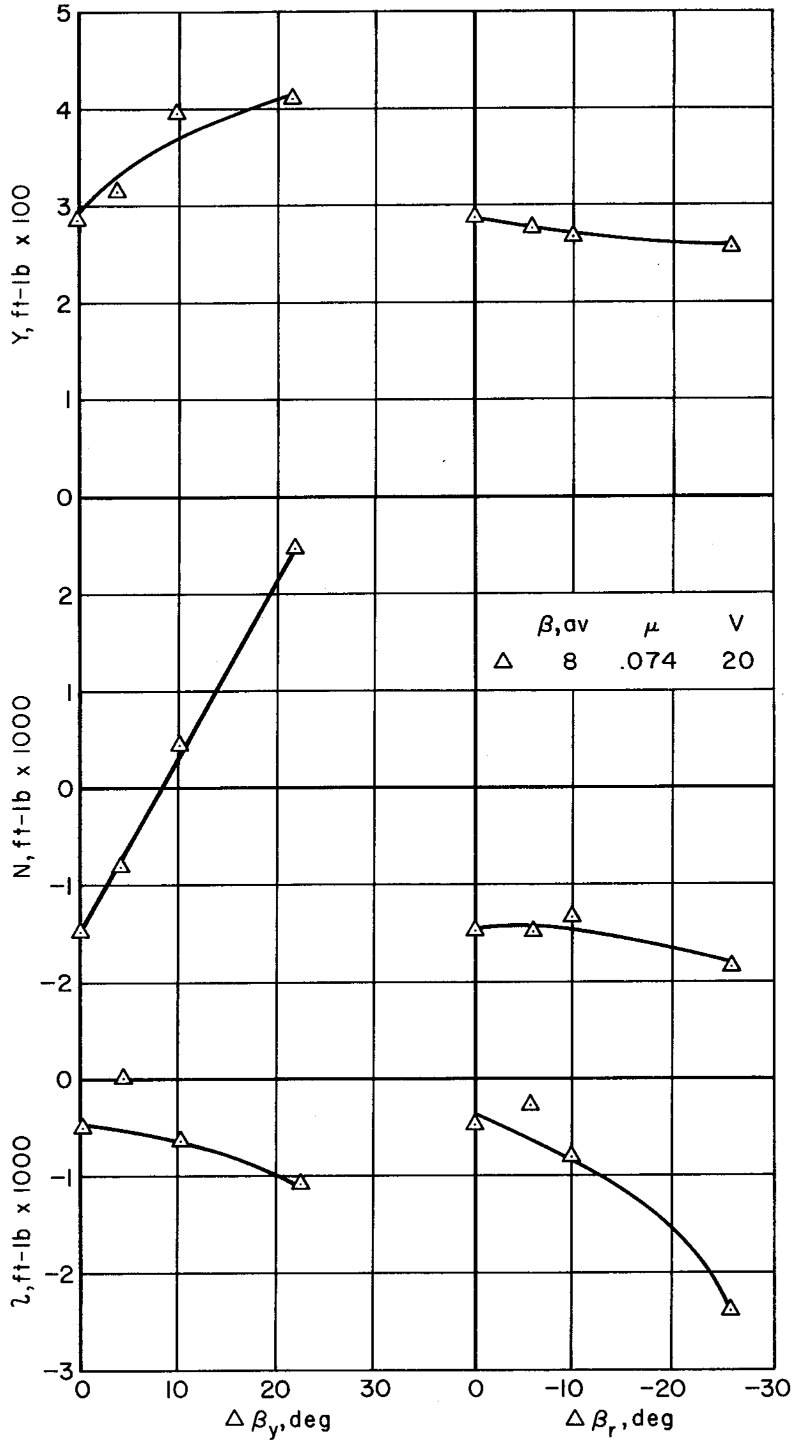

(b) Lateral-directional characteristics.

Figure 52.- Concluded.

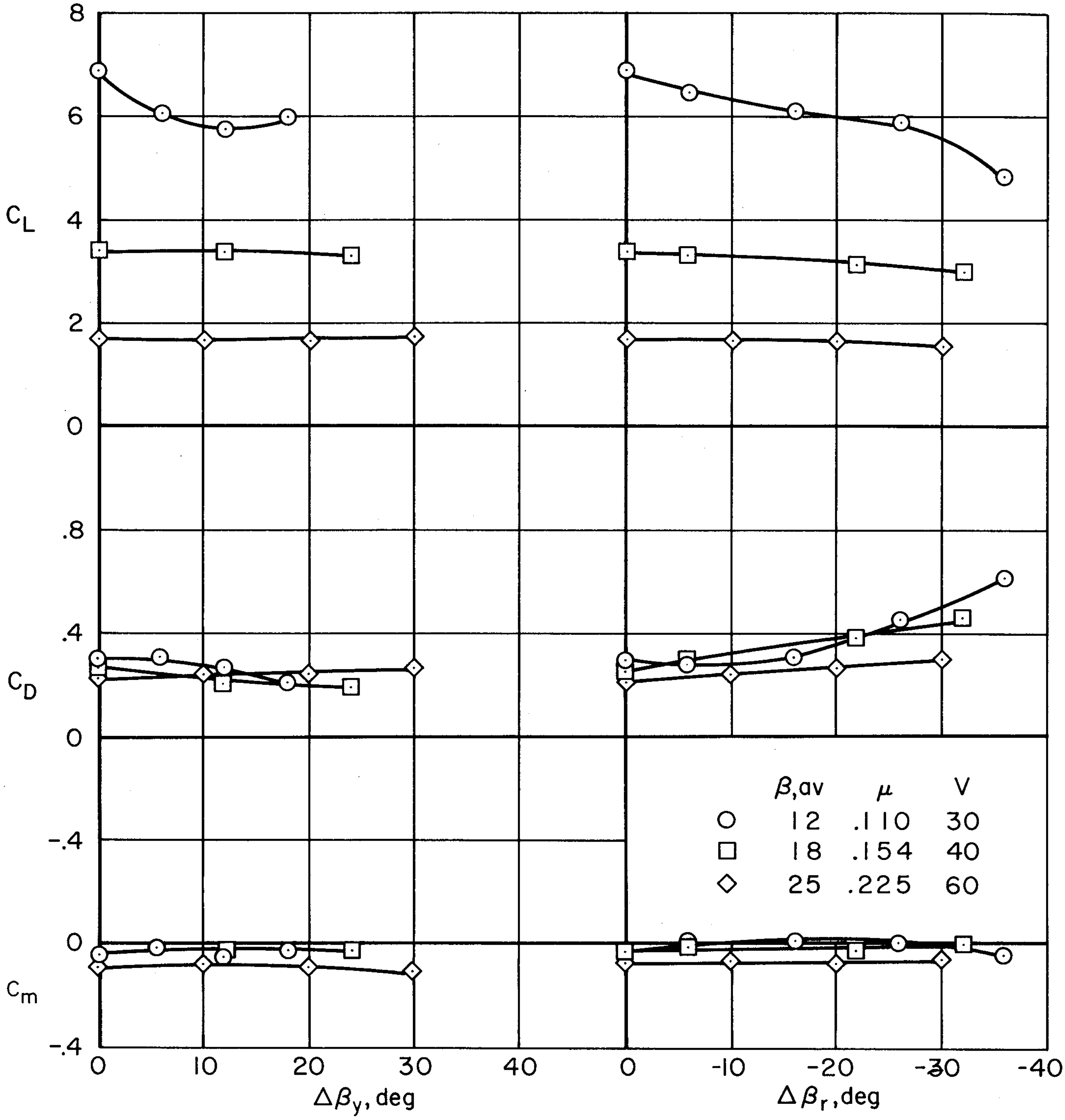

(a) Longitudinal characteristics.

Figure 53.- Effect of yaw and roll control on aerodynamic characteristics; $h/D = 3.85$, $\alpha = 0^\circ$, $\beta_s = -12^\circ$, tail on, $i_t = 20^\circ$, $\delta_f = 45^\circ$, straight louvers, 1700 RPM.

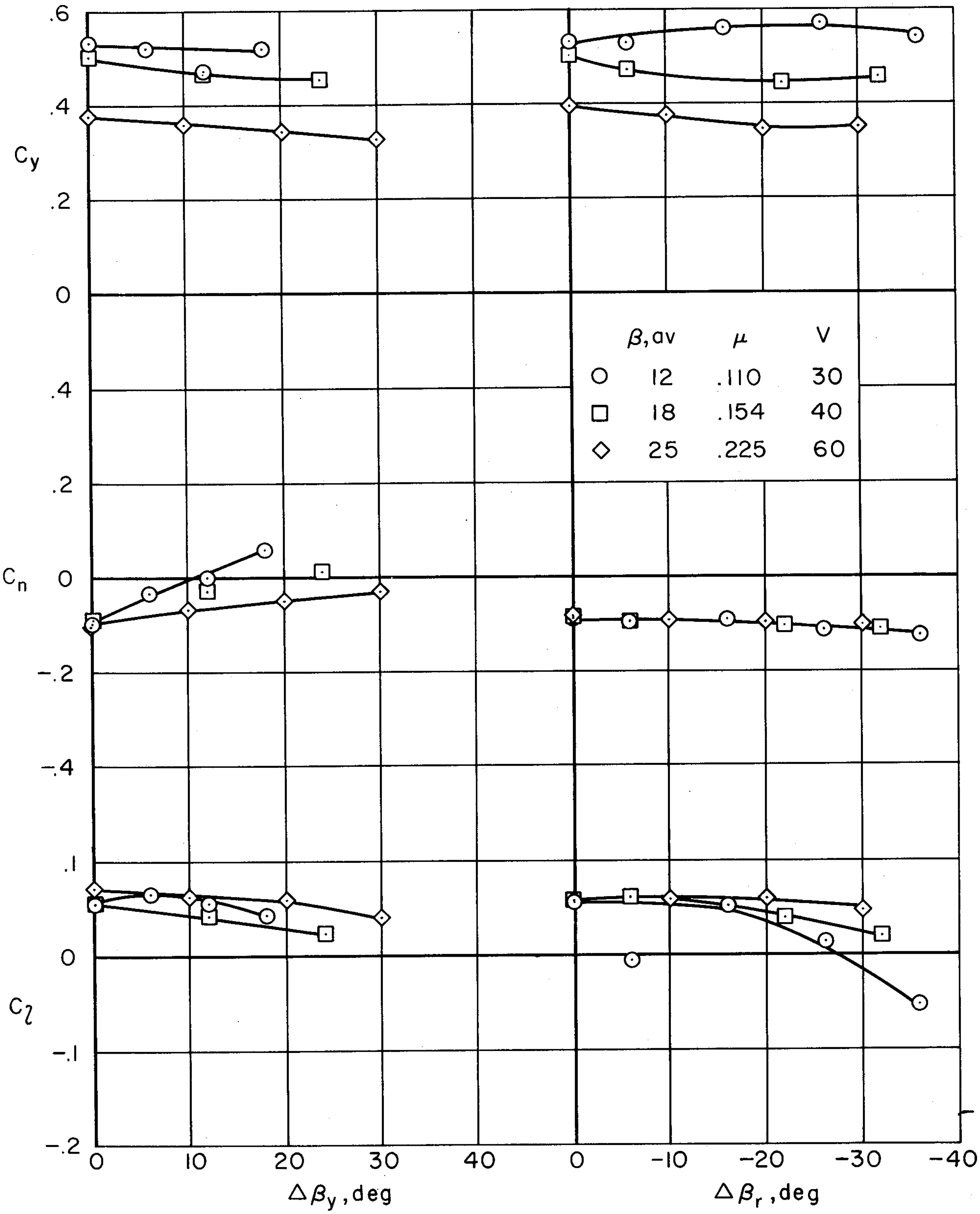

(b) Lateral-directional characteristics.

Figure 53.- Concluded.

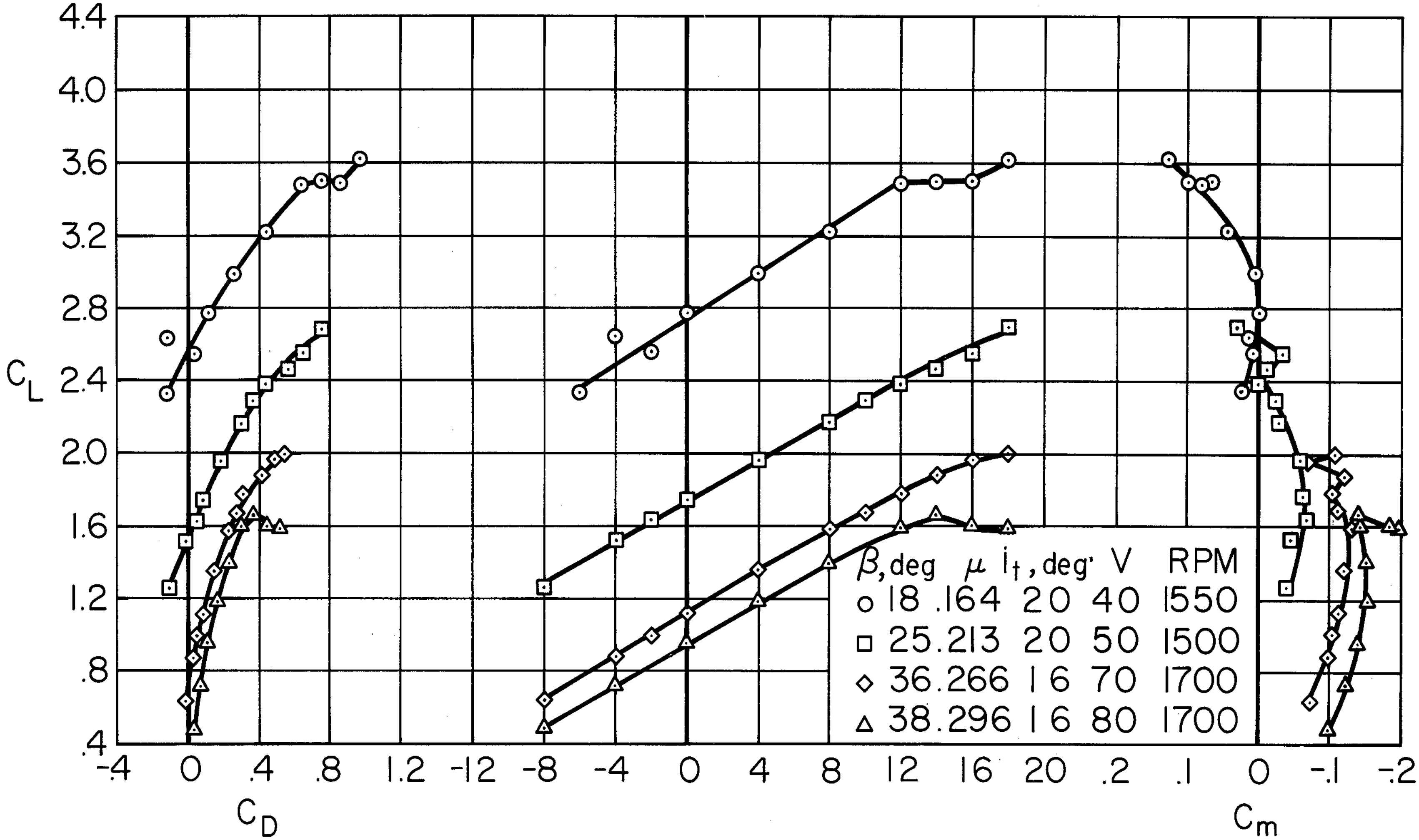

(a) h/D = 3.85, pitch fan off and faired.

Figure 54.- Longitudinal characteristics near trimmed conditions; $\delta_f = 45^\circ$, straight louvers.

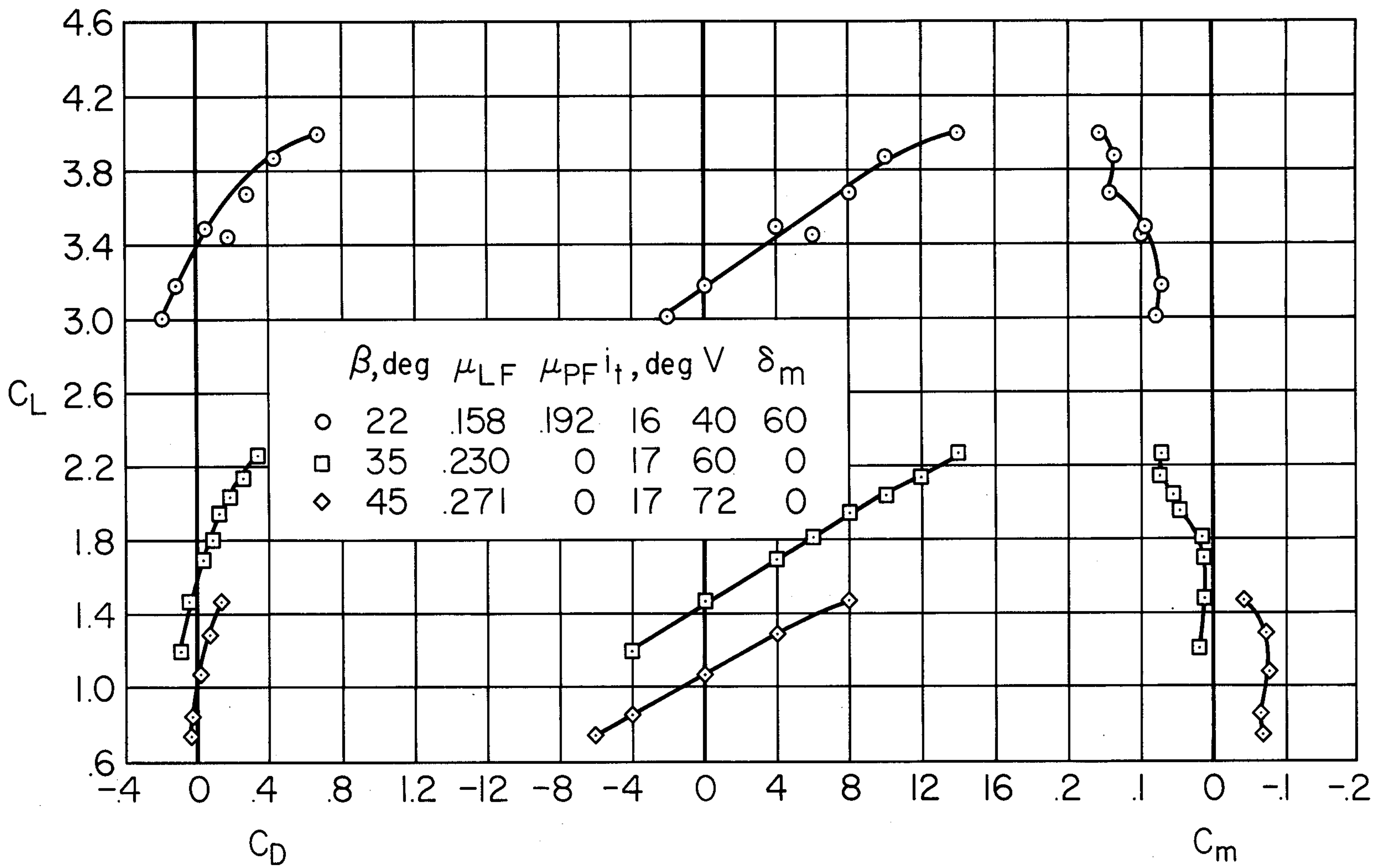

(b) h/D = 2.2

Figure 54.- Continued.

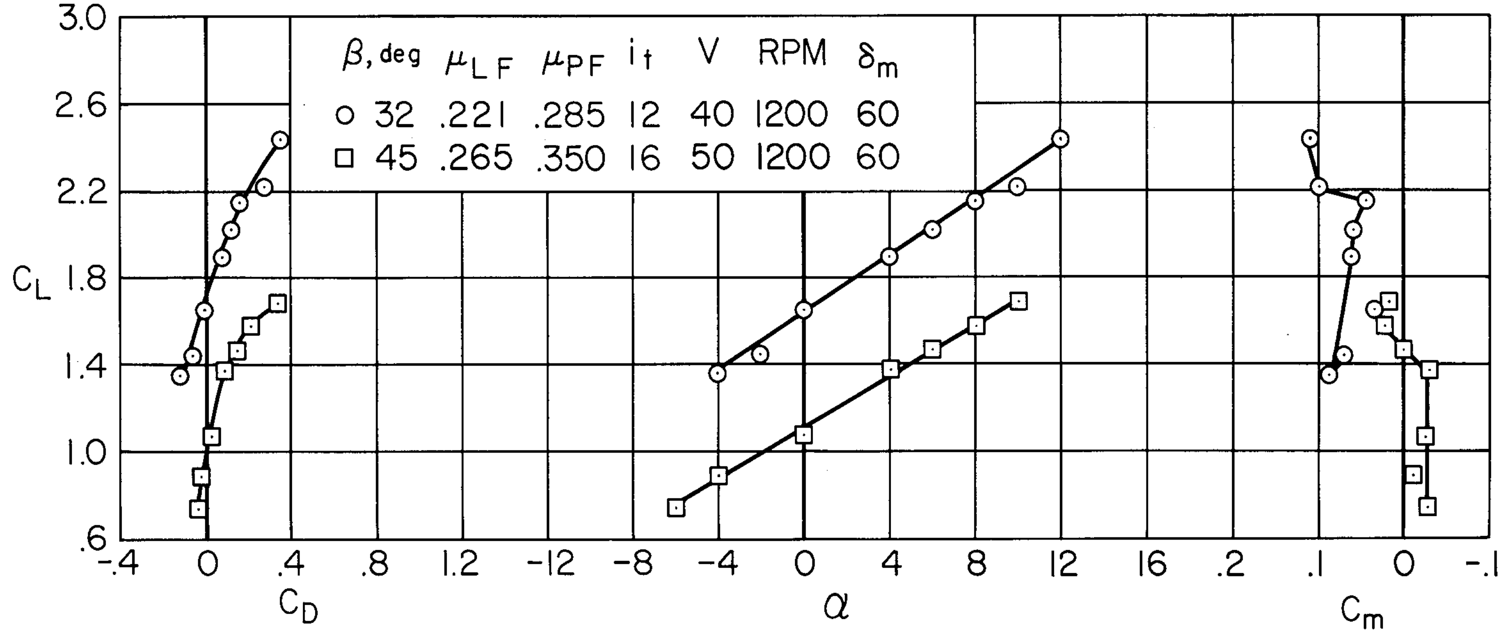

(c) h/D = 1.7

Figure 54.- Concluded.

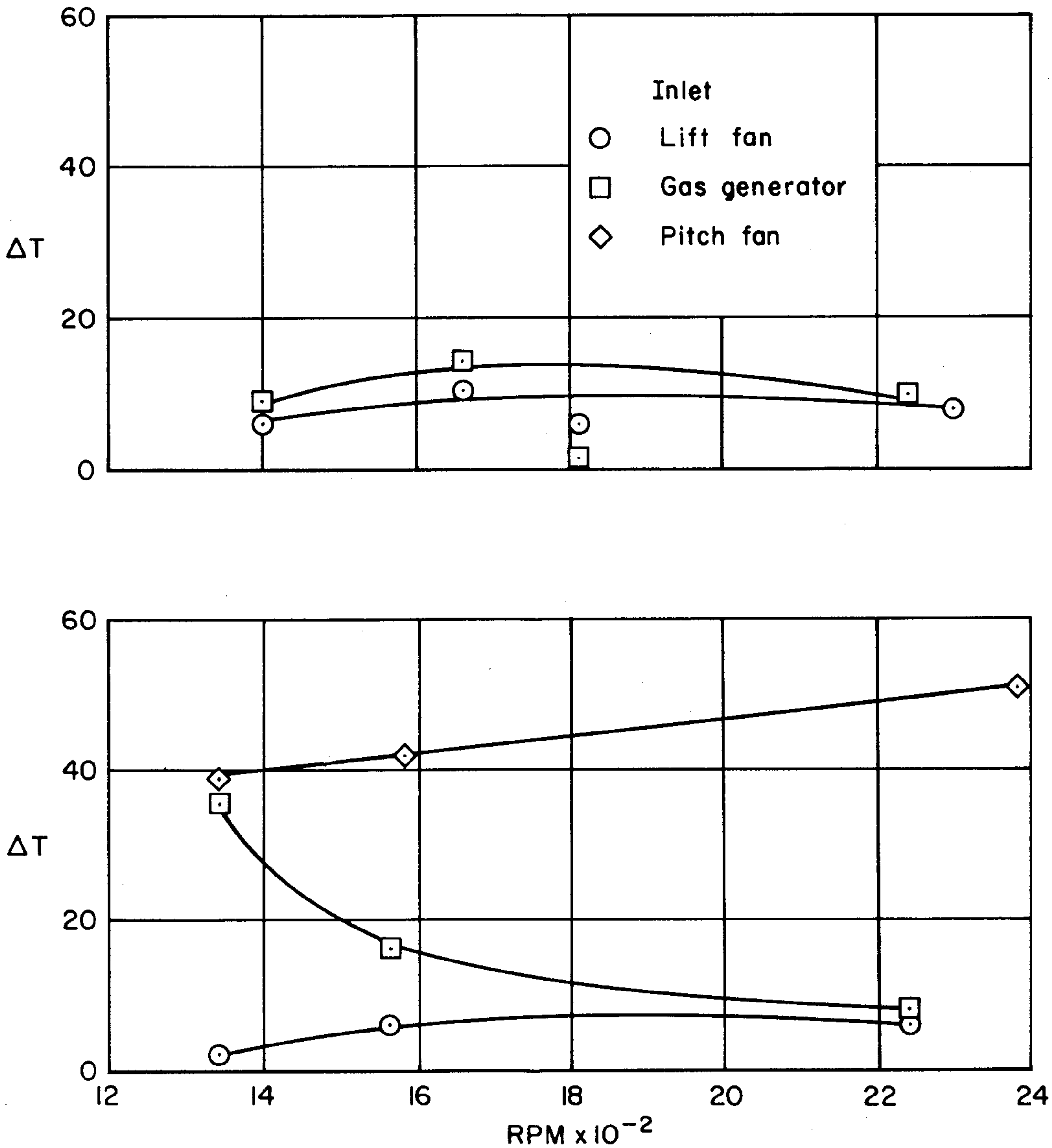

(a) Straight louvers.

Figure 55.- Inlet temperatures due to ingestion; $h/D = 1.0$, $\alpha = 0^{\circ}$, $\beta = 0^{\circ}$, $\delta_f = 45^{\circ}$, $V = 0$ to 5 knots.

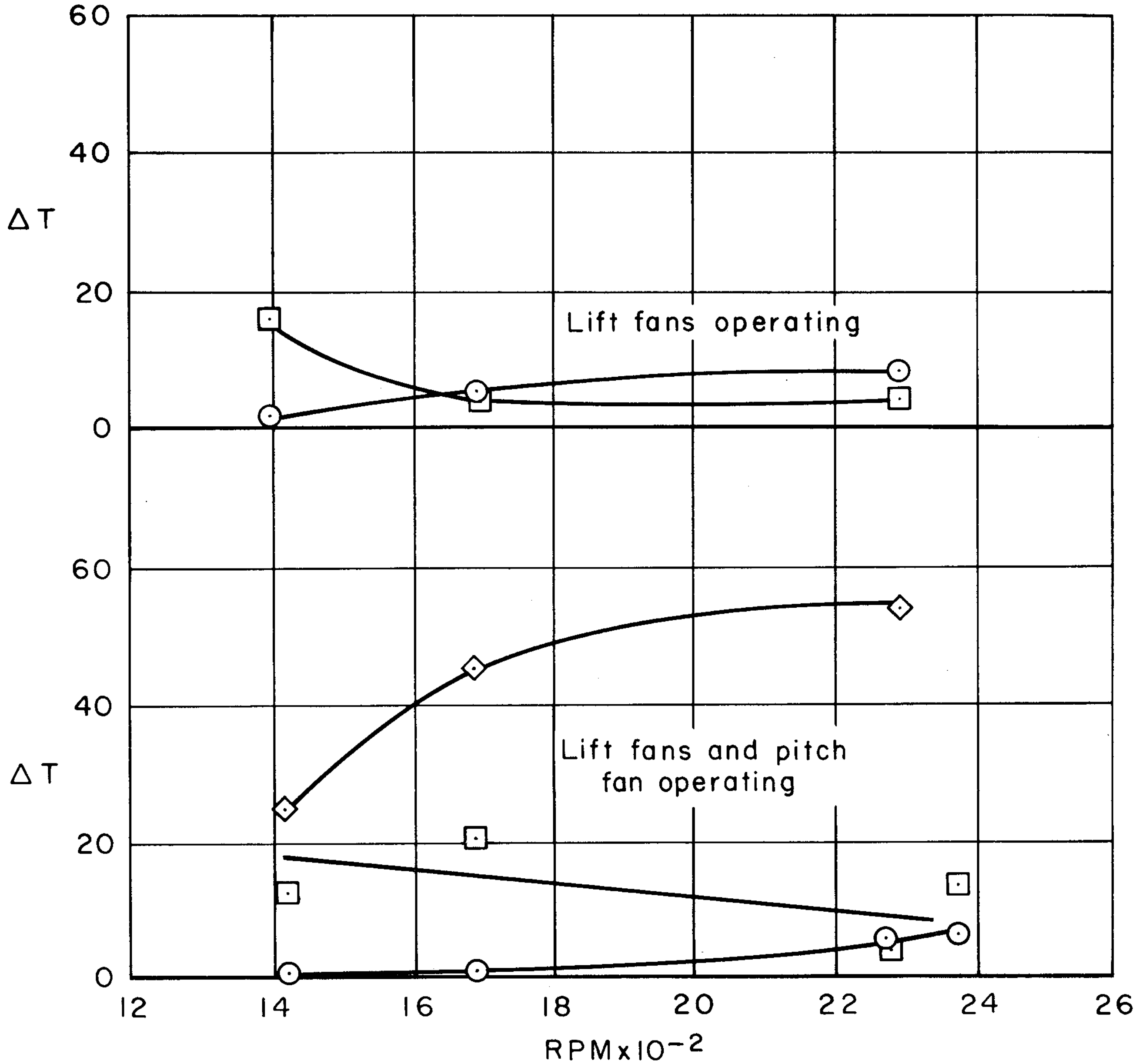

(b) Staggered louvers.

Figure 55.- Concluded.

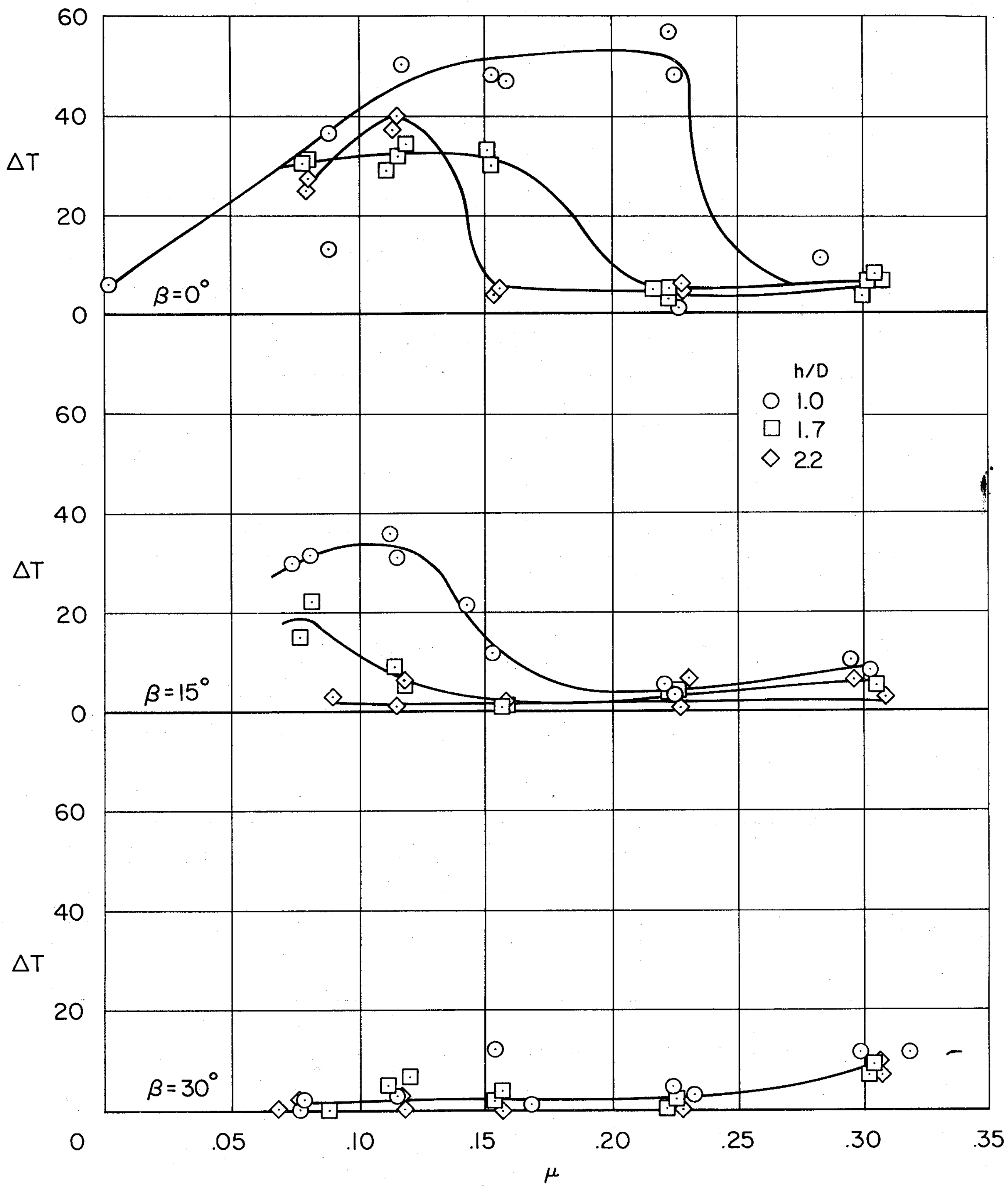

Figure 56.- Effect of ground height and exit louver angle on temperature rise in lift-fan inlets due to ingestion; $\alpha = 0^{\circ}$, $\delta_f = 45^{\circ}$, staggered louvers.

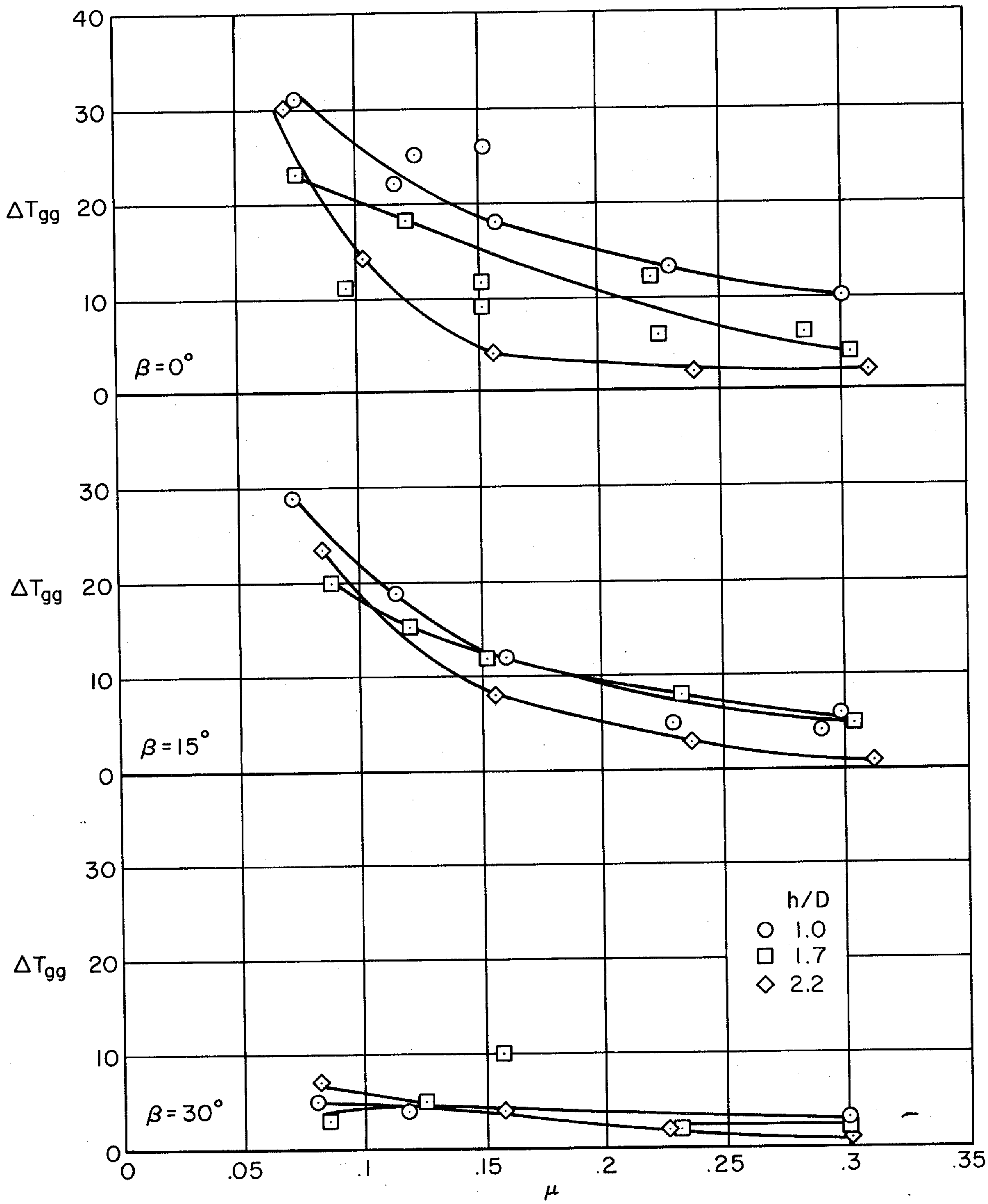

(a) Straight louvers.

Figure 57.- Effect of ground height and exit louver angle on temperature rise in gas generator inlets due to reingestion; $\alpha = 0^\circ$, $\delta_f = 45^\circ$.

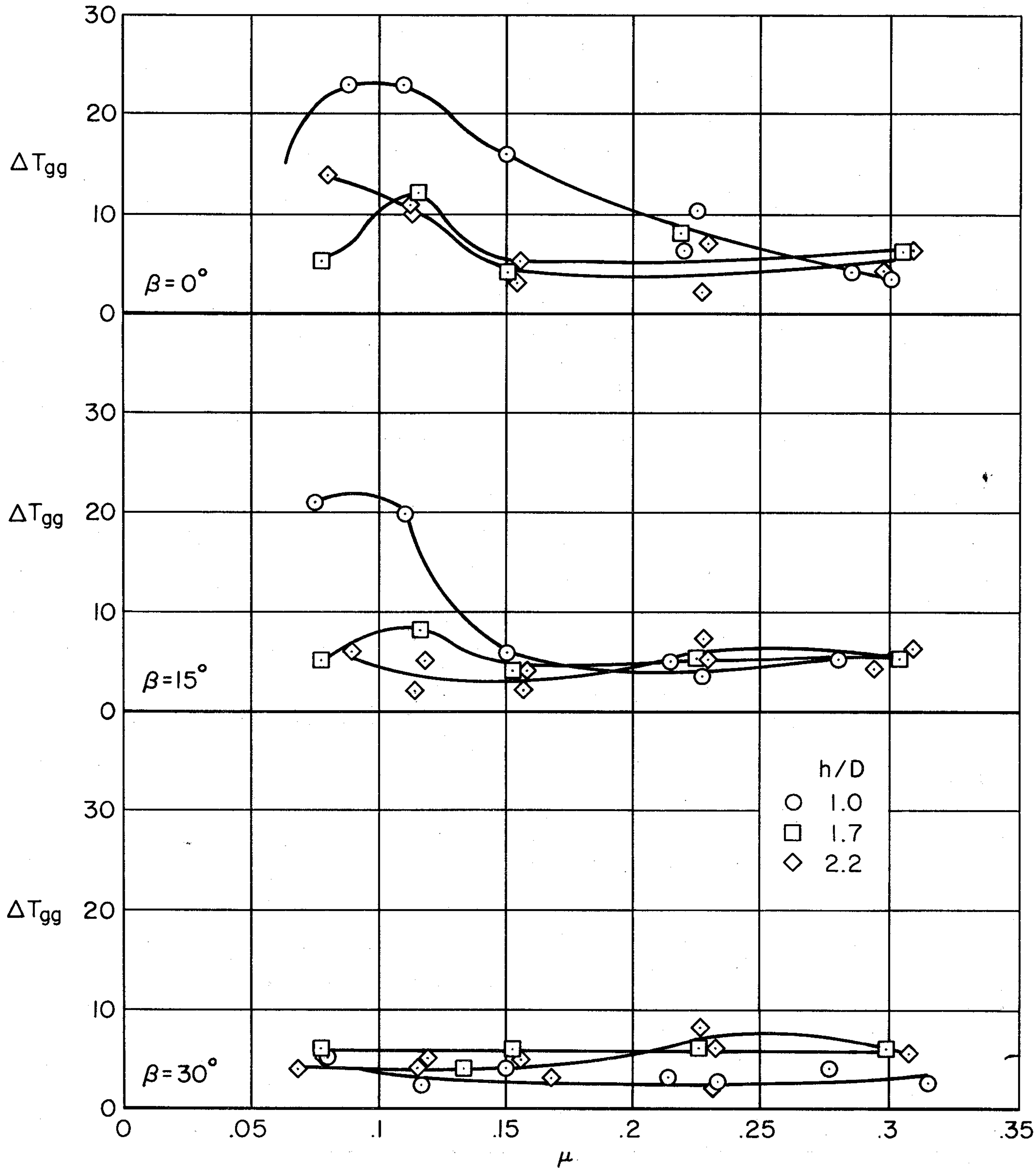

(b) Staggered louvers.

Figure 57.- Concluded.

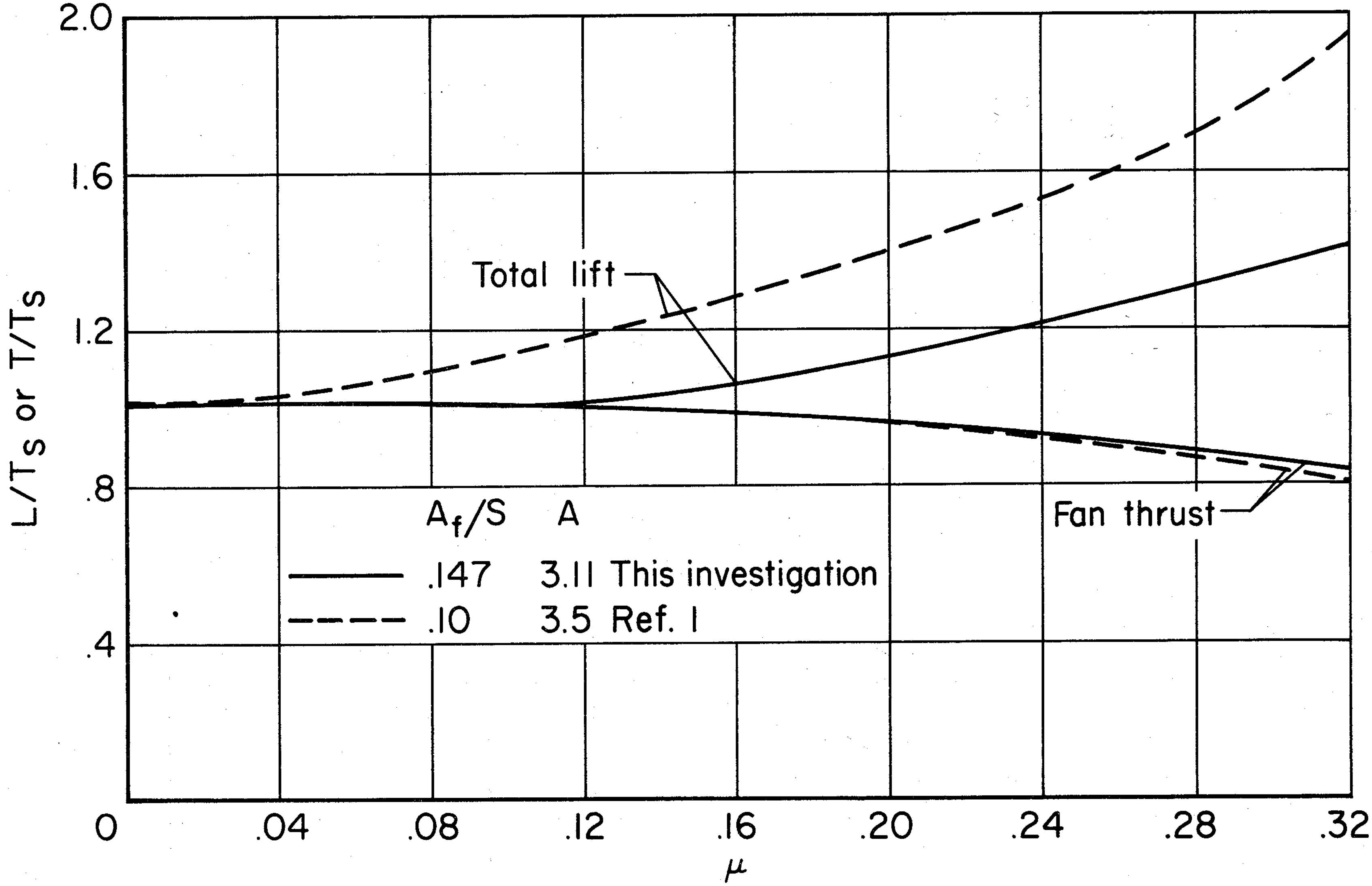

Figure 58.- Comparison of large-scale fan-in-wing variation of lift with airspeed; $\alpha = 0^{\circ}$, tail off, $\delta_f = 0^{\circ}$.

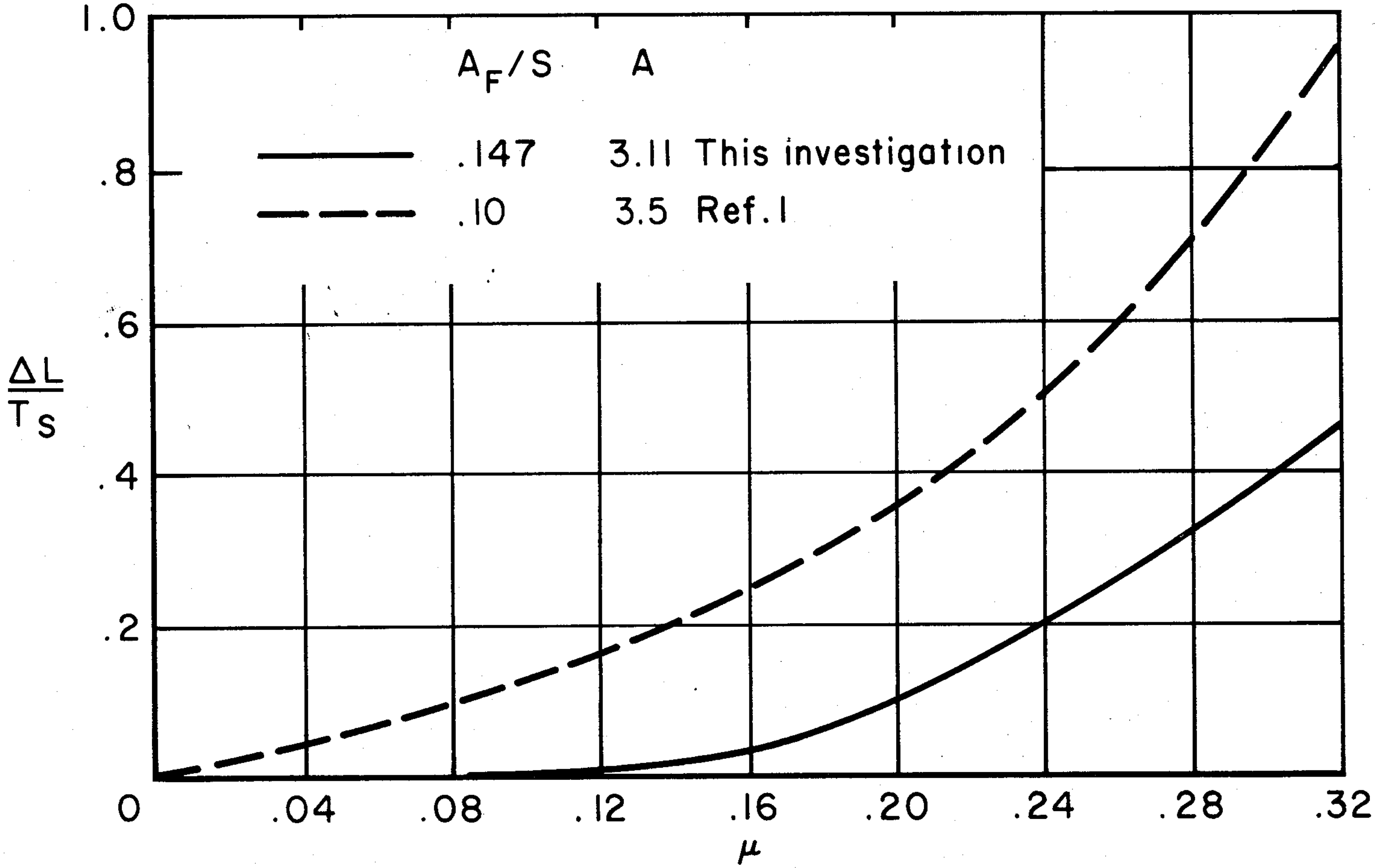

Figure 59.- Comparison of the variation of fan induced lift with airspeed; $\alpha = 0^{\circ}$, $\beta = 0^{\circ}$, $\delta_f = 0^{\circ}$.

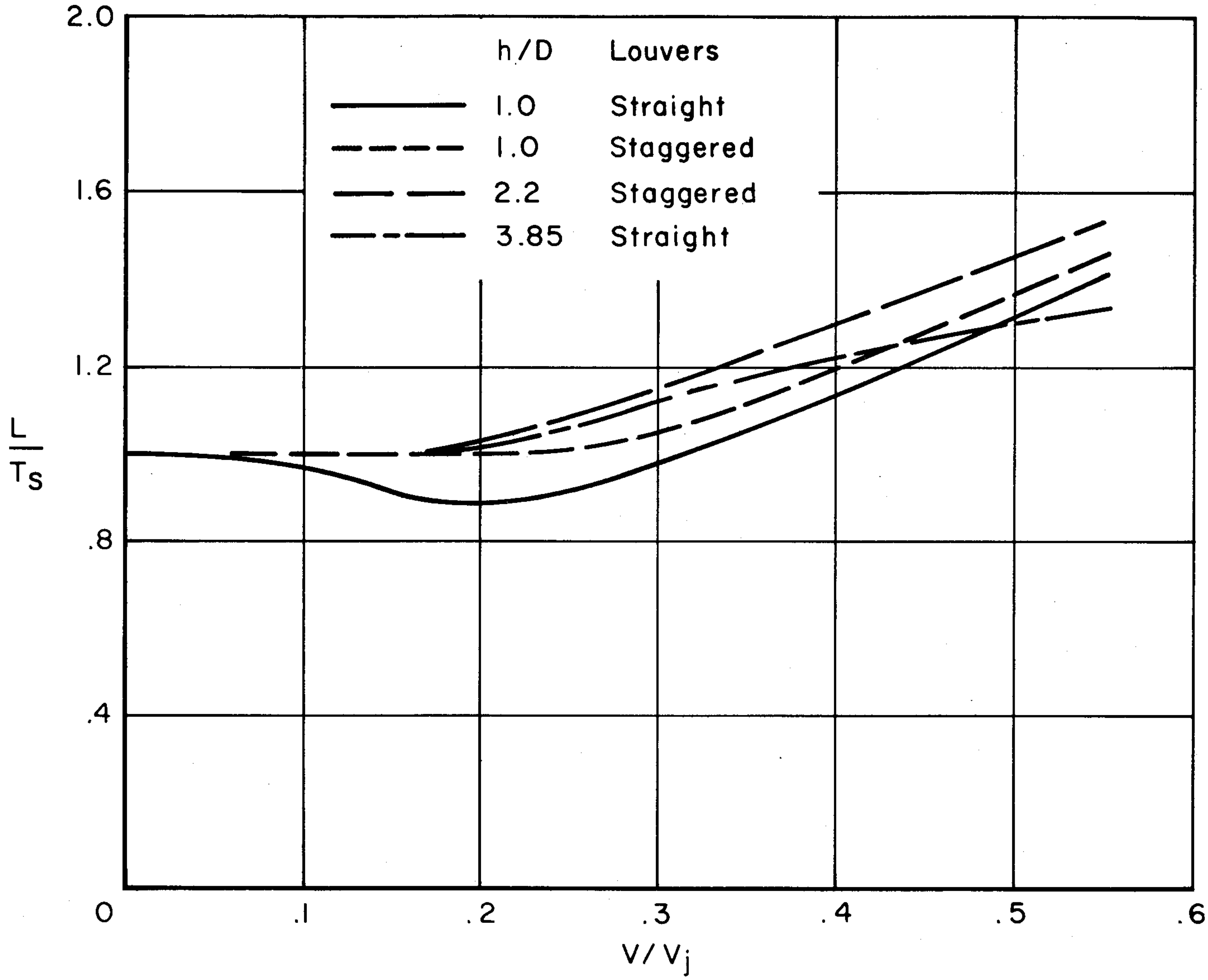

Figure 60.- Constant fan RPM; tail on, $\delta_f = 45^{\circ}$.

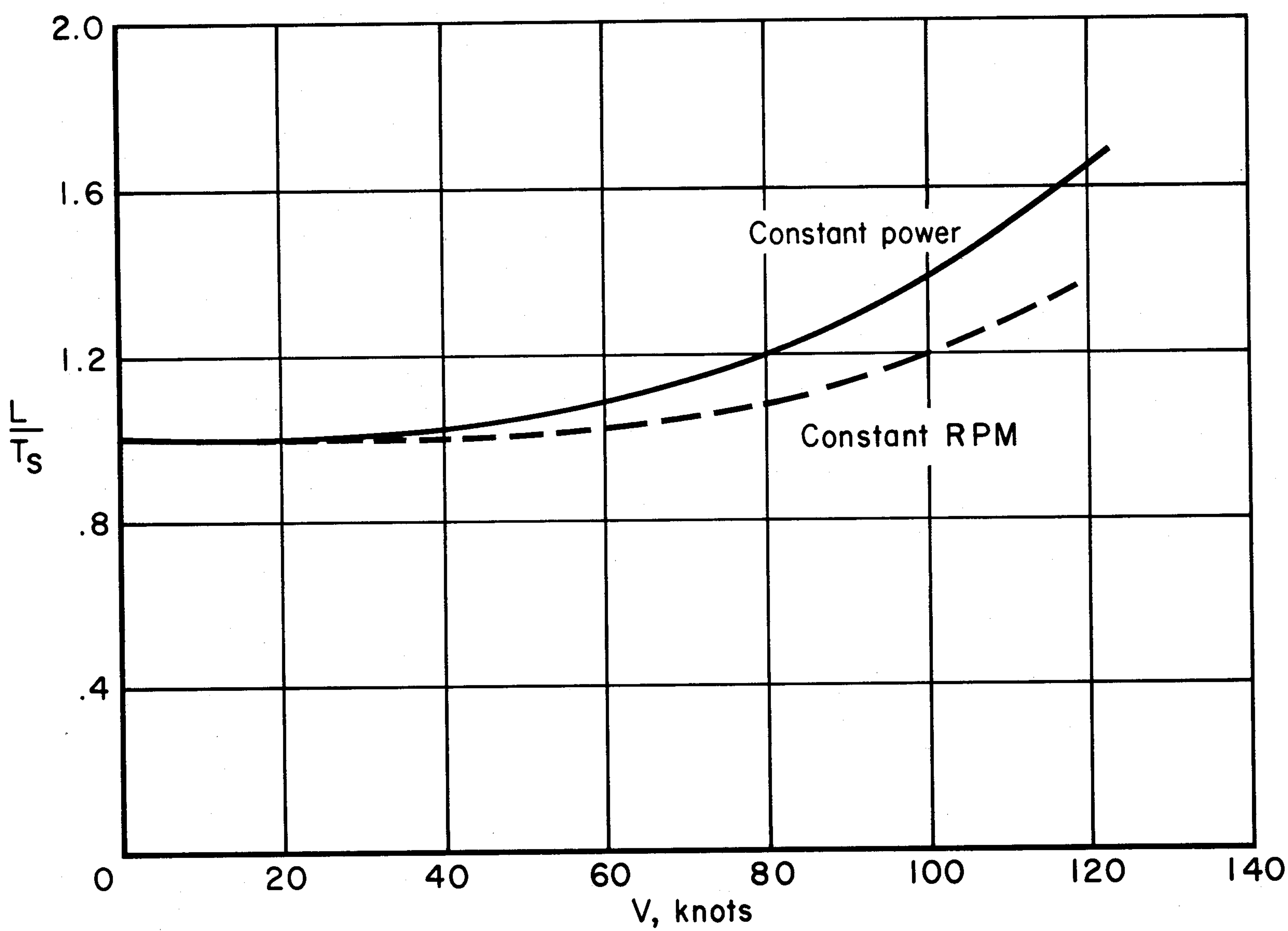

Figure 61.- Effect of constant power; $h/D = 1.0$, $\beta = 0^{\circ}$, tail on, $\delta_f = 45^{\circ}$.

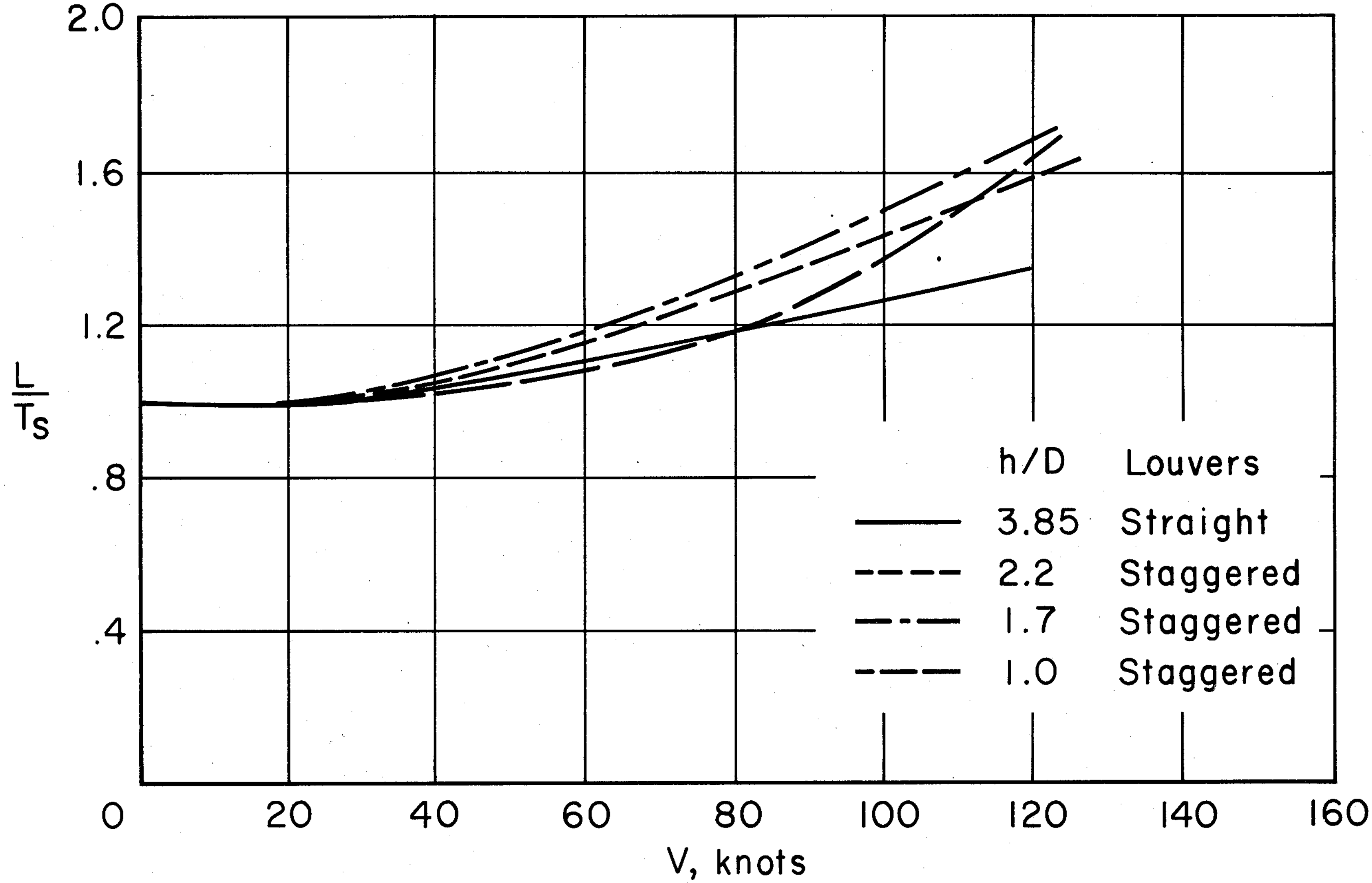

Figure 62.- Equivalent power setting; tail on, $\delta_f = 45^{\circ}$.

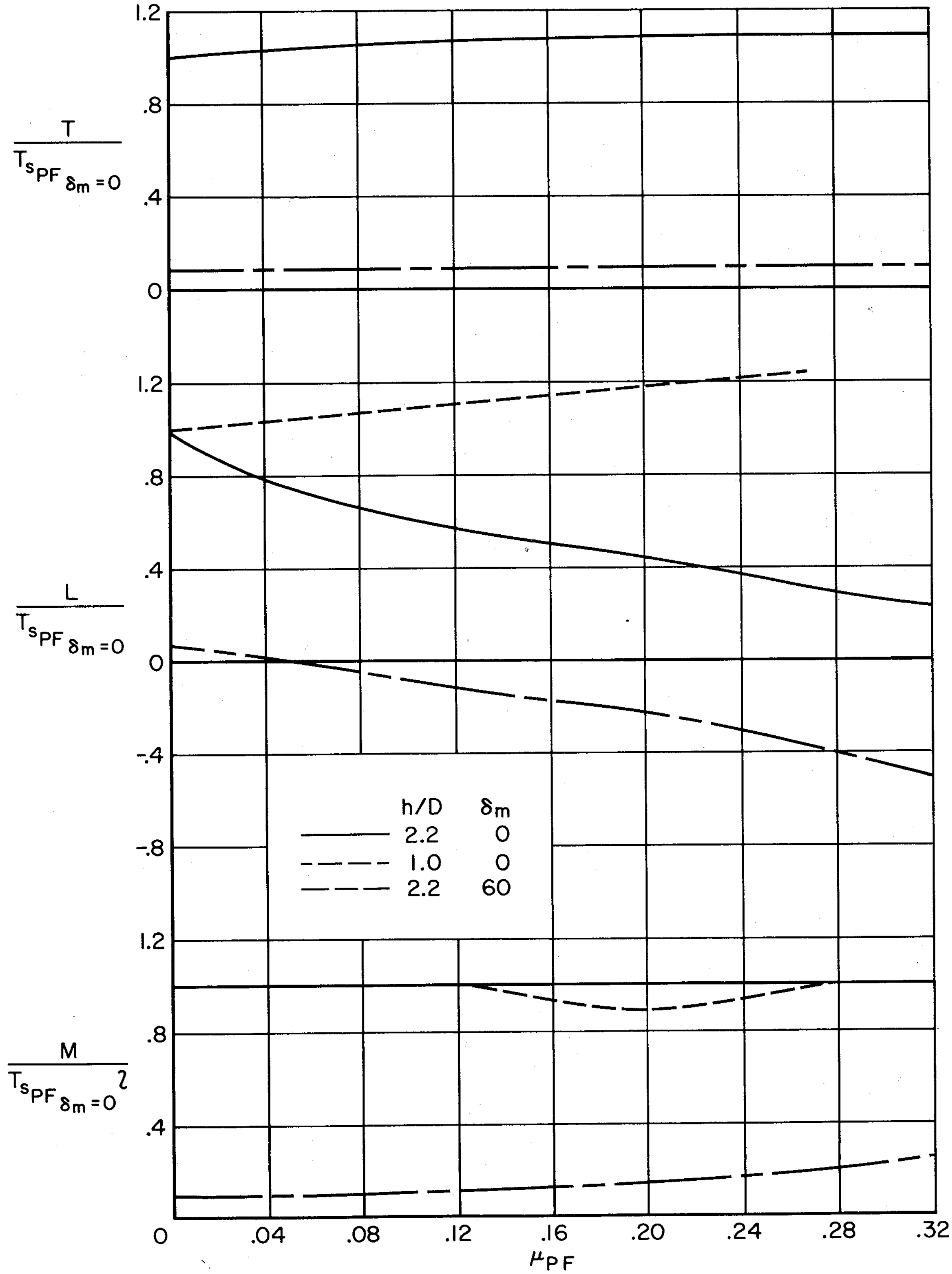

Figure 63.- Effect of airspeed on the variation of lift and moment due to pitch-fan operation.

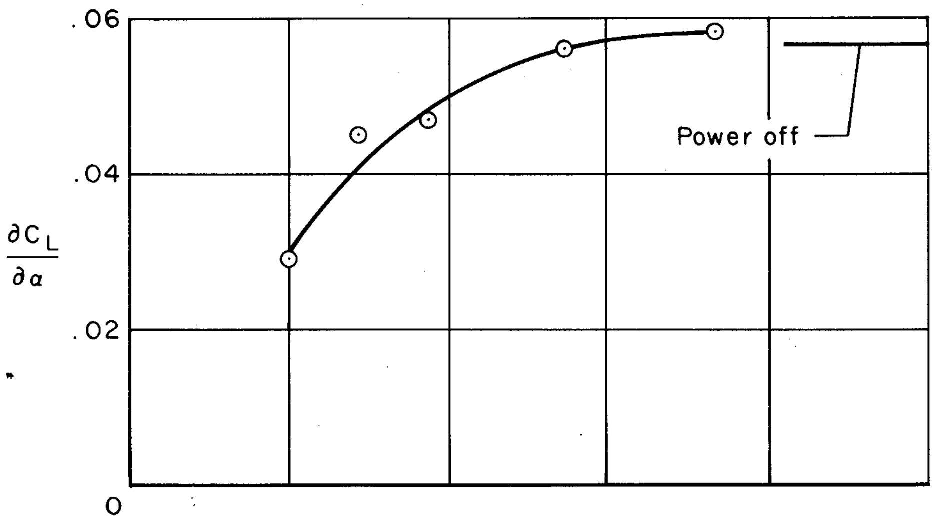

(a) Lift-curve slope; pitch fan only operating, tail off.

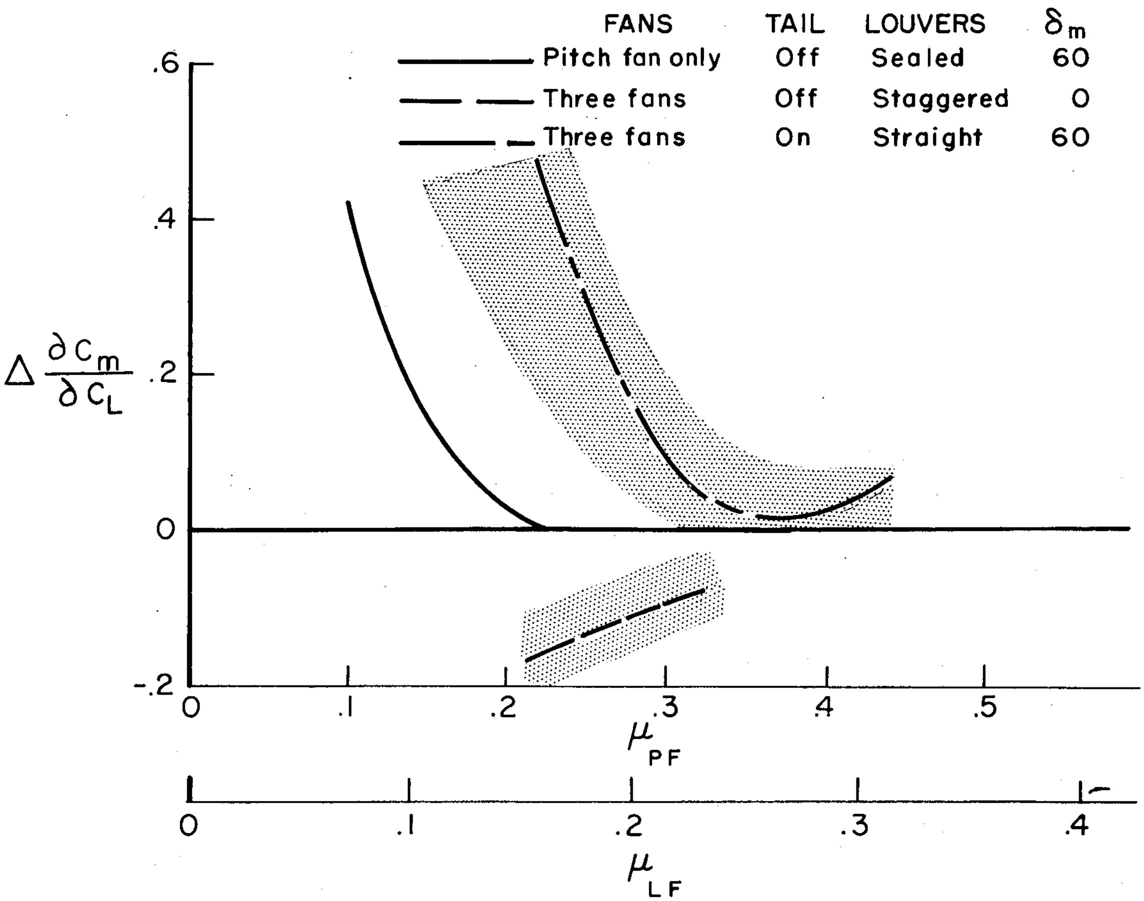

(b) Static margin.

Figure 64.- Effect of pitch-fan operation on lift-curve slope and longitudinal stability; h/D = 2.2, δ_f = 45°.

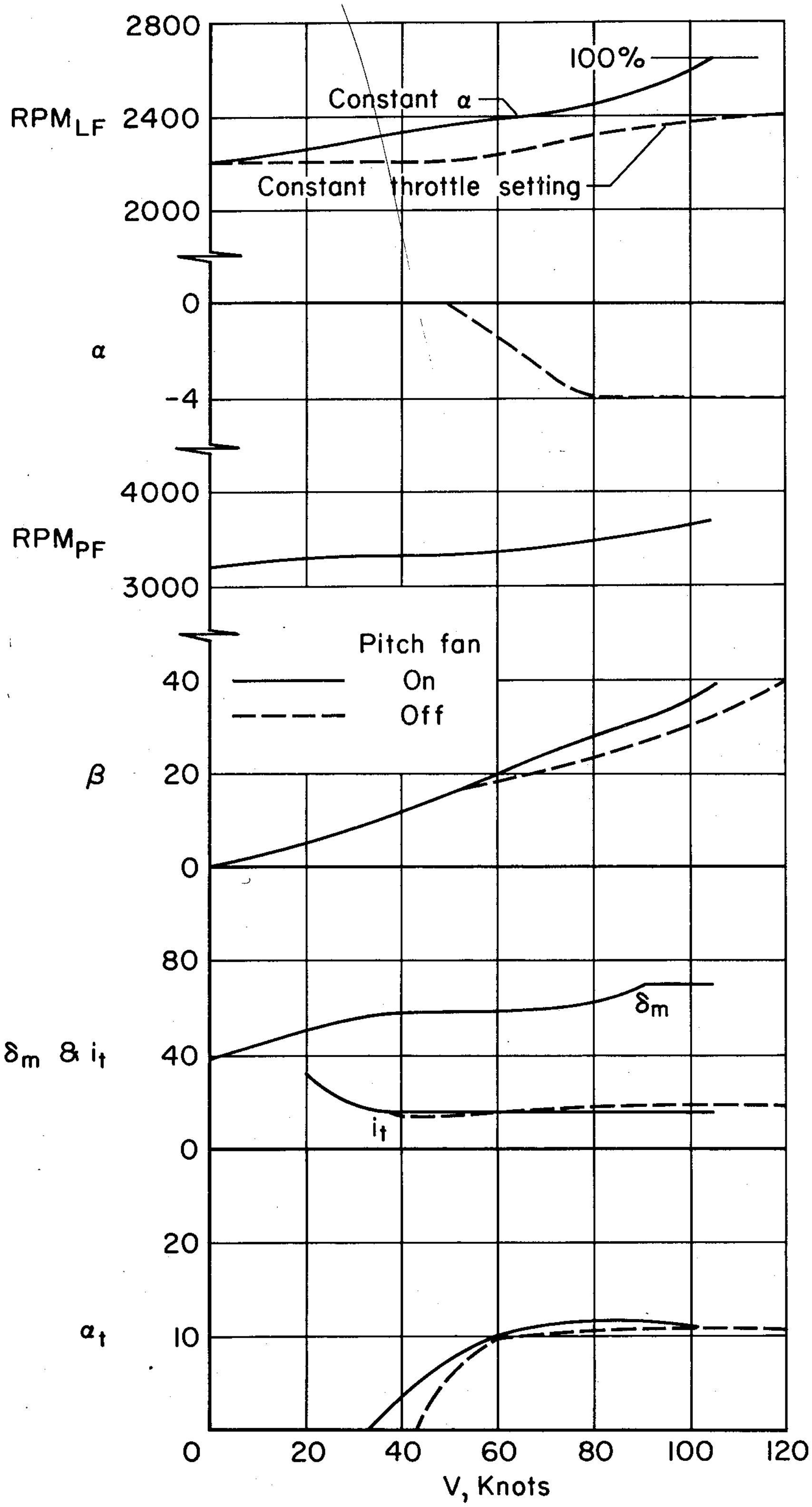

Figure 65.- Power and longitudinal control requirements for unaccelerated flight; $\delta_f = 45^\circ$, W = 9500 lb.